Cranfield University

M. J. Provost

The Use of Optimal Estimation Techniques in the Analysis of Gas Turbines

1994

School of Mechanical Engineering
Department of Thermal Power

Ph.D Thesis

CRANFIELD UNIVERSITY

SCHOOL OF MECHANICAL ENGINEERING

DEPARTMENT OF THERMAL POWER

PhD Thesis

Academic Year 1994-5

M J PROVOST

The Use of Optimal Estimation Techniques in the Analysis of Gas Turbines

Supervisor: R Singh

December 1994

ABSTRACT

This thesis discusses several methods that can be used to analyse gas turbines, based on an optimal estimation algorithm called the Kalman Filter. These techniques overcome the difficulties of more 'traditional' analysis methods, which can give misleading results because they do not explicitly consider the possibility of measurement error.

An enhancement to the Kalman Filter (the 'Concentrator') is presented, which overcomes the Kalman Filter's tendency to 'smear' the effects of genuine changes in a small number of component changes and/or sensor biasses over the whole set of changes and biasses being considered. To complement this, methods of optimising some of the statistical inputs to the Kalman Filter in order to improve the ability of the 'Concentrator' to carry out the required analysis are discussed. These are based on analytical methods developed to determine the sensitivity of the Kalman Filter to its inputs.

Techniques are also presented for determining the gas-path measurements in a gas turbine that are needed to enable the required analysis of component changes and/or sensor biasses to be performed, including determination of both possible measurement redundancy and the ability of a set of measurements to successfully differentiate between all the component changes and sensor biasses being sought.

A recursive algorithm for time series analysis (the Smoothing/Trending Algorithm) is also presented. This produces, for each point in a time series, best estimates of the underlying levels and trends (rates of change of level) of the process generating the observations. A method of combining the 'Concentrator' and the Smoothing/Trending Algorithm is also presented, which reduces the effects of sensor noise on the analysis of component changes and sensor biasses from time series data.

Many types of prime movers and process plant could be effectively analysed using the methods described in this thesis.

ACKNOWLEDGEMENTS

'If I have seen further it is by standing on the shoulders of giants'

- Isaac Newton, in a letter to Robert Hooke, 5th February 1675

Without the help of many people in Rolls-Royce plc, the work described in this thesis could not have happened. I would particularly like to mention the contributions made by the following friends and colleagues:

Mr John Chantry, Mr Barry Curnock and Mr Michael Barwell, who offered encouragement, guidance and the sorts of awkward questions that set off new lines of enquiry or force a better way of explaining things;

Mr David Nevell, who helped my early understanding of the Kalman Filter and offered some ideas on the 'Concentrator';

Mr Colin Williams and Mr Graham Lomas, who helped with the integration onto the Rolls-Royce mainframe computer of the FORTRAN program that implements the methods described in this thesis;

Mr Michael Ward and Mr David Streeter, who provided routines that plotted out the results from the Smoothing/Trending Algorithm and Trend 'Concentration';

Mrs Pauline Graham and Mr Andrew Wright, who helped with many of the diagrams;

Mrs Audrey Richardson, Miss Lisa Dowd and Mrs Charlotte Elsey, who helped with typing the first draft;

Special thanks are due to Mr Simon Hart, who allowed the project to continue when I joined his department.

Several members of Cranfield University also made invaluable contributions, notably my supervisor Professor Riti Singh, who gave freely of his knowledge, experience and wisdom. Dr Johnathan Blackledge and Dr Roy Bannister, the other members of my PhD review committee, offered constructive criticisms and comments each time we met.

My wife Sheila, and children Nicholas and Simon, tolerated the disruption to family life that such a project inevitably brings with good humour. Sheila also inked in all the special symbols the computer couldn't handle.

All responsibility for errors or omissions lies with me. Opinions expressed are my own, and are not necessarily endorsed by either Rolls-Royce plc or Cranfield University.

M.J. Pratt

CONTENTS

		Page
CHAPTER 1:	SUBJECT MATTER COVERED BY THIS THESIS	1
CHAPTER 2:	INTRODUCTION	3
2.1	Gas Turbine Modelling	4
2.2	Facets of Gas Turbine Analysis	5
2.3	Difficulties with the Analysis Process	6
2.4	The 'Traditional' Approach to Gas Turbine Analysis	8
2.5	An Alternative Approach to Gas Turbine Analysis	10
2.6	Optimal Estimation and Kalman Filtering	12
2.7	The Kalman Filter Equations	13
2.8	Problems with the Kalman Filter	15
2.9	Literature Search	16
2.10	Extension of Kalman Filtering to Time Series Analysis	17
CHAPTER 3:	DETERMINATION OF NECESSARY MEASUREMENTS	18
3.1	Determination of Possible Gas-Path Measurements	19
3.2	Generation of Exchange Rate Tables	20
3.3	Correlations Between Measurements	23
3.4	Inclusion of Sensor Bias	28
3.5	Correlations Between Component Changes and Sensor Biasses	29
3.6	Observability	33
3.7	Detection Ratio	44
CHAPTER 4:	KALMAN FILTERING APPLIED TO GAS TURBINE ANALYSIS	45
4.1	The Analysis Situation	45
4.2	Theory of Estimation Methods	46
4.3	Formal Derivation of the Kalman Filter	49
4.4	Meaning of Results	54
4.5	Kalman Filter 'Concentrator'	57
4.6	Input Required for the Kalman Filter	60
4.7	Sensitivity Analysis	62
4.8	'Tuning' the Kalman Filter	64
4.9	Methods of Deriving Component Change and Sensor Bias Standard Deviations	65
4.10	Use of Sensitivity Analysis	66
4.11	Analysis Using 'Tuned' Standard Deviations	72
4.12	Automatic 'Tuning'	74
CHAPTER 5:	SMOOTHING AND TRENDING USING KALMAN FILTER THEORY	77
5.1	Basic Assumptions	77
5.2	Derivation of Smoothing/Trending Equations	79
5.3	Meaning of Results	83
5.4	Input Required	84
5.5	Comparison with Moving Average and Exponential Smoothing	84
5.6	Trend 'Concentration'	85
5.7	'Tuning' the Smoothing/Trending Algorithm	87
5.8	Examples	88

Page

CHAPTER 6: EXAMPLES 97
6.1 Single Component Changes and Sensor Biasses 98
6.2 Single Component Changes and Sensor Biasses with Normally-Distributed Sensor Non-Repeatability 101
6.3 Pairs of Component Changes and/or Sensor Biasses 112
6.4 Smoothing/Trending Algorithm Demonstration 114
6.5 Trend 'Concentration' 117

CHAPTER 7: DISCUSSION 155

CHAPTER 8: CONCLUSIONS 160

CHAPTER 9: RECOMMENDATIONS FOR FURTHER WORK 162

CHAPTER 10: REFERENCES 165

APPENDIX A: GAS TURBINE MEASUREMENTS AND 'TRADITIONAL' ANALYSIS TECHNIQUES 170
A1 Measurements 170
A2 Thrust 170
A3 Fuel Flow 173
A4 Pressures 174
A5 Temperatures 180
A6 Airflow 188
A7 Shaft Speeds 188
A8 Engine Geometry 188
A9 Correction of Measurements to 'True' Values 189
A10 Calculation of Unmeasured Parameters 190
A11 Calculation of TET from HP Turbine Capacity 190
A12 Calculation of Core Flow Using a Heat Balance 191
A13 Calculation of Other Unmeasured Parameters 193
A14 Correction of Measurements to Standard Day Conditions 196
A15 Calculation of Component Performance 199
A16 Measurement Error 200
A17 Iterative Analysis 202

APPENDIX B: CALCULATION OF OBSERVABILITY EIGENVALUES AND EIGENVECTORS 206

APPENDIX C: CALCULATION OF SENSOR NON-REPEATABILITY STANDARD DEVIATIONS 208

FIGURES

		Page
1	A single-spool axial flow turbojet	3
2	The Analysis Process	7
3	Apparent compressor improvement due to rematching	10
4	Diagrammatic representation of analysis situation	11
5	The System Matrix	11
6	Exchange Rate Table for typical two-shaft turbofan	21
7	Typical two-shaft turbofan configuration	22
8	Component and Environment Exchange Rates	24
9	Two-dimensional 'Component Change Space'	25
10	Measurement Correlation Matrix (components only)	27
11	Generation of System Matrix	29
12	Measurement Correlation Matrix (whole system)	30
13	Two-dimensional 'Measurement Space'	31
14	System Correlation Matrix	33
15	Example of indistinguishable combinations of component changes	34
16	Example of poorly-observable system	36
17	Example of easily observable system	37
18	System Correlation Matrices and Eigenvalues/vectors	40
19	Non-observability when number of component changes + sensor biasses greater than number of measurements	41
20	Eigenvalues/Eigenvectors of full System Matrix	42
21	Eigenvalues/Eigenvectors: no sensor biasses	43
22	The Analysis Situation	46
23	Use of prior information	56
24	'Concentrator' performance for -1% HPC ETA, +0.5% P2 bias, +1% T49 bias	59
25	Diagrammatic representation of $\underline{C}$' matrix	61
26	Kalman Gain Matrix on first pass	67
27	First pass analyses	68
28	Normalised analysis	69
29	Normalised analysis/normalised analysis of input component change or sensor bias	70
30	Partial derivatives of normalised analysis ratios	71
31	'Concentrator' performance for 'Tuned' input	73
32	'Concentrator' performance for 'Tuned' input (2)	75
33	Diagrammatic representation of time series model	78
34	Calculation procedure for smoothing/trending	82
35	Typical relationship of level, trend estimate gains	89
36	Smoothing/trending of step: no noise	90
37	Smoothing/trending of step: noise in series	91
38	Smoothing/trending of ramp: no noise	92
39	Smoothing/trending of ramp: noise in series	93
40	Smoothing/trending of outlier: no noise	94
41	Smoothing/trending of outlier: noise in series	95
42	Kalman Gain Matrix on first pass: 'Auto-Tuned' $\underline{Q}$ Matrix	98
43	First pass analyses: 'Auto-Tuned' $\underline{Q}$ Matrix	99
44	Normalised analysis/normalised analysis of input component change or sensor bias: 'Auto-Tuned $\underline{Q}$ Matrix	100
45	Fan Tip Efficiency Analysis Distribution	102
46	Fan Tip Capacity Analysis Distribution	102
47	LP Compressor Efficiency Analysis Distribution	103

		Page
48	HP Compressor Efficiency Analysis Distribution	103
49	HP Compressor Capacity Analysis Distribution	104
50	HP Turbine Efficiency Analysis Distribution	104
51	HP Turbine Capacity Analysis Distribution	105
52	LP Turbine Efficiency Analysis Distribution	105
53	EPR Bias Analysis Distribution	106
54	Inlet Pressure Bias Analysis Distribution	106
55	Inlet Temperature Bias Analysis Distribution	107
56	Fuel Flow Bias Analysis Distribution	107
57	HPC Entry Pressure Bias Analysis Distribution	108
58	HPC Entry Temperature Bias Analysis Distribution	108
59	HPC Exit Pressure Bias Analysis Distribution	109
60	HPC Exit Temperature Bias Analysis Distribution	109
61	LPT Exit Temperature Bias Analysis Distribution	110
62	Fan Tip Exit Pressure Bias Analysis Distribution	110
63	Net Thrust Bias Analysis Distribution	111
64	Total Inlet Airflow Bias Analysis Distribution	111
65	Smoothing/Trending of Car Fuel Consumption Records	115
66	Relationships between Kalman Filter and 'Concentrator', Smoothing/Trending and Trend 'Concentration'	118
67	Fuel Flow Measurement Differences	121
68	HPC Entry Total Pressure Measurement Differences	122
69	HPC Entry Total Temperature Measurement Differences	123
70	HPC Exit Total Pressure Measurement Differences	124
71	HPC Exit Total Temperature Measurement Differences	125
72	LPT Exit Total Temperature Measurement Differences	126
73	Fan Tip Exit Total Pressure Measurement Differences	127
74	LP Speed Measurement Differences	128
75	HP Speed Measurement Differences	129
76	Net Thrust Measurement Differences	130
77	Total Inlet Airflow Measurement Differences	131
78	Fan Tip Efficiency Analyses	132
79	Fan Tip Capacity Analyses	133
80	LP Compressor Efficiency Analyses	134
81	HP Compressor Efficiency Analyses	135
82	HP Compressor Capacity Analyses	136
83	HP Turbine Efficiency Analyses	137
84	HP Turbine Capacity Analyses	138
85	LP Turbine Efficiency Analyses	139
86	EPR Sensor Bias Analyses	140
87	Inlet Total Pressure Sensor Bias Analyses	141
88	Inlet Total Temperature Sensor Bias Analyses	142
89	Fuel Flow Sensor Bias Analyses	143
90	HPC Entry Total Pressure Sensor Bias Analyses	144
91	HPC Entry Total Temperature Sensor Bias Analyses	145
92	HPC Exit Total Pressure Sensor Bias Analyses	146
93	HPC Exit Total Temperature Sensor Bias Analyses	147
94	LPT Exit Total Temperature Sensor Bias Analyses	148
95	Fan Tip Exit Total Pressure Sensor Bias Analyses	149
96	Net Thrust Sensor Bias Analyses	150
97	Total Inlet Airflow Sensor Bias Analyses	151

		Page
98	System Architecture for Enhancements to Kalman Filter Based Analysis Methods	163
99	Engine thrust measurement system	171
100	Diagram of indoor test bed	172
101	Typical positive displacement flow meter	174
102	Typical pressure rake (1)	176
103	Typical pressure rake (2)	177
104	Typical pressure rake (3)	178
105	Typical Scanivalve arrangement	179
106	Typical temperature rake (1)	181
107	Typical temperature rake (2)	182
108	Typical verniered temperature rakes	184
109	Typical combined pressure and temperature rake	185
110	Composite picture of typical pressure and temperature measurements in the compressor section of an engine	186
111	Composite picture of typical pressure and temperature measurements in the turbine section of an engine	187
112	Core flow calculation using heat balance	192
113	Two-shaft turbofan: summary of analysis	194

TABLES

		Page
1	Comparison of 'Concentrator' outputs with various inputs to the Q matrix	76
2	Square Roots of Diagonal Elements of Q Matrix	97
3	'Concentrator' Results: Single Component Changes and Sensor Biasses	99
4	Failures of +1%/+1% Component Changes and/or Sensor Biasses	113
5	Failures of -1%/+1% Component Changes and/or Sensor Biasses	113
6	Time Series of Simulated HP Compressor Efficiency Changes	117
7	Typical theta exponents	198

NOTATION

A	Area
$\underline{A}$	Matrix defining how $\underline{x}$ varies over time
$\underline{C}$	System Matrix
$\underline{C}'$	Matrix which contains both the environmental exchange rate table and a unit matrix
CALVAL	Fuel Calorific Value
CAP	Flow capacity
Cov(a,b)	Covariance of a and b
Cp	Specific heat at constant pressure
Cv	Specific heat at constant volume
$\underline{e}$	Vector of errors
E[ ]	Expectation operator
FG÷W√T	Semi-dimensional gross thrust
FN	Net thrust
FN÷Pamb	Semi-dimensional thrust
$\underline{G}$	Weighting matrix
$\underline{I}$	Unit matrix of appropriate dimension
J	Sum of squares
$\underline{K}$	Kalman Gain Matrix
Level	True level of process generating time series
m	Number of gas-path measurements
n	Number of component changes + sensor biasses
N(a,b)	Normally-distributed random variable, with mean a, variance b
N	Shaft speed
N÷√T	Semi-dimensional shaft speed
$\underline{P}$	Covariance matrix of $\hat{\underline{x}}$
$\underline{P}'$	Covariance update

P	Total pressure
Pamb	Ambient static pressure
P13	Fan Tip exit total pressure
P2	Engine inlet total pressure
P26	HP Compressor entry total pressure
P3	HP Compressor exit total pressure
$\underline{Q}$	System covariance matrix
q_{11}	Level variance
q_{12}	Level-trend covariance
q_{22}	Trend variance
$\underline{R}$	Measurement repeatability covariance matrix
t	Number of intervals (time, cycles, etc) between current and previous observation in time series
T	Total temperature
T2	Engine inlet total temperature
T26	HP Compressor entry total temperature
T3	HP Compressor exit total temperature
T49	LP Turbine exit total temperature
Trend	True trend (rate of change of level) of process generating time series
$\underline{V}$	diagonal matrix of squares of standard deviations of repeatabilities
$\underline{W}$	Weighting matrix
W	Mass flow rate
W1A	Total inlet airflow
WFE	Fuel flow
WFE÷(P$\sqrt{T}$)	Semi-dimensional fuel flow
W$\sqrt{T}$÷P	Semi-dimensional airflow
W$\sqrt{T}$÷AP	Another form of semi-dimensional airflow, also known as Q

wl	Noise term in level
wt	Noise term in trend
XN	Shaft speed
XNH	HP shaft speed
XNL	LP shaft speed
$\underline{x}$	System state vector
$\underline{Y}$	Vector of observations
γ	Ratio of specific heats = Cp÷Cv
δ	$P2_{test} \div P2_{corrected}$
δ_{amb}	$Pamb_{test} \div Pamb_{corrected}$
η , ETA	Efficiency
λ	Eigenvalue
Θ	$T2_{test} \div T2_{corrected}$

Subscript k denotes current time

Subscript k-1 denotes immediately previous time

Subscript 0 denotes estimate before any measurements taken

Superscript T denotes matrix transpose

Superscript -1 denotes matrix inverse

Superscript # denotes matrix pseudo-inverse

Superscript ^ denotes best estimate

Superscript - denotes mean

Please note that the dot product symbol • has been used throughout to indicate multiplication, since it was felt that the use of x would introduce excessive confusion with the symbol used to indicate the system state vector.

ABBREVIATIONS

AGARD	Advisory Group for Aerospace Research and Development
AIAA	American Institute of Aeronautics and Astronautics
AIDS	Aircraft Integrated Data System
ASME	American Society of Mechanical Engineers
COMPASS	COndition Monitoring and Performance Analysis Software System
ECM	Engine Condition Monitoring
ECS	Environmental Control System
EGT	Exhaust Gas Temperature
EPR	Engine Pressure Ratio
GEM	General Engine Monitoring
GPA	Gas Path Analysis
HP	High Pressure
HPC	High Pressure Compressor
HPT	High Pressure Turbine
IEEE	Institute of Electrical and Electronic Engineers
ISA	International Standard Atmosphere
LP	Low Pressure
LPC	Low Pressure Compressor
LPT	Low Pressure Turbine
MAP	Module Analysis Program
NASA	National Aeronautics and Space Administration
NGV	Nozzle Guide Vane
NMR	Nuclear Magnetic Resonance
RRAP	Rolls-Royce Aero-engine Performance
SAE	Society of Automotive Engineers
SFC	Specific Fuel Consumption

SOAPP	State-Of-the-Art Performance Programming
TEAM	Turbine Engine Analysis Module
TGT	Turbine Gas Temperature
TEMPER	Turbine Engine Module Performance Estimation Routine
TET	Turbine Entry Temperature
UTR	Uniform Temperature Reference

GLOSSARY OF TERMS

Accuracy

The range of possible error in a measurement. Unfortunately, the word is used in a very loose way, so the reader is warned to beware of quoted 'accuracy' values!

Analysis

The process of deducing the performance of the individual components of a gas turbine from gas-path measurements.

Analytical Redundancy

The use of software such as the Kalman Filter to calculate the values that would have been read by failed sensors.

Bias

A fixed component of measurement error, which remains constant no matter how many times the measurement is taken.

Capacity

A measure of the ability of a component to accept airflow; usually expressed semi-dimensionally (as $W\sqrt{T}\div P$).

Component Change Space

A space formed by defining vectors whose coordinates are specified by the elements in each gas-path measurement row in an Exchange Rate Table.

Component Exchange Rate Table

A matrix relating changes of gas-path measurements (the dependent variables) to changes in component performance parameters (the independent variables).

Component Performance Parameters

Thermodynamic parameters such as efficiency and flow capacity which are used to describe the performance of individual components in the gas turbine. The term is also used to describe parameters such as cooling bleed which may be dependent on the configuration of several components.

Concatenation

The process of extending a matrix by adding extra rows or columns from another matrix to it.

Concentrator

The enhancement to the Kalman Filter developed by the author which removes the under-estimation of genuine component changes and/or sensor biasses caused by the least-squares basis of the Kalman Filter.

Condition Monitoring

The gathering of data from a gas turbine in service, in order to understand its condition and optimise its operating costs.

Constant Error

See Bias.

Cooling/Sealing Bleed

Air taken from the compressor(s) of a gas turbine to cool hot components such as turbine NGVs, turbine blades and turbine disks.

Correlation

A measure of the relationship between two parameters, indicating whether changes in one of them are accompanied by changes in the other.

Covariance

A statistical measure of how two random variables vary together. The covariance of two random variables a and b is defined as $E[(a-\bar{a})\bullet(b-\bar{b})]$.

Covariance Matrix

A symmetrical matrix showing the covariance of each possible pair of elements in two random vectors.

Detection Ratio

A measure of the invertibility of a Component Exchange Rate Table.

Dimensions

The number of rows and columns in a matrix, denoted by $(n\bullet m)$, where n is the number of rows and m is the number of columns.

Enthalpy

The total energy (potential, kinetic and thermal) of a fluid.

Environmental Control System

The system on an aircraft that takes air bleed from an engine and uses it to pressurise the fuselage and supply air for the occupants to breathe.

Environmental Exchange Rate Table

A matrix relating changes of gas-path measurements (the dependent variables) to changes in the environmental measurements (the independent variables).

Environmental Measurements

Measurements of flight condition (inlet total pressure, inlet total temperature, ambient static pressure) and power-setting parameter that are used to define expected levels of gas-path measurements.

Error Covariance Matrix

A matrix, calculated by the Kalman Filter, that quantifies the possible 'spread' of the estimates produced by the Kalman Filter.

Exchange Rate Table

A matrix relating changes of gas-path measurements (the dependent variables) to changes in component performance parameters and/or environmental measurements (the independent variables).

Expectation Operator

An operator E[] which denotes a meaning process. For n values of a random variable a, $E[a] = \left(\sum_{i=1}^{n} a_i \right) \div n$

Expected Value

A value calculated using the expectation operator.

Expected Value of Gas-Path Measurement

The value of a gas-path measurement that would be observed, at a given flight condition and power setting, if the gas turbine was behaving as expected, ie with no component changes or sensor biasses.

Exponential Smoothing

A commonly-used method of smoothing a time series, by adding a 'weighted' value of the current observation to a 'weighted' value of the previous estimate of the 'true' value of the series.

Flight Condition Measurement

A measurement that can be used to calculate environmental measurements, eg altitude, Mach Number.

Flow Capacity

See Capacity.

Gas-Path Analysis

A commonly-used term for performance analysis.

Gas-Path Measurement

A measurement taken on a gas turbine that can be used to analyse component performance. Measurements taken may be a combination of those needed to determine air properties (eg total pressure, total temperature) and other relevant parameters such as shaft rotational speeds, fuel flow and thrust.

Handling Bleed

Air bleed taken off the compressor(s) of a gas turbine at low powers to ensure stable operation.

Hardware Redundancy

The provision of multiple sensors to measure the same parameter.

International Standard Atmosphere

An internationally-agreed relationship between altitude, ambient pressure and 'normal' ambient temperature.

Kalman Filter

An algorithm for producing best estimates of the component changes and sensor biasses that produced an observed set of gas-path measurement differences from expectation.

Kalman Gain Matrix

The matrix used to calculate best estimates of component changes and sensor biasses from observed gas-path measurement differences from expectation.

Level Estimate Gain

The value used to calculate the best estimate of level in a noisy time series from an expected level and the difference between the actual and predicted observation.

Measurement Space

A space formed by defining vectors whose coordinates are specified by the elements in each component change or sensor bias column in an Exchange Rate Table.

Modelling

See Synthesis.

Module

A part of a gas turbine, containing one or more components, that can be replaced as a unit during maintenance.

Module Performance Analysis

A commonly-used term for performance analysis.

Moving Average

A commonly-used method of smoothing a time series, by averaging several points to reduce the effects of random noise in the observations.

Normal Distribution

An important probability distribution used widely in the study of variability in measurements, components, etc.

Nozzle Discharge Coefficient

The ratio of the actual non-dimensional airflow passing through a nozzle to the ideal airflow at the same pressure ratio.

Nozzle Guide Vanes

A row of stator blades on a turbine, so called because they accelerate the air before entry to the rotor blades in the same way that a nozzle accelerates the gas leaving a gas turbine to produce a propulsive jet.

Nozzle Velocity Coefficient

The ratio of the actual non-dimensional thrust produced by a nozzle to the ideal thrust at the same pressure ratio and airflow.

Over-determined Matrix

A System Matrix with more rows than columns.

Power-Setting Parameter

A gas-path measurement (or a parameter derived from other measurements) that is used to define the power setting of a gas turbine.

Precision Error

See Repeatability.

Prior Information

Information available before an analysis is carried out.

Pseudo-Inverse

An 'inverse' of a non-square matrix, calculated as follows:

$$\underline{B}^{\#} = (\underline{B}^{T} \bullet \underline{B})^{-1} \bullet \underline{B}^{T} \text{ if } \underline{B} \text{ has more rows than columns}$$

$$\underline{B}^{\#} = \underline{B}^{T} \bullet (\underline{B} \bullet \underline{B}^{T})^{-1} \text{ if } \underline{B} \text{ has more columns than rows}$$

The above definitions satisfy the basic defining equations of the inverse:

$$\underline{B} \bullet \underline{B}^{\#} = \underline{B}^{\#} \bullet \underline{B} = \underline{I}$$

Random Error

See Repeatability

Recursive

An algorithm is said to be recursive if the calculations it carries out are dependent on the current input(s) and the results from immediately previous calculations only.

Rematching

The movement of gas turbine component operating points due to changes in component performance parameters.

Repeatability

A random component of measurement error caused by numerous small effects which cause disagreements between repeated measurements of the same quantity.

Scanivalve

A device that enables many pressures to be measured by the same transducer.

Sensitivity Analysis

The process of calculating how sensitive the Kalman Filter is to its inputs.

Slope Table

See Environmental Exchange Rate Table.

Smearing

The tendency of the Kalman Filter to calculate changes in all the component changes and sensor biasses being searched for, and thereby possibly under-estimating genuine changes.

Synthesis

The calculation of the performance of a gas turbine from knowledge of the performance of its individual components.

Systematic Error

See Bias.

System Matrix

A matrix relating changes of gas-path measurements (dependent variables) to changes in both component performance parameters and sensor biasses (independent variables).

Traditional Analysis

The analysis of a gas turbine by using the gas-path measurements to calculate both unmeasured gas-path parameters and component performance parameters directly.

Trend Estimate Gain

The value used to calculate the best estimate of trend in a noisy time series from an expected trend and the difference between the actual and predicted observation.

Under-determined Matrix

A System Matrix with more columns than rows.

CHAPTER 1: SUBJECT MATTER COVERED BY THIS THESIS

The Introduction briefly discusses the thermodynamic cycle of a gas turbine, and the calculation methods that enable the whole gas turbine to be modelled from knowledge of the performance characteristics of its individual components (synthesis). The inverse process, calculating gas turbine component performance parameters from gas-path measurements taken from it during testing or while it is in service (analysis) is introduced, and the difficulties of the 'traditional' approach of direct calculation without considering the influences of measurement error are discussed. An alternative view of the gas turbine performance analysis problem is presented, which leads to the use of an algorithm called the Kalman Filter. The Kalman Filter equations are introduced, and problems with the Kalman Filter approach, which are addressed in subsequent chapters of the thesis, are identified.

The chapter on Determination of Necessary Measurements lists the choices of component performance parameters to be analysed and the gas-path measurements that may be made available to do this, and discusses the generation of Exchange Rate Tables that show how changes in gas-path measurements relate to changes in component performance parameters. The calculation of possible correlations between pairs of measurements is presented, as a way of indicating whether there is redundancy in the gas-path measurement set. The possibility of sensor bias is then introduced, and the calculation of correlations between pairs of component changes and/or sensor biasses is presented, as a way of indicating whether the component changes and sensor biasses being sought can be separately identified. Observability theory is then introduced, as a way of looking for combinations of multiple component changes and/or sensor biasses that cannot be detected with the gas-path measurement set that is available. Finally, a simple method of testing the invertibility of Exchange Rate Tables is presented.

The chapter on Kalman Filtering Applied to Gas Turbine Analysis discusses the situation faced by the analyst, which is one of many more unknowns (component changes and sensor biasses) than knowns (gas-path measurements). The possible estimation methods to deal with this situation are discussed, which lead to the Kalman Filter. The Kalman Filter equations are then derived, and the meaning of the various terms discussed. The 'Concentrator' enhancement to the Kalman Filter, developed by the author to overcome the limitations of the Kalman Filter when analysing a small number of distinct changes, is then presented. The input to the Kalman Filter is then discussed, relating it to the considerations normally taken into account when 'traditional' analysis is carried out. A sensitivity analysis of the Kalman Filter equations to the various statistical inputs is then presented, followed by methods

of 'tuning' the Kalman Filter to optimise its ability to do the required analysis.

The chapter on Smoothing and Trending Using Kalman Filter Theory discusses the basic assumptions behind time-series analysis, and develops a set of equations, based on the Kalman Filter, that produce best estimates of the level and trend (rate of change) at each point in time in a noisy time series. Comparisons of the characteristics of this approach with more traditional methods of time series analysis such as Moving Average and Exponential Smoothing are made, followed by a description of a combination of this method of time-series analysis and the 'Concentrator' called Trend 'Concentration' that can be applied to sets of time series of gas-path measurements. Ways of 'tuning' the algorithm are discussed, and examples of its response to typical time series both with and without random noise added to the observations are presented.

The chapter on Examples shows the results from a number of demonstrations of the 'Concentrator', the Smoothing/ Trending Algorithm and Trend 'Concentration', using simulated gas turbine data. The universal applicability of the Smoothing/Trending Algorithm is demonstrated by using it to analyse fuel consumption figures gathered from the author's car.

The main body of the thesis concludes with a Discussion of what has been achieved, Conclusions and Recommendations for Further Work.

Appendix A discusses current gas turbine measurement practice at Rolls-Royce and 'traditional' analysis techniques in more detail.

Appendix B discusses the calculation of observability Eigenvalues and Eigenvectors.

Appendix C derives the sensor non-repeatability standard deviations used in the examples given throughout the thesis.

CHAPTER 2: INTRODUCTION

The gas turbine cycle is one of the most important ways of converting the chemical energy of a fuel into useful work. The basic theory behind it has been known for over a century; a diagram of a machine that implements it is shown in Figure 1.

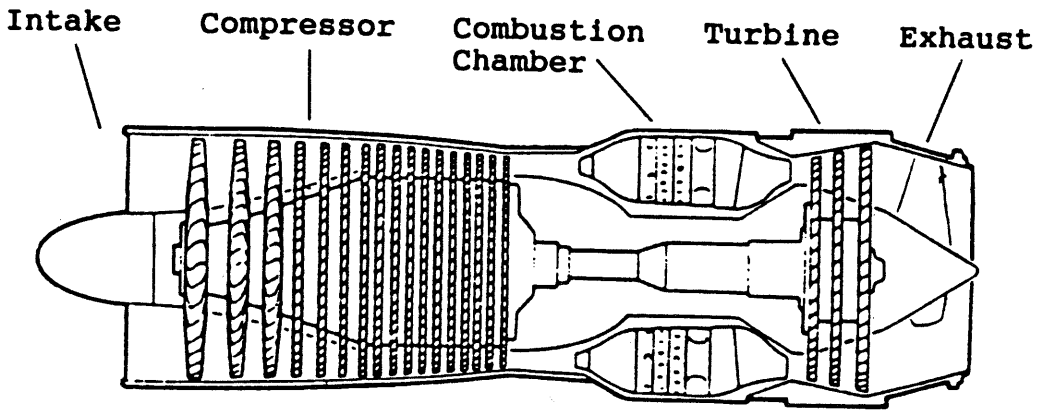

Figure 1: A single-spool axial flow turbojet: an example of a gas turbine engine (from Reference 1)

Air, the working fluid for the cycle, flows continuously from left to right in the diagram. The air first passes through an intake, then enters a compressor, which, as its name implies, compresses it to many times atmospheric pressure. Fuel is then introduced and burnt in a combustion chamber. The resulting mixture of air and combustion products is then expanded through a turbine, which extracts enough power to drive the compressor. Only part of the fuel energy is needed to drive the compressor: the rest appears as a stream of hot, high-pressure gas in the exhaust, which can be expanded through either a further turbine to extract shaft power from the gas or a nozzle which converts the pressure of the gas into a high-speed jet. The momentum of this jet is balanced (according to Newton's Third Law of Motion) by a force on the engine which can be used to propel a vehicle.

It was Whittle who first realised that a gas turbine producing such a jet would be an ideal device for aircraft propulsion, since it offered the prospect of compact, high power-to-weight ratio engines with the ability to produce useful propulsive force at much higher speeds and altitudes than are possible with piston engine/propeller combinations. His efforts, together with parallel efforts by Constant in Britain, von Ohain in Germany and others in America who were given access to Whittle's pioneering work, led to the necessary development of high-strength, high-temperature materials that made the gas turbine engine a practical reality and truly revolutionised aircraft performance. Further applications have rapidly

followed, with the result that the gas turbine is now the natural choice for gas pumping, electricity generation and ship propulsion in situations where compactness, light weight and quick starting and acceleration to demanded power are paramount.

Undoubtedly one of the main stimulants to the developments of thermodynamic modelling of the gas turbine has been the steady-flow nature of the cycle. Unlike a piston engine, in which a comparatively small quantity of gas is subject to intermittent compression, combustion and expansion, the flow through the gas turbine is continuous. At a steady operating condition, the pressures, temperatures and mass flow rates of the working fluid at the boundaries between the components of a gas turbine are constant: this contrasts with the piston engine in which, at a constant throttle position, the pressures and temperatures in the cylinders are fluctuating rapidly.

The steady-flow nature of the gas turbine cycle makes it much more amenable to accurate mathematical calculation than the piston engine cycle. The slide-rule methods that Whittle used to calculate the performance of his engines are, with comparatively small modifications, still in widespread use in today's computer age. Whittle has written in his description of the design and testing of the W2/500 engine that powered the Gloster Meteor jet fighter (Reference 2) that "On September 2, 1942 it was run up to full speed and the results plotted so exactly on the design curves that I was foolish enough to declare that 'jet engine design has become an exact science'". He recalled afterwards (Reference 3) that his engineers got a lot of pleasure quoting that back at him later when they ran into trouble!

2.1 Gas Turbine Modelling

The ease of calculation of gas turbine cycles has led to the development of many tools (such as the Rolls-Royce RRAP, Pratt and Whitney SOAPP and Cranfield TURBOMATCH systems) that model gas turbines using characteristics of the components that make them up. If the flow, pressure ratio and efficiency characteristics of the compressor and turbine are known, as well as the pressure loss characteristics of the intake, combustion chamber and exhaust and the temperature rise characteristics of the fuel used, then the performance of the whole engine (pressures, temperatures and flows at each component boundary, fuel flow rate, etc) can be calculated by finding operating points on each of the above characteristics that satisfy the laws of gas dynamics and laws of conservation of mass and energy for the whole gas turbine, expressed in ways such as:

Power absorbed by Compressor
= Power produced by Turbine

Mass flow out of Compressor - Cooling bleed flow
= Mass flow into Combustion Chamber

Mass flow into Combustion Chamber + fuel flow
= Mass flow out of Combustion Chamber

Enthalpy into Combustion Chamber + Fuel Enthalpy
= Enthalpy out of Combustion Chamber

If local Mach No = 1, then

$$\frac{\text{Mass flow} \bullet \sqrt{\text{Temperature}}}{\text{Area} \bullet \text{Pressure}} = \text{Constant}$$

Etc

This process, known as synthesis, has received a great deal of attention in the literature, and will not be discussed in any further detail here. However, the inverse process, analysis, (the calculation of component performance from pressures, temperatures, flows, etc measured on a complete gas turbine, using measurement and calculation methods discussed in Appendix A) has not received the attention it deserves, because it has been assumed to be a fairly trivial extension of synthesis, rather than an exercise with its own special problems and difficulties that are addressed in this thesis.

2.2 Facets of Gas Turbine Analysis

The objectives of synthesis are fairly clear; use component characteristics and thermodynamic relationships to build a mathematical model of a gas turbine from its parts. Analysis, on the other hand, can have different objectives depending on what the results will be used for. If, for instance, the analysis is being done to determine if a gas turbine is acceptable to the customer, then the calculations to determine its acceptability or otherwise will almost certainly be laid down in a contract specification. Depending on the skills and sophistication of the parties involved, this analysis may bear little relation to current thermodynamic understanding of the gas turbine in question.

Analysis of gas turbines undergoing performance development testing will have as its objective the detailed understanding of the behaviour of all the components. This understanding, and the methods used to achieve it, develops as analysis proceeds, and should not be constrained by contract specification niceties.

Condition monitoring of gas turbines in service requires an intermediate approach, in which fairly detailed and up-to-date analysis methods need to be agreed between the manufacturer and end user in order to achieve cost-effective maintenance.

Using one set of methods to achieve another set of objectives is usually a recipe for confusion and misunderstanding. The performance analysis methods developed in this thesis address firstly the detailed performance understanding requirement, but can also be applied to condition monitoring.

It should be noted that the gas turbine performance analyst is rarely asked to explain the absolute levels of overall and component performance that are calculated; usually, performance of gas turbines and components is expressed relative to some appropriate datum. For example, the statement that the specific fuel consumption (SFC) of the gas turbine he is analysing is 10 g/kNs is not nearly as useful as the statement that the SFC is 3% worse than expected: a stated compressor efficiency of 89% sounds quite good, until comparison with the results of a compressor test rig shows it to be 2% lower than design. Ultimately, the purpose of gas turbine analysis is to identify physical (hardware) faults in the engine, by looking at deviations in measurable parameters (such as fuel flow, rotor speeds, pressures, temperatures) from expectation. A very famous diagram produced by L A Urban of Hamilton Standard and reproduced as Figure 2 shows the various relationships in the analysis process: the analyst is working from right to left on this diagram, hoping to isolate the faults that moved the gas turbine from left to right.

2.3 Difficulties with the Analysis Process

Superficially, the analysis process as shown in Figure 2 looks easy; calculate appropriate component performance parameter deviations from gas-path measurement deviations relative to a datum, then use the results to guide the search for hardware faults. In practice, the analysis process is corrupted by errors in the measurements taken to determine how the gas turbine is behaving.

Errors can have serious effects on any analysis, because they result in incorrect component performance calculations which lead to misleading hardware fault diagnosis. Every experienced analyst can recall instances of measurement errors discovered when analysing gas turbines on-line that either prevented the test being terminated prematurely (due to incorrect calculation of critical gas-path parameters such as turbine entry temperature) or stopped a potentially worthless or dangerous test from proceeding (fuel leaks in altitude test plants, in which the gas turbine itself is sealed inside a test chamber and not visible by the test crew).

Failure to detect measurement errors can have serious financial consequences, as time and effort are spent searching (on the basis of flawed calculations) for non-existent faults in one part of the gas turbine while

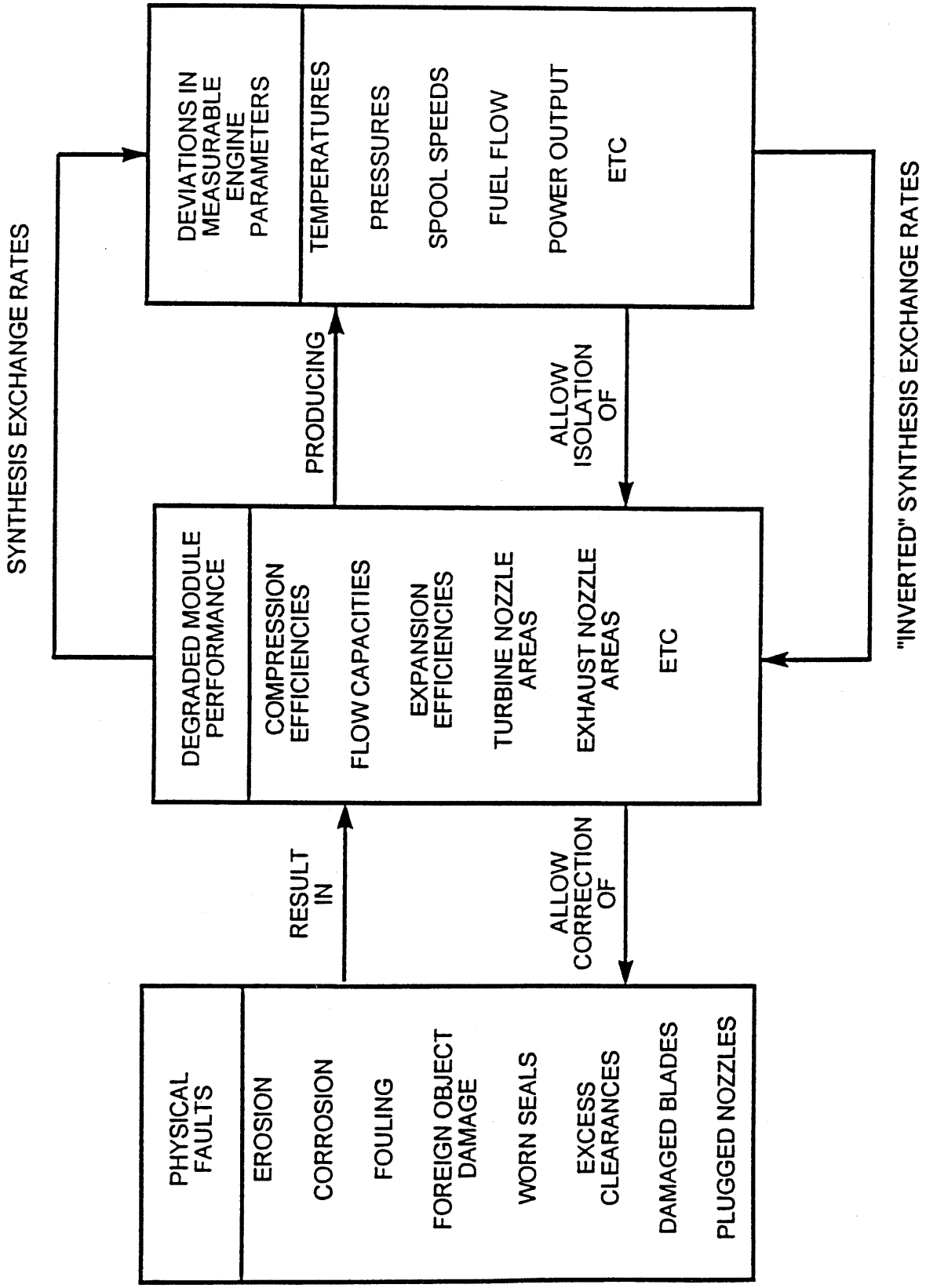

Figure 2: The Analysis Process (adapted from Reference 4)

genuine faults go undetected. Any analyst who ignores the possibility of corruption of his calculations by erroneous measurements is treading on dangerous ground, and is certain to run into problems: indeed, such individuals soon gain a reputation for recklessness bordering on irresponsibility.

The experienced performance analyst learns to look for characteristic 'signatures' of typical single measurement errors: these are usually recognised by calculation of better than expected performance of one or more components, accompanied by worse than expected performance on other components (so-called 'reciprocal changes'). However, when more than one error is present and/or genuine changes in components that make up error 'signatures' have happened, the task of finding errors becomes very much more difficult. It is not unusual for even the most experienced analyst to spend days or weeks trying to produce a credible assessment of overall and component behaviour when multiple errors are present: engineering judgement, trial and error calculations, patience and a certain amount of luck are all required if any sense is to be made of the results. The need to speed up an inefficient, time consuming and demoralising process is the main motivation behind the research that has been conducted.

2.4 The 'Traditional' Approach to Gas Turbine Analysis

The 'Traditional' analysis approach, covered in detail in Appendix A, can be summarised in four steps:

1) Use appropriate gas-path measurements to calculate component performance parameters (efficiencies and flow capacities of the turbomachinery, duct pressure losses, nozzle discharge and thrust coefficients, excess cooling and sealing bleed flows, etc), depending on what measurements are available;

2) Calculate the differences between the component performance parameter values worked out in 1) above and the datum values of those same parameters;

3) Calculate the differences between the observed gas-path measurement values and the datum values of the measurements;

4) Do a consistency check to see if the differences in component performance account for the differences in overall gas turbine performance.

The above method has the following drawbacks:

1) The required calculations may not be possible, due to missing measurements. For example, the calculation of compressor efficiency uses the formula:

$$\text{Compressor Efficiency} = \frac{(P_{out} \div P_{in})^{((\gamma-1)\div\gamma)} - 1}{(T_{out} \div T_{in}) - 1}$$

where P_{out} = outlet total pressure
P_{in} = inlet total pressure
T_{out} = outlet total temperature
T_{in} = inlet total temperature
γ = ratio of specific heats of air

Clearly, if any one or more of the required pressure and temperature measurements are missing, then the calculation is not possible;

2) The possibility of measurement errors is not considered, at least initially;

3) The consistency checks at the end of the analysis process do not directly indicate the presence of errors in the measurements, since the 'reciprocal changes' in component performance parameters discussed earlier will conspire to 'explain' all of the measurements;

4) The consistency checks also fail if the analyst omits to calculate some of the component performance parameters: often, nozzle performance is omitted from the calculation process, with the result that thrust accounting is misleading;

5) Rematching effects (in which the change of performance of the set of components causes movements of component working points along their characteristics that alter component performance expectations) are not explicitly accounted for. A classic example of this is compressor efficiency, which falls off as the flow through the compressor approaches the maximum possible. If the engine has been uprated, say, the airflows are high and the compressor efficiency is lower than its peak as a consequence. Poor performance of components will tend to reduce the airflow through the gas turbine, moving the compressor back towards peak efficiency (which may, of course, be lower than design intent). The situation often arises where the calculated efficiency is higher than datum, even though the basic characteristic is poorer than design: see Figure 3.

The experienced performance analyst is aware of the above pitfalls, and makes allowances for them in his calculations: however, as indicated earlier, the process is time-consuming and heavily dependent on skill and judgement.

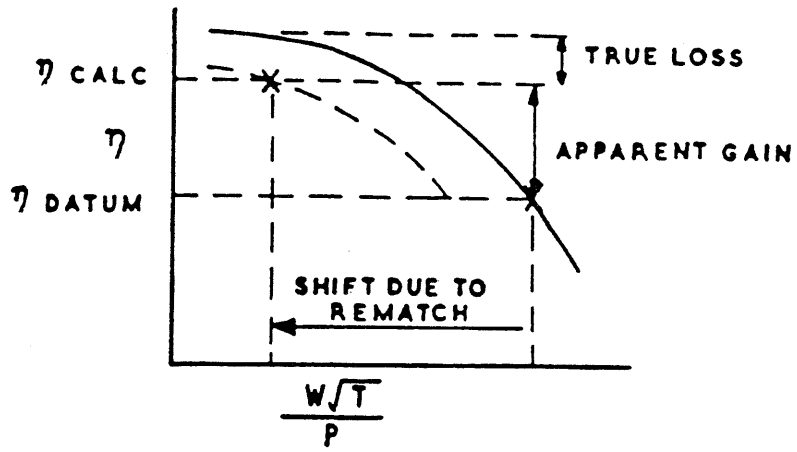

Figure 3: Apparent improvement of compressor performance due to rematching effects: the Greek symbol η represents efficiency, while $W\sqrt{T} \div P$ is the compressor airflow parameter

2.5 An Alternative Approach to Gas Turbine Analysis

An alternative approach recognises that the differences between observed and expected measurements from a gas turbine can be caused by up to four distinct causes:

1) Genuine component performance changes;

2) Biasses (shifts of calibration) of the measurements used to define the flight conditions and power setting of the gas turbine. These measurements essentially define the expected levels of the measurements added to the gas turbine for diagnostic purposes: if they are erroneous, then the expectations will also be wrong. Typically, if the power-setting parameter is measured high (say), then the diagnostic measurements will appear low, because the actual power is lower than measured. Similarly, if the measurement of flight condition pressure is high, then all the diagnostic pressures and other pressure-sensitive measurements will appear low, because the environmental air pressure is lower than measured, and if the measurement of flight condition temperature is high, then all the diagnostic temperatures and other temperature-sensitive measurements will appear low, because the environmental air temperature is lower than measured;

3) Biasses (shifts of calibration) in the measurements added to the gas turbine for diagnostic purposes: these affect each observed measurement shift independently;

4) Random scatter of all the measurements, both those used to define the flight condition and power setting of the gas turbine and those added for diagnostic purposes.

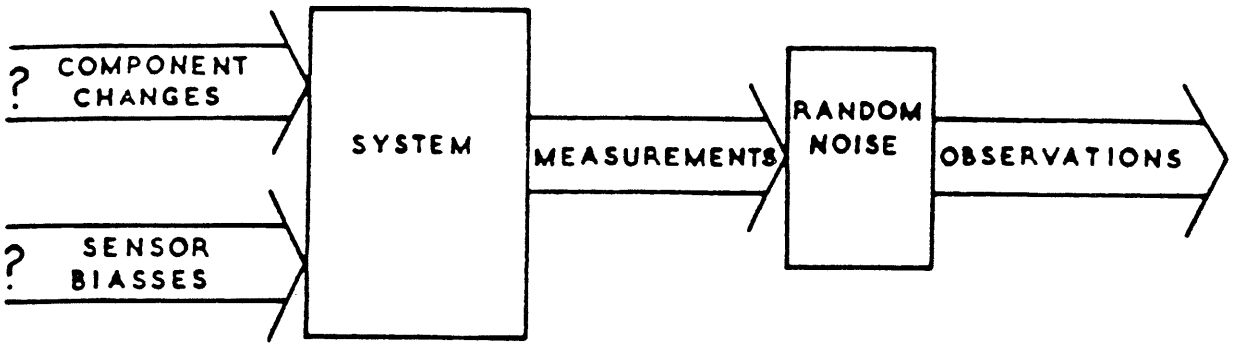

Figure 4: Diagrammatic representation of analysis situation

Figure 4 shows the above situation in diagrammatic form: unknown component changes and sensor biasses affect the 'system' of gas turbine thermodynamic relationships and measurement dynamics, resulting in a set of measurements which are then corrupted by random noise to produce a set of observed values. The analyst has to use these to diagnose component and sensor performance, and ultimately deduce which hardware problems are affecting both the gas turbine components and the measurement system.

The 'System' referred to above can be thought of as a matrix, shown diagrammatically in Figure 5.

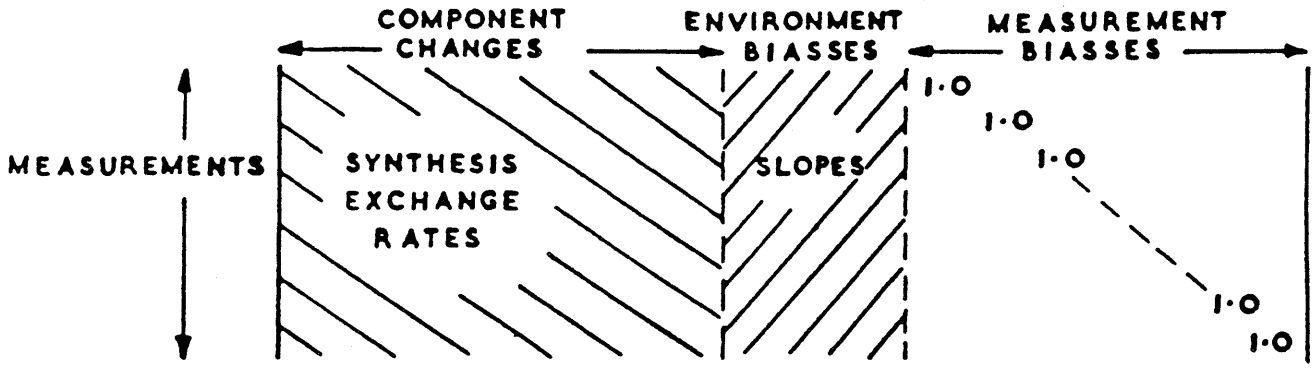

Figure 5: The System Matrix

In this matrix, the effects of component changes on the differences between the observed and expected measurements can be represented by a set of synthesis exchange rates: each column of exchange rates represents the effect of a 1% change in each of the component performance parameters in turn. Similarly, the effects of power-setting and flight condition measurement biasses (environment biasses) can be represented by a set of slopes, representing the

effects of 1% shifts in the power-setting and flight condition measurement calibrations on each of the diagnostic measurements. The final part of the matrix represents the effects of 1% shifts in each of the diagnostic measurement calibrations in turn: as indicated above, these effects are independent, so can be represented by a unit matrix of appropriate dimension. It is seen that a 1% shift in the n'th diagnostic measurement (say), would alter the n'th observed difference by 1%, leaving the others unaltered.

It is immediately obvious from the shape of the matrix represented in Figure 5 that there are many more unknowns (component changes and sensor biasses) than knowns (measurement differences from expectation). There are therefore an infinite number of solutions to the problem of diagnosing the component changes and sensor biasses that caused the observed measurement differences. Two of these solutions are apparent by inspection:

1) If the sensor bias columns are removed, leaving as many component changes to be diagnosed as there are measurement differences (the usual situation in most methods of 'traditional' analysis), then a unique solution for the set of component changes that produced the set of observed measurement differences can be found;

2) If the component change and environment bias columns are removed, leaving the unit matrix of diagnostic measurement bias effects, then this implies that all the measurement shifts are caused by measurement bias: the gas turbine component performance parameters are unchanged.

The true situation is usually somewhere between the two extremes outlined above: some component performance parameters have changed, while some measurements are biassed. The question the analyst is trying to answer is: which ones? Faced with an apparently infinite set of answers to this question, the situation looks hopeless.

2.6 Optimal Estimation and Kalman Filtering

The history of techniques that can address the above situation begins with (according to Reference 5) the work done by Gauss in 1795 to calculate comet and planetary motion from uncertain astronomical measurements using least-squares. The maximum likelihood methods of R A Fisher in 1912 also provided a stimulus, by giving some theoretical and probabilistic backing to the arithmetic of least-squares. Kolmogorov in 1941 and Weiner in 1942 independently developed a linear least-squares estimation technique which, while somewhat cumbersome, received considerable attention and laid the foundations for the subsequent developments in Kalman Filter Theory.

R E Kalman's first paper on discrete-time, recursive mean-square filtering in 1960 (Reference 6) was greeted with enthusiasm by both engineers and mathematicians alike because his general approach to the problem and his use of state-space techniques unified known results, and the recursive nature of the equations that now bear his name are ideally suited to computer implementation. His approach can also be related to the work of Bayes in the early 18th Century, since it (like the famous result in probability theory known as Bayes' Theorem) depends very heavily on prior (pre-observation) information which is then combined with observations to produce posterior (post-observation) estimates. Kalman's work produced an explosion of subsequent theoretical work, as well as inspiring engineers in such diverse fields as spacecraft navigation, missile guidance and control systems analysis to use this new theory to either proceed with problems initially thought intractable or improve the accuracy of existing control and navigation systems by calculation instead of expensive hardware improvements.

L A Urban and A J Volponi at Hamilton Standard (a division of United Technologies, who also own Pratt and Whitney aero-engines) began work on the use of Kalman Filtering in the analysis of gas turbines in the late 1970's (see References 4, 7 and 8). Their interest was mainly in the analysis of data from civil turbofans gathered in service for maintenance purposes, and their apparent success with the technique has resulted in similar initiatives from both General Electric (References 9 and 10) and Rolls-Royce (Reference 11) in the field of condition monitoring. Before discussing the problems of applying Kalman Filtering to gas turbine analysis (which the author believes have not been fully appreciated by Urban et al), it is instructive to review the Kalman Filter equations.

2.7 The Kalman Filter Equations

The Kalman Filter, in its full recursive form, consists of four equations:

$$1) \quad \underline{\hat{x}}_k = \underline{A} \bullet \underline{\hat{x}}_{k-1} + \underline{K} \bullet (\underline{Y}_k - \underline{C} \bullet \underline{A} \bullet \underline{\hat{x}}_{k-1})$$

$$2) \quad \underline{K} = \underline{P}' \bullet \underline{C}^T \bullet (\underline{C} \bullet \underline{P}' \bullet \underline{C}^T + \underline{R})^{-1}$$

$$3) \quad \underline{P}' = \underline{A} \bullet \underline{P}_{k-1} \bullet \underline{A}^T + \underline{Q}$$

$$4) \quad \underline{P}_k = (\underline{I} - \underline{K} \bullet \underline{C}) \bullet \underline{P}'$$

where:

$\underline{\hat{x}}$ = best estimate of system state vector: in the gas turbine analysis case, the best estimate of component changes and sensor biasses;

$\underline{Y}$ = vector of observations: in the gas turbine

analysis case, the set of measurement differences from expectation;

$\underline{C}$ = System Matrix: in the gas turbine analysis case, this is the matrix shown in Figure 5. Ideally:

$$\underline{y} = \underline{C} \bullet \underline{x};$$

$\underline{K}$ = Kalman Gain Matrix: the weighting matrix used to update state estimates from observations;

$\underline{Q}$ = system covariance matrix: the uncertainties in the system are assumed to be normally distributed, with mean $\underline{0}$ and covariance $\underline{Q}$;

$\underline{R}$ = measurement repeatability covariance matrix: the random errors in the measurements are assumed to be normally distributed, with mean $\underline{0}$ and covariance $\underline{R}$;

$\underline{A}$ = matrix defining how $\underline{x}$ varies over time: ideally

$$\underline{x}_k = \underline{A} \bullet \underline{x}_{k-1} ;$$

$\underline{P}'$= covariance update;

$\underline{P}$ = covariance matrix of $\hat{\underline{x}}$; the errors in the estimate $\hat{\underline{x}}$ are assumed to be normally distributed, with mean $\underline{0}$ and covariance $\underline{P}$;

$\underline{I}$ = unit matrix of appropriate dimension;

Subscripts k, k-1 denote current time and immediately previous time respectively;

Superscripts T, -1 denote matrix transpose and matrix inverse respectively.

If, however, a single 'snapshot' analysis of a gas turbine with no previous historical data from it is being done, a simplified non-recursive form of the Kalman Filter can be used, consisting of just three equations:

1) $\hat{\underline{x}} = \hat{\underline{x}}_0 + \underline{K} \bullet (\underline{y} - \underline{C} \bullet \hat{\underline{x}}_0)$

2) $\underline{K} = \underline{Q} \bullet \underline{C}^T \bullet (\underline{C} \bullet \underline{Q} \bullet \underline{C}^T + \underline{R})^{-1}$

3) $\underline{P} = (\underline{I} - \underline{K} \bullet \underline{C}) \bullet \underline{Q}$

where all the terms have the meanings given above. $\hat{\underline{x}}_0$ is the estimate of the system state before any measurements are taken, which in the gas turbine case is a zero vector if the datum set of component changes and sensor biasses corresponds to the datum set of measurements used to generate the measurement differences $\underline{y}$. This, of course,

then gives the final simplification of the first Kalman Filter equation:

$$1) \quad \hat{\underline{x}} = \underline{K} \bullet \underline{y}$$

The Kalman Gain Matrix $\underline{K}$ can be considered to be a form of 'inverse' of the System Matrix $\underline{C}$: $\underline{K}$ gives us state estimates from known observations, while $\underline{C}$ gives us observations from known states. In the limit, as the measurement repeatability covariance matrix $\underline{R}$ tends to zero, $\underline{K}$ tends to a true inverse of $\underline{C}$ if $\underline{C}$ is square (or a pseudo-inverse of $\underline{C}$ if $\underline{C}$ is either over- or under-determined) and the uncertainty in the estimate $\hat{\underline{x}}$ given by $\underline{P}$ also tends to zero. Conversely, if $\underline{R}$ becomes large compared to the system covariance matrix $\underline{Q}$, then $\underline{K}$ tends to zero and the measurements cease to influence the estimate $\hat{\underline{x}}$.

Various derivations of the Kalman Filter equations are widely available (References 12 to 20). The following points are worthy of note:

1) There are two basic forms for the Kalman Gain Matrix $\underline{K}$ in the literature:

$$\underline{K} = \underline{P}' \bullet \underline{C}^T \bullet (\underline{C} \bullet \underline{P}' \bullet \underline{C}^T + \underline{R})^{-1} \quad \text{(as above)}$$

$$= (\underline{P}'^{-1} + \underline{C}^T \bullet \underline{R}^{-1} \bullet \underline{C})^{-1} \bullet \underline{C}^T \bullet \underline{R}^{-1}$$

   The first form generally involves inversion of a matrix of smaller dimension than the second form, which is preferable for accuracy and speed reasons;

2) Whatever the starting points for the various derivations (linearity of system and/or normality of noise terms and/or simple least-squares), the same filter equations result.

While the Kalman Filter is obviously a very powerful tool that can be used in a huge variety of applications, it has several problems which should be considered.

2.8 Problems with the Kalman Filter

One problem of major practical importance when considering applying the Kalman Filter to gas turbine analysis is the fact that, given a set of measurement differences from a datum, it calculates changes in all the component changes and sensor biasses being considered in the problem, even when it is known that those measurement differences are due to a small subset of the component changes and sensor biasses being considered. This 'smearing' effect results from the least-squares basis of the filter, and can produce potentially misleading analyses by indicating that more hardware changes are present in the gas turbine than is actually the case. Under-estimation of magnitudes of

synthesised faults of 50% or more is possible: the analyst, faced with both under-estimated genuine faults and spurious indications of hardware changes that are not present, can rapidly lose confidence in the technique. Selecting the single 'biggest' change as being the only fault worth investigating is unsatisfactory, since it is perfectly possible for two or three faults (say one component change and one or two sensor biasses) to be present simultaneously, all of which require investigation. This thesis has developed a method to overcome this.

Another problem is ensuring that the inputs of the prior knowledge of the system to the Kalman Filter (represented by the System Matrix $\underline{C}$ and the covariance matrices $\underline{Q}$ and $\underline{R}$) are such that meaningful analyses will result. The appropriateness of the measurements used to determine the component changes and sensor biasses being sought needs to be assessed, and the elements in the system covariance matrix $\underline{Q}$ (which cannot normally be determined from engine data due to insufficient data) need to be optimised to achieve the desired analysis capability. These difficulties have also been addressed in this thesis.

2.9 Literature Search

Much of the work reported on performance analysis techniques has been carried out to satisfy the requirements of gas turbine condition monitoring. The objective of condition monitoring is to gather data periodically from sensors attached to gas turbines in service, then process it to produce information that can be used to optimise both the subsequent operation of the gas turbine and the maintenance, repair and overhaul actions that are performed on it, thus minimising the total life-cycle costs. Reference 21 shows that performance analysis is only one of a large number of techniques that can be used. Reference 22 gives a list of condition monitoring requirements for large civil turbofan engines, which includes gas-path analysis, a commonly-used term for gas turbine performance analysis in service. Such lists of requirements have been the key drivers behind the production of the MPA, ECM, TEAM, GEM, TEMPER and COMPASS condition monitoring systems developed by Pratt and Whitney, General Electric and Rolls-Royce and described in References 7 to 11. References 23 to 25 show typical results from in-service use of several of the above systems; however, while use of the Kalman Filter is mentioned, no details are given of the input supplied to make the filter work, other than the $\underline{y}$ vectors that, together with the $\underline{\hat{x}}$ output vectors, are the main interest of the users of the output. Some discussion of the problems seen in using the Kalman Filter for performance analysis is given in Reference 10; however, the proposed solution technique of focusing on the biggest component change or sensor bias and ignoring the others is

unsatisfactory for the reasons given above. Reference 26 also gives details of the performance analysis of a military aero-engine using a Kalman Filter; it appears to recognise the 'smearing' effect mentioned above as a problem, and attempts to reduce it by unspecified 'improvements' to the Kalman Filter inputs.

References 27 to 32 discuss implementations of Kalman Filters in aero-engine control systems, in order to provide information that can be used to optimise the control of engines in real time. References 29 to 32 focus on the detection of single large sensor biasses, which is acceptable over the very short time cycles of a gas turbine control system but not over the much longer time periods (hours or days) between data sets gathered for condition monitoring purposes, during which many changes in both components and sensor biasses could have occurred.

Some authors appear to advocate side-stepping the problems of the Kalman Filter discussed above by using expert systems to supplement or replace Kalman Filtering (References 33 and 34). However, expert systems only work when they are given clearly-defined rules based on experience; when rules are not available, such as during a gas turbine development programme or in the initial stages of service operation, expert system techniques cannot be used with any confidence.

None of the references studied appear to satisfactorily address the problems of determining sets of appropriate measurements needed to diagnose the component changes being sought (a problem touched on but not pursued fully in Reference 35), or of determining a suitable $\underline{Q}$ matrix to achieve the desired analysis capability. As mentioned above, methods to carry out these very important tasks are discussed in this thesis.

2.10 Extension of Kalman Filtering to Time Series Analysis

Smoothing and detecting underlying trends in time series data gathered from gas turbines is another important analysis technique. This thesis discusses an application of the Kalman Filter that can be used to perform this process, as well as a method of combining time series and 'snapshot' analysis techniques to reduce the sensitivity of the latter to sensor noise and improve the computational efficiency of the analysis of gas-path measurement time series.

CHAPTER 3: DETERMINATION OF NECESSARY MEASUREMENTS

This chapter discusses the work done to develop methods of determining the ability of different gas turbine measurement sets to provide the information needed to perform the required analysis of component changes from nominal and/or sensor biasses. This area seems to be neglected in the literature, but is one of the key requirements before any analysis, no matter how sophisticated, is attempted.

Before beginning an analysis, the performance analyst should first decide what hardware changes are to be looked for. Generally, the analysis is restricted to changes that affect the gas-path of the engine; also, because component thermodynamic performance can be affected in the same way by many different types and combinations of mechanical faults, actual hardware changes are re-expressed in terms of changes in component performance parameters, eg efficiency, flow capacity. For example, a typical list may read:

Turbine tip seal rubs	=>	turbine efficiency changes
Nozzle Guide Vane (NGV) platform seal gaps, blocked cooling holes	=>	turbine capacity or cooling bleed changes
Compressor blade tip erosion, dirt on compressor blades, foreign object damage	=>	compressor efficiency changes
Mis-shaped final nozzle	=>	nozzle discharge and velocity coefficient changes
Seal gap increases	=>	Cooling bleed changes
Customer air offtake pipe leaks	=>	Environmental Control System (ECS) bleed changes
etc.		

Hardware changes are thus transformed into component performance parameter changes. Typically, a full list of component performance parameter changes may read:

Fan Tip efficiency and capacity changes;

Fan Root/Booster efficiency and capacity changes;

Core compressor efficiency and capacity changes;

Turbine efficiency and capacity changes;

Combustion Chamber pressure loss changes;

Bypass Duct pressure loss changes;

Nozzle discharge and velocity coefficient changes;

Cooling/sealing bleed changes;

ECS bleed and power offtake changes.

All these changes will affect overall gas turbine performance parameters such as cruise Specific Fuel Consumption (SFC), take-off Turbine Entry Temperature (TET), compressor working line levels, etc. The purpose of analysis is to use measurements to resolve the causes of such overall performance parameter changes, by identification of the individual component performance parameter changes that caused them.

3.1 Determination of Possible Gas-Path Measurements

The performance analyst should then determine what gas-path measurements are available to diagnose component performance changes. The list will vary a great deal, depending on the engine being analysed. Production engines (particularly when installed in aircraft) will have a very limited set of measurements available (usually cockpit parameters only): development engines will have anything from a limited set tailored to the monitoring of endurance running to a full set of pressure/temperature rakes in many planes designed specifically for detailed component performance determination. Usually, the gas-path measurements that are available are:

Shaft rotational speeds;

Fuel flow;

Thrust (on the test-bed);

Total inlet airflow, derived from total and static pressure and total temperature measurements in the intake;

Total and/or static pressures in the engine gas-path, either single or multi-tapping;

Total and/or 'static' temperatures in the engine gas path, either single or multi-tapping; 'static' temperatures are wall-mounted transducers with calibration factors applied;

Shaft torque;

Power-setting parameter, eg Engine Pressure Ratio (EPR).

In addition, measurements defining the flight conditions

(air inlet conditions and forward speed) must be available, eg altitude, Mach number, total air inlet temperature (flight), cell static pressure and air intake total temperature (test-bed), wet and dry bulb temperatures (for humidity determination). This set of measurements (with the possible, but not desirable, omission of humidity-related measurements), plus one measurement from the above gas-path measurement list (eg thrust, shaft speed, EPR) must always be available before any form of analysis can proceed, because they define the basic conditions in which the gas turbine is operating: in effect, they are needed to define a 'datum' against which any subsequent analysis can be compared.

Note that the gas-path measurement list does not include derived parameters such as core airflow, TET and SFC, which are sometimes thought of as 'measurements'. This is because these parameters are calculated from other gas-path measurements, and therefore do not contain any extra information about the gas turbine over and above that provided by the measurements used in their derivation.

3.2 Generation of Exchange Rate Tables

Having generated two lists, one containing possible component performance parameter changes and the other containing available measurements, the performance analyst then has to generate an Exchange Rate Table showing the percentage change in each gas-path measurement for a 1% change in each component performance parameter (or unit change if the datum value is zero) in turn, at the flight conditions and power level at which the analysis is to be done. Note that, by tradition, parameters normally thought of in terms of percentages (eg efficiency, cooling bleed flow) have their exchange rates calculated by adding 1% (eg 88% => 89%; 3% => 4%), while other parameters (eg flow capacity) have their exchange rates calculated by factoring by 1.01 (eg 1000 => 1010). Figure 6 shows the typical output from such a set of calculations done on a typical two-shaft turbofan engine synthesis using the Rolls-Royce RRAP system; a sketch of the engine configuration is shown in Figure 7.

If sensor bias determination is to be included in the analysis, it is also necessary to determine the effect of 1% biasses in flight condition and power-setting parameter measurements, all of which are fixed when the above exchange rate table is generated. This is done by changing the flight condition parameters and the power setting parameter by -1%, and calculating the resulting percentage changes in the gas-path measurements. The presence of the negative sign is to account for the fact that, if the power setting parameter (say) is read high (ie a positive bias), all the gas-path measurements will appear to read low. Figure 6 also shows these exchange rates.

SMALL CHANGE MATRIX
COEFFICIENTS BASED ON PERCENTAGE STEPS ARE PRINTED BELOW FOR 1% STEPS.
STEP TYPE : '*' - % FACTOR , ' ' - % DELTA , '+/-' - ABSOLUTE DELTA.

BASE PARAMETERS :-
ALT 0.0 XM 0.0 EPR 1.300

INDEPENDENT PARAMETERS NAME	DATUM		STEP	WFE 6891.496	P26 22.914	T26 334.038	P3 359.878	T3 792.131	T49 804.896	P13 21.477	XNL 4574.059	XNH 13712.281	FN 20371.078
FAN ETA	0.0		0.02	-0.289	0.022	0.000	-0.187	-0.061	-0.060	0.156	-0.043	-0.053	0.390
FAN CAP	1.000	*	0.02	0.059	-0.406	-0.121	-0.008	0.005	0.066	-0.014	-0.341	0.045	-0.021
LPC ETA	0.005		0.02	-0.168	0.330	-0.038	0.013	-0.128	-0.198	-0.006	-0.014	-0.100	-0.013
LPC CAP	1.000	*	0.02	-0.080	0.310	0.073	0.034	-0.014	-0.084	-0.026	-0.043	-0.033	-0.069
HPC ETA	0.004		0.02	-1.051	-0.432	-0.097	0.252	-0.582	-1.261	-0.045	-0.046	0.125	-0.100
HPC CAP	1.000	*	0.02	0.128	0.050	0.011	-0.058	0.023	0.153	0.006	0.006	-0.212	0.013
HPT ETA	-0.023		0.02	-1.393	-0.576	-0.130	0.563	0.195	-1.665	-0.065	-0.065	0.373	-0.138
HPT CAP	23.756	*	0.02	0.160	0.067	0.015	-1.033	-0.335	0.202	0.007	0.007	-0.152	0.017
LPT ETA	-0.013		0.02	-0.177	0.388	0.114	-0.064	-0.027	-0.432	0.235	0.305	-0.060	0.589
LPT CAP	147.390	*	0.02	-0.458	-0.455	-0.118	0.254	0.090	-0.425	-0.162	-0.201	0.181	-0.395
EPR	1.300	*	0.02	-3.605	-0.760	-0.286	-2.608	-0.776	-0.726	-1.065	-1.255	-0.576	-3.249
P2	0.0	*	0.02	-0.993	-1.002	-0.001	-0.998	0.005	0.012	-1.004	-0.006	0.003	-1.011
T2	0.0	*	0.02	-0.572	0.031	-0.989	0.013	-0.923	-0.952	0.012	-0.486	-0.502	0.036

INDEPENDENT PARAMETERS NAME	DATUM		STEP	W1A 759.925
FAN ETA	0.0		0.02	0.286
FAN CAP	1.000	*	0.02	-0.020
LPC ETA	0.005		0.02	0.008
LPC CAP	1.000	*	0.02	-0.036
HPC ETA	0.004		0.02	0.040
HPC CAP	1.000	*	0.02	-0.005
HPT ETA	-0.023		0.02	0.051
HPT CAP	23.756	*	0.02	-0.006
LPT ETA	-0.013		0.02	0.368
LPT CAP	147.390	*	0.02	-0.194
EPR	1.300	*	0.02	-1.596
P2	0.0	*	0.02	-1.008
T2	0.0	*	0.02	0.527

KEY

WFE	Fuel Flow	EPR	Engine Pressure Ratio (power-setting parameter)
P26	HP Compressor Entry Pressure		
T26	HP Compressor Entry Temperature	P2	Engine Inlet Pressure
P3	HP Compressor Exit Pressure	T2	Engine Inlet Temperature
T3	HP Compressor Exit Temperature		
T49	LP Turbine Exit Temperature	NB	Note sign change of EPR, P2, T2 rows (-1% changes)
P13	Fan Exit Pressure		
XNL	LP Shaft Speed		
XNH	HP Shaft Speed		
FN	Net Thrust		
W1A	Total Inlet Airflow		
ETA	Efficiency		
CAP	Flow Capacity		

Figure 6: Exchange Rate Table for typical two-shaft turbofan

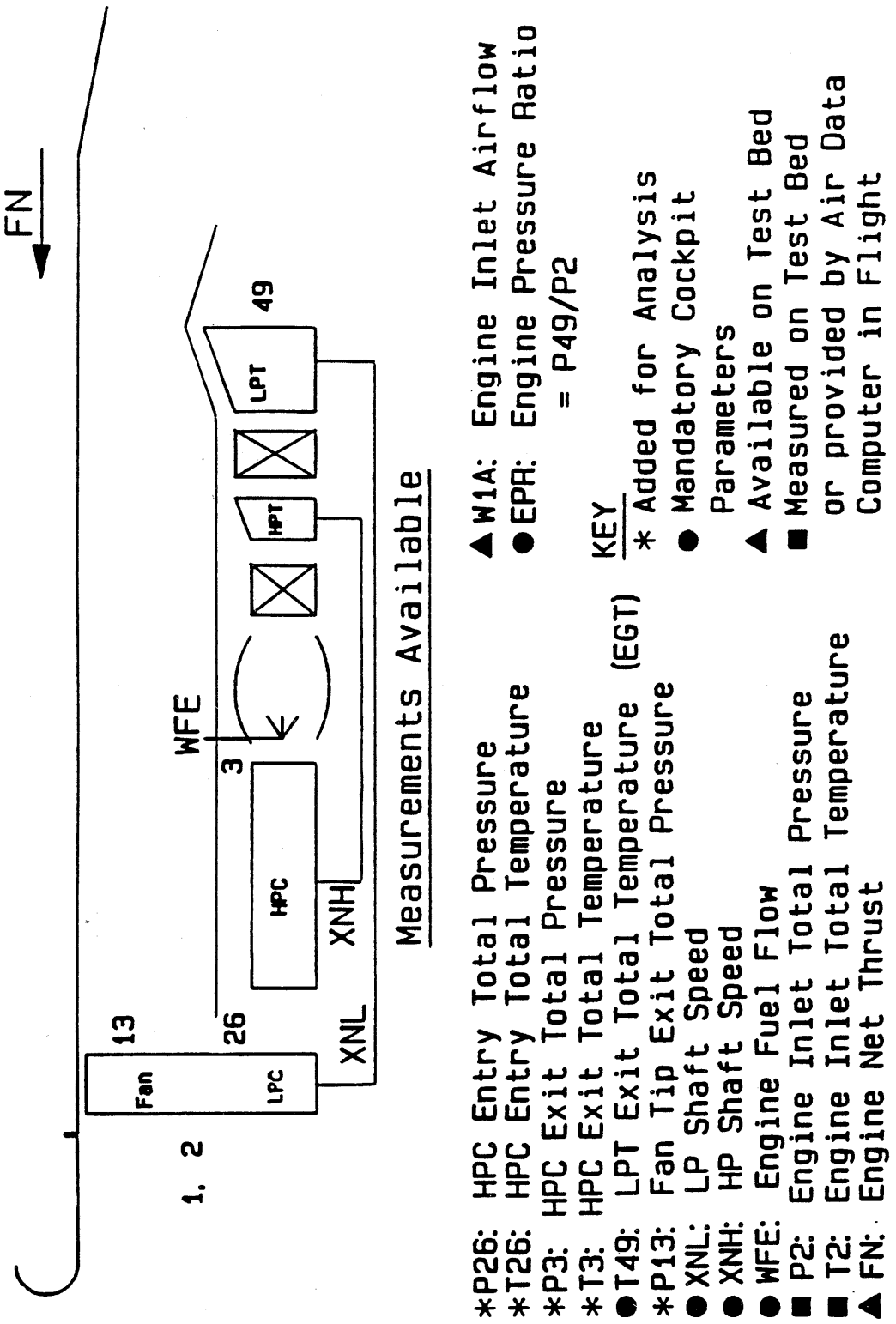

Figure 7: Typical two-shaft turbofan configuration

Figure 8 shows two tables generated from the above processes; note that:

1) the single table in Figure 6 has been split into two, one showing the effects of component changes on the measurements (the Component Exchange Rate Table) and the other showing the effects of environmental and power-setting parameter measurement biasses on the measurements (the Environmental Exchange Rate or Slope Table);

2) The tables have been transposed, since an accident of history in the Rolls-Royce presentation of such tables makes their format incompatible with the subsequent matrix algebra!

3.3 Correlations Between Measurements

The first thing that should be checked is whether any of the gas-path measurements chosen respond in similar ways to other measurements to all (or nearly all) of the component changes. This test indicates whether there is any redundancy between the measurements. This may be beneficial if the measurements are present for reasons other than performance analysis, but may be an indication of over-specification of required measurements if the analyst is trying to determine an optimum set of measurements for analysis in the future. An example of each situation is:

1) Fuel flow and Exhaust Gas Temperature (EGT) (both mandatory cockpit measurements) may respond in similar ways to the component changes being sought. Since these measurements are mandatory, no action would be taken to remove one of them for cost reasons;

2) HP Compressor entry pressure and HP Compressor entry temperature may respond in similar ways to the component changes being sought. Since these measurements may be present purely for performance analysis, deletion of one of them may be considered if the cost of providing such instruments is high.

Note, however, that with a small number of gas-path measurements, the presence of redundancy between the measurements may indicate that there is insufficient information to do the required analysis, because the measurement set is so small that all the component changes are indistinguishable.

The method of checking whether the chosen gas-path measurements respond in similar ways to the component changes being sought is a general one, which can best be understood by imagining a multi-dimensional 'Component Change Space' coordinate system in which each component is represented by an axis which is perpendicular to all the

Figure 8: Component and Environment Exchange Rates

** EXCHANGE RATE TABLES: ACTIVE COMPONENT CHANGES & MEASUREMENT BIASSES STARRED; ROWS FOR ABSENT MEASUREMENTS NOT PRINTED **

** TABLE DETAILS: SEA LEVEL STATIC ISA CORRECTED DATA EXCHANGE RATES AT 1.3 EPR **

** COMPONENT EXCHANGE RATES **

		FAN ETA	FAN CAP	LPC ETA	LPC CAP	HPC ETA	HPC CAP	HPT ETA	HPT CAP	LPT ETA
		*	*	*	*	*	*	*	*	*
		*	*	*	*	*	*	*	*	*
WFE	**	-0.2890	0.0590	-0.1680	-0.0800	-1.0510	0.1280	-1.3930	0.1600	-0.1770
P26	**	0.0220	-0.4060	0.3300	0.3100	-0.4320	0.0500	-0.5760	0.0670	0.3880
T26	**	0.0	-0.1210	-0.0380	0.0730	-0.0970	0.0110	-0.1300	0.0150	0.1140
P3	**	-0.1870	-0.0080	0.0130	0.0340	0.2520	-0.0580	0.5630	-1.0330	-0.0640
T3	**	-0.0610	0.0050	-0.1280	-0.0140	-0.5820	0.0230	0.1950	-0.3350	-0.0270
T49	**	-0.0600	0.0660	-0.1980	-0.0840	-1.2610	0.1530	-1.6650	0.2020	-0.4320
P13	**	0.1560	-0.0140	-0.0060	-0.0260	-0.0450	0.0060	-0.0650	0.0070	0.2350
XNL	**	-0.0430	-0.3410	-0.0140	-0.0430	-0.0460	0.0060	-0.0650	0.0070	0.3050
XNH	**	-0.0530	0.0450	-0.1000	-0.0330	0.1250	-0.2120	0.3730	-0.1520	-0.0600
FN	**	0.3900	-0.0210	-0.0130	-0.0690	-0.1000	0.0130	-0.1380	0.0170	0.5890
W1A	**	0.2860	-0.0200	0.0080	-0.0360	0.0400	-0.0050	0.0510	-0.0060	0.3680

		LPT CAP
		*
		*
WFE	**	-0.4580
P26	**	-0.4550
T26	**	-0.1180
P3	**	0.2540
T3	**	0.0900
T49	**	-0.4250
P13	**	-0.1620
XNL	**	-0.2010
XNH	**	0.1810
FN	**	-0.3950
W1A	**	-0.1940

** ENVIRONMENT EXCHANGE RATES **

		EPR	P2	T2
		*	*	*
		*	*	*
WFE	**	-3.6050	-0.9930	-0.5720
P26	**	-0.7600	-1.0020	0.0310
T26	**	-0.2860	-0.0010	-0.9890
P3	**	-2.6080	-0.9980	0.0130
T3	**	-0.7760	0.0050	-0.9230
T49	**	-0.7260	0.0120	-0.9520
P13	**	-1.0650	-1.0040	0.0120
XNL	**	-1.2550	-0.0060	-0.4860
XNH	**	-0.5760	0.0030	-0.5020
FN	**	-3.2490	-1.0110	0.0360
W1A	**	-1.5960	-1.0080	0.5270

other component axes. While human experience is limited to three dimensions, matrix algebra recognises no such limitations, so the above 'Component Change Space' coordinate system is quite valid, even if more than three component changes are considered. Examples given here will, of course, be limited to two dimensions; it is hoped that the reader will be able to grasp the concepts, even if imagining a 10-dimensional space can be a little difficult!

The 'Component Change Space' described above will contain measurement vectors for each gas-path measurement being considered; the coordinates of the end-points of the vectors will be defined by the elements in each gas-path measurement row; see Figure 9.

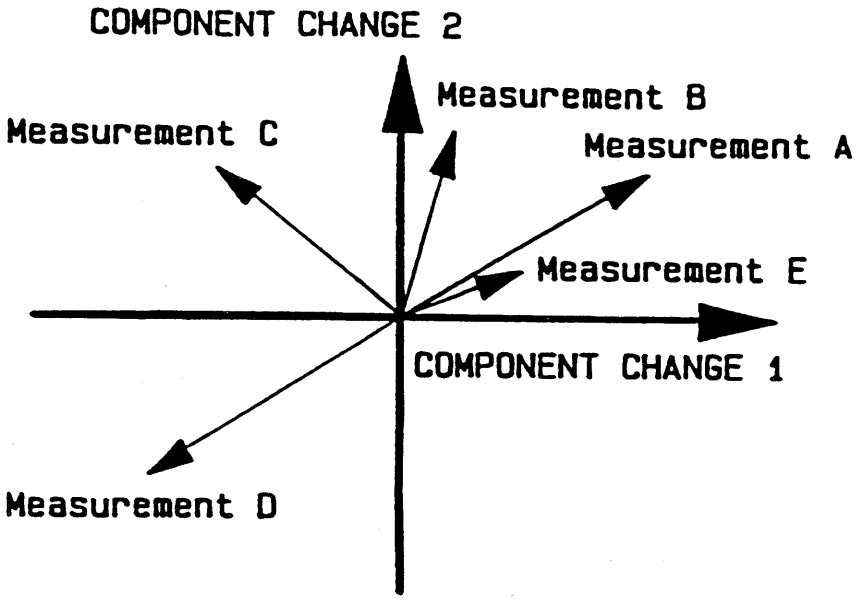

Figure 9: Two-dimensional 'Component Change Space'; five measurement vectors

Some of the measurement vectors will be nearly parallel to others; eg in Figure 9, Measurement Vectors A, D and E are nearly parallel (the fact that D 'points' in the opposite direction does not affect the argument), whereas Measurement Vectors B and C are not, either with each other or with A, D and E. Parallel measurement vectors indicate similar response by the measurements to the component changes; eg in Figure 9, it will be difficult to distinguish Component Change 1 from Component Change 2 using only Measurements A, D and E.

It is obvious that the direction, not the length, of the vectors is important, and that we should evaluate the angles between pairs of vectors to see if they are nearly parallel or not.

This is done as follows:

1) Divide each element in each row of the Component Exchange Rate Table by the square root of the sum of squares of the elements in that row; this normalises the rows defining the measurement vectors by converting them to unit length;

2) Multiply this matrix by its transpose; this effectively works out the dot product of every pair of normalised measurement vectors, which produces the cosine of the angle between them;

3) The resulting symmetric matrix of cosines can then be inspected for possible correlations between the measurements, ie measurements which respond in similar ways to the component changes being sought. The values will vary between +1 and -1 with:

   +1 indicating perfect positive correlation; the pair of measurements change in the same direction, but not necessarily by the same amount, for all the component changes being sought;

   0 indicating no correlation; the pair of measurements do not respond in the same way;

   -1 indicating perfect negative correlation; the pair of measurements change in the opposite direction, but not necessarily by opposite amounts, for all the component changes being sought.

Cosines with magnitudes greater than 0.7 are worthy of note; levels above this value may indicate that the pair of measurements only respond differently to a small sub-set of the component changes. The following simple classifications can therefore be made:

1) 0.7 => 0.8 indicates some correlation;

2) 0.8 => 0.9 indicates a high degree of correlation;

3) 0.9 => 1.0 indicates a very high degree of correlation; the measurements are effectively redundant.

Figure 10 shows the results of the above calculations for the Component Exchange Rate Table in Figure 8.

Correlations of interest include:

1) Fuel Flow (WFE) and LP Turbine exit total temperature (T49), which are both measures of the energy going into the core of the gas turbine;

2) Fan Tip exit total pressure (P13), net thrust (FN) and total inlet airflow (W1A), which are all measures of LP

```
** MEASUREMENT CORRELATION MATRIX (COMPONENTS ONLY) **

** SINCE MATRIX IS SYMMETRIC, ONLY LOWER TRIANGULAR ELEMENTS ARE PRINTED **

          WFE      P26      T26       P3       T3      T49      P13      XNL      XNH

WFE    1.0000
P26    0.6265   1.0000
T26    0.6176   0.8986   1.0000
P3    -0.5517  -0.4524  -0.4335   1.0000
T3     0.2194   0.0204   0.0805   0.3803   1.0000
T49    0.9852   0.5806   0.5602   0.5635   0.2201   1.0000
P13    0.2074   0.5888   0.6399   0.3379  -0.0746   0.1725   1.0000
XNL    0.1868   0.6787   0.7894   0.1843  -0.0303   0.0968   0.6409   1.0000
XNH   -0.7568  -0.7799  -0.6787  -0.7150  -0.2135  -0.7482  -0.4711  -0.3637   1.0000
FN     0.1764   0.5637   0.6146   0.3229  -0.0783   0.1412   0.9993   0.6288  -0.4457
H1A   -0.1826   0.3317   0.3838   0.1287  -0.1547  -0.2053   0.9230   0.5451  -0.1750

          FN      H1A

FN     1.0000
H1A    0.9346   1.0000

** MATRIX ANALYSIS **

** WARNING ** WFE     AND T49    VERY HIGHLY CORRELATED;  FACTOR=   0.9852
** WARNING ** WFE     AND XNH    CORRELATED;              FACTOR=  -0.7568
** WARNING ** P26     AND T26    HIGHLY CORRELATED;       FACTOR=   0.8986
** WARNING ** P26     AND XNH    CORRELATED;              FACTOR=  -0.7799
** WARNING ** T26     AND XNL    CORRELATED;              FACTOR=   0.7894
** WARNING ** P3      AND XNH    CORRELATED;              FACTOR=   0.7150
** WARNING ** T49     AND XNH    CORRELATED;              FACTOR=  -0.7482
** WARNING ** P13     AND FN     VERY HIGHLY CORRELATED;  FACTOR=   0.9993
** WARNING ** P13     AND H1A    VERY HIGHLY CORRELATED;  FACTOR=   0.9230
** WARNING ** FN      AND H1A    VERY HIGHLY CORRELATED;  FACTOR=   0.9346
```

Figure 10: Measurement Correlation Matrix (Components only)

system output;

3) the negative correlation of HP shaft speed (XNH) with WFE and T49, reflecting the fact that, as component efficiencies go down (which would raise WFE and T49), the core airflow is reduced, reducing XNH.

3.4 Inclusion of Sensor Bias

The effects of the inclusion of sensor bias in the analysis on the correlation between measurements can be done in a similar manner to that described above; however, a matrix that includes the effects of sensor bias must first be created.

An analysis that includes the effects of sensor bias is looking for three distinct sets of items:

1) Component changes;

2) Environmental (flight condition and power level) sensor biasses;

3) Gas-path measurement sensor biasses.

The information about the way that the gas-path measurements change when the above-mentioned component changes and sensor biasses occur is given by:

1) The Component Exchange Rate Table;

2) The Environmental Exchange Rate Table (Slope Table);

3) An identity matrix, which merely states that a 1% sensor bias in a gas-path measurement produces a change of 1% in that measurement, while leaving the other measurements unaffected.

A combined matrix, subsequently called the System Matrix, is created by concatenating the columns of the Environmental Exchange Rate Table and the identity matrix to the end of the Component Exchange Rate Table to extend it: Figure 11 shows the process diagrammatically. Note that, if some gas-path sensor biasses are not considered possible (eg speeds), then the appropriate columns are removed from the identity matrix at the end of the System Matrix.

Having done this, the System Matrix can be analysed in exactly the same way as the Component Exchange Rate Table was previously to determine which pairs of measurements respond in a similar manner to both component changes and sensor biasses. Generally, there will be fewer correlations, due to the diagonal nature of the identity matrix. Figure 12 shows the results of the above calculations for the System Matrix made up of the tables

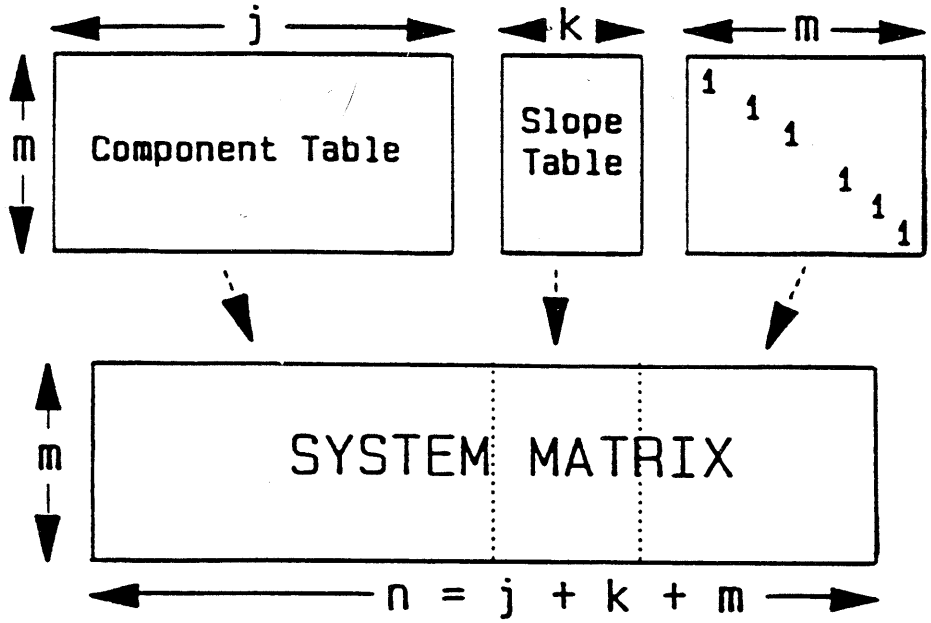

Figure 11: Generation of System Matrix, showing dimensions

in Figure 8. Note that the correlations printed out follow from the large changes in these measurements with EPR and P2 (inlet total pressure) biasses.

3.5 Correlations Between Component Changes and/or Sensor Biasses

The next thing the performance analyst needs to check is whether any of the component changes and/or sensor biasses produce similar changes to any other change or bias in all (or nearly all) of the gas-path measurements. This test indicates whether any component changes or sensor biasses cannot be distinguished from one another, which may be unacceptable. Classic cases of such situations are:

1) HP Compressor efficiency changes and HP Turbine efficiency changes cannot be distinguished from one another if HP Compressor delivery temperature is unavailable;

2) Generally, HP Turbine capacity changes, cooling bleed changes and HP Compressor delivery pressure sensor biasses cannot be distinguished from one another.

The method of checking whether component changes and sensor biasses are distinguishable from each other is similar to the methods for checking measurement redundancy. A multi-dimensional 'Measurement Space' coordinate system, in which each measurement is represented by an axis which is perpendicular to all the other measurement axes, is considered, which contains component/bias vectors for each component change and

** MEASUREMENT CORRELATION MATRIX (WHOLE SYSTEM) **

** SINCE MATRIX IS SYMMETRIC, ONLY LOWER TRIANGULAR ELEMENTS ARE PRINTED **

	WFE	P26	T26	P3	T3	T49	P13	XNL	XNH
WFE	1.0000								
P26	0.5918	1.0000							
T26	0.3021	0.1619	1.0000						
P3	0.6535	0.3730	0.1246	1.0000					
T3	0.4839	0.1696	0.4567	0.4233	1.0000				
T49	0.6142	0.3674	0.3771	0.0370	0.3850	1.0000			
P13	0.6346	0.5766	0.1338	0.6266	0.2547	0.1802	1.0000		
XNL	0.6568	0.3881	0.3709	0.5596	0.4671	0.3135	0.4575	1.0000	
XNH	0.2749	-0.0145	0.2830	0.4469	0.4216	0.0087	0.2119	0.3639	1.0000
FN	0.8220	0.5617	0.1943	0.7805	0.3879	0.2615	0.7234	0.6786	0.3335
H1A	0.6419	0.5491	-0.0030	0.7008	0.1772	0.0679	0.7058	0.4787	0.1964

	FN	H1A
FN	1.0000	
H1A	0.8046	1.0000

** MATRIX ANALYSIS **

** WARNING ** WFE	AND FN	HIGHLY CORRELATED;	FACTOR=	0.8220
** WARNING ** P3	AND FN	CORRELATED;	FACTOR=	0.7805
** WARNING ** P3	AND H1A	CORRELATED;	FACTOR=	0.7008
** WARNING ** P13	AND FN	CORRELATED;	FACTOR=	0.7234
** WARNING ** P13	AND H1A	CORRELATED;	FACTOR=	0.7058
** WARNING ** FN	AND H1A	HIGHLY CORRELATED;	FACTOR=	0.8046

Figure 12: Measurement Correlation Matrix (Whole System)

sensor bias being considered. The co-ordinates of the end-points of the vectors will be defined by the elements in each component change or sensor bias column in the System Matrix; see Figure 13.

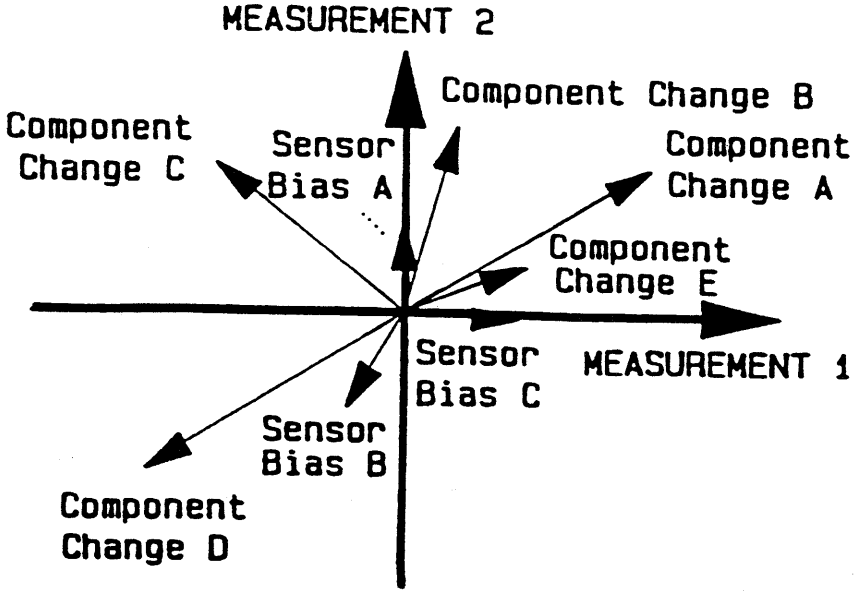

Figure 13: Two-dimensional 'Measurement Space'; five component change vectors and three sensor bias vectors

Some of the component change or sensor bias vectors will be nearly parallel to others; eg, in Figure 13, Component Change Vectors A, D and E and Sensor Bias Vector B are nearly parallel (the fact that D 'points' in the opposite direction does not affect the argument), whereas the others are not, either with each other or the group stated above. Parallel component change and/or sensor bias vectors indicate that they have similar effects on the measurements; eg in Figure 13, it will be difficult to distinguish 2% changes in Component E or -1% changes in Component D from 1% changes in Component A. As before, the direction, not the length, of the vectors is important; again, we need to evaluate the angles between pairs of vectors to see if they are nearly parallel or not.

This is done as follows:

1) Divide each element in each column of the System Matrix by the square root of the sum of squares of the elements in that column; this normalises the columns defining the component change and sensor bias vectors by converting them to unit length;

2) Multiply the transpose of this matrix by the matrix; this effectively works out the dot product of every pair of normalised component change and sensor bias vectors, which produces the cosine of the angle between

them;

3) The resulting symmetric matrix of cosines can then be inspected for possible correlations between component changes and sensor biasses, ie component changes and/or sensor biasses that will be difficult to distinguish from one another. Again, all the values will vary between +1 and -1 with:

   +1 indicating perfect positive correlation; the pair of component changes or sensor biasses affect the measurements in the same sense, and are therefore indistinguishable;

   0 indicating no correlation; the pair of component changes or sensor biasses are distinguishable;

   -1 indicating perfect negative correlation; the pair of component changes or sensor biasses affect the measurements in exactly the opposite sense, and are therefore indistinguishable.

Again, cosines with magnitudes greater than 0.7 are worthy of note; levels above this value may indicate that the pair of component changes and/or sensor biasses affect most of the measurements in the same way. As before:

1) 0.7 => 0.8 indicates some correlation;

2) 0.8 => 0.9 indicates a high degree of correlation;

3) 0.9 => 1.0 indicates a very high degree of correlation, the component changes and/or sensor biasses are effectively indistinguishable.

Figure 14 shows the results of the above calculations for the System Matrix made up of the tables in Figure 8. Correlations of interest include:

1) HP Compressor and HP Turbine efficiencies, which, as inspection of Figure 8 will verify, affect all measurements except HP Compressor exit total temperature (T3) in a similar way;

2) HP Turbine capacity and HP Compressor exit total pressure (P3) bias, which are difficult to distinguish because P3 is by far the largest measurement change when this turbine capacity changes (see Figure 8);

3) Fan Tip and LP Turbine efficiencies, which are difficult to distinguish because of the lack of temperature measurements in the bypass duct and the absence of LP Turbine inlet temperature measurements;

4) Fan Root/Booster (LPC) efficiency and capacity, and HP Compressor entry total pressure (P26) bias, reflecting

```
** SYSTEM CORRELATION MATRIX **

** SINCE MATRIX IS SYMMETRIC, ONLY LOWER TRIANGULAR ELEMENTS ARE PRINTED **

              FAN ETA     FAN CAP     LPC ETA     LPC CAP     HPC ETA     HPC CAP     HPT ETA     HPT CAP     LPT ETA
FAN ETA       1.0000
FAN CAP      -0.0943      1.0000
LPC ETA       0.2666     -0.6090      1.0000
LPC CAP      -0.0370     -0.6594      0.8501      1.0000
HPC ETA       0.2885      0.0596      0.4305      0.1885      1.0000
HPC CAP      -0.1064     -0.0910     -0.1354     -0.0300     -0.7373      1.0000
HPT ETA       0.2077      0.0731      0.3859      0.0948      0.9101     -0.8019      1.0000
HPT CAP       0.2621     -0.0147     -0.0021     -0.0868     -0.2625      0.4090     -0.4899      1.0000
LPT ETA       0.7314     -0.6070      0.5189      0.2960      0.2581     -0.1415      0.2372      0.0070      1.0000
LPT CAP      -0.2285      0.4265     -0.8079     -0.8822      0.7257     -0.6858      0.8216     -0.4657     -0.3588
EPR          -0.0526      0.1813      0.2468      0.1823      0.4598     -0.2187      0.3712      0.3175     -0.3684
P2           -0.2536      0.3049     -0.1520     -0.1537      0.2934     -0.1779      0.2644      0.2839     -0.5477
T2            0.4022      0.1268      0.5773      0.1327      0.6728     -0.2512      0.4724      0.0315      0.2789
WFE          -0.4633      0.1065     -0.3712     -0.2255     -0.5764      0.4231     -0.5694      0.1418     -0.1752
P26           0.0353     -0.7331      0.7292      0.8736     -0.2349      0.1483     -0.2437      0.0596      0.3841
T26           0.0        -0.2185     -0.0840      0.2057     -0.0532      0.0346     -0.0350      0.0133      0.1128
P3           -0.2998     -0.0144      0.0287      0.0058      0.1382     -0.1917      0.2382     -0.9152     -0.0634
T3           -0.0978      0.0090     -0.2828     -0.0395     -0.3192      0.0760      0.0825     -0.2968     -0.8267
T49          -0.0962      0.1192     -0.4375     -0.2367     -0.6916      0.5058     -0.7045      0.1790     -0.4276
P13           0.2301     -0.0253     -0.0133     -0.0733     -0.0247      0.0198     -0.0275      0.0062      0.2326
XNL          -0.0689     -0.6157     -0.0309     -0.1212     -0.0252      0.0198     -0.0275      0.0062      0.3019
XNH          -0.0830      0.0812     -0.2210     -0.0938      0.0686     -0.7008      0.1578     -0.1367     -0.0594
FN            0.4252     -0.0379     -0.0287     -0.1945     -0.0548      0.0430     -0.0584      0.0151      0.5831
M1A           0.4584     -0.0361      0.0177     -0.1815      0.0219     -0.0165      0.0216     -0.0053      0.3643

              LPT CAP     EPR         P2          T2          WFE         P26         T26         P3          T3
LPT CAP       1.0000
EPR           0.5798      1.0000
P2            0.5816      0.8551      1.0000
T2            0.2986      0.3013     -0.0144      1.0000
WFE          -0.4634     -0.5869     -0.4045     -0.2922      1.0000
P26          -0.4603     -0.1237     -0.4088      0.8156      0.0         1.0000
T26          -0.1194     -0.0466     -0.0004     -0.5032      0.0         0.0         1.0000
P3            0.2578     -0.4246     -0.4063      0.0066      0.0         0.0         0.0         1.0000
T3            0.0911     -0.1263      0.0020     -0.4715      0.0         0.0         0.0         0.0         1.0000
T49          -0.4300     -0.1182      0.0049     -0.4863      0.0         0.0         0.0         0.0         0.0
P13          -0.1639     -0.1734     -0.4088      0.0861      0.0         0.0         0.0         0.0         0.0
XNL          -0.2833     -0.2043     -0.0024     -0.2483      0.0         0.0         0.0         0.0         0.0
XNH           0.1851     -0.0938      0.0012     -0.2564      0.0         0.0         0.0         0.0         0.0
FN           -0.3996     -0.5289     -0.4116      0.0184      0.0         0.0         0.0         0.0         0.0
M1A          -0.1963     -0.2598     -0.4104      0.2692      0.0         0.0         0.0         0.0         0.0

              T49         P13         XNL         XNH         FN          M1A
T49           1.0000
P13           0.0         1.0000
XNL           0.0         0.0         1.0000
XNH           0.0         0.0         0.0         1.0000
FN            0.0         0.0         0.0         0.0         1.0000
M1A           0.0         0.0         0.0         0.0         0.0         1.0000

** MATRIX ANALYSIS **

** WARNING ** FAN ETA  AND LPT ETA  CORRELATED.              FACTOR=  0.7314
** WARNING ** FAN CAP  AND P26      CORRELATED.              FACTOR= -0.7331
** WARNING ** LPC ETA  AND LPC CAP  HIGHLY CORRELATED.       FACTOR=  0.8501
** WARNING ** LPC ETA  AND P26      CORRELATED.              FACTOR=  0.7292
** WARNING ** LPC CAP  AND P26      HIGHLY CORRELATED.       FACTOR=  0.8736
** WARNING ** HPC ETA  AND HPC CAP  CORRELATED.              FACTOR= -0.7373
** WARNING ** HPC ETA  AND HPT ETA  VERY HIGHLY CORRELATED.  FACTOR=  0.9101
** WARNING ** HPC ETA  AND LPT CAP  CORRELATED.              FACTOR=  0.7257
** WARNING ** HPC CAP  AND HPT ETA  HIGHLY CORRELATED.       FACTOR= -0.8019
** WARNING ** HPC CAP  AND XNH      CORRELATED.              FACTOR= -0.7008
** WARNING ** HPT ETA  AND LPT CAP  HIGHLY CORRELATED.       FACTOR=  0.8216
** WARNING ** HPT ETA  AND T49      CORRELATED.              FACTOR= -0.7045
** WARNING ** HPT CAP  AND P3       VERY HIGHLY CORRELATED.  FACTOR= -0.9152
** WARNING ** EPR      AND P2       HIGHLY CORRELATED.       FACTOR=  0.8551
```

Figure 14: System Correlation Matrix

the fact that Fan Root/Booster performance has a large effect on P26 levels.

3.6 Observability

The work in the preceding sections has covered pairs of component changes and/or sensor biasses which may affect the measurements in the same way. However, there may be situations where, if two (or more) component changes and/or sensor biasses are combined, this combination may be indistinguishable from another component change or sensor bias. Figure 15 shows such a possibility, for a three-dimensional case.

The Figure shows that, while the pairs of Component Changes A and B, B and C and A and C are not correlated (because the angles between them are large), the

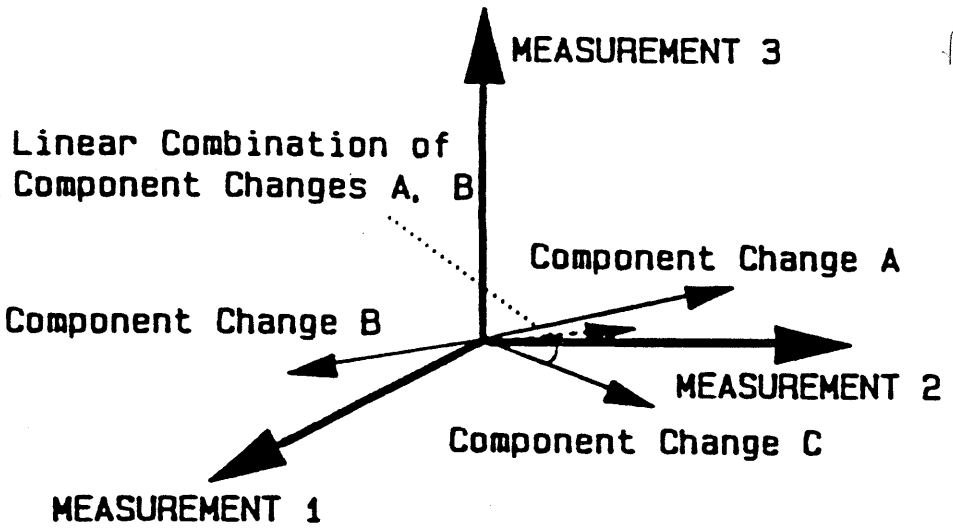

Figure 15: Example of indistinguishable combinations of component changes

combination of Component Changes A and B shown by the dotted line is very highly correlated with Component Change C, since the angle between them is small. A classic case of such a situation is the diagnosis of turbine NGV capacity changes in multi-shaft gas turbines, which cannot be distinguished from reciprocal changes in the efficiencies of the turbines on either side of the NGVs in question. Note that an alternative, but equally valid, way of looking at such a situation is to reverse the direction of Component Change C, which would then result in a combination of Component Changes A, B and C which would produce very small (or zero) changes in all the measurements; this combination would obviously not be detectable. Observability Theory enables us to determine very easily which particular combinations of component changes and/or sensor biasses are not detectable with a given set of measurements; this is obviously useful information when trying to assess the analysis capabilities of the measurements being considered.

A steady-state system is said to be observable if all the system states (in the performance analysis case, component changes and sensor biasses being searched for) can be uniquely determined from the set of outputs (in the performance analysis case, gas-path measurements). As pointed out in Reference 36 (which, incidentally, quotes a different definition for observability for dynamic systems), the most common test for observability (the invertibility or otherwise of the System Matrix) produces a 'yes or no' type answer which is not very useful. Reference 36 proposes a different method of testing for observability (expanded on in Reference 37 and discussed in the context of performance analysis in Reference 38), which is developed in the following paragraphs.

Consider two analysis systems, each trying to determine HP Compressor efficiency (HPC ETA) and HP Turbine efficiency (HPT ETA) changes from two measurements, using, in the first case, HP Compressor entry total pressure (P26) and HP Compressor exit total pressure (P3), and, in the second case, HP Compressor exit total pressure (P3) and HP Compressor exit total temperature (T3). The appropriate matrices (sub-matrices of Figure 8) are given below:

System 1:

	ΔHPC ETA	ΔHPT ETA
ΔP26	-0.432	-0.576
ΔP3	0.252	0.563

System 2:

	ΔHPC ETA	ΔHPT ETA
ΔP3	0.252	0.563
ΔT3	-0.582	0.195

In doing an analysis, we are, in effect, trying to find the intersection of equations as given below:

System 1:

$$-0.432 \bullet \Delta\text{HPC ETA} - 0.576 \bullet \Delta\text{HPT ETA} = \Delta P26 = -0.5\% \text{ (say)}$$
$$0.252 \bullet \Delta\text{HPC ETA} + 0.563 \bullet \Delta\text{HPT ETA} = \Delta P3 = 0.5\% \text{ (say)}$$

System 2:

$$0.252 \bullet \Delta\text{HPC ETA} + 0.563 \bullet \Delta\text{HPT ETA} = \Delta P3 = 0.5\% \text{ (say)}$$
$$-0.582 \bullet \Delta\text{HPC ETA} + 0.195 \bullet \Delta\text{HPT ETA} = \Delta T3 = 0.5\% \text{ (say)}$$

The values on the right-hand side are known from measurements and are, of course, subject to measurement error. Figures 16 and 17 show the above equations plotted (as functions of ΔHPC ETA and ΔHPT ETA) for each system, in the areas labelled 'Component Change Space'. In both cases, the exact solution, ie the point of intersection of the solid lines, is indicated.

The acute angle of intersection of the lines in Figure 16, relative to the angle in Figure 17, becomes important when measurement error is considered. Lines appropriate to shifts in the measurements of ± 0.05% have been included on both plots; it is seen that the exact solution point has now become an area of uncertainty, which is much larger in Figure 16 (covering a range of 1.1% ΔHPC ETA and nearly 0.7% ΔHPT ETA) than it is in Figure 17 (covering about 0.2% in both ΔHPC ETA and ΔHPT ETA), due entirely to the different angles of intersection. Obviously, the situation in Figure 17 is the more acceptable of the two, because there is much less uncertainty in the answers. This argument could, of course, be extended to the intersections in more than two dimensions.

The two Figures also show, in the parts of the diagrams

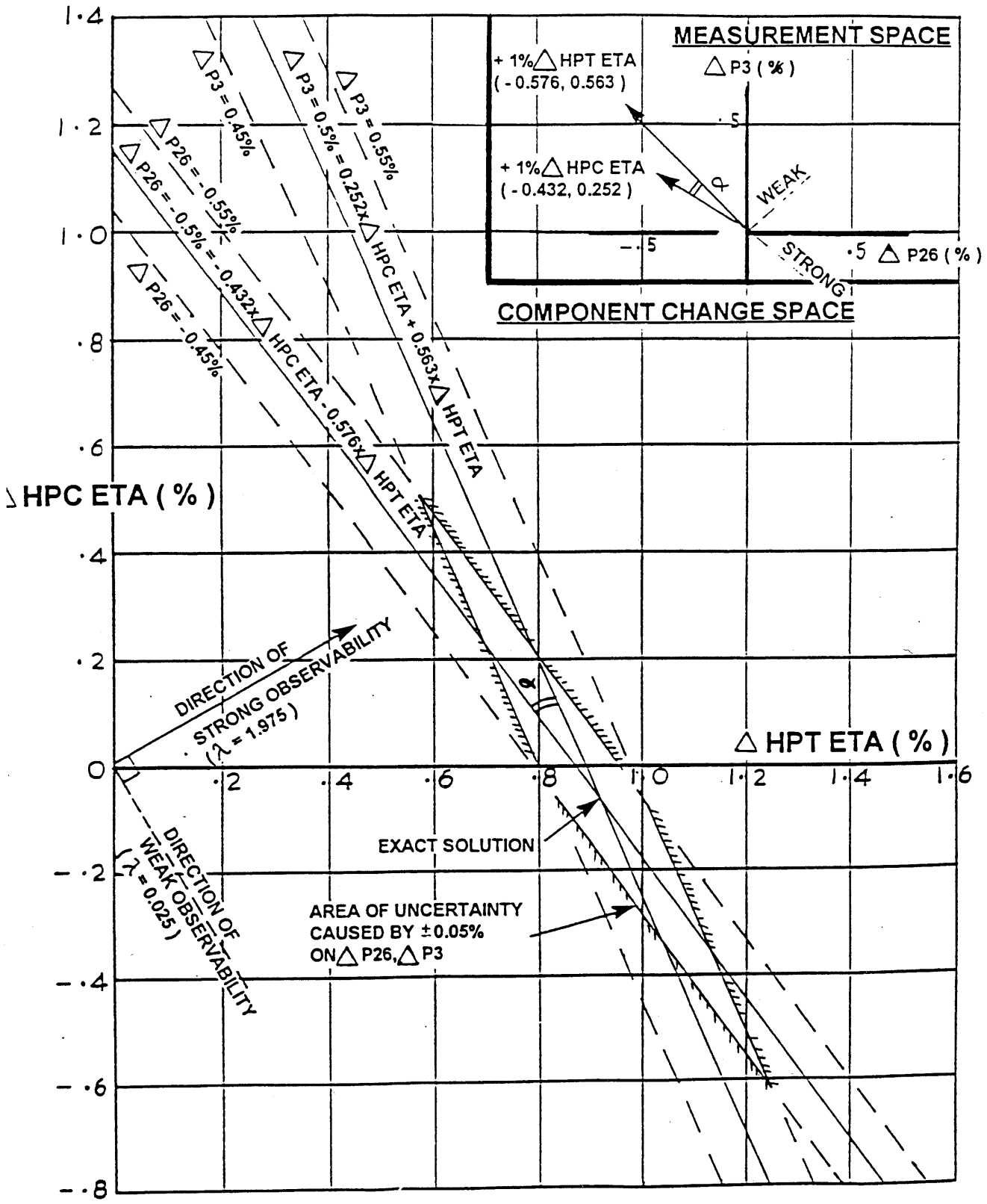

Figure 16: Example of poorly-observable system: ΔHPC ETA, ΔHPT ETA from ΔP26, ΔP3 (Problem-1)

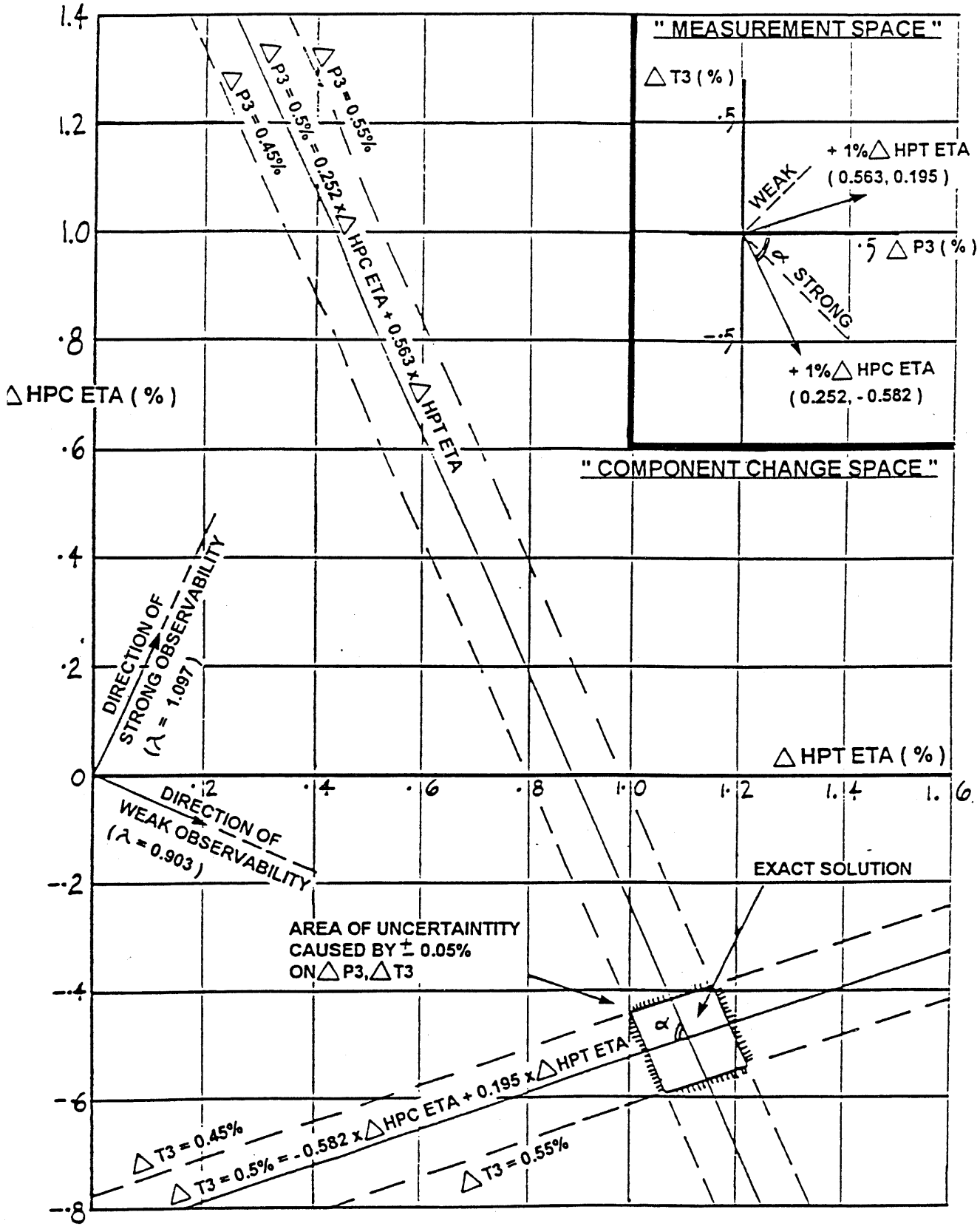

Figure 17: Example of easily observable system: ΔHPC ETA, ΔHPT ETA from ΔP3, ΔT3

labelled 'Measurement Space', the shift in the measurements appropriate to 1% changes in ΔHPC ETA and ΔHPT ETA; these are merely pictorial representations of the columns of the matrices given above. Since the angles between the lines in 'Component Change Space' and the vectors in 'Measurement Space' (indicated as α on the Figures) are equal, we can therefore assess the shapes of the areas of uncertainty by dealing directly with the angles between the vectors made up by the columns in the System Matrix; indeed, this is a variation on the procedure used in the correlation analysis approaches described earlier.

This approach, while being valid for more than two dimensions, becomes rapidly unworkable as the number of dimensions (component changes and sensor biasses) in 'Component Change Space' increases. However, if we imagine adding an extra vector to the 'Measurement Space', which is approximately perpendicular to the vectors for ΔHPC ETA and ΔHPT ETA, we see that this is easy to do where the angle between the component change vectors is small (Figure 16), but not possible where the angle between the component change vectors is large (Figure 17). This test works no matter how many vectors (ie component changes and sensor biasses) or how many dimensions (ie number of gas-path measurements) there are in the 'Measurement Space'; indeed, there may be several vectors, each pointing in a unique direction, which are perpendicular to component change or sensor bias vectors. As another example, it is seen that it would be possible to 'insert' an extra vector into the 'Measurement Space' of Figure 15 that is approximately perpendicular to all the vectors appropriate to Component Changes A, B and C; according to the previous argument, this would indicate a very mis-shaped three-dimensional 'volume of uncertainty' in the determination of the magnitude of Component Changes A, B and C from Measurements 1, 2 and 3 which, of course, would lead to problems in analysis. The ability to 'insert' an extra vector into the 'Measurement Space' that is approximately perpendicular to the component change and sensor bias vectors already in that space implies that there is a certain amount of linear dependency between those vectors; if the component change and sensor bias vectors 'fill' the 'Measurement Space' such that they are not linearly dependent, then it would be impossible to 'insert' an extra vector that is perpendicular to all those vectors.

The calculation of this 'extra' vector, which can be used to define the observability of the system, is detailed in Appendix B. The theory does, in fact, produce a set of vectors, equal in number to the total number of component changes and sensor biasses being searched for, which are perpendicular to one another. These Eigenvectors have associated Eigenvalues which express the level of observability of the system in the direction of their

associated vectors. The smallest Eigenvalue is associated with the Eigenvector which points in the direction of weakest observability: Figures 16 and 17 show that this direction is parallel to the longest diagonal of the parallelogram in 'Component Change Space' defining the area of uncertainty. Conversely, the largest Eigenvalue is associated with the Eigenvector which points in the direction of strongest observability: Figures 16 and 17 show that this direction is parallel to the shortest diagonal of the parallelogram in 'Component Change Space' defining the area of uncertainty. Figure 16 shows very clearly that, for poorly-observable systems in 'Measurement Space', the direction of strongest observability bisects the angle between the two component change vectors, while the direction of weakest observability is nearly at right angles to both the component change vectors. Figure 18 shows the system correlation matrices and Eigenvalues/Eigenvectors for the two situations illustrated in Figures 16 and 17; note the large difference in correlation between HPC ETA and HPT ETA.

Generally, the following statements can be made about the Eigenvalues and Eigenvectors produced from an observability analysis of a system where m gas-path measurements are used to search for a total of n component changes and sensor biasses:

1) n Eigenvectors and associated Eigenvalues are produced;

2) The Eigenvectors are perpendicular to one another, except where the Eigenvalues are equal; in this case, the Eigenvectors are identical;

3) The sum of all the Eigenvalues is m;

4) If $n > m$, then there are at least $(n-m)$ Eigenvectors representing combinations of component changes and sensor biasses that are not observable. These Eigenvectors are characterised by:

   - very small associated Eigenvalues;

   - the fact that, if all the measurement differences appropriate to all the component changes and sensor biasses in the Eigenvectors are worked out, they are all zero (hence non-observability!);

5) Each element of each Eigenvector can be multiplied by the same factor to give a new vector with the same properties, ie the direction of the Eigenvector, not its magnitude, is important.

The explanation of 4) above is quite straightforward. If we imagine an analysis where three component changes are being searched for using two gas-path measurements (so

A) POORLY-OBSERVABLE SYSTEM

```
** SYSTEM CORRELATION MATRIX **
** SINCE MATRIX IS SYMMETRIC, ONLY LOWER TRIANGULAR ELEMENTS ARE PRINTED **
            HPC ETA     HPT ETA
HPC ETA       1.0000
HPT ETA       0.9699      1.0000
** MATRIX ANALYSIS **
** WARNING ** HPC ETA  AND HPT ETA  VERY HIGHLY CORRELATED: FACTOR=   0.9699


** EIGENVALUES AND EIGENVECTORS OF DETERMINISTIC OBSERVABILITY MATRIX: PERF=    0.03 **
** EIGENVALUES AND EIGENVECTORS ARE PRINTED OUT IN THE ORDER STRONG ------- WEAK OBSERVABILITY
EIGENVAL    1.975       .2468E-01
HPC ETA      -0.5074     -0.8617
HPT ETA      -0.8617      0.5074
** MEASUREMENT DIFFERENCES CORRESPONDING TO ABOVE EIGENVECTORS **
P26           0.7155      0.0800
P3           -0.6130      0.0685
```

B) EASILY-OBSERVABLE SYSTEM

```
** SYSTEM CORRELATION MATRIX **
** SINCE MATRIX IS SYMMETRIC, ONLY LOWER TRIANGULAR ELEMENTS ARE PRINTED **
            HPC ETA     HPT ETA
HPC ETA       1.0000
HPT ETA       0.0751      1.0000
** MATRIX ANALYSIS **
** NO SIGNIFICANT CORRELATIONS DETECTED **


** EIGENVALUES AND EIGENVECTORS OF DETERMINISTIC OBSERVABILITY MATRIX: PERF=    0.02 **
** EIGENVALUES AND EIGENVECTORS ARE PRINTED OUT IN THE ORDER STRONG ------- WEAK OBSERVABILITY
EIGENVAL    1.097       .9026
HPC ETA      0.9158     -0.4017
HPT ETA      0.4017      0.9158
** MEASUREMENT DIFFERENCES CORRESPONDING TO ABOVE EIGENVECTORS **
P3           0.4569      0.4144
T3          -0.4547      0.4123
```

Figure 18: System Correlation Matrices and Eigenvalues/ Eigenvectors

n - m = 1), the 'Measurement Space' would look like the left-hand side of Figure 19:

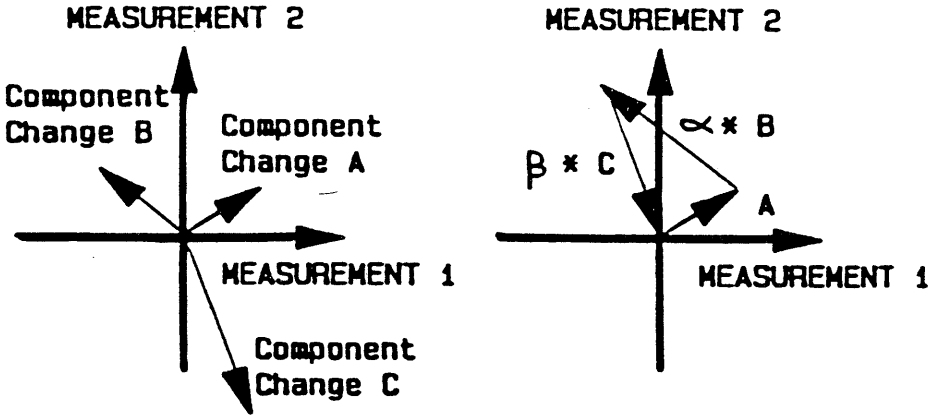

Figure 19: Non-observability when number of component changes + sensor biasses greater than number of measurements

The right-hand side of Figure 19 shows how one combination of component changes A, B and C, in the ratio 1:α:β, can be chosen to give zero measurement differences in both Measurement 1 and Measurement 2.

Figure 20 shows the observability Eigenvalues and Eigenvectors for the System Matrix made up of the tables in Figure 8. Note:

1) the 11 large Eigenvalues (all greater than 0.05) that correspond to the 11 Eigenvectors pointing in the strongly observable directions;

2) the 9 distinct small Eigenvalues (all less than 10^{-5}) that correspond to the 9 distinct Eigenvectors pointing in the weakly observable directions; note that the measurement differences corresponding to the component changes and sensor biasses in these Eigenvectors are all zero;

3) 4 Eigenvalues and Eigenvectors appear as pairs.

Figure 21 shows the observability Eigenvalues and Eigenvectors for the Component Exchange Rate Table only, ie without sensor biasses included. It is seen that the combination of the following three changes:

-0.3322% HP Turbine efficiency

+0.4637% LP Turbine efficiency

+0.8210% LP Turbine capacity

is not observable, in spite of there being more gas-path measurements (11) than component changes being sought

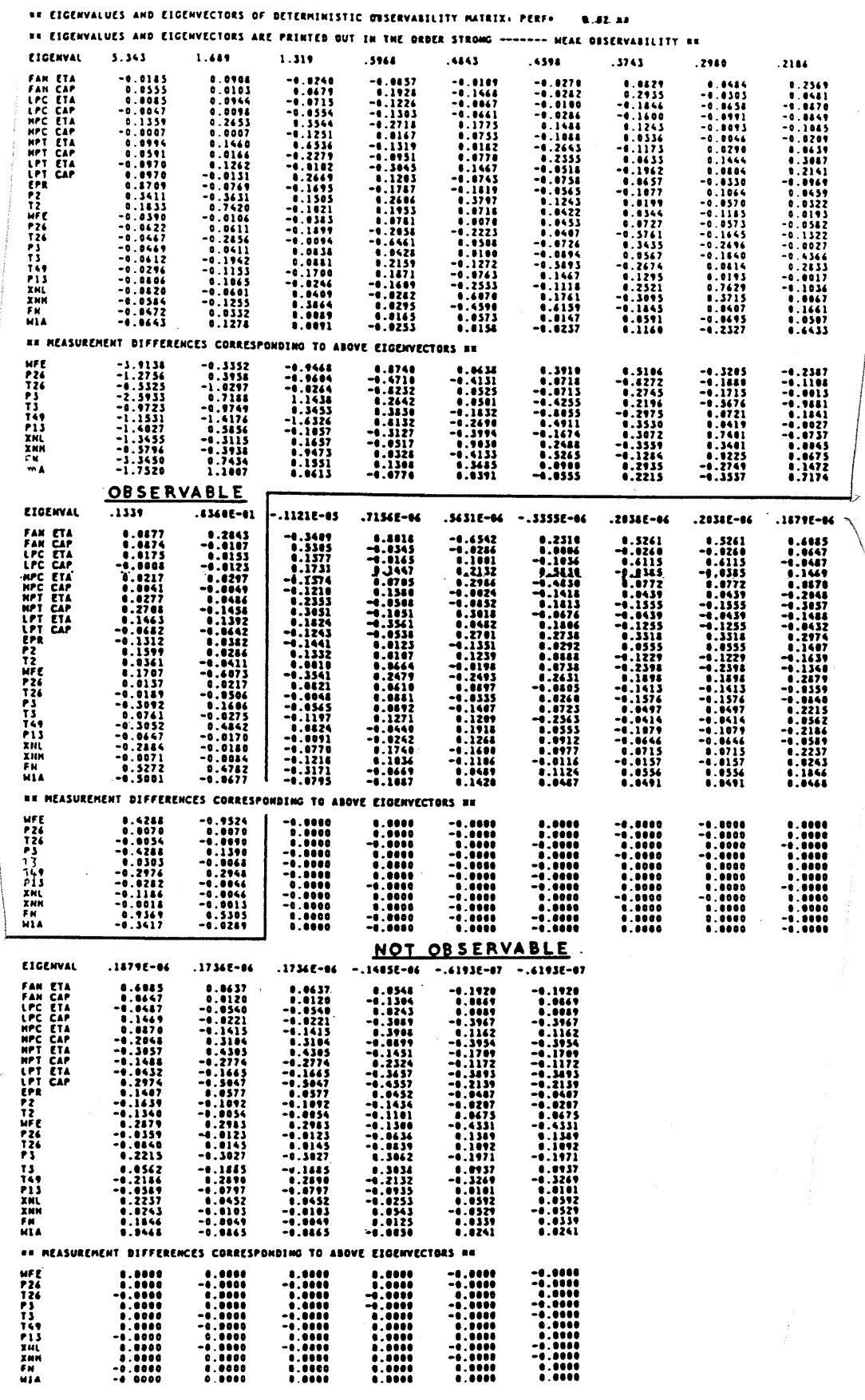

** EIGENVALUES AND EIGENVECTORS OF DETERMINISTIC OBSERVABILITY MATRIX: PERF= 0.02 **

** EIGENVALUES AND EIGENVECTORS ARE PRINTED OUT IN THE ORDER STRONG ------- WEAK OBSERVABILITY **

EIGENVAL	5.343	1.689	1.319	.5968	.4843	.4598	.3743	.2980	.2186
FAN ETA	-0.0185	0.0908	-0.0240	-0.0857	-0.0189	-0.0270	0.0829	0.0484	0.2569
FAN CAP	0.0555	0.0103	0.0679	0.1928	-0.1468	-0.0242	0.2935	-0.0303	0.0481
LPC ETA	0.0085	0.0944	-0.0715	-0.1226	-0.0067	-0.0100	-0.1446	-0.0658	-0.0870
LPC CAP	-0.0047	0.0098	-0.0556	-0.1303	-0.0661	-0.0286	-0.1600	-0.0991	-0.0849
HPC ETA	0.1359	0.2653	0.3564	-0.2718	0.1775	0.1488	0.1243	-0.0093	-0.1065
HPC CAP	-0.0007	0.0007	-0.1251	0.0167	0.0753	-0.1088	0.0336	-0.0844	-0.0209
HPT ETA	0.0996	0.1460	0.6536	-0.1319	0.0182	-0.2643	-0.1173	0.0290	0.0639
HPT CAP	0.0591	0.0166	-0.2279	-0.0951	0.0778	0.2355	0.0633	0.1444	0.3887
LPT ETA	-0.0970	0.1262	-0.0182	-0.3045	0.1467	-0.0518	-0.1962	0.0804	0.2141
LPT CAP	0.0970	-0.0131	0.2669	0.1203	-0.8745	-0.0758	0.0657	-0.0330	-0.0969
EPR	0.8709	-0.0769	-0.1695	-0.1787	-0.1819	-0.0565	-0.1077	0.1064	0.0459
P2	0.3411	-0.3651	0.1585	0.2686	0.3797	0.1243	0.0199	-0.0570	0.0322
T2	0.1833	0.7620	-0.1821	0.1953	0.0716	0.0422	0.0344	-0.1185	0.0193
WFE	-0.0390	-0.0106	-0.0383	0.0781	0.0078	0.0453	0.0727	-0.0573	-0.0582
P26	-0.0622	0.0611	-0.1899	-0.2858	-0.2223	0.0407	-0.5761	-0.1665	-0.1322
T26	-0.0467	-0.2856	-0.0094	-0.4661	0.0588	-0.0726	0.3635	-0.2496	-0.0027
P3	-0.0449	0.0411	0.0838	0.0628	0.0100	-0.0894	0.0567	-0.1640	-0.6366
T3	-0.0612	-0.1962	0.0881	0.2159	-0.1272	-0.5893	-0.2674	0.0614	0.2833
T49	-0.0296	-0.1153	-0.1700	0.1871	-0.0763	0.1467	0.1295	0.0193	-0.0017
P13	-0.0806	0.1065	-0.0246	-0.1609	-0.2535	-0.1116	0.2321	0.7629	-0.1036
XNL	-0.0828	-0.0601	0.0409	-0.0282	0.6070	0.1761	-0.3895	0.3715	0.0867
XNM	-0.0586	-0.1255	0.3864	0.0295	-0.4598	0.6159	-0.1845	0.0407	0.1661
FN	-0.0672	0.0332	0.0889	0.0165	0.0573	0.0147	0.0591	-0.0695	0.0507
MIA	-0.0643	0.1278	0.0891	-0.0253	0.0158	-0.0237	0.1160	-0.2327	0.6433

** MEASUREMENT DIFFERENCES CORRESPONDING TO ABOVE EIGENVECTORS **

WFE	-3.9138	-0.3352	-0.9468	0.8740	0.0638	0.3919	0.5106	-0.3205	-0.2387
P26	-1.2756	0.3958	-0.9604	-0.4718	-0.4131	0.0718	-0.8272	-0.1888	-0.1108
T26	-0.5325	-1.0297	-0.0264	-0.8232	0.0525	-0.0715	0.2745	-0.1715	-0.0013
P3	-2.5933	0.7188	1.1438	0.2642	0.0501	-0.4255	0.2196	-0.5676	-0.9881
T3	-0.9725	-0.9749	0.3455	0.3830	-0.1832	-0.8855	-0.2975	0.0721	0.1841
T49	-1.1531	-1.4176	-1.6326	-0.8132	-0.2698	0.4911	0.3530	0.0419	-0.0027
P13	-1.4027	0.5856	-0.1057	-0.3127	-0.3994	-0.1674	0.3072	0.7401	-0.0737
XNL	-1.3455	-0.3115	0.1657	-0.0517	0.0938	0.2488	-0.3559	0.3401	0.0863
XNM	-0.5796	-0.3938	0.9473	0.0328	-0.4153	0.5265	-0.1286	0.0225	0.0675
FN	-3.3650	0.7434	0.1551	0.1308	0.3485	0.0898	0.2935	-0.2749	0.1472
MIA	-1.7520	1.1807	0.0613	-0.0770	0.0391	-0.0355	0.2215	-0.3537	0.7174

OBSERVABLE

EIGENVAL	.1339	.6360E-01	-.1121E-05	.7156E-06	.5631E-06	-.3355E-06	.2038E-06	.2038E-06	.1879E-06
FAN ETA	0.0877	0.2843	-0.3489	0.8818	-0.6542	0.2318	0.5261	0.5261	0.6885
FAN CAP	0.0876	-0.0187	0.5305	-0.0345	-0.0286	0.0006	-0.0260	-0.0260	0.0647
LPC ETA	0.0175	0.0153	0.1577	-0.0165	0.1001	-0.1036	0.6115	0.6115	-0.0487
LPC CAP	-0.0008	-0.0123	0.1731	0.3447	0.2132	0.5818	-0.0385	-0.0385	0.1449
HPC ETA	0.0217	0.0207	-0.1574	0.0705	0.2966	-0.4830	0.0772	0.0772	0.0870
HPC CAP	0.0061	-0.0049	-0.1210	0.1588	-0.0024	-0.1418	0.0439	0.0439	-0.2048
HPT ETA	0.0277	0.0486	0.2353	-0.0508	-0.0832	0.1813	-0.1555	-0.1555	-0.3857
HPT CAP	0.2708	-0.1458	0.3851	-0.1051	0.3018	-0.0676	-0.0439	-0.0439	-0.1488
LPT ETA	0.1463	0.1392	0.1824	-0.3541	0.0482	0.1806	-0.1255	-0.1255	-0.0432
LPT CAP	-0.0682	-0.0642	-0.1245	-0.0538	-0.2701	0.2736	0.3318	0.3318	0.2976
EPR	-0.1312	0.0382	-0.1441	0.0123	-0.1351	0.0292	0.0555	0.0555	0.1407
P2	0.1599	0.0286	0.1332	0.0107	0.1239	0.0888	-0.1229	-0.1229	-0.1639
T2	0.0361	-0.0411	0.0810	0.0464	-0.0198	0.0738	-0.2398	-0.2398	-0.1368
WFE	0.1707	-0.6873	-0.3541	0.2479	-0.2693	0.2631	0.1898	0.1898	0.2879
P26	0.0137	0.0217	0.0621	0.0610	0.0897	-0.0805	-0.1613	-0.1613	-0.0359
T26	-0.0189	-0.0506	-0.0048	0.0861	-0.0555	0.0268	-0.1576	-0.1576	-0.0848
P3	-0.3092	0.1686	-0.0565	0.0892	-0.1407	0.0723	0.0497	0.0497	0.2215
T3	0.0761	-0.0275	-0.1197	0.1271	0.1209	-0.2563	-0.0414	-0.0414	0.0562
T49	-0.3052	0.4862	0.0824	-0.0440	0.1918	0.0555	-0.1079	-0.1079	-0.2186
P13	-0.0647	-0.0170	-0.0091	-0.0242	0.1268	0.0912	-0.0646	-0.0646	-0.0589
XNL	-0.2884	-0.0188	-0.0770	0.1740	-0.1690	0.0977	0.0715	0.0715	0.2237
XNM	-0.0871	-0.0084	-0.1218	0.1836	-0.1186	-0.0116	-0.0157	-0.0157	0.0243
FN	0.5272	0.4782	-0.3171	-0.0669	0.0689	0.1126	0.0556	0.0556	0.1866
MIA	-0.5881	-0.0677	-0.0795	-0.1087	0.1428	0.0487	0.0491	0.0491	0.0468

** MEASUREMENT DIFFERENCES CORRESPONDING TO ABOVE EIGENVECTORS **

WFE	0.4288	-0.9524	-0.0000	0.0000	-0.0000	0.0000	-0.0000	-0.0000	0.0000
P26	0.0070	0.0070	0.0000	0.0000	-0.0000	0.0000	-0.0000	-0.0000	0.0000
T26	-0.0054	-0.0090	0.0000	-0.0000	0.0000	-0.0000	0.0000	0.0000	-0.0000
P3	-0.4288	0.1390	-0.0000	0.0000	-0.0000	0.0000	-0.0000	-0.0000	0.0000
T3	0.0303	-0.0068	-0.0000	0.0000	-0.0000	-0.0000	0.0000	0.0000	0.0000
T49	-0.2976	0.2948	-0.0000	0.0000	-0.0000	-0.0000	0.0000	0.0000	0.0000
P13	-0.0282	-0.0044	0.0000	-0.0000	0.0000	-0.0000	0.0000	0.0000	-0.0000
XNL	-0.1186	-0.0046	-0.0000	0.0000	-0.0000	0.0000	-0.0000	-0.0000	0.0000
XNM	-0.0018	-0.0013	-0.0000	0.0000	-0.0000	0.0000	0.0000	0.0000	0.0000
FN	0.9369	0.5305	0.0000	-0.0000	-0.0000	-0.0000	0.0000	0.0000	-0.0000
MIA	-0.3417	-0.0289	0.0000	-0.0000	0.0000	-0.0000	0.0000	0.0000	-0.0000

NOT OBSERVABLE

EIGENVAL	.1879E-06	.1736E-06	.1736E-06	-.1485E-06	-.6193E-07	-.6193E-07
FAN ETA	0.6885	0.0637	0.0637	0.0548	-0.1920	-0.1920
FAN CAP	0.0647	0.0120	0.0120	-0.1304	0.0869	0.0869
LPC ETA	-0.0487	-0.0540	-0.0540	0.0243	0.0089	0.0089
LPC CAP	0.1449	-0.0221	-0.0221	-0.3089	-0.3967	-0.3967
HPC ETA	0.0870	-0.1415	-0.1415	0.3908	0.1162	0.1162
HPC CAP	-0.2048	0.3104	0.3104	-0.0899	-0.3954	-0.3954
HPT ETA	-0.3857	0.4305	0.4305	-0.1451	-0.1709	-0.1709
HPT CAP	-0.1488	-0.2774	-0.2774	0.2324	-0.1172	-0.1172
LPT ETA	-0.0432	-0.1665	-0.1665	-0.3657	-0.3893	-0.3893
LPT CAP	0.2976	-0.5047	-0.5047	-0.4557	-0.2139	-0.2139
EPR	0.1407	0.0577	0.0577	0.0452	-0.0487	-0.0487
P2	-0.1639	-0.1092	-0.1092	-0.1436	-0.0207	-0.0207
T2	-0.1368	-0.0856	-0.0856	-0.1101	0.0675	0.0675
WFE	0.2879	0.2985	0.2985	-0.1308	-0.4331	-0.4331
P26	-0.0359	-0.0123	-0.0123	-0.0634	0.1349	0.1349
T26	-0.0848	0.0145	0.0145	-0.0839	0.1092	0.1092
P3	0.2215	-0.3027	-0.3027	0.3062	-0.1971	-0.1971
T3	0.0562	-0.1885	-0.1885	0.3034	0.0937	0.0937
T49	-0.2186	0.2890	0.2890	-0.2132	-0.3269	-0.3269
P13	-0.0589	-0.0797	-0.0797	-0.0935	0.0101	0.0101
XNL	0.2237	0.0452	0.0452	-0.0253	0.0592	0.0592
XNM	0.0243	-0.0103	-0.0103	0.0543	-0.0529	-0.0529
FN	0.1866	-0.0049	-0.0049	0.0125	0.0339	0.0339
MIA	0.0468	-0.0865	-0.0865	-0.0850	0.0241	0.0241

** MEASUREMENT DIFFERENCES CORRESPONDING TO ABOVE EIGENVECTORS **

WFE	0.0000	0.0000	0.0000	0.0000	-0.0000	-0.0000
P26	0.0000	-0.0000	-0.0000	0.0000	-0.0000	-0.0000
T26	-0.0000	0.0000	0.0000	-0.0000	0.0000	0.0000
P3	0.0000	0.0000	0.0000	-0.0000	-0.0000	-0.0000
T3	0.0000	-0.0000	-0.0000	0.0000	-0.0000	-0.0000
T49	0.0000	-0.0000	-0.0000	0.0000	0.0000	0.0000
P13	-0.0000	0.0000	0.0000	0.0000	0.0000	0.0000
XNL	0.0000	-0.0000	-0.0000	0.0000	-0.0000	-0.0000
XNM	0.0000	0.0000	0.0000	0.0000	-0.0000	-0.0000
FN	-0.0000	0.0000	0.0000	0.0000	0.0000	0.0000
MIA	-0.0000	0.0000	0.0000	0.0000	0.0000	0.0000

Figure 20: Eigenvalues/Eigenvectors of full System Matrix

Figure 21: Eigenvalues/Eigenvectors: no sensor biasses

** EIGENVALUES AND EIGENVECTORS OF DETERMINISTIC OBSERVABILITY MATRIX: PERF= 0.09 **

** EIGENVALUES AND EIGENVECTORS ARE PRINTED OUT IN THE ORDER STRONG ------- WEAK OBSERVABILITY **

EIGENVAL	5.583	2.691	1.367	.7361	.2847	.1716	.1012	.5254E-01	.1173E-01
FAN ETA	-0.1913	0.3658	0.1604	-0.5293	0.0996	0.1817	0.1066	0.1320	0.6721
FAN CAP	0.2326	-0.0990	0.1898	-0.7270	0.2270	-0.0171	0.1505	-0.0331	-0.5440
LPC ETA	-0.0264	0.0205	0.1646	0.1465	0.4478	0.5479	-0.1987	-0.6404	0.0003
LPC CAP	-0.0444	-0.0638	-0.0342	0.2528	0.2267	0.5088	0.6350	0.4455	-0.1300
HPC ETA	0.3394	0.4043	0.6102	0.3226	0.3169	-0.3521	0.0415	0.1371	-0.0002
HPC CAP	-0.1000	-0.0969	0.0522	-0.0262	0.2441	0.2257	-0.7096	0.5924	-0.1094
HPT ETA	0.5490	0.5025	-0.2366	-0.0201	-0.3510	0.3610	-0.1218	0.0299	-0.1008
HPT CAP	-0.1858	-0.1455	0.6818	0.0133	-0.6226	0.2828	-0.0175	-0.0067	-0.1058
LPT ETA	-0.4594	0.6173	-0.1168	0.0188	-0.0706	0.0007	-0.0226	-0.0300	-0.4153
LPT CAP	0.4842	-0.1560	-0.0199	-0.0146	-0.1042	0.1498	-0.0484	0.0353	0.1721

** MEASUREMENT DIFFERENCES CORRESPONDING TO ABOVE EIGENVECTORS **

WFE	-1.2275	-1.3083	-0.2263	-0.2437	0.0390	-0.3136	0.0193	-0.0900	-0.1116
P26	-1.0000	-0.1329	-0.1451	0.2960	0.1839	0.2560	0.1013	-0.1319	0.0016
T26	-0.2481	-0.0125	-0.0603	0.0760	-0.0155	-0.0052	0.0426	0.0425	-0.0010
P3	0.7768	0.3921	-0.7149	0.1682	0.4824	-0.1622	-0.0119	0.0172	0.0034
T3	0.0423	-0.1460	-0.6566	-0.1922	-0.1116	0.1108	-0.0513	0.0134	-0.0019
T49	-1.3665	-1.6182	-0.1978	-0.4430	0.0724	-0.2925	0.0584	-0.0562	0.1709
P13	-0.2710	0.1779	-0.0090	-0.0863	0.0097	-0.0163	0.0034	-0.0041	-0.0045
XNL	-0.3594	0.1873	-0.1117	0.2528	-0.0930	-0.0654	-0.0760	-0.0256	0.0061
XNH	0.4366	0.1916	-0.1386	0.0049	-0.1104	-0.0551	0.1055	-0.0472	0.0019
FN	-0.6521	0.4606	-0.0183	-0.2233	0.0215	-0.0366	0.0061	-0.0121	-0.0194
W1A	-0.2778	0.4096	0.0135	-0.1231	0.0109	0.0111	0.0032	0.0034	0.0176

← OBSERVABLE →

EIGENVAL	.5091E-05
FAN ETA	0.0161
FAN CAP	-0.0080
LPC ETA	-0.0014
LPC CAP	-0.0008
HPC ETA	-0.0018
HPC CAP	-0.0132
HPT ETA	-0.3522
HPT CAP	-0.0105
LPT ETA	0.4637
LPT CAP	0.8210

NOT OBSERVABLE

low values not observable

** MEASUREMENT DIFFERENCES CORRESPONDING TO ABOVE EIGENVECTORS **

WFE	-0.0017
P26	-0.0000
T26	-0.0000
P3	0.0000
T3	0.0000
T49	0.0008
P13	0.0001
XNL	0.0000
XNH	0.0000
FN	0.0010
W1A	-0.0008

(ALL VALUES VERY NEAR ZERO)

(10). This shows the inability of separating turbine capacity and efficiency changes without extra measurements that was mentioned earlier.

3.7 Detection Ratio

As discussed in the next chapter, the gas turbine performance analyst is attempting to find solutions to the equation $\underline{y} = \underline{C} \bullet \underline{x}$, where the terms have the meanings given in the Introduction. The equation can obviously be solved if $\underline{C}$ can be inverted. A useful check on the invertibility of $\underline{C}$ is to attempt to solve the above equation for all the $\underline{y}$ vectors that make up the columns of $\underline{C}$, ie vectors which represent the effects on the gas-path measurements of 1% changes in all the component changes and sensor biasses being sought. The equations:

$$\underline{y} = \underline{C} \bullet \underline{x}$$

$$\underline{x} = \underline{C}^{\#} \bullet \underline{y}$$

are effectively extended to become:

$$\underline{C} = \underline{C} \bullet \underline{I}$$

$$\underline{I} = \underline{C}^{\#} \bullet \underline{C}$$

where $\underline{C}^{\#}$ is either the inverse or pseudo-inverse of $\underline{C}$ and $\underline{I}$ is the unit matrix. If, however, $\underline{C}$ is ill-conditioned,

then $\underline{C}^{\#} \bullet \underline{C}$ will not equal $\underline{I}$, but some other matrix $\underline{B}$ with diagonal terms that are less than unity and off-diagonal terms that are non-zero. Each diagonal element of $\underline{B}$ corresponding to each component change or sensor bias being sought is called the Detection Ratio for that change or bias: it varies between zero (component change or sensor bias not detectable) and unity (component change or sensor bias perfectly detectable). A table of such diagonal elements effectively shows the proportion of any actual component change or sensor bias present that the chosen set of gas-path measurements can ideally detect, and gives a quick 'feel' for the ability of that set of gas-path measurements to differentiate between the component changes and sensor biasses being sought.

Because inclusion of sensor bias always makes $\underline{C}$ ill-conditioned, this calculation is only useful when $\underline{C}$ consists of the Component Exchange Rate Table only. Calculation of Detection Ratios is not a very robust test of analysis capability, but it is a useful way of summarising and explaining the analysis abilities of a set of gas-path measurements to those who would find the other methods described above somewhat daunting! Trials have shown that Detection Ratios of unity for all the component changes being sought is a necessary, but not sufficient, condition for a viable analysis scheme.

CHAPTER 4: KALMAN FILTERING APPLIED TO GAS TURBINE ANALYSIS

This chapter discusses the Kalman Filter; an algorithm that, given additional information regarding measurement non-repeatability and component change/sensor bias 'spread', calculates best estimates of the component changes and sensor biasses that generated the observed gas-path measurements. A modification to the basic Kalman Filter developed to improve the answers produced and make them more meaningful to the analyst is also discussed, followed by the relationship between the input required by the Kalman Filter and the knowledge used by an experienced performance analyst when analysing a gas turbine. A sensitivity analysis of the Kalman Filter equations to the various statistical inputs is then presented, followed by a discussion of various methods of 'tuning' the Filter to give acceptable analyses.

4.1 The Analysis Situation

The basic equation defining the analysis situation, which forms the starting point for the development of the Kalman Filter, is:

$$\underline{y} = \underline{C} \bullet \underline{x} + \underline{v}$$

where:

$\underline{y}$ = (m•1) column vector of percentage differences between observed and expected levels of gas-path measurements;

$\underline{C}$ = (m•n) System Matrix, defining the effect on the gas-path measurements of 1% changes in component performance parameters, environmental measurement sensor biasses and gas-path measurement sensor biasses; its derivation from component exchange rates and environmental exchange rates was discussed in the previous chapter. Note that n is usually much greater than m, ie the matrix is under-determined;

$\underline{x}$ = (n•1) column vector of percentage changes in component performance parameters and sensor biasses;

$\underline{v}$ = (m•1) column vector of noise terms in the gas-path measurements. These terms are assumed to be normally distributed, with a mean of zero and a known covariance $\underline{R}$.

The situation is shown diagrammatically in Figure 22. The performance analyst is trying to determine the vector $\underline{x}$ from the vector $\underline{y}$, where $\underline{y}$ has been 'corrupted' from its 'true' vector $\underline{y}'$ by measurement noise $\underline{v}$. Since the number

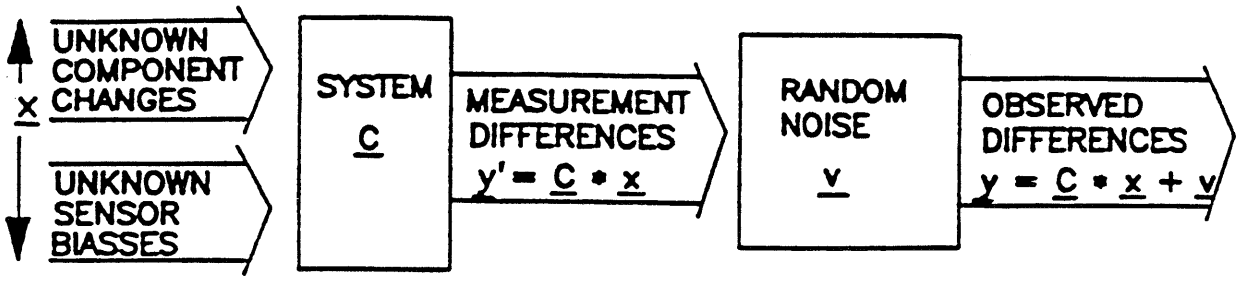

Figure 22: The Analysis Situation

of terms in $\underline{x}$ (n) is usually considerably greater than the number of terms in $\underline{y}$ (m) (typically, the performance analyst would be searching for approximately m component changes, approximately 3 environmental sensor biasses, and m gas-path sensor biasses (corresponding to the m gas-path measurements), so $n \approx 2 \bullet m + 3$), there is not a unique solution to the question 'what $\underline{x}$ generated $\underline{y}$?'; indeed, there are an infinite number of solutions. The performance analyst is forced to accept a 'best estimate', ie the most likely vector of component changes and sensor biasses $\hat{\underline{x}}$ that generated the observed vector of measurement differences $\underline{y}$; the Kalman Filter is merely an algorithm for generating such an estimate.

4.2 Theory of Estimation Methods

Before proceeding with the theory behind estimation methods (which leads ultimately to the Kalman Filter), some criteria are stated for evaluation of the possible methods of deriving the 'best estimate' of $\underline{x}$ referred to earlier. If $\hat{\underline{x}}$ is defined as the $(n \bullet 1)$ vector of best estimates of the component changes and sensor biasses that produced $\underline{y}$, then:

1) The method of calculating $\hat{\underline{x}}$ must be unbiassed; on average, $\hat{\underline{x}}$ must equal the 'true' vector $\underline{x}$ of component changes and sensor biasses;

$$E[\hat{\underline{x}}] = \underline{x}$$

2) The method of calculating $\hat{\underline{x}}$ must be consistent; as the number of sets of measurements $\underline{y}$ is increased, $\hat{\underline{x}}$ must move closer to $\underline{x}$;

3) The method of calculating $\hat{\underline{x}}$ must be efficient; the variance of $\hat{\underline{x}}$ relative to $\underline{x}$ must be as small as possible;

$$E[(\hat{\underline{x}}-\underline{x})^2] = \text{minimum.}$$

The estimation methods described here, which can be thought of as 'stepping-stones' to the Kalman Filter, rely on some method of minimising the errors between the observed measurement differences $\underline{y}$ and the measurement

differences that would be generated by $\hat{\underline{x}}$ ($\underline{C} \bullet \hat{\underline{x}}$), ie:

$$\underline{e} = \underline{y} - \underline{C} \bullet \hat{\underline{x}}$$

is minimised.

The easiest method of doing this is to minimise the sum of squares of the elements in $\underline{e}$. This is done by forming the scalar quantity:

$$J = \underline{e}^T \bullet \underline{e} = (\underline{y} - \underline{C} \bullet \hat{\underline{x}})^T \bullet (\underline{y} - \underline{C} \bullet \hat{\underline{x}})$$

Minimising the value of J with respect to $\hat{\underline{x}}$ leads to the Least Squares Estimate:

$$\hat{\underline{x}}_{LS} = (\underline{C}^T \bullet \underline{C})^{-1} \bullet \underline{C}^T \bullet \underline{y}$$

If m=n, this reduces to:

$$\hat{\underline{x}}_{LS} = \underline{C}^{-1} \bullet \underline{y}$$

However, for n>m, the term $(\underline{C}^T \bullet \underline{C})^{-1}$ does not exist, so this simple approach is of no direct use to the performance analyst. A Weighted Least Squares Estimate can be derived by including an (m•m) symmetrical weighting matrix $\underline{W}$ in the expression for J:

$$J = (\underline{y} - \underline{C} \bullet \hat{\underline{x}})^T \bullet \underline{W} \bullet (\underline{y} - \underline{C} \bullet \hat{\underline{x}})$$

Minimisation of J leads to:

$$\hat{\underline{x}}_{WLS} = (\underline{C}^T \bullet \underline{W} \bullet \underline{C})^{-1} \bullet \underline{C}^T \bullet \underline{W} \bullet \underline{y}$$

If $\underline{W}$ is equal to the inverse of the covariance matrix of the measurement noise ($\underline{R}$), then one obtains the Gauss-Markov Estimate:

$$\hat{\underline{x}}_{GM} = (\underline{C}^T \bullet \underline{R}^{-1} \bullet \underline{C})^{-1} \bullet \underline{C}^T \bullet \underline{R}^{-1} \bullet \underline{y}$$

If the measurement noise is normally distributed, the above equation can be derived by maximising the likelihood of $\hat{\underline{x}}$, given that $\underline{y}$ has occurred; this produces the Maximum Likelihood Estimate:

$$\hat{\underline{x}}_{ML} = (\underline{C}^T \bullet \underline{R}^{-1} \bullet \underline{C})^{-1} \bullet \underline{C}^T \bullet \underline{R}^{-1} \bullet \underline{y} \quad \text{for } \underline{v} = N(\underline{0}, \underline{R})$$

In order to extend the above estimates to include cases where n>m, an Extended Weighted Least Squares Estimate is derived, by considering $\hat{\underline{x}}$ to be distributed round a vector $\hat{\underline{x}}_0$; the expression for J now becomes:

$$J = (\hat{\underline{x}}-\hat{\underline{x}}_0)^T \bullet \underline{G} \bullet (\hat{\underline{x}}-\hat{\underline{x}}_0) + (\underline{y} - \underline{C} \bullet \hat{\underline{x}})^T \bullet \underline{W} \bullet (\underline{y} - \underline{C} \bullet \hat{\underline{x}})$$

where $\underline{G}$ is an (n•n) symmetrical weighting matrix. Minimisation of J leads to:

$$\hat{\underline{x}}_{EWLS} = \hat{\underline{x}}_0 + (\underline{G} + \underline{C}^T \bullet \underline{W} \bullet \underline{C})^{-1} \bullet \underline{C}^T \bullet \underline{W} \bullet (\underline{y} - \underline{C} \bullet \hat{\underline{x}}_0)$$

If $\underline{x}$ is considered to be a vector of random variables (mean $\bar{\underline{x}}$ and covariance $\underline{P}$), then the Minimum Variance Estimate:

$$\hat{\underline{x}}_{MV} = \bar{\underline{x}} + (\underline{P}^{-1} + \underline{C}^T \bullet \underline{R}^{-1} \bullet \underline{C})^{-1} \bullet \underline{C}^T \bullet \underline{R}^{-1} \bullet (\underline{y} - \underline{C} \bullet \bar{\underline{x}})$$

can be derived. If both the measurement noise and the component changes/sensor biasses are normally-distributed random variables, then application of Bayes' Theorem leads to the Bayes' Estimate:

$$\hat{\underline{x}}_B = \bar{\underline{x}} + (\underline{P}^{-1} + \underline{C}^T \bullet \underline{R}^{-1} \bullet \underline{C})^{-1} \bullet \underline{C}^T \bullet \underline{R}^{-1} \bullet (\underline{y} - \underline{C} \bullet \bar{\underline{x}})$$

$$= \bar{\underline{x}} + \underline{P} \bullet \underline{C}^T \bullet (\underline{C} \bullet \underline{P} \bullet \underline{C}^T + R)^{-1} \bullet (\underline{y} - \underline{C} \bullet \bar{\underline{x}})$$

$$\text{for } \underline{v} = N(\underline{0}, \underline{R}),\ \underline{x} = N(\bar{\underline{x}}, \underline{P})$$

The discussion above shows how, by adding extra information, different estimates for $\hat{\underline{x}}$ can be produced. Note that all the above estimates can be considered as more general cases of the Bayes' Estimate, as shown below.

If $\hat{\underline{x}} = \hat{\underline{x}}_0 + (\underline{G} + \underline{C}^T \bullet \underline{W} \bullet \underline{C})^{-1} \bullet \underline{C}^T \bullet \underline{W} \bullet (\underline{y} - \underline{C} \bullet \hat{\underline{x}}_0)$

then:

1) $\hat{\underline{x}}_0 = \underline{0},\ \underline{G} = \underline{0},\ \underline{W} = \underline{I} \Rightarrow \hat{\underline{x}} = \hat{\underline{x}}_{LS}$ Least Squares

2) $\hat{\underline{x}}_0 = \underline{0},\ \underline{G} = \underline{0},\ \underline{W} \neq \underline{I} \Rightarrow \hat{\underline{x}} = \hat{\underline{x}}_{WLS}$ Weighted Least Squares

3) $\hat{\underline{x}}_0 = \underline{0},\ \underline{G} = \underline{0},\ \underline{W} = \underline{R}^{-1} \Rightarrow \hat{\underline{x}} = \hat{\underline{x}}_{GM}$ Gauss Markov

4) $\hat{\underline{x}}_0 = \underline{0},\ \underline{G} = \underline{0},\ \underline{W} = \underline{R}^{-1}$, $\underline{v}$ normally distributed $\Rightarrow \hat{\underline{x}} = \hat{\underline{x}}_{ML}$ Maximum Likelihood

5) $\hat{\underline{x}}_0 = \underline{0},\ \underline{G} \neq \underline{0},\ \underline{W} \neq \underline{0} \Rightarrow \hat{\underline{x}} = \hat{\underline{x}}_{EWLS}$ Extended Weighted Least Squares

6) $\hat{\underline{x}}_0 = \bar{\underline{x}},\ \underline{G} = \underline{P}^{-1},\ \underline{W} = \underline{R}^{-1} \Rightarrow \hat{\underline{x}} = \hat{\underline{x}}_{MV}$ Minimum Variance

7) $\hat{\underline{x}}_0 = \bar{\underline{x}},\ \underline{G} = \underline{P}^{-1},\ \underline{W} = \underline{R}^{-1}$, $\bar{\underline{x}}$, $\underline{v}$ normally distributed $\Rightarrow \hat{\underline{x}} = \hat{\underline{x}}_B$ Bayes

Given the correct input, all the above estimates are unbiassed and consistent; however, the efficiency improves as we move down the list from Least Squares to Bayes. Since we require the best possible estimate of the vector of n component changes and sensor biasses ($\hat{\underline{x}}$) from the vector of m gas-path measurement differences ($\underline{y}$), in situations where n>m, we therefore concentrate our

attention on the Bayes estimator. Such an estimator is also known as the Kalman Filter, after the man who first formulated the estimator in a form that is suitable for easy recursive computation (Reference 6).

4.3 Formal Derivation of the Kalman Filter

There are many methods of deriving the equations that make up the Kalman Filter, reflecting the fact that it is applicable over a fairly general range of conditions. The derivation given below is based on that given in Reference 12; other derivations, starting from other standpoints, can be found in References 13 to 20. The Kalman Filter is normally used to produce sequential estimates from an ordered time sequence of gas-path measurement vectors; however, this recursive feature is not suitable for practical performance analysis, for three reasons:

1) Most sets of measurements to be analysed come from 'stand-alone' testing; they do not relate to any previous sets in a defined way;

2) The recursive feature imposes constraints on the input (to prevent the situation where the filter stops responding to the measurements) which could cause problems;

3) Even if the constraints of 1) and 2) are not present, the fact that the same measurement vector could produce different analyses, depending on its position in the time sequence, could cause confusion for the users.

The derivation of the Kalman Filter equations given here is therefore done for the calculation of a single 'best estimate' of the vector of component changes and sensor biasses that generated a given vector of gas-path measurement differences from expectation.

The starting-point for the Kalman Filter derivation is the following pair of equations:

$$1)\quad \underline{x} = \underline{\hat{x}}_0 + \underline{w}$$

where:

$\underline{x}$ = (n•1) vector of true component changes and sensor biasses;

$\underline{\hat{x}}_0$ = (n•1) datum vector of assumed component changes and sensor biasses (usually zero), considered to represent the estimate of the state of the gas turbine before any measurements are taken;

$\underline{w}$ = (n•1) normally distributed random vector of component changes and sensor biasses, with a mean of zero and a covariance of $\underline{Q}$ (n•n).

This equation represents our assumption that the gas turbine being analysed is considered to be one of a family whose component changes and sensor biasses are normally distributed about a mean defined by $\underline{\hat{x}}_0$, with 'spread' defined by $\underline{Q}$. Because changes in gas turbine components and sensor biasses can be thought of as arising from a summation of many small effects, the Central Limit Theorem leads to the justification of the assumption of normality.

2) $\underline{y} = \underline{C} \bullet \underline{x} + \underline{v}$

where:

$\underline{y}$ = (m•1) vector of percentage differences between observed and expected levels of gas-path measurements;

$\underline{C}$ = (m•n) System Matrix;

$\underline{x}$ = (n•1) vector of true component changes and sensor biasses, defined previously;

$\underline{v}$ = (m•1) vector of gas-path measurement noise terms, assumed to be normally distributed with a mean of zero and a covariance of $\underline{R}$ (m•m).

This measurement equation states the relationship between the gas-path measurement differences from expectation and the component changes and sensor biasses that generated them. The noise terms represent the 'corruption' of the gas-path measurements by non-repeatability in the measurement system.

The derivation runs as follows:

We require an estimator of the form:

$$\underline{\hat{x}} = \underline{K}' \bullet \underline{\hat{x}}_0 + \underline{K} \bullet \underline{y}$$

where:

$\underline{\hat{x}}$ = vector of best estimates of component changes and sensor biasses;

$\underline{\hat{x}}_0$, $\underline{y}$ defined previously;

$\underline{K}'$, $\underline{K}$ are weighting matrices.

This equation states that the desired form of the component change and sensor bias estimates is a weighted linear combination of the estimates of the component changes and sensor biasses before any measurements are taken and the information contained in the gas-path measurement differences from expectation. $\underline{K}'$ and $\underline{K}$ will be functions of $\underline{Q}$ (the assumed 'spread' of component changes

and sensor biasses), $\underline{R}$ (the 'spread' of gas-path measurement noise) and $\underline{C}$ (the System Matrix). The derivation of $\underline{K}'$ and $\underline{K}$ will lead to the formulae for the Kalman Filter.

If the estimation error before the measurements are taken is denoted by $\tilde{\underline{x}}(-)$, and the estimation error after the measurements are taken is denoted by $\tilde{\underline{x}}(+)$ then:

$$\hat{\underline{x}}_0 = \underline{x} + \tilde{\underline{x}}(-)$$

$$\hat{\underline{x}} = \underline{x} + \tilde{\underline{x}}(+)$$

ie estimated state = true state + estimation error

Using the previous formula for $\hat{\underline{x}}$:

$$\underline{x} + \tilde{\underline{x}}(+) = \underline{K}' \bullet (\underline{x} + \tilde{\underline{x}}(-)) + \underline{K} \bullet \underline{y}$$

Using the measurement equation, and rearranging:

$$\tilde{\underline{x}}(+) = \underline{K}' \bullet \underline{x} + \underline{K}' \bullet \tilde{\underline{x}}(-) + \underline{K} \bullet \underline{C} \bullet \underline{x} + \underline{K} \bullet \underline{v} - \underline{x}$$

$$= (\underline{K}' + \underline{K} \bullet \underline{C} - \underline{I}) \bullet \underline{x} + \underline{K}' \bullet \tilde{\underline{x}}(-) + \underline{K} \bullet \underline{v}$$

If we take expectations on both sides:

$$E[\tilde{\underline{x}}(+)] = (\underline{K}' + \underline{K} \bullet \underline{C} - \underline{I}) \bullet E[\underline{x}] + \underline{K}' \bullet E[\tilde{\underline{x}}(-)] + \underline{K} \bullet E[\underline{v}]$$

Now:

$E[\underline{v}] = \underline{0}$ by definition;

$E[\tilde{\underline{x}}(+)] = E[\tilde{\underline{x}}(-)] = \underline{0}$ if estimation unbiassed;

$E[\underline{x}] \neq \underline{0}$

Therefore, the only way that the above equation can be true is if:

$$\underline{K}' + \underline{K} \bullet \underline{C} - \underline{I} = \underline{0}$$

$$\underline{K}' = \underline{I} - \underline{K} \bullet \underline{C}$$

Therefore:

$$\hat{\underline{x}} = (\underline{I} - \underline{K} \bullet \underline{C}) \bullet \hat{\underline{x}}_0 + \underline{K} \bullet \underline{y}$$

$$\hat{\underline{x}} = \hat{\underline{x}}_0 + \underline{K} \bullet (\underline{y} - \underline{C} \bullet \hat{\underline{x}}_0)$$

==========

This is the basic equation for the Kalman Filter. In words:

Estimate after measurements taken
= Estimate before measurements taken plus weighting matrix multiplied by the difference between observed measurement differences and measurement differences predicted from estimate before measurements taken

If $\underline{K}$ is small, $\hat{\underline{x}}$ is essentially $\hat{\underline{x}}_0$, because the measurements are considered to carry little information about $\hat{\underline{x}}$: if $\underline{K}$ is large, $\hat{\underline{x}}_0$ is modified by $(\underline{y} - \underline{C} \bullet \hat{\underline{x}}_0)$ to produce an estimate $\hat{\underline{x}}$ that uses the information contained in the measurements.

To derive $\underline{K}$, we proceed as follows:

$$\underline{x} + \tilde{\underline{x}}(+) = (\underline{I} - \underline{K} \bullet \underline{C}) \bullet (\underline{x} + \tilde{\underline{x}}(-)) + \underline{K} \bullet \underline{C} \bullet \underline{x} + \underline{K} \bullet \underline{v}$$

$$\Rightarrow \tilde{\underline{x}}(+) = (\underline{I} - \underline{K} \bullet \underline{C}) \bullet \tilde{\underline{x}}(-) + \underline{K} \bullet \underline{v}$$

If we define:

$$\underline{P}_1 = E[\tilde{\underline{x}}(+) \bullet \tilde{\underline{x}}(+)^T]$$

$$\underline{P}_0 = E[\tilde{\underline{x}}(-) \bullet \tilde{\underline{x}}(-)^T]$$

and note:

$$E[\underline{v} \bullet \underline{v}^T] = \underline{R}$$

$$E[\tilde{\underline{x}}(-) \bullet \underline{v}^T] = \underline{0} \quad \text{(noise and estimation errors uncorrelated)}$$

then:

$$\begin{aligned}
\underline{P}_1 &= E[((\underline{I} - \underline{K} \bullet \underline{C}) \bullet \tilde{\underline{x}}(-) + \underline{K} \bullet \underline{v}) \bullet \\
&\qquad ((\underline{I} - \underline{K} \bullet \underline{C}) \bullet \tilde{\underline{x}}(-) + \underline{K} \bullet \underline{v})^T] \\
&= E[((\underline{I} - \underline{K} \bullet \underline{C}) \bullet \tilde{\underline{x}}(-)) \bullet (\tilde{\underline{x}}(-)^T \bullet (\underline{I} - \underline{K} \bullet \underline{C})^T)] \\
&\quad + E[\underline{K} \bullet \underline{v} \bullet (\tilde{\underline{x}}(-)^T \bullet (\underline{I} - \underline{K} \bullet \underline{C})^T)] \\
&\quad + E[((\underline{I} - \underline{K} \bullet \underline{C}) \bullet \tilde{\underline{x}}(-)) \bullet \underline{v}^T \bullet \underline{K}^T] \\
&\quad + E[\underline{K} \bullet \underline{v} \bullet \underline{v}^T \bullet \underline{K}^T] \\
&= (\underline{I} - \underline{K} \bullet \underline{C}) \bullet \underline{P}_0 \bullet (\underline{I} - \underline{K} \bullet \underline{C})^T + \underline{K} \bullet \underline{R} \bullet \underline{K}^T
\end{aligned}$$

$\underline{K}$ is chosen to minimise the sum of the diagonal elements of $\underline{P}_1$; ie the total of the variances of the estimation errors of the component changes and sensor biasses is minimised. This sum is known as the trace of the matrix. A result used to derive $\underline{K}$ is:

$$\frac{\delta}{\delta A}\ (\text{trace}\ (\underline{A} \bullet \underline{B} \bullet \underline{A}^T)) = 2 \bullet \underline{A} \bullet \underline{B} = \underline{0}\ \text{for minimum}$$

Therefore:

$$-2 \bullet (\underline{I} - \underline{K} \bullet \underline{C}) \bullet \underline{P}_0 \bullet \underline{C}^T + 2 \bullet \underline{K} \bullet \underline{R} = \underline{0}$$

$$\Rightarrow \underline{K} = \underline{P}_0 \bullet \underline{C}^T \bullet (\underline{C} \bullet \underline{P}_0 \bullet \underline{C}^T + \underline{R})^{-1}$$

If $\underline{P}_0$ is assumed to equal $\underline{Q}$, the covariance of the component changes and sensor biasses round $\hat{\underline{x}}_0$, then:

$$\underline{K} = \underline{Q} \bullet \underline{C}^T \bullet (\underline{C} \bullet \underline{Q} \bullet \underline{C}^T + \underline{R})^{-1}$$

This is the equation for the weighting matrix used to adjust the estimate of the component changes and sensor biasses before the measurements were taken by the difference between the observed gas-path measurement differences and those predicted from the pre-measurement estimate.

As a final result, we note that:

$$\underline{P}_1 = (\underline{I} - \underline{K} \bullet \underline{C}) \bullet \underline{Q} \bullet (\underline{I} - \underline{K} \bullet \underline{C})^T + \underline{K} \bullet \underline{R} \bullet \underline{K}^T$$

$$= (\underline{I} - \underline{K} \bullet \underline{C}) \bullet \underline{Q} - (\underline{I} - \underline{K} \bullet \underline{C}) \bullet \underline{Q} \bullet \underline{C}^T \bullet \underline{K}^T + \underline{K} \bullet \underline{R} \bullet \underline{K}^T$$

$$= (\underline{I} - \underline{K} \bullet \underline{C}) \bullet \underline{Q} - (\underline{Q} \bullet \underline{C}^T - \underline{K} \bullet (\underline{C} \bullet \underline{Q} \bullet \underline{C}^T + \underline{R})) \bullet \underline{K}^T$$

When $\underline{K}$ is substituted into the second term, it disappears, leaving:

$$\underline{P}_1 = (\underline{I} - \underline{K} \bullet \underline{C}) \bullet \underline{Q}$$

This equation gives the covariance of the estimates for the component changes and sensor biasses round $\hat{\underline{x}}$.

The Kalman Filter equations can therefore be summarised as:

1) $\hat{\underline{x}} = \hat{\underline{x}}_0 + \underline{K} \bullet (\underline{y} - \underline{C} \bullet \hat{\underline{x}}_0)$

2) $\underline{K} = \underline{Q} \bullet \underline{C}^T \bullet (\underline{C} \bullet \underline{Q} \bullet \underline{C}^T + \underline{R})^{-1}$

3) $\underline{P}_1 = (\underline{I} - \underline{K} \bullet \underline{C}) \bullet \underline{Q}$

where:

$\hat{\underline{x}}$ = vector of best estimates of component changes and sensor biasses after gas-path measurement

differences from expectations are observed;

$\hat{\underline{x}}_0$ = vector of best estimates of component changes and sensor biasses before gas-path measurement differences from expectation are observed. This vector is usually zero; in this case, $\hat{\underline{x}} = \underline{K} \bullet \underline{y}$;

$\underline{y}$ = vector of gas-path measurement differences from expectation;

$\underline{K}$ = Kalman Gain Matrix;

$\underline{C}$ = System Matrix, relating gas-path measurement differences to component changes and sensor biasses;

$\underline{Q}$ = covariance matrix of component changes and sensor biasses (usually diagonal);

$\underline{R}$ = measurement repeatability covariance matrix;

$\underline{P}_1$ = covariance matrix of best estimates of component changes and sensor biasses;

$\underline{I}$ = identity matrix.

4.4 Meaning of Results

Before proceeding with an explanation of what the Kalman Filter equations represent in simple terms, it is useful to summarise what the various terms in the equations mean.

$\hat{\underline{x}}$ is what we are trying to determine; the best estimate of component changes and sensor biasses that generated the observed gas-path measurement differences $\underline{y}$.

$\underline{C}$ contains the information that enables us to derive gas-path measurement differences from component changes and sensor biasses.

$\hat{\underline{x}}_0$, $\underline{Q}$ and $\underline{R}$ contain prior information (ie information known before $\underline{y}$ is observed) about the expected levels of component changes and sensor biasses, the 'spread' or uncertainty of component changes and sensor biasses around $\hat{\underline{x}}_0$, and the 'spread' or uncertainty of gas-path measurement differences due to non-repeatability in the measurement system respectively.

To explain what $\underline{K}$ and $\underline{P}_1$ represent, it is helpful to write the equations for them in different forms:

$$\underline{K} = \underline{Q} \bullet \underline{C}^T \bullet (\underline{C} \bullet \underline{Q} \bullet \underline{C}^T + \underline{R})^{-1}$$

$$\underline{K} \bullet (\underline{C} \bullet \underline{Q} \bullet \underline{C}^T + \underline{R}) = \underline{Q} \bullet \underline{C}^T$$

$$\underline{K} \bullet (\underline{I} + \underline{C} \bullet \underline{Q} \bullet \underline{C}^T \bullet \underline{R}^{-1}) = \underline{Q} \bullet \underline{C}^T \bullet \underline{R}^{-1}$$

$$\underline{K} = (\underline{I} - \underline{K} \bullet \underline{C}) \bullet \underline{Q} \bullet \underline{C}^T \bullet \underline{R}^{-1}$$

$$\Rightarrow \underline{K} = \underline{P}_1 \bullet \underline{C}^T \bullet \underline{R}^{-1}$$

$$\underline{P}_1 = (\underline{I} - \underline{K} \bullet \underline{C}) \bullet \underline{Q}$$

$$= (\underline{I} - \underline{P}_1 \bullet \underline{C}^T \bullet \underline{R}^{-1} \bullet \underline{C}) \bullet \underline{Q}$$

$$\underline{I} = (\underline{P}_1^{-1} - \underline{C}^T \bullet \underline{R}^{-1} \bullet \underline{C}) \bullet \underline{Q}$$

$$\underline{Q}^{-1} = \underline{P}_1^{-1} - \underline{C}^T \bullet \underline{R}^{-1} \bullet \underline{C}$$

$$\Rightarrow \underline{P}_1 = (\underline{Q}^{-1} + \underline{C}^T \bullet \underline{R}^{-1} \bullet \underline{C})^{-1}$$

$$\Rightarrow \underline{K} = (\underline{Q}^{-1} + \underline{C}^T \bullet \underline{R}^{-1} \bullet \underline{C})^{-1} \bullet \underline{C}^T \bullet \underline{R}^{-1}$$

It is seen that $\underline{K}$ is proportional to the uncertainty in the estimate $\hat{\underline{x}}$, and inversely proportional to the uncertainty in the measurements $\underline{y}$. If the uncertainty in the measurements $\underline{R}$ (ie the measurement noise) is large relative to the uncertainty in the estimate ($\underline{P}_1$) then $\underline{K}$ will be small, and only small changes to the prior estimate $\hat{\underline{x}}_0$ will be made; ie noisy measurements do not carry enough 'weight' to alter our previous estimates of the component changes and sensor biasses. If the uncertainty in the measurements ($\underline{R}$) is small relative to the uncertainty in the estimate ($\underline{P}_1$) then $\underline{K}$ will be large, and large changes will be made to the prior estimate $\hat{\underline{x}}_0$; ie the measurements contain 'good' information that enables us to modify a previous estimate of the component changes and sensor biasses. If $\underline{C}$ is square, and $\underline{R}$ tends to zero, then $\underline{K}$ tends to $\underline{C}^{-1}$; if $\hat{\underline{x}}_0$ is zero (the usual case), then:

$$\hat{\underline{x}} = \underline{C}^{-1} \bullet \underline{y}$$

This equation is equivalent to 'traditional' analysis, where $\underline{C}^{-1}$, the inverse of the component exchange rate table, is a table of test bed analysis exchange rates: in this table, the percentage change in each component performance parameter for a 1% change in each gas-path measurement is shown. Note that, in this case, no prior information about $\underline{Q}$ and $\underline{R}$ is required.

The inverse of $\underline{P}_1$ is seen to be the sum of the inverse of

$\underline{Q}$ and a term proportional to the inverse of $\underline{R}$. If the uncertainty in the measurements $\underline{R}$ is large, then $\underline{P}_1$ will not be substantially different from $\underline{Q}$; ie noisy measurements do not improve our uncertainty about the estimates of the component changes and sensor biasses. If the uncertainty in the measurements $\underline{R}$ is small, then $\underline{P}_1$ will be reduced; ie 'good' measurements reduce our uncertainty about the estimates of the component changes and sensor biasses. If $\underline{C}$ is square and $\underline{R}$ tends to zero, then, because $\underline{K}$ tends to $\underline{C}^{-1}$, $\underline{P}_1$ tends to zero (as $\underline{K} \bullet \underline{C}$ tends to $\underline{I}$); there is no uncertainty about the estimates of component changes in this case.

The use of prior information about expected levels of component changes and sensor biasses, uncertainties in both the expected levels of component changes and sensor biasses and uncertainties in the measurements is an unfamiliar concept to many people. To illustrate the concept of using prior information, consider a scalar variable b which is thought to be linearly related to a scalar variable a; see Figure 23.

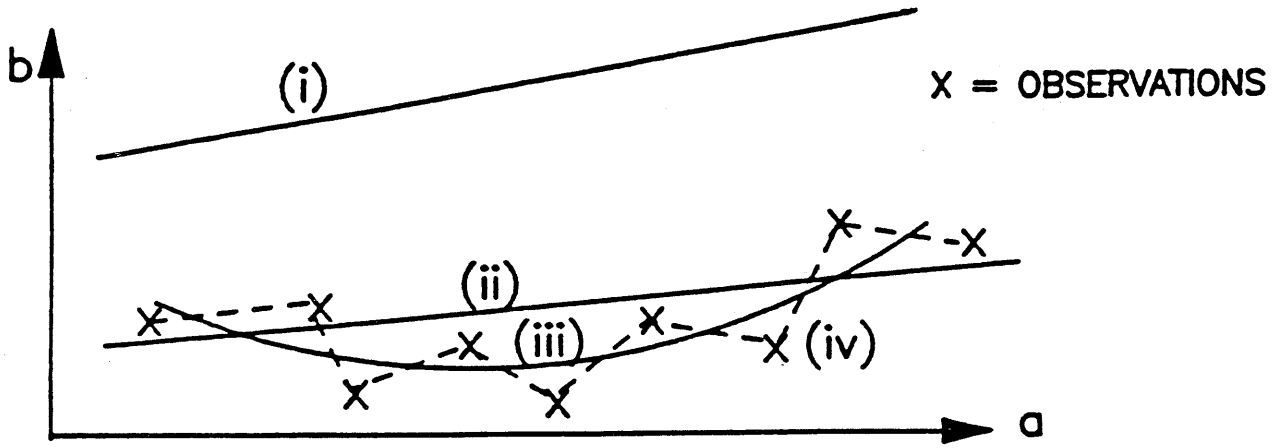

Figure 23: Use of prior information

Line (i) in Figure 23 shows the expected prior relationship between b and a before the observations are taken. If the noise in the observations is thought to be very large, and the uncertainty about the position of line (i) is thought to be zero, then the estimate of the relationship between b and a will not be altered by the observations, and line (i) will be the 'best estimate' of the actual relationship. Line (ii) shows the 'best estimate' of the actual relationship between b and a if the noise in the observations is considered to be smaller, and the uncertainty about the prior relationship between b and a (line (i)) is increased, while still being considered to be linear. Line (iii) shows the 'best

estimate' of the actual relationship between b and a if a non-linear form is considered. The dotted line (iv) shows the 'best estimate' of the actual relationship between b and a if the noise in the observations is considered to be zero, and the uncertainty about the prior relationship between b and a (line (i)) is very large. It is obvious that, given different prior information, very different estimates of the actual relationship between b and a are produced. Note that least-squares curve fitting uses prior information about the shape of a relationship (expressed as the order of the curve-fit), but does not use any information about the noise in the observations; it would therefore produce yet another estimate of the relationship between b and a, based on less prior information.

4.5 Kalman Filter 'Concentrator'

The Kalman Filter has one property which can cause problems; the least-squares basis of the Filter causes the estimates of all the possible component changes and sensor biasses included in the system matrix to be non-zero, even if it is known that the gas-path measurement differences input to the Filter are due to only a sub-set of the possible component changes and sensor biasses. This results in under-estimation of the 'genuine' component changes and sensor biasses that were known to have caused the observed gas-path measurement differences, and analysis of component changes and sensor biasses that were not part of the set that caused those measurement differences. Because it was felt that this 'smearing' would cause confusion among users, a 'Concentrator' has been developed, which removes spurious component changes and sensor biasses from the analysis, while retaining those component changes and sensor biasses that caused the observed gas-path measurement differences. The methods used by the 'Concentrator' are discussed below.

The objective of the 'Concentrator' is to selectively remove individual component changes and/or sensor biasses from the problem (by setting their uncertainties to zero), while still ensuring that enough component changes and/or sensor biasses remain to 'explain' the observed gas-path measurement differences. The procedure is as follows:

1) Run the Kalman Filter as described above, including all the component changes and sensor biasses in the System Matrix;

2) Evaluate an Objective Function:

$$f = (\underline{y} - \underline{C} \bullet \underline{\hat{x}})^T \bullet \underline{R}^{-1} \bullet (\underline{y} - \underline{C} \bullet \underline{\hat{x}})$$

This gives a measure of the amount of unexplained measurement change, and is distributed as chi-square, with the number of degrees of freedom equal to the number of gas-path measurements;

3) Normalise each element of the vector $\hat{\underline{x}}$ by dividing by the square root of the respective diagonal element of the $\underline{P}_1$ matrix to produce a vector $\hat{\underline{x}}_n$:

$$\text{i'th element of } \hat{\underline{x}}_n = \frac{\text{i'th element of } \hat{\underline{x}}}{\sqrt{(\text{i'th diagonal element of } \underline{P}_1)}}$$

4) To start the 'Concentrator' off, component changes and sensor biasses whose elements in $\hat{\underline{x}}_n$ have absolute values less than the average of all the absolute values of the elements in $\hat{\underline{x}}_n$ are removed. Once the 'Concentrator' has been started, component changes and sensor biasses whose elements in $\hat{\underline{x}}_n$ have absolute values that reduce as the 'Concentrator' proceeds are removed. In all cases, at least one, but not all, of the component changes and sensor biasses are removed;

5) The Kalman Filter is re-run, including only those component changes and sensor biasses that have not been removed by 4), to produce a new vector $\hat{\underline{x}}$ of best estimates of component changes and sensor biasses;

6) Steps 2) to 5) are repeated until only one component change or sensor bias is left. The series of vectors of best estimates of component changes and sensor biasses (each with a different number of changes and biasses) produced by each run of the Kalman Filter are numbered sequentially in the order in which they were generated;

7) A maximum value for the objective function value is selected, either from user input or calculated from a chi-square probability distribution, the number of degrees of freedom and a user-defined probability level. The highest-numbered $\hat{\underline{x}}$ vector whose corresponding objective function value is less than this maximum is selected as the 'best answer', ie the smallest set of component changes and/or sensor biasses that successfully 'explains' the observed gas-path measurement differences. If none of the objective function values are less than the maximum, the basic Kalman Filter result from 1) above is taken as the 'best answer';

8) The 'best answer' is further modified by rejecting component changes and sensor biasses whose elements in $\hat{\underline{x}}$ have absolute values less than a user-specified number of standard deviations. The user is therefore presented with the most significant set of estimated component changes and sensor biasses that generated the observed gas-path measurement differences.

Figure 24 shows how the 'Concentrator' produces an improvement on the answer produced by the basic Kalman Filter, by producing estimates of component changes and

A) BEST ESTIMATES ($\hat{x}$) FROM 'CONCENTRATOR'

		①	②	③	④	⑤ ← PASS N°
	FAN ETA	0.133	0.0	0.0	0.0	0.0
	FAN CAP	-0.092	0.0	0.0	0.0	0.0
	LPC ETA	-0.295	0.0	0.0	0.0	0.0
	* LPC CAP	0.0	0.0	0.0	0.0	0.0
-1% —	HPC ETA	-0.627	-0.977	-1.117	-1.108	-1.718
	HPC CAP	-0.047	0.0	0.0	0.0	0.0
	HPT ETA	-0.499	-0.102	0.0	0.0	0.0
	HPT CAP	-0.116	0.0	0.0	0.0	0.0
	LPT ETA	-0.271	0.0	0.0	0.0	0.0
	* LPT CAP	0.0	0.0	0.0	0.0	0.0
	EPR	0.051	0.0	0.0	0.0	0.0
+0.5% —	P2	0.281	0.370	0.435	0.0	0.0
	T2	-0.209	-0.094	0.0	0.0	0.0
	WFE	-0.222	-0.067	0.0	0.0	0.0
	P26	-0.083	0.0	0.0	0.0	0.0
	T26	-0.209	-0.094	0.0	0.0	0.0
	P3	0.016	0.0	0.0	0.0	0.0
	T3	0.049	0.0	0.0	0.0	0.0
+1% —	T49	0.343	0.789	0.835	0.826	0.0
	P13	-0.094	0.0	0.0	0.0	0.0
	* XNL	0.0	0.0	0.0	0.0	0.0
	* XNH	0.0	0.0	0.0	0.0	0.0
	FN	0.022	0.0	0.0	0.0	0.0
	W1A	0.082	0.0	0.0	0.0	0.0
	TOTAL SS	63.971	121.810	133.197	286.126	626.406
	CHNGE SS	57.191	102.242	119.880	98.900	73.802
	MEAS SS	6.780	19.568	13.317 →	187.227	552.604 ← OBJECTIVE FUNCTION

(LIMIT 19.7)

ACTUAL COMPONENT CHANGES AND SENSOR BIASSES USED TO GENERATE MEASUREMENT DIFFERENCES

BASIC KALMAN FILTER (NOTE UNDERESTIMATES FOR HPCETA, P2, T49; OVERESTIMATES FOR OTHERS, E.G. HPT ETA)

BEST ANSWER (VERY CLOSE TO ACTUAL CHANGES + BIASSES)

(NOTE LARGE JUMP IN OBJECTIVE FUNCTION WHEN P2 BIAS REMOVED)

* = THESE COMPONENT CHANGES AND SENSOR BIASSES NOT ACTIVATED

B) STANDARD DEVIATIONS (SQUARE ROOTS OF P1 DIAGONAL ELEMENTS) FOR ABOVE

FAN ETA	0.16552	0.0	0.0	0.0	0.0
FAN CAP	0.13883	0.0	0.0	0.0	0.0
LPC ETA	0.17926	0.0	0.0	0.0	0.0
* LPC CAP	0.0	0.0	0.0	0.0	0.0
HPC ETA	0.13323	0.09671	0.03422	0.03421	0.00868
HPC CAP	0.15976	0.0	0.0	0.0	0.0
HPT ETA	0.10311	0.05266	0.0	0.0	0.0
HPT CAP	0.13844	0.0	0.0	0.0	0.0
LPT ETA	0.14240	0.0	0.0	0.0	0.0
* LPT CAP	0.0	0.0	0.0	0.0	0.0
EPR	0.04306	0.0	0.0	0.0	0.0
P2	0.06773	0.04074	0.03516	0.0	0.0
T2	0.05870	0.03409	0.0	0.0	0.0
WFE	0.08776	0.07400	0.0	0.0	0.0
P26	0.07398	0.0	0.0	0.0	0.0
T26	0.05073	0.03079	0.0	0.0	0.0
P3	0.09055	0.0	0.0	0.0	0.0
T3	0.08121	0.0	0.0	0.0	0.0
T49	0.08412	0.05205	0.04478	0.04477	0.0
P13	0.05592	0.0	0.0	0.0	0.0
* XNL	0.0	0.0	0.0	0.0	0.0
* XNH	0.0	0.0	0.0	0.0	0.0
FN	0.08774	0.0	0.0	0.0	0.0
W1A	0.06230	0.0	0.0	0.0	0.0

Figure 24: 'Concentrator' performance for -1% HPC ETA, +0.5% P2 bias, +1% T49 bias

sensor biasses that are very close to those used to generate the gas-path measurement differences analysed.

4.6 Input Required for the Kalman Filter

This section discusses the input to the Kalman Filter algorithm that the performance analyst has to provide, and compares this input with the knowledge used by the experienced performance analyst when analysing a gas turbine.

The Kalman Filter requires:

1) Component Exchange Rate and Environmental Exchange Rate tables, as discussed in the previous chapter, which are used to produce the System Matrix. These tables contain the necessary thermodynamic relationships between component changes and gas-path measurement changes, and the apparent changes in gas-path measurements due to environmental measurement errors.

   The experienced performance analyst would always have such tables available, to refer to during the analysis process;

2) A set of expected levels of gas-path measurements, at the flight conditions and power setting at which the analysis is to be done, for a datum gas turbine; ie an engine whose performance is at some desired level with which others can be compared. Since the best estimates of component changes and sensor biasses produced by the Kalman Filter will be relative to this datum, it follows that the datum gas turbine component changes and sensor biasses are all zero ($\underline{\hat{x}}_0 = \underline{0}$). To do an analysis, percentage differences between observed and expected levels of gas-path measurements are input into the Kalman Filter to produce the desired best estimates of component changes and sensor biasses that produced those differences.

   The experienced performance analyst will always have some idea of the values of gas-path measurements and component performance parameters that he would expect to see from the gas turbine he is analysing; the above information (expected values of gas-path measurements, component changes and sensor biasses all zero) is exactly analogous to this;

3) A set of standard deviations of the repeatabilities in both the gas-path measurements, flight condition measurements and power-setting parameter measurements. These are used to calculate the $\underline{R}$ matrix as follows:

$$\underline{R} = \underline{C}' \bullet \underline{V} \bullet \underline{C}'^{T}$$

where:

$\underline{R}$ = measurement noise covariance matrix, as used in the Kalman Filter;

$\underline{V}$ = (t•t) diagonal matrix of squares of standard deviations of repeatabilities, where t = number of environmental parameters + number of gas-path measurements;

$\underline{C}'$ = (m•t) matrix, which contains both the environmental exchange rate table and a unit matrix, as shown in Figure 25;

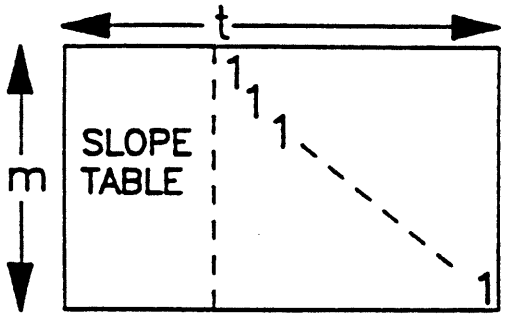

Figure 25: Diagrammatic representation of $\underline{C}'$ matrix

The $\underline{R}$ matrix therefore contains the variances and covariances of the apparent non-repeatabilities in the gas-path measurement differences, due to both the non-repeatability in the observed gas-path measurements and the non-repeatability in the expected gas-path measurements due to non-repeatability in the flight condition and power-setting parameter measurements that define the levels of the expected gas-path measurements.

The experienced performance analyst will always have in mind (if only subjectively) some idea of how repeatable the measurements are, in order to give more 'weight' in his analysis to the more repeatable measurements; this is exactly analogous to the way the $\underline{R}$ matrix is used in the Kalman Filter;

4) A set of standard deviations of the component changes and sensor biasses about their nominal levels. The $\underline{Q}$ matrix is set up by creating a diagonal matrix containing the squares of these standard deviations.

The experienced performance analyst will always have in mind (if only subjectively) some idea of the possible 'spread' of component change and sensor bias around the datum gas turbine, in order to assess the potential for component change and sensor bias in the engine he is analysing. Effectively, he is 'weighting' some

component changes and sensor biasses more than others, and will tend to adjust his analysis to reflect these beliefs. This is exactly analogous to the function of the $\underline{Q}$ matrix in the Kalman Filter.

It is seen, therefore, that the Kalman Filter requires essentially the same information that the experienced performance analyst needs when doing a gas turbine analysis, except that qualitative 'feels' for measurement non-repeatability and component change/sensor bias possibilities are replaced by quantitative values in the $\underline{R}$ and $\underline{Q}$ matrices. The values for the $\underline{R}$ matrix can usually be deduced from repeatability studies on the measurement system, but the values for the $\underline{Q}$ matrix require more thought; the setting up of these values will be discussed later.

4.7 Sensitivity Analysis

The sensitivity of the Kalman Filter to its input, particularly the elements of the (usually diagonal) $\underline{V}$ and $\underline{Q}$ matrices discussed above, can easily be found by differentiating the equations defining the Kalman Filter with respect to the individual elements in those matrices. We have:

$$\underline{K} = \underline{Q} \bullet \underline{C}^T \bullet (\underline{C} \bullet \underline{Q} \bullet \underline{C}^T + \underline{R})^{-1}$$

$$\underline{R} = \underline{C}' \bullet \underline{V} \bullet \underline{C}'^T$$

$$\underline{P}_1 = (\underline{I} - \underline{K} \bullet \underline{C}) \bullet \underline{Q}$$

where the terms have the meanings defined previously.

Differentiation with respect to an element q_i in the matrix $\underline{Q}$ is done as follows:

$$\underline{K} \bullet (\underline{C} \bullet \underline{Q} \bullet \underline{C}^T + \underline{R}) = \underline{Q} \bullet \underline{C}^T$$

$$\frac{\delta \underline{K}}{\delta q_i} \bullet (\underline{C} \bullet \underline{Q} \bullet \underline{C}^T + \underline{R}) + \underline{K} \bullet (\underline{C} \bullet \frac{\delta \underline{Q}}{\delta q_i} \bullet \underline{C}^T) = \frac{\delta \underline{Q}}{\delta q_i} \bullet \underline{C}^T$$

$$\frac{\delta \underline{K}}{\delta q_i} = ((\underline{I} - \underline{K} \bullet \underline{C}) \bullet \frac{\delta \underline{Q}}{\delta q_i} \bullet \underline{C}^T) \bullet (\underline{C} \bullet \underline{Q} \bullet \underline{C}^T + \underline{R})^{-1}$$

Since $q_i = s_i^2$, where s_i is the user-supplied standard deviation:

$$\frac{\delta q_i}{\delta s_i} = 2 \bullet s_i$$

$$\frac{\delta \underline{K}}{\delta s_i} = \frac{\delta \underline{K}}{\delta q_i} \bullet \frac{\delta q_i}{\delta s_i}$$

$$\frac{\delta \underline{K}}{\delta s_i} = 2 \bullet s_i \bullet ((\underline{I} - \underline{K} \bullet \underline{C}) \bullet \frac{\delta \underline{Q}}{\delta q_i} \bullet \underline{C}^T) \bullet (\underline{C} \bullet \underline{Q} \bullet \underline{C}^T + \underline{R})^{-1}$$

Note that $\frac{\delta \underline{Q}}{\delta q_i}$ is a zero matrix with 1 in row i, column i.

All the other terms are as defined previously.

Also:

$$\frac{\delta \underline{P}_1}{\delta q_i} = (\underline{I} - \underline{K} \bullet \underline{C}) \bullet \frac{\delta \underline{Q}}{\delta q_i} - \frac{\delta \underline{K}}{\delta q_i} \bullet \underline{C} \bullet \underline{Q}$$

$$\frac{\delta \underline{P}_1}{\delta s_i} = \frac{\delta \underline{P}_1}{\delta q_i} \bullet \frac{\delta q_i}{\delta s_i}$$

$$\frac{\delta \underline{P}_1}{\delta s_i} = 2 \bullet s_i \bullet (\underline{I} - \underline{K} \bullet \underline{C}) \bullet \frac{\delta \underline{Q}}{\delta q_i} - \frac{\delta \underline{K}}{\delta s_i} \bullet \underline{C} \bullet \underline{Q}$$

$\underline{P}_1$ is a variance matrix, and we are interested in the variation of standard deviations; we therefore define a new matrix $\underline{T}$, whose elements are the square roots of the elements of $\underline{P}_1$. If the element of interest in $\underline{T}$ is denoted by t_j, and has a corresponding element p_j in $\underline{P}_1$, then:

$$p_j = t_j^2$$

$$\frac{\delta p_j}{\delta t_j} = 2 \bullet t_j$$

$$\frac{\delta t_j}{\delta s_i} = \frac{\delta p_j}{\delta s_i} \bullet \frac{\delta t_j}{\delta p_j}$$

$$\frac{\delta t_j}{\delta s_i} = \frac{1}{2 \bullet t_j} \bullet (2 \bullet s_i \bullet (\underline{I} - \underline{K} \bullet \underline{C}) \bullet \frac{\delta \underline{Q}}{\delta q_i} - \frac{\delta \underline{K}}{\delta s_i} \bullet \underline{C} \bullet \underline{Q})$$

Differentiation with respect to an element v_i in the matrix $\underline{V}$ is done as follows:

$$\underline{K} \bullet (\underline{C} \bullet \underline{Q} \bullet \underline{C}^T + \underline{C}' \bullet \underline{V} \bullet \underline{C}'^T) = \underline{Q} \bullet \underline{C}^T$$

$$\frac{\delta \underline{K}}{\delta v_i} \bullet (\underline{C} \bullet \underline{Q} \bullet \underline{C}^T + \underline{R}) + \underline{K} \bullet \underline{C}' \bullet \frac{\delta \underline{V}}{\delta v_i} \bullet \underline{C}'^T = \underline{0}$$

$$\frac{\delta \underline{K}}{\delta v_i} = (-\underline{K} \bullet \underline{C}' \bullet \frac{\delta \underline{V}}{\delta v_i} \bullet \underline{C}'^T) \bullet (\underline{C} \bullet \underline{Q} \bullet \underline{C}^T + \underline{R})^{-1}$$

Since $v_i = r_i^2$, where r_i is the user-supplied standard deviation:

$$\frac{\delta v_i}{\delta r_i} = 2 \bullet r_i$$

$$\frac{\delta K}{\delta r_i} = \frac{\delta K}{\delta v_i} \bullet \frac{\delta v_i}{\delta r_i}$$

$$\frac{\delta K}{\delta r_i} = 2 \bullet r_i \bullet (-\underline{K} \bullet \underline{C}' \bullet \frac{\delta V}{\delta v_i} \bullet \underline{C}'^{T}) \bullet (\underline{C} \bullet \underline{Q} \bullet \underline{C}^{T} + \underline{R})^{-1}$$

Note that $\frac{\delta V}{\delta v_i}$ is a zero matrix with 1 in row i, column i.

All the other terms are as defined previously.

Also:

$$\frac{\delta P_1}{\delta r_i} = - \frac{\delta K}{\delta r_i} \bullet \underline{C} \bullet \underline{Q}$$

Using the previous definition of the $\underline{T}$ matrix, and the results that followed:

$$\frac{\delta t_j}{\delta r_i} = \frac{\delta p_j}{\delta r_i} \bullet \frac{\delta t_j}{\delta p_j}$$

$$\frac{\delta t_j}{\delta r_i} = \frac{1}{2 \bullet t_j} \bullet - \frac{\delta K}{\delta r_i} \bullet \underline{C} \bullet \underline{Q}$$

These formulae can be used to calculate the sensitivity of the Kalman Gain Matrix and the standard deviations of the estimates (which are used in the 'Concentrator') to the assumptions made about measurement non-repeatability and component change and sensor bias standard deviations; these results can be used in the 'tuning' of the Kalman Filter, which is discussed in the next section.

Differentiation with respect to the elements of the $\underline{C}$ matrix is also possible, but the formulae are quite complex and, since the number of elements in the $\underline{C}$ matrix is large, the results from a complete differentiation would be quite voluminous.

4.8 'Tuning' the Kalman Filter

As stated at the end of the previous section, the Kalman Filter requires, as part of its input, standard deviations of component changes and sensor biasses, which reflect the relative probabilities of occurrence of individual changes and biasses. This input is critical to the performance of the filter, but is unfortunately very difficult to derive formally (as stated in Reference 4). This section discusses the various methods that can be used to determine these standard deviations; the adjustment of

these values to give an acceptable analysis is known as 'tuning'.

4.9 Methods of Deriving Component Change and Sensor Bias Standard Deviations

1) Engineering Judgement

The performance analyst using the Kalman Filter can set up the component change and sensor bias standard deviations in a way that reflects his assessment of the relative amounts of change that are possible in each individual change and bias; large standard deviations are set up for component changes and sensor biasses that are more likely to have occurred, whereas small standard deviations are set up for component changes and sensor biasses that are less likely to have occurred.

This method is obviously easy to implement (since it requires no data, other than experience), but is not formalised in any way, and carries no guarantee of 'correctness'.

2) Calculations Using Measurement Scatter

Given enough data, the $\underline{Q}$ matrix can be calculated directly as follows. We have:

$$\underline{y} = \underline{C} \bullet \underline{x} + \underline{v}$$

where the terms have the usual meanings. Therefore:

$$\text{Cov}(\underline{y}) = \underline{Z} = \underline{C} \bullet \underline{Q} \bullet \underline{C}^T + \underline{R}$$

$$\underline{C} \bullet \underline{Q} \bullet \underline{C}^T = (\underline{Z} - \underline{R})$$

Using the concept of the pseudo-inverse:

$$\underline{Q} = \underline{C}^{\#} \bullet (\underline{Z} - \underline{R}) \bullet \underline{C}^{\#T}$$

$\underline{Z}$ can be calculated as $E[(\underline{y}-\bar{\underline{y}}) \bullet (\underline{y}-\bar{\underline{y}})^T]$: $\underline{R}$ and $\underline{C}$ are known, so $\underline{Q}$ can be calculated. The required standard deviations of the component changes and sensor biasses can be calculated by taking the square roots of the diagonal elements in the $\underline{Q}$ matrix; this removes spurious cross-correlations between component changes and sensor biasses that are not 'physically' connected but may arise purely from the choice of gas turbines in the sample.

This method is the most justifiable one on theoretical grounds; it does, however, require a very large sample of gas turbines containing representative sets of component changes and sensor biasses. In practice, because of improvements and modifications made to

gas turbines over time, this latter requirement is hardly ever met.

3) Calculations Using Analysis Scatter

Given enough data, the $\underline{Q}$ matrix can be calculated from the covariance of the analysis of a number of engines, $E[(\underline{\hat{x}}-\underline{\bar{x}})\bullet(\underline{\hat{x}}-\underline{\bar{x}})^T]$. As before, the required standard deviations of the component changes and sensor biasses can be calculated by taking the square roots of the diagonal elements in the above matrix.

This method is the least satisfactory of the three methods presented; the covariance of the analysis depends on the standard deviations being searched for (since $\underline{\hat{x}}$ depends on these), and it does require the same large sample of gas turbines as the previous method.

4) Other Possible Calculations

Previous sections showed that the Kalman Filter effectively minimises the quantity:

$$J = (\underline{\hat{x}} - \underline{\hat{x}}_0)^T \bullet \underline{Q}^{-1} \bullet (\underline{\hat{x}} - \underline{\hat{x}}_0) + (\underline{y} - \underline{C} \bullet \underline{\hat{x}})^T \bullet \underline{R}^{-1} \bullet (\underline{y} - \underline{C} \bullet \underline{\hat{x}})$$

where the terms have the usual meanings. Reference 14 shows that:

$$E[J] = m \div 2$$

where m = number of gas-path measurements.

Therefore, if the value of J is evaluated for a number of analyses and averaged (to produce E[J]), a factor $\sqrt{(2 \bullet E[J] \div m)}$ can be calculated that, when applied to the measurement repeatability standard deviations and component change/sensor bias standard deviations, will adjust the value of E[J] to its required level. Note that, because this scale factor appears in the numerator and denominator of the Kalman Gain Matrix, the best estimates of component changes and sensor biasses will be unaffected; the values in the $\underline{Q}$ and $\underline{R}$ matrices have just been scaled equally.

4.10 Use of Sensitivity Analysis

It is seen from the above discussion that engineering judgement is the most practical source of the standard deviations of the component changes and sensor biasses required by the Kalman Filter. However, it is desirable to adjust these values to allow for the fact that some component changes and sensor biasses will be more easily

detectable than others; results from the sensitivity analysis discussed previously can be used to do this.

A typical Kalman Gain Matrix is shown in Figure 26.

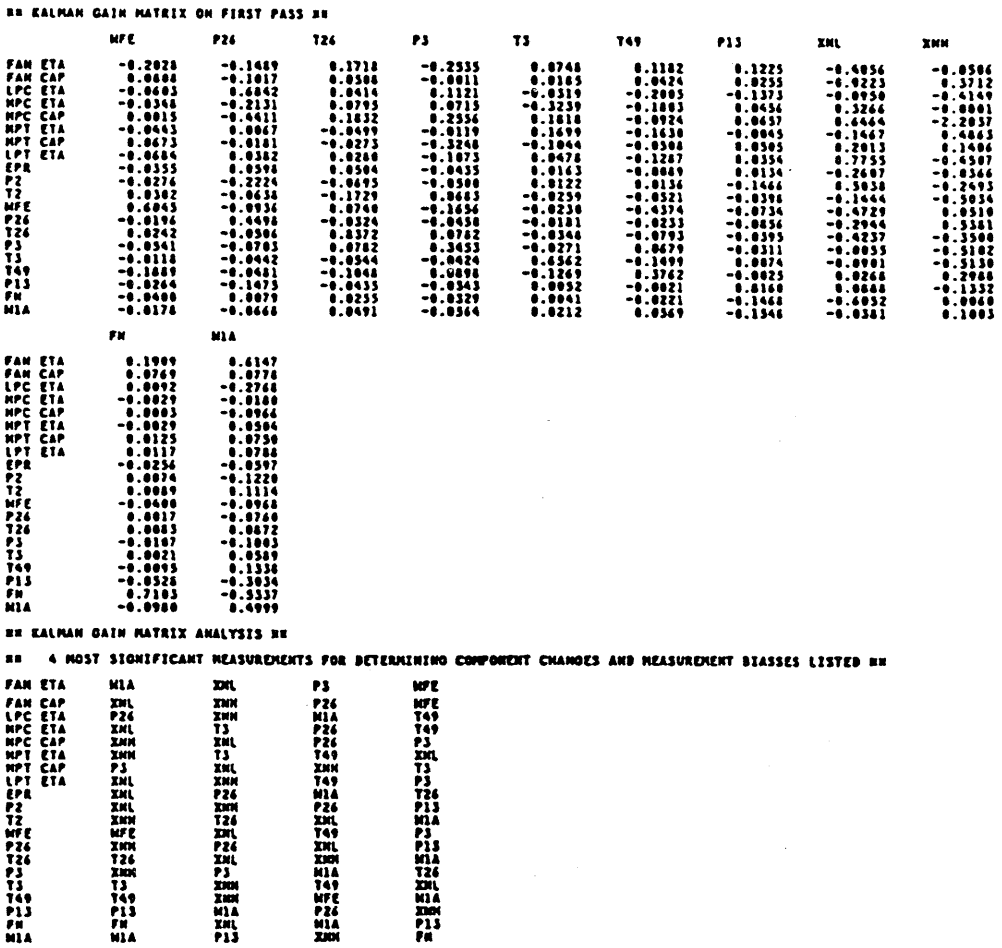

** KALMAN GAIN MATRIX ON FIRST PASS **

	WFE	P26	T26	P3	T3	T49	P13	XNL	XNH
FAN ETA	-0.2028	-0.1489	0.1718	-0.2535	0.0748	0.1182	0.1225	-0.4056	-0.0586
FAN CAP	0.0888	-0.1017	0.0588	-0.0811	0.0185	0.0424	0.0255	-0.0223	0.3712
LPC ETA	-0.0603	0.6842	0.0414	0.1121	-0.0319	-0.2085	-0.1373	-0.0950	-0.4149
HPC ETA	-0.0348	-0.2131	0.0795	0.0715	-0.3239	-0.1883	0.0434	0.3266	-0.0001
HPC CAP	0.0015	-0.0411	0.1832	0.2356	0.1818	-0.0924	0.0437	0.6464	-2.2037
HPT ETA	-0.0443	0.0867	-0.0499	-0.0119	0.1699	-0.1638	-0.0045	-0.1667	0.4865
HPT CAP	0.0673	-0.0181	-0.0273	-0.3248	-0.1044	-0.0508	0.0505	0.2013	0.1406
LPT ETA	-0.0684	0.0382	0.0268	-0.1073	0.0478	-0.1287	0.0356	0.7755	-0.4507
EPR	-0.0355	0.0598	0.0504	-0.0435	0.0163	-0.0869	0.0134	-0.2607	-0.0366
P2	-0.0276	-0.2224	-0.0695	-0.0508	0.0122	0.0136	-0.1466	0.3038	-0.2693
T2	0.0302	-0.0638	-0.1729	0.0683	-0.0259	-0.0521	-0.0398	-0.1444	-0.5034
WFE	0.6045	-0.0936	0.0740	-0.1656	-0.0238	-0.4374	-0.0734	-0.4729	0.0510
P26	-0.0196	0.4498	-0.0326	-0.0658	-0.0181	-0.0253	-0.0856	-0.2944	0.3581
T26	0.0242	-0.0586	0.8372	0.0762	-0.0346	-0.0793	-0.0395	-0.4237	-0.3508
P3	-0.0341	-0.0705	0.0782	0.3453	-0.0271	0.0479	-0.0311	-0.0035	-0.3102
T3	-0.0118	-0.0442	-0.0544	-0.0424	0.6562	-0.1499	0.0074	-0.0981	-0.3138
T49	-0.1889	-0.0481	-0.1048	0.0898	-0.1269	0.3762	-0.0825	0.0268	0.2988
P13	-0.0264	-0.1473	-0.0435	-0.0343	0.0052	-0.0821	0.8168	0.0888	-0.1332
FN	-0.0498	0.0079	0.0255	-0.0329	0.0041	-0.0221	-0.1468	-0.6052	0.0068
M1A	-0.0178	-0.0468	0.0491	-0.0364	0.0212	0.0369	-0.1346	-0.0381	0.1003

	FN	M1A
FAN ETA	0.1909	0.6147
FAN CAP	0.0769	0.0778
LPC ETA	0.0092	-0.2764
HPC ETA	-0.0029	-0.0188
HPC CAP	0.0003	-0.0966
HPT ETA	-0.0029	0.0586
HPT CAP	0.0125	0.0750
LPT ETA	0.0117	0.0788
EPR	-0.0256	-0.0597
P2	0.0074	-0.1220
T2	0.0089	0.1114
WFE	-0.0408	-0.0968
P26	0.0017	-0.0766
T26	0.0083	0.0872
P3	-0.0107	-0.1043
T3	0.0021	0.0589
T49	-0.0095	0.1338
P13	-0.0526	-0.3034
FN	0.7103	-0.3537
M1A	-0.0988	0.4999

** KALMAN GAIN MATRIX ANALYSIS **

** 4 MOST SIGNIFICANT MEASUREMENTS FOR DETERMINING COMPONENT CHANGES AND MEASUREMENT BIASSES LISTED **

FAN ETA	M1A	XNL	P3	WFE
FAN CAP	XNL	XNH	P26	WFE
LPC ETA	P26	XNH	M1A	T49
HPC ETA	XNL	T3	P26	T49
HPC CAP	XNH	XNL	P26	P3
HPT ETA	XNH	T3	T49	XNL
HPT CAP	P3	XNL	XNH	T3
LPT ETA	XNL	XNH	T49	P3
EPR	XNL	P26	M1A	T26
P2	XNL	XNH	P26	P13
T2	XNH	T26	XNL	M1A
WFE	WFE	XNL	T49	P3
P26	XNH	P26	XNL	P13
T26	T26	XNL	XNH	M1A
P3	XNH	P3	M1A	T26
T3	T3	XNH	T49	XNL
T49	T49	XNH	WFE	M1A
P13	P13	M1A	P26	XNH
FN	FN	XNL	M1A	P13
M1A	M1A	P13	XNH	FN

Figure 26: Kalman Gain Matrix on first pass

By post-multiplying by the System Matrix (to produce the product $\underline{K} \bullet \underline{C}$), a set of column vectors of best estimates of component changes and sensor biasses from the analysis of measurement differences appropriate to 1% changes in each component change or sensor bias being searched for in turn is produced; see Figure 27. The 'Concentrator' enhancement to the Kalman Filter works using normalised estimated component changes and sensor biasses, where:

$$\text{Normalised change or bias} = \frac{\text{Estimated change or bias}}{\sqrt{(\text{Element from } \underline{P}_1 \text{ diagonal})}}$$

By dividing by the square roots of the appropriate diagonal elements from the $\underline{P}_1$ matrix, a set of column vectors of normalised estimates of component changes and sensor biasses from the analysis of 1% changes in individual component changes and sensor biasses is produced; see Figure 28. Obviously, in Figure 28, it is

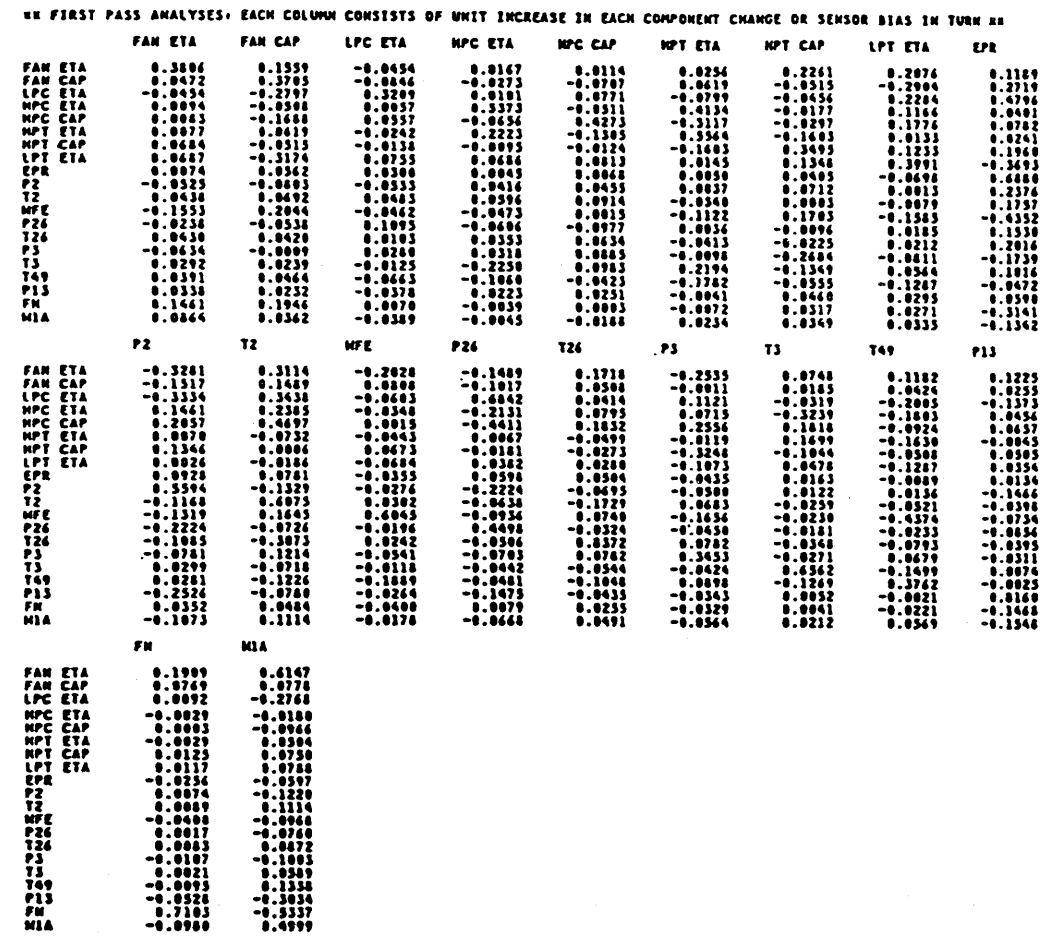

** FIRST PASS ANALYSES: EACH COLUMN CONSISTS OF UNIT INCREASE IN EACH COMPONENT CHANGE OR SENSOR BIAS IN TURN **

	FAN ETA	FAN CAP	LPC ETA	HPC ETA	HPC CAP	HPT ETA	HPT CAP	LPT ETA	EPR
FAN ETA	0.3806	0.1559	-0.0656	0.0167	0.0114	0.0256	0.2261	0.2076	0.1189
FAN CAP	0.0472	0.3705	-0.0846	-0.0273	-0.0707	0.0619	-0.0515	-0.2906	0.2719
LPC ETA	-0.0454	-0.2797	0.3289	0.0191	0.0771	-0.0799	-0.0656	0.2284	0.4796
HPC ETA	0.0094	-0.0588	0.0057	0.3373	-0.0311	0.4134	-0.0177	0.1166	0.0401
HPC CAP	0.0063	-0.1668	0.0557	-0.0656	0.4273	-0.3117	-0.0297	0.1776	0.0782
HPT ETA	0.0077	0.0619	-0.0242	0.2223	-0.1305	0.5564	-0.1683	0.0133	0.0261
HPT CAP	0.0684	-0.0515	-0.0134	-0.0095	-0.0124	-0.1683	0.3695	0.1233	0.1968
LPT ETA	0.0687	-0.3174	0.0755	0.0686	0.0813	0.0145	0.1348	0.3991	-0.3693
EPR	0.0074	0.0362	0.0300	0.0045	0.0068	0.0050	0.0405	-0.0698	0.6888
P2	-0.0525	-0.0683	-0.0533	0.0416	0.0455	0.0837	0.0712	0.0813	0.2376
T2	0.0438	0.0492	0.0483	0.0596	0.0914	-0.0560	0.0803	-0.0879	0.1757
MFE	-0.1553	0.2044	-0.0462	-0.0473	0.0815	-0.1122	0.1705	-0.1585	-0.4352
P26	-0.0236	-0.0538	0.1095	-0.0606	-0.0977	0.0036	-0.0096	0.0185	0.1538
T26	0.0430	0.0428	0.0183	0.0353	0.0634	-0.0413	-0.0225	0.0212	0.2016
P3	-0.0634	-0.0809	0.0260	0.0318	0.0885	-0.0098	-0.2684	-0.0811	-0.1739
T3	0.0292	0.0239	-0.0125	-0.2250	0.0983	0.2194	-0.1349	0.0564	0.1816
T49	0.0191	0.0464	-0.0663	-0.1060	-0.0423	-0.1782	-0.0555	-0.1267	-0.0472
P13	0.0138	0.0232	-0.0378	0.0223	0.0251	-0.0061	0.0460	0.0295	0.0598
FN	0.1461	0.1946	0.0070	-0.0039	0.0083	-0.0072	0.0317	0.0271	-0.3141
M1A	0.0864	0.0362	-0.0389	-0.0045	-0.0188	0.0234	0.0349	0.0335	-0.1362

	P2	T2	MFE	P26	T26	P3	T3	T49	P13
FAN ETA	-0.3281	0.3114	-0.2028	-0.1489	0.1718	-0.2535	0.0748	0.1182	0.1225
FAN CAP	-0.1517	0.1489	0.0808	-0.1017	0.0588	-0.0811	0.0185	0.0426	0.0255
LPC ETA	-0.3334	0.3438	-0.0603	0.6042	0.0414	0.1121	-0.0319	-0.2005	-0.1373
HPC ETA	0.1461	0.2385	-0.0348	-0.2131	0.0795	0.0715	-0.3239	-0.1803	0.0456
HPC CAP	0.2057	0.4697	0.0015	-0.4411	0.1832	0.2556	0.1818	-0.0924	0.0637
HPT ETA	0.0870	-0.0732	-0.0443	0.0067	-0.0499	-0.0119	0.1699	-0.1630	-0.0065
HPT CAP	0.1346	0.0806	0.0673	-0.0181	-0.0273	-0.3246	-0.1044	-0.0508	0.0305
LPT ETA	0.0826	-0.0186	-0.0684	0.0362	0.0288	-0.1073	0.0478	-0.1287	0.0354
EPR	0.0928	0.0761	-0.0355	0.0598	0.0509	-0.0435	0.0163	-0.0089	0.0134
P2	0.3594	-0.1329	-0.0276	-0.2226	-0.0695	-0.0588	0.0122	0.0136	-0.1446
T2	-0.1168	0.6975	0.0302	-0.0438	-0.1729	0.0683	-0.0259	-0.0521	-0.0398
MFE	-0.1319	0.1645	0.6845	-0.0934	0.0740	-0.1656	-0.0230	-0.4376	-0.0734
P26	-0.2224	-0.0726	-0.0196	0.6498	-0.0324	-0.0458	-0.0181	-0.0233	-0.0856
T26	-0.1085	-0.1073	0.0242	-0.0586	0.8372	0.0782	-0.0368	-0.0793	-0.0395
P3	-0.0781	0.1214	-0.0541	-0.0703	0.0762	0.3453	-0.0271	0.0479	-0.0311
T3	0.0299	-0.0718	-0.0118	-0.0442	-0.0544	-0.0624	0.6562	-0.1409	0.0076
T49	0.0281	-0.1226	-0.1889	-0.0481	-0.1048	0.0898	-0.1269	0.3762	-0.0825
P13	-0.2524	-0.0780	-0.0264	-0.1475	-0.0435	-0.0343	0.0052	-0.0021	0.8160
FN	0.0352	0.0484	-0.0490	0.0079	0.0255	-0.0329	0.0041	-0.0221	-0.1468
M1A	-0.1073	0.1114	-0.0178	-0.0648	0.0491	-0.0564	0.0212	0.0569	-0.1548

	FN	M1A
FAN ETA	0.1999	0.6167
FAN CAP	0.0769	0.0778
LPC ETA	0.0092	-0.2768
HPC ETA	-0.0029	-0.0188
HPC CAP	0.0003	-0.0966
HPT ETA	-0.0029	0.0304
HPT CAP	0.0125	0.0730
LPT ETA	0.0117	0.0788
EPR	-0.0234	-0.0597
P2	0.0074	-0.1220
T2	0.0089	0.1114
MFE	-0.0400	-0.0968
P26	0.0017	-0.0760
T26	0.0083	0.0472
P3	-0.0107	-0.1003
T3	0.0021	0.0349
T49	-0.0093	0.1338
P13	-0.0528	-0.3034
FN	0.7103	-0.5337
M1A	-0.0980	0.4999

Figure 27: First pass analyses

desirable that, for any column vector produced by an analysis of a single component change or sensor bias, the element corresponding to the component change or sensor bias being analysed should be the largest; other elements with absolute values larger than or close to this value indicate potential problems in the analysis. This is most easily checked if the ratio:

$$\frac{\text{Normalised change or bias}}{\text{Normalised change or bias being analysed}}$$

is created: column vectors of these ratios are shown in Figure 29. Trials have shown that, for good analysis capability, the following criteria should be applied to the ratios in Figure 29:

1) No ratio should be greater than 1.0;

2) The number of ratios greater than 0.6 should be minimised;

3) As far as possible, ratios greater than 0.6 should be 'paired-off'; ie if A could be analysed instead of B, then B could also be analysed instead of A;

** FIRST PASS ANALYSES. AS ABOVE. BUT EACH ROW DIVIDED BY STANDARD DEVIATIONS OF ESTIMATES ON FIRST PASS **

	FAN ETA	FAN CAP	LPC ETA	HPC ETA	HPC CAP	HPT ETA	HPT CAP	LPT ETA	EPR
FAN ETA	1.2889	0.4955	-0.1443	0.0531	0.0363	0.0812	0.7184	0.6596	0.3777
FAN CAP	0.2702	2.1227	-0.4847	-0.1566	-0.4049	0.3546	-0.2948	-1.6637	1.5577
LPC ETA	-0.1378	-0.8484	0.9735	0.0305	0.2339	-0.2423	-0.1383	0.6928	1.6550
HPC ETA	0.0460	-0.2491	0.0277	2.6327	-0.2504	2.0255	-0.0868	0.5716	0.1963
HPC CAP	0.0321	-0.6368	0.2165	-0.2551	1.6607	-1.2116	-0.1154	0.6981	0.3039
HPT ETA	0.0528	0.4225	-0.1669	1.5171	-0.0908	3.7977	-1.0940	0.0985	0.1665
HPT CAP	0.3655	-0.2980	-0.0777	-0.0537	-0.0701	-0.9836	1.9699	0.6950	1.1946
LPT ETA	0.3651	-1.7883	0.4235	0.3843	0.4557	0.0813	0.7560	2.2386	-2.0713
EPR	0.1330	1.0857	0.5366	0.0797	0.1211	0.0891	0.7249	-1.2498	12.3171
P2	-0.4943	-0.7557	-0.5025	0.3913	0.4269	0.0348	0.6702	0.0119	2.2369
T2	0.4660	0.7364	0.5165	0.4345	0.9729	-0.3421	0.8827	-0.0843	1.8788
WFE	-0.7034	0.9288	-0.2097	-0.2151	0.0070	-0.3098	0.7738	-0.7199	-1.9776
P26	-0.2808	-0.4534	0.9224	-0.5106	-0.8231	0.0300	-0.0886	0.1559	1.2689
T26	0.5324	0.5207	0.1261	0.4366	0.7857	-0.3114	-0.2793	0.2626	2.4973
P3	-0.3917	-0.0057	0.1733	0.1963	0.5466	-0.0606	-1.6367	-0.5014	-1.0748
T3	0.1993	0.1630	-0.0858	-1.3347	0.6706	1.4966	-0.9281	0.3858	0.6936
T49	0.2151	0.2554	-0.3649	-0.3834	-0.2326	-0.9810	-0.3054	-0.7087	-0.2396
P13	0.3749	0.2560	-0.4289	0.2461	0.2781	-0.0451	0.5199	0.3274	0.6353
FN	0.7756	1.0331	0.0373	-0.0206	0.0016	-0.0363	0.1685	0.1448	-1.6672
M1A	0.8150	0.3411	-0.3669	-0.0424	-0.1772	0.2288	0.3286	0.3159	-1.2655
AV ABS()	0.3911	0.6661	0.3387	0.4989	0.4524	0.6539	0.5799	0.6084	1.7517

	P2	T2	WFE	P26	T26	P3	T3	T49	P13
FAN ETA	-1.0422	0.9893	-0.6442	-0.4731	0.5459	-0.8054	0.2576	0.3755	0.3892
FAN CAP	-0.8693	0.8528	0.4627	-0.3828	0.2913	-0.0864	0.1060	0.2432	0.1461
LPC ETA	-1.0114	1.0429	-0.1829	2.0758	0.1255	0.3602	-0.0967	-0.6881	-0.4164
HPC ETA	0.7159	1.1688	-0.1704	-1.0441	0.3897	0.3503	-1.5474	-0.8855	0.2235
HPC CAP	0.7993	1.8257	0.0857	-1.7145	0.7122	0.9936	0.7066	-0.3591	0.2552
HPT ETA	0.0476	-0.4996	-0.3026	0.0459	-0.3488	-0.0810	1.1595	-1.1128	-0.0383
HPT CAP	0.7584	0.0831	0.3793	-0.1828	-0.1537	-1.8304	-0.3887	-0.2861	0.2647
LPT ETA	0.0146	-0.1964	-0.3838	0.2145	0.1572	-0.6819	0.2679	-0.7221	0.1985
EPR	1.6613	1.3983	-0.6341	1.0698	0.9821	-0.7784	0.2912	-0.1596	0.2396
P2	5.2674	-1.2518	-0.2596	-2.0940	-0.6340	-0.6707	0.1353	0.1281	-1.3807
T2	-1.2426	6.4648	0.3215	-0.6787	-1.8396	0.7269	-0.2751	-0.5547	-0.4233
WFE	-0.5995	0.7473	2.7465	-0.4253	0.3344	-0.7523	-0.1046	-1.9878	-0.3335
P26	-1.8738	-0.6114	-0.1648	3.7896	-0.2731	-0.3793	-0.1527	-0.1968	-0.7213
T26	-1.3447	-3.8082	0.2995	-0.6275	10.3736	0.9693	-0.4312	-0.9822	-0.4891
P3	-0.6827	0.7504	-0.3341	-0.4347	0.4834	2.1341	-0.1678	0.4196	-0.1924
T3	0.2940	-0.4899	-0.8802	-0.3018	-0.3709	-0.2894	4.4766	-1.0229	0.0587
T49	0.1547	-0.6747	-1.0397	-0.2646	-0.3771	0.4944	-0.6986	2.8712	-0.8139
P13	-2.8048	-0.8635	-0.2936	-1.6371	-0.4831	-0.3811	0.9362	-0.8233	0.8579
FN	0.1871	0.2547	-0.2125	0.0420	0.1353	-0.1745	0.0220	-0.1171	-0.7792
M1A	-1.0112	1.0498	-0.1676	-0.6296	0.4627	-0.5321	0.1999	0.3365	-1.4594
AV ABS()	1.1046	1.2427	0.4544	0.9124	0.9804	0.6546	0.3872	0.6394	0.8343

	FN	M1A
FAN ETA	0.6864	1.9527
FAN CAP	0.4485	0.4439
LPC ETA	0.0279	-0.8397
HPC ETA	-0.0140	-0.0881
HPC CAP	0.0811	-0.3753
HPT ETA	-0.0195	0.3439
HPT CAP	0.0787	0.4226
LPT ETA	0.0637	0.4419
EPR	-0.4598	-1.0481
P2	0.0693	-1.8491
T2	0.0945	1.2850
WFE	-0.1818	-0.0397
P26	0.0139	-0.6402
T26	0.1031	1.0811
P3	-0.0663	-0.6201
T3	0.0144	0.4018
T49	-0.0523	0.7345
P13	-0.3666	-3.3680
FN	3.7706	-2.8331
M1A	-0.0242	4.7133
AV ABS()	0.3791	1.1573

Figure 28: $\frac{\text{First pass analysis}}{\text{Standard deviations of estimates}}$ = Normalised Analysis

4) For any column, the number of ratios greater than the average of the absolute values of all the ratios should be minimised;

5) The average of the absolute values of all the ratios should be minimised.

Both of the latter criteria help the 'Concentrator' focus more quickly on the more significant component changes and sensor biasses. By varying the standard deviations of the component changes and sensor biasses input to the Kalman Filter, the performance analyst can make changes to his assumed levels of these standard deviations in order to meet the above criteria. To help him do this, the sensitivity analysis described previously can be extended as follows:

$$\frac{\delta}{\delta s}(\underline{K} \bullet \underline{C}) = \frac{\delta \underline{K}}{\delta s} \bullet \underline{C}$$

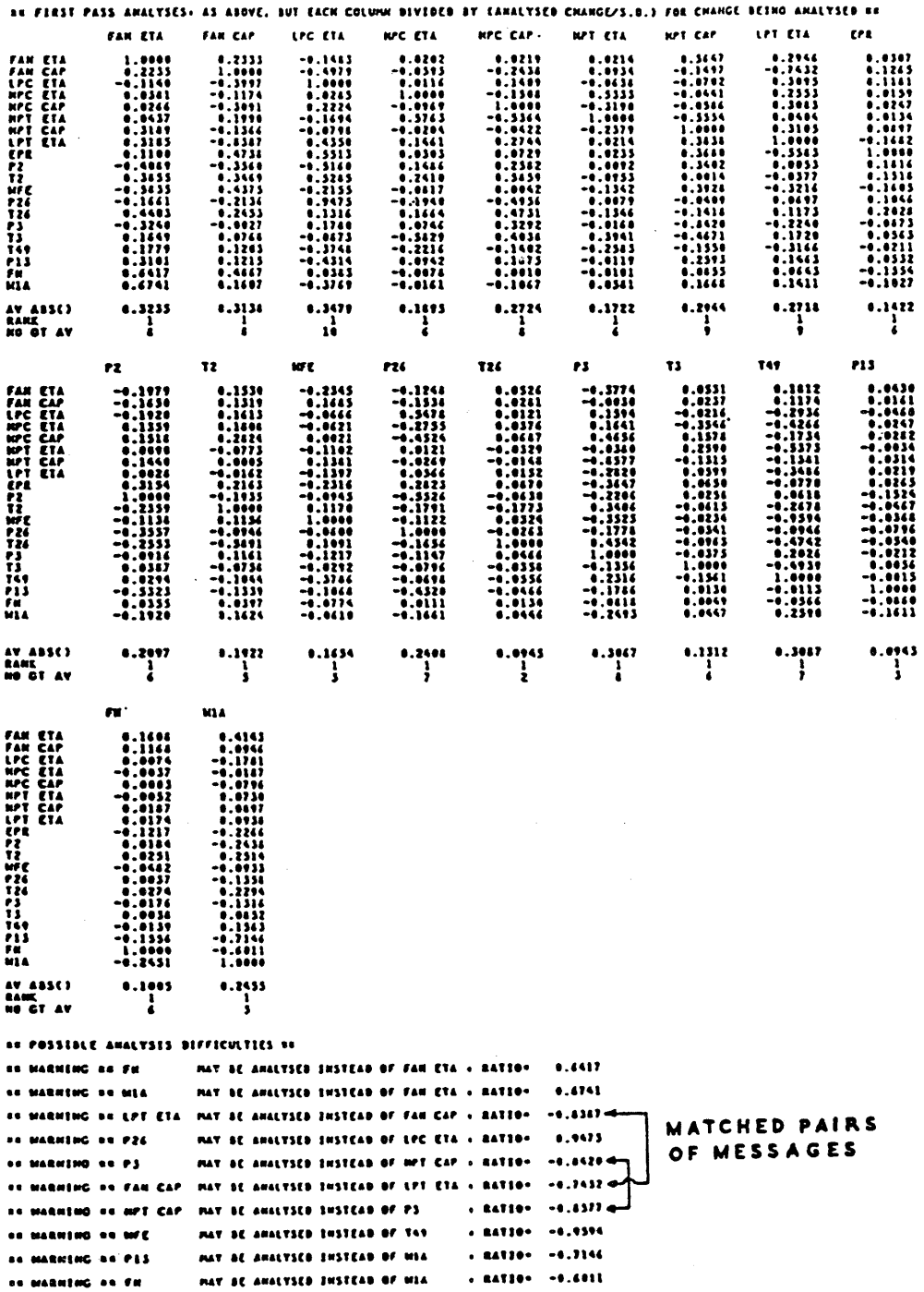

** FIRST PASS ANALYSES+ AS ABOVE, BUT EACH COLUMN DIVIDED BY (ANALYSED CHANGE/S.D.) FOR CHANGE BEING ANALYSED **

	FAN ETA	FAN CAP	LPC ETA	HPC ETA	HPC CAP	HPT ETA	HPT CAP	LPT ETA	EPR
FAN ETA	1.0000	0.2333	-0.1483	0.0202	0.0219	0.0214	0.3647	0.2946	0.0307
FAN CAP	0.2235	1.0000	-0.4979	-0.0393	-0.2436	0.0934	-0.1497	-0.7432	0.1245
LPC ETA	-0.1140	-0.3997	1.0000	0.0116	0.1499	-0.0638	-0.0702	0.3095	0.1161
HPC ETA	0.0381	-0.1174	0.0265	1.0000	-0.1508	0.5333	-0.0441	0.2533	0.0159
HPC CAP	0.0266	-0.3091	0.2224	-0.0969	1.0000	-0.3198	-0.0566	0.3083	0.0267
HPT ETA	0.0437	0.1998	-0.1694	0.5763	-0.5364	1.0000	-0.3556	0.0484	0.0134
HPT CAP	0.3189	-0.1366	-0.0798	-0.0284	-0.0422	-0.2379	1.0000	0.3183	0.0497
LPT ETA	0.3185	-0.8387	0.4558	0.1661	0.2744	0.0214	0.3838	1.0000	-0.1482
EPR	0.1188	0.0738	0.3513	0.0303	0.0729	0.0235	0.3668	-0.5563	1.0000
P2	-0.4869	-0.3568	-0.5160	0.1686	0.2582	0.0892	0.3402	0.0853	0.1414
T2	0.3655	0.3469	0.5265	0.2618	0.3459	-0.0955	0.0814	-0.0377	0.1316
WFE	-0.3635	0.4373	-0.2155	-0.0817	0.0842	-0.1342	0.3928	-0.3214	-0.1605
P26	-0.1661	-0.2134	0.9473	-0.4940	-0.4936	0.0879	-0.0609	0.0697	0.1066
T26	0.4483	0.2653	0.1316	0.1664	0.4731	-0.1366	-0.1418	0.1173	0.2028
P3	-0.3240	-0.0027	0.1748	0.0746	0.3292	-0.0168	-0.4620	-0.2240	-0.0473
T3	0.1649	0.0766	-0.0673	-0.3629	0.4036	0.3941	-0.4671	0.1720	0.0363
T49	0.1779	0.1263	-0.3746	-0.2216	-0.1402	-0.2383	-0.1558	-0.3166	-0.0211
P13	0.3101	0.1213	-0.4314	0.0942	0.1673	-0.0119	0.2593	0.1663	0.0532
FH	0.6417	0.4667	0.0363	-0.0078	0.0010	-0.0101	0.0833	0.0643	-0.1356
M1A	0.6741	0.1607	-0.3769	-0.0161	-0.1867	0.0341	0.1668	0.1411	-0.1027
AV ABS()	0.3235	0.3136	0.3479	0.1893	0.2724	0.1722	0.2944	0.2718	0.1422
RANK	1	1	1	1	1	1	1	1	1
NO GT AV	6	6	10	6	6	6	9	9	6

	P2	T2	WFE	P26	T26	P3	T3	T49	P13
FAN ETA	-0.1979	0.1530	-0.2345	-0.1268	0.0526	-0.3774	0.0531	0.1812	0.0430
FAN CAP	-0.1650	0.1319	0.1665	-0.1534	0.0281	-0.0030	0.0237	0.1174	0.0161
LPC ETA	-0.1920	0.1613	-0.0666	0.5678	0.0121	0.1594	-0.0216	-0.2936	-0.0460
HPC ETA	0.1359	0.1808	-0.0821	-0.2755	0.0376	0.1641	-0.3564	-0.4266	0.0267
HPC CAP	0.1518	0.2624	0.0021	-0.4526	0.0647	0.4656	0.1578	-0.1734	0.0282
HPT ETA	0.0898	-0.0773	-0.1102	0.0121	-0.0329	-0.0368	0.2590	-0.5373	-0.0034
HPT CAP	0.1448	0.0885	0.1381	-0.0269	-0.0148	-0.0577	-0.1315	-0.1341	0.0314
LPT ETA	0.0826	-0.0162	-0.1397	0.0366	0.0152	-0.2828	0.0599	-0.3686	0.0219
EPR	0.3154	0.2163	-0.2316	0.2823	0.0670	-0.3647	0.0650	-0.0778	0.0265
P2	1.0000	-0.1935	-0.0945	-0.5326	-0.0638	-0.2206	0.0256	0.0618	-0.1326
T2	-0.2359	1.0000	0.1178	-0.1791	-0.1773	0.3606	-0.0615	-0.2678	-0.0467
WFE	-0.1138	0.1186	1.0000	-0.1122	0.0326	-0.3525	-0.0234	-0.5596	-0.0368
P26	-0.3537	-0.0946	-0.0600	1.0000	-0.0263	-0.1778	-0.0541	-0.0946	-0.0796
T26	-0.2353	-0.3691	0.1691	-0.1656	1.0000	0.4542	-0.0843	-0.4742	-0.0540
P3	-0.0916	0.1161	-0.1217	-0.1147	0.0466	1.0000	-0.0375	0.2026	-0.0212
T3	0.0187	-0.0736	-0.0292	-0.0796	-0.0338	-0.1356	1.0000	-0.4939	0.0036
T49	0.0294	-0.1044	-0.3746	-0.0698	-0.0556	0.2316	-0.1561	1.0000	-0.0815
P13	-0.5323	-0.1339	-0.1864	-0.4328	-0.0466	-0.1786	0.0130	-0.0113	1.0000
FH	0.0355	0.0397	-0.0774	0.0111	0.0138	-0.0414	0.0069	-0.0566	-0.0660
M1A	-0.1920	0.1624	-0.0610	-0.1661	0.0446	-0.2493	0.0467	0.2598	-0.1611
AV ABS()	0.2097	0.1922	0.1634	0.2498	0.0945	0.3067	0.1312	0.3087	0.0945
RANK	1	1	1	1	1	1	1	1	1
NO GT AV	6	5	5	7	2	6	6	7	3

	FH	M1A
FAN ETA	0.1686	0.4143
FAN CAP	0.1164	0.0944
LPC ETA	0.0074	-0.1741
HPC ETA	-0.0037	-0.0187
HPC CAP	0.0083	-0.0796
HPT ETA	-0.0052	0.0730
HPT CAP	0.0187	0.0697
LPT ETA	0.0174	0.0936
EPR	-0.1217	-0.2246
P2	0.0184	-0.2436
T2	0.0251	0.2314
WFE	-0.0462	-0.0933
P26	0.0037	-0.1358
T26	0.0274	0.2294
P3	-0.0176	-0.1316
T3	0.0036	0.0832
T49	-0.0139	0.1363
P13	-0.1356	-0.7146
FH	1.0000	-0.6011
M1A	-0.2451	1.0000
AV ABS()	0.1005	0.2455
RANK	1	1
NO GT AV	6	3

** POSSIBLE ANALYSIS DIFFICULTIES **

** WARNING ** FH MAY BE ANALYSED INSTEAD OF FAN ETA . RATIO= 0.6417
** WARNING ** M1A MAY BE ANALYSED INSTEAD OF FAN ETA . RATIO= 0.6741
** WARNING ** LPT ETA MAY BE ANALYSED INSTEAD OF FAN CAP . RATIO= -0.8387
** WARNING ** P26 MAY BE ANALYSED INSTEAD OF LPC ETA . RATIO= 0.9473
** WARNING ** P3 MAY BE ANALYSED INSTEAD OF HPT CAP . RATIO= -0.8420
** WARNING ** FAN CAP MAY BE ANALYSED INSTEAD OF LPT ETA . RATIO= -0.7432
** WARNING ** HPT CAP MAY BE ANALYSED INSTEAD OF P3 . RATIO= -0.8377
** WARNING ** WFE MAY BE ANALYSED INSTEAD OF T49 . RATIO= -0.9596
** WARNING ** P13 MAY BE ANALYSED INSTEAD OF M1A . RATIO= -0.7146
** WARNING ** FH MAY BE ANALYSED INSTEAD OF M1A . RATIO= -0.6011

MATCHED PAIRS OF MESSAGES

Figure 29: Normalised analysis

Normalised analysis of input change or bias

where s = standard deviation of any component change or sensor bias.

$$\frac{\delta}{\delta s}\left(\underline{K} \bullet \underline{C} \div p\right) = \left(p \bullet \frac{\delta}{\delta s}\left(\underline{K} \bullet \underline{C}\right) - \left(\underline{K} \bullet \underline{C}\right) \bullet \frac{\delta p}{\delta s}\right) \div p^2$$

where p = square root of appropriate element in $\underline{P}_1$

diagonal (different for each row of the $\underline{K} \bullet \underline{C}$ matrix).

$$\frac{\delta}{\delta s}\left((\underline{K} \bullet \underline{C} \div p) \div r\right) = \left(r \bullet \frac{\delta}{\delta s}(\underline{K} \bullet \underline{C} \div p) - (\underline{K} \bullet C \div p) \bullet \frac{\delta r}{\delta s}\right) \div r^2$$

where r = normalised component change or sensor bias for change or bias being analysed (different for each column of the $(\underline{K} \bullet \underline{C} \div p)$ matrix).

A typical matrix of these partial derivatives of the ratios is shown in Figure 30.

** PARTIAL DERIVATIVES OF (FIRST PASS ANALYSES/S.D.) DIVIDED BY (FIRST PASS ANALYSIS/S.D.) FOR CHANGE BEING ANALYSED **
** WITH RESPECT TO FAN ETA SYSTEM STANDARD DEVIATION **

	FAN ETA	FAN CAP	LPC ETA	HPC ETA	HPC CAP	HPT ETA	HPT CAP	LPT ETA	EPR
FAN ETA	0.0	0.3913	-0.2355	0.0313	0.0339	0.0332	0.6671	0.5264	0.0479
FAN CAP	-0.7788	0.0	0.0578	-0.0070	-0.0025	-0.0116	-0.1927	-0.2804	-0.0150
LPC ETA	0.3964	0.0025	0.0	0.0043	0.0039	0.0049	0.0599	0.1352	0.0073
HPC ETA	-0.1315	-0.0319	0.0119	0.0	-0.0017	-0.0005	-0.0388	0.0392	-0.0020
HPC CAP	-0.0916	-0.0314	0.0162	-0.0012	0.0	-0.0019	-0.0349	0.0583	-0.0012
HPT ETA	-0.1508	0.0059	0.0058	-0.0010	-0.0028	0.0	-0.1856	-0.0149	-0.0026
HPT CAP	-1.1197	-0.1518	0.0915	-0.0111	-0.0108	0.0005	0.0	-0.1234	-0.0227
LPT ETA	-1.1162	-0.1994	0.0814	-0.0205	-0.0291	-0.0142	-0.1548	0.0	-0.0189
EPR	-0.3886	0.0066	0.0491	-0.0044	-0.0050	-0.0046	0.0264	-0.1986	0.0
P2	1.4512	0.1706	-0.0854	0.0015	-0.0078	0.0158	0.3468	0.2308	0.0086
T2	-1.3640	-0.1567	0.0839	-0.0352	-0.0661	-0.0077	-0.2672	-0.2218	-0.0336
MFE	2.1300	0.2282	-0.1303	0.0385	0.0234	0.0501	0.4378	0.3146	0.0638
P26	0.5759	0.0498	-0.0245	0.0091	0.0142	0.0067	0.1044	0.1086	0.0094
T26	-1.3698	-0.1918	0.1145	-0.0354	-0.0712	-0.0031	-0.3293	-0.2323	-0.0459
P3	1.1382	0.1437	-0.0953	0.0080	-0.0062	0.0141	0.0401	0.1621	0.0231
T3	-0.5716	-0.0644	0.0444	0.0016	-0.0127	-0.0118	-0.2381	-0.0563	-0.0098
T49	-0.6173	-0.0658	0.0422	-0.0032	-0.0058	-0.0032	-0.1641	-0.1692	-0.0183
P13	-1.0877	-0.1269	0.0946	-0.0178	-0.0221	-0.0120	-0.1569	-0.1673	-0.0206
FN	-2.3694	-0.3396	0.1733	-0.0227	-0.0269	-0.0237	-0.4419	-0.3688	-0.0847
M1A	-2.3058	-0.3214	0.2753	-0.0216	0.0081	-0.0427	-0.4653	-0.3819	-0.0134
AV ABS()	-0.9773	-0.0284	0.0125	-0.0025	-0.0089	-0.0024	0.0493	0.0094	-0.0063

	P2	T2	MFE	P26	T26	P3	T3	T49	P13
FAN ETA	-0.3562	0.2674	-0.4709	-0.2003	0.0098	-0.6954	0.0039	0.2951	0.0700
FAN CAP	0.0474	-0.0427	0.1722	0.0490	-0.0188	0.1597	-0.0225	-0.0711	-0.0174
LPC ETA	-0.0898	0.0641	-0.0818	-0.0008	0.0132	-0.0362	0.0110	0.0181	0.0059
HPC ETA	0.0484	-0.0241	0.0113	-0.0060	0.0021	0.0755	-0.0151	-0.0468	-0.0011
HPC CAP	0.0481	0.0484	0.0128	-0.0187	0.0031	0.1558	0.0026	-0.0229	0.0001
HPT ETA	0.0187	-0.0288	-0.0318	0.0110	-0.0095	0.0202	0.0037	-0.0574	-0.0038
HPT CAP	0.1478	-0.0928	0.1976	0.0759	-0.0336	0.0278	-0.0267	-0.1128	-0.0254
LPT ETA	0.1205	-0.0950	0.0862	0.0755	-0.0304	0.1625	-0.0338	-0.1170	-0.0256
EPR	0.1166	0.0095	-0.0557	0.0398	0.0021	-0.0256	-0.0095	-0.0635	-0.0070
P2	0.0	0.0994	-0.2167	-0.0739	0.0372	-0.3369	0.0396	0.1399	0.0359
T2	0.1063	0.0	0.2157	0.0972	-0.0511	0.3474	-0.0356	-0.1310	-0.0313
MFE	-0.2257	0.1699	0.0	-0.1225	0.0571	-0.4525	0.0628	0.3155	0.0520
P26	-0.1463	0.0511	-0.1007	0.0	0.0129	-0.1687	0.0162	0.0512	0.0084
T26	0.1305	-0.1788	0.2343	0.1142	0.0	0.3983	-0.0367	-0.1359	-0.0343
P3	-0.1396	0.1103	-0.1930	-0.0763	0.0369	0.0	0.0338	0.1155	0.0261
T3	0.0712	-0.0619	0.0606	0.0360	-0.0216	0.0887	0.0	-0.0884	-0.0131
T49	0.0738	-0.0707	-0.0675	0.0397	-0.0255	0.1916	-0.0282	0.0	-0.0146
P13	0.0127	-0.1094	0.0953	0.0739	-0.0358	0.1882	-0.0316	-0.1072	0.0
FN	0.2420	-0.1885	0.2695	0.1584	-0.0653	0.4345	-0.0658	-0.2122	-0.0388
M1A	0.2565	-0.2071	0.2890	0.1951	-0.0725	0.4770	-0.0785	-0.2806	-0.0255
AV ABS()	0.0647	0.0288	0.0640	0.0046	0.0075	0.0623	-0.0050	0.0445	0.0000

	FN	M1A
FAN ETA	0.3193	0.9718
FAN CAP	-0.0207	-0.1036
LPC ETA	0.0381	-0.0508
HPC ETA	-0.0133	-0.0449
HPC CAP	-0.0080	-0.0044
HPT ETA	-0.0156	0.0236
HPT CAP	-0.0985	-0.1853
LPT ETA	-0.0969	-0.1819
EPR	-0.0060	-0.0658
P2	0.1314	0.1918
T2	-0.1092	-0.1253
MFE	0.1671	0.4042
P26	0.0524	0.0249
T26	-0.1259	-0.1903
P3	0.0925	0.1586
T3	-0.0488	-0.0634
T49	-0.0603	-0.0186
P13	-0.1542	-0.7739
FN	0.0	-0.8404
M1A	-0.2483	0.0
AV ABS()	0.0183	0.0724

Figure 30: Partial derivatives of normalised analysis ratios

Matrices like this can be generated for the standard deviations of all the component changes and sensor biasses in the analysis, as well as for the measurement repeatability standard deviations; these latter matrices are used for information only.

The performance analyst wishing to adjust a standard deviation to make a particular ratio fit the criteria better can calculate the required change to the standard deviation using the formula:

$$\frac{\text{Required change in ratio}}{\text{Change in standard deviation}} \approx \frac{\delta \text{ ratio}}{\delta s}$$

which rearranges to:

$$\text{Change in standard deviation} \approx \frac{\text{Required change in ratio}}{\frac{\delta \text{ ratio}}{\delta s}}$$

The layout of the tables is such that, if a message:

WARNING A MAY BE ANALYSED INSTEAD OF B: RATIO = z

is to be eliminated, the values of $\frac{\delta \text{ ratio}}{\delta s}$ can be found by looking in the partial derivatives table appropriate to either A or B's deviation (depending on which standard deviation is to be modified) in Column B Row A.

Generally, a situation where a component change or sensor bias A could be analysed instead of a component change or sensor bias B can be alleviated if either the standard deviation appropriate to A is reduced, and/or the standard deviation appropriate to B is increased. The examples given in Figures 26 to 29 show the results of 'tuning' using the above method; several pages of messages showing possible analysis difficulties before 'tuning' have been reduced to the few messages in Figure 29, some of which are 'paired'.

4.11 Analysis Using 'Tuned' Standard Deviations

Figure 31 shows a typical analysis of a combination of component changes and sensor biasses done using the Kalman Filter. The first column, labelled DEL COMP, is the vector of component changes equivalent to 'traditional' analysis; it is seen that this analysis, by not considering the possibility of sensor bias, is completely wrong. The second column, labelled DEL MEAS, is the vector of gas-path measurement differences produced by -1% HPC ETA, +0.5% P2 sensor bias, and +1% T49 sensor bias. The next three columns show the input to the Kalman Filter:

1) SYSTM SD = Square roots of diagonal elements of $\underline{Q}$ matrix;

2) INST SD = Square roots of diagonal elements of $\underline{V}$ matrix, used to generate $\underline{R}$: the derivation of these values is given in Appendix C;

3) EXPECTED = $\underline{\hat{x}}_0$ vector, assumed to be zero in this case;

```
** ANALYSIS OF  -1.0000 * HPC ETA  COLUMN +   0.5000 * P2      COLUMN +   1.0000 * T49      COLUMN **

** DATA SUPPLIED AS DIFFERENCES **

** EXPECTED VALUES OF COMPONENT CHANGES AND MEASUREMENT BIASSES NOT SUPPLIED, VALUES OF ZERO HAVE BEEN ASSUMED **

          DEL COMP    DEL MEAS    SYSTM SD    INST SD    EXPECTED    KALMAN      BEST OBJ    BEST ANS

FAN ETA     2.857       0.0         0.400       0.0        0.0       -0.063       0.0         0.0
FAN CAP    -3.138       0.0         0.220       0.0        0.0       -0.006       0.0         0.0
LPC ETA    -1.447       0.0         0.400       0.0        0.0       -0.377       0.0         0.0
LPC CAP     0.0         0.0         0.0         0.0        0.0        0.0         0.0         0.0
HPC ETA    -0.938       0.0         0.300       0.0        0.0       -0.645      -1.018      -1.018   ***
HPC CAP     0.419       0.0         0.340       0.0        0.0       -0.076       0.0         0.0
HPT ETA     0.212       0.0         0.220       0.0        0.0       -0.382       0.0         0.0
HPT CAP     0.280       0.0         0.220       0.0        0.0       -0.026       0.0         0.0
LPT ETA    -3.218       0.0         0.230       0.0        0.0       -0.196       0.0         0.0
LPT CAP     0.0         0.0         0.0         0.0        0.0        0.0         0.0         0.0

EPR         0.0         0.0         0.100       0.031      0.0        0.033       0.0         0.0
P2          0.0         0.0         0.160       0.032      0.0        0.252       0.473       0.473   ***
T2          0.0         0.0         0.150       0.021      0.0       -0.170       0.0         0.0

HFE         0.0         0.554       0.350       0.100      0.0       -0.456       0.0         0.0
P26         0.0        -0.069       0.160       0.039      0.0       -0.074       0.0         0.0
T26         0.0         0.096       0.200       0.020      0.0       -0.169       0.0         0.0
P3          0.0        -0.751       0.200       0.102      0.0       -0.003       0.0         0.0
T3          0.0         0.585       0.250       0.084      0.0        0.090       0.0         0.0
T49         0.0         2.267       0.230       0.008      0.0        0.496       0.973       0.973   ****
P13         0.0        -0.457       0.210       0.033      0.0       -0.151       0.0         0.0
XNL         0.0         0.043       0.0         0.007      0.0        0.0         0.0         0.0
XNH         0.0        -0.123       0.0         0.007      0.0        0.0         0.0         0.0
FN          0.0        -0.405       0.350       0.147      0.0       -0.001       0.0         0.0
H1A         0.0        -0.544       0.150       0.015      0.0        0.008       0.0         0.0

** NOTES **

1) ITEMS REJECTED FROM BEST ANSWER IF LESS THAN  0.50 STANDARD DEVIATION(S)

2) BEST ANSWER BASED ON PASS THROUGH KALMAN FILTER GIVING BEST VALUE OF OBJECTIVE FUNCTION

3) WARNING MESSAGES PRINTED IN MATRIX ANALYSIS BLOCKS (IF ANY) SHOULD BE READ IN ADDITION TO THESE NOTES

4) STARS AGAINST ITEMS IN BEST ANSWER SHOW APPROXIMATE NUMBER OF STANDARD DEVIATIONS OF CHANGE IN EACH ITEM

5)  5 PASSES THROUGH KALMAN FILTER, BEST VALUE OF OBJECTIVE FUNCTION    0.789 REACHED ON PASS    3
```

Figure 31: 'Concentrator' performance for -1% HPC ETA, +0.5% P2 bias, +1% T49 bias: 'Tuned' input

The column labelled KALMAN is the answer from the basic Kalman Filter, which exhibits the 'smearing' mentioned above. The next column, labelled BEST OBJ, is the output from the 'Concentrator', while the final column, labelled BEST ANS, contains only those items in BEST OBJ whose magnitude is greater than 0.5 times SYSTM SD. It is clearly seen that the output from the 'Concentrator' is very close to the input component changes and sensor biasses.

Figure 32 shows the progress of the 'Concentrator', and is exactly equivalent to Figure 24. The large jump in the objective function from pass 3 to pass 4, reflecting the inability to explain the measurement differences when the P2 sensor bias is removed, is evident.

4.12 Automatic 'Tuning'

Another approach that can be taken to find the standard deviations of the component changes and sensor biasses required by the Kalman Filter is based on the recognition that the 'tuning' process described above is really attempting to make the matrix in Figure 29 as close to a unit matrix as possible by making the off-diagonal elements of this matrix as close to zero as possible. This process can be automated by using an optimisation algorithm such as the downhill simplex method of Nelder and Mead (described in Reference 39), which has the inputs to the $\underline{Q}$ matrix as variables and the sum of the absolute values of the off-diagonal elements of the matrix in Figure 29 as the function to be minimised. This function can be further refined to force the algorithm to produce a matrix that satisfies the criteria referred to above by:

1) double-counting off-diagonal elements whose absolute values are greater than 0.6;

2) triple-counting off-diagonal elements whose absolute values are greater than 1.0;

In addition, to avoid the calculation of values for the $\underline{Q}$ matrix that are very far from those first assumed, the function value can be set very high if the algorithm attempts to calculate standard deviations whose values are less than half or greater than double those starting values supplied by the analyst.

This process speeds up the 'tuning' of the Kalman Filter quite considerably, and further reduces the difference between values of synthesised faults in components and sensors and values calculated by the 'Concentrator', as shown in Table 1.

A) BEST ESTIMATES ($\hat{x}$) FROM 'CONCENTRATOR'

		①	②	③	④	⑤ ← PASS N°
	FAN ETA	-0.063	0.0	0.0	0.0	0.0
	FAN CAP	-0.006	0.0	0.0	0.0	0.0
	LPC ETA	-0.377	0.0	0.0	0.0	0.0
*	LPC CAP	0.0	0.0	0.0	0.0	0.0
	HPC ETA	-0.645	-0.870	-1.018	-1.009	-1.720
	HPC CAP	0.076	0.0	0.0	0.0	0.0
	HPT ETA	-0.382	-0.095	0.0	0.0	0.0
	HPT CAP	0.026	0.0	0.0	0.0	0.0
	LPT ETA	-0.196	0.0	0.0	0.0	0.0
*	LPT CAP	0.0	0.0	0.0	0.0	0.0
	EPR	0.033	0.0	0.0	0.0	0.0
	P2	0.252	0.416	0.473	0.0	0.0
	T2	-0.170	-0.063	0.0	0.0	0.0
	WFE	-0.456	-0.012	0.0	0.0	0.0
	P26	-0.074	0.0	0.0	0.0	0.0
	T26	-0.169	-0.056	0.0	0.0	0.0
	P3	-0.003	0.0	0.0	0.0	0.0
	T3	0.090	0.0	0.0	0.0	0.0
	T49	0.496	0.963	0.973	0.962	0.0
	P13	-0.151	-0.041	0.0	0.0	0.0
*	XNL	0.0	0.0	0.0	0.0	0.0
*	XNH	0.0	0.0	0.0	0.0	0.0
	FN	-0.001	0.0	0.0	0.0	0.0
	W1A	0.008	0.0	0.0	0.0	0.0
	TOTAL SS	21.459	35.990	38.946	206.203	585.363
	CHNGE SS	21.131	33.166	38.157	28.781	32.869
	MEAS SS	0.328	2.824	0.789	177.422	552.494 ← OBJECTIVE FUNCTION (LIMIT 19·7)
		BASIC KALMAN FILTER		BEST ANSWER		

* = THESE COMPONENT CHANGES AND SENSOR BIASSES NOT ACTIVATED

B) STANDARD DEVIATIONS (SQUARE ROOTS OF $\underline{P}$I DIAGONAL ELEMENTS) FOR ABOVE

	FAN ETA	0.31481	0.0	0.0	0.0	0.0
	FAN CAP	0.17455	0.0	0.0	0.0	0.0
	LPC ETA	0.32963	0.0	0.0	0.0	0.0
*	LPC CAP	0.0	0.0	0.0	0.0	0.0
	HPC ETA	0.20407	0.12005	0.03755	0.03755	0.00869
	HPC CAP	0.25730	0.0	0.0	0.0	0.0
	HPT ETA	0.14652	0.06400	0.0	0.0	0.0
	HPT CAP	0.17743	0.0	0.0	0.0	0.0
	LPT ETA	0.17829	0.0	0.0	0.0	0.0
*	LPT CAP	0.0	0.0	0.0	0.0	0.0
	EPR	0.05586	0.0	0.0	0.0	0.0
	P2	0.10620	0.04994	0.03657	0.0	0.0
	T2	0.09397	0.04159	0.0	0.0	0.0
	WFE	0.22011	0.10796	0.0	0.0	0.0
	P26	0.11868	0.0	0.0	0.0	0.0
	T26	0.08070	0.03722	0.0	0.0	0.0
	P3	0.16182	0.0	0.0	0.0	0.0
	T3	0.14659	0.0	0.0	0.0	0.0
	T49	0.18165	0.06413	0.04939	0.04938	0.0
	P13	0.09009	0.04135	0.0	0.0	0.0
*	XNL	0.0	0.0	0.0	0.0	0.0
*	XNH	0.0	0.0	0.0	0.0	0.0
	FN	0.18838	0.0	0.0	0.0	0.0
	W1A	0.10607	0.0	0.0	0.0	0.0

Figure 32: 'Concentrator' performance for 'Tuned' input

	HPC ETA	P2 Bias	T49 Bias
Synthesised Faults	-1.0%	+0.5%	+1.0%
Original 'Concentrator' with 'Untuned' input (Figure 24)	-1.117%	+0.435%	+0.835%
'Concentrator' with 'Tuned' input (Figure 32)	-1.018%	+0.473%	+0.973%
'Concentrator with 'Auto-Tuned' input	-1.002%	+0.476%	+0.995%

Table 1: Comparison of 'Concentrator' outputs with various inputs to the Q matrix

CHAPTER 5: SMOOTHING AND TRENDING USING KALMAN FILTER THEORY

The ability to smooth and detect underlying trends in a time series is a common requirement in engineering. This chapter describes an application of the Kalman Filter to the analysis of such series, in which the underlying level and trend (rate of change of level) in a process generating noisy observations can be estimated. The equations for this application of the Kalman Filter are derived, and the meaning of the results is discussed, including comparisons with other often-used smoothing algorithms such as Moving Average and Exponential Smoothing. Finally, an application of the 'Concentrator' described in the previous chapter to the analysis of related time series of component changes and sensor biasses is also discussed.

5.1 Basic Assumptions

A time series may be defined as a series of related points gathered sequentially. To proceed with the analysis, the following assumptions are made regarding the relationships that apply from point to point:

1) $Level_k = (Level_{k-1} + wl_{k-1}) + t \bullet (Trend_{k-1} + wt_{k-1})$

2) $Trend_k = (Trend_{k-1} + wt_{k-1})$

where:

Level = true level of process generating series;

Trend = true trend (rate of change of level) of process generating series;

t = number of intervals (time, cycles, etc) between current and previous observation;

wl, wt = noise terms in level and trend respectively; these are assumed to be normally distributed with means of zero and variances of q_{11}, q_{22} respectively. They are also assumed to have a covariance of q_{12};

Subscript k denotes value at time current observation of time series taken;

Subscript k-1 denotes value at time previous observation of time series taken.

Expressed in words:

Level 'now' = Level 'then' plus term to allow for level variability plus number of intervals multiplied by (Trend 'then' plus term to

allow for trend variability)

Trend 'now' = Trend 'then' plus term to allow for trend variability

3) $Obs_k = Level_k + v_k$

where:

Obs = observation of parameter value in time series;

v = noise in observation, assumed to be normally distributed with a mean of zero and a variance r;

k, Level, defined above.

Expressed in words:

Observation 'now' = Level 'now' plus noise in observation

Figure 33 shows the situation diagrammatically.

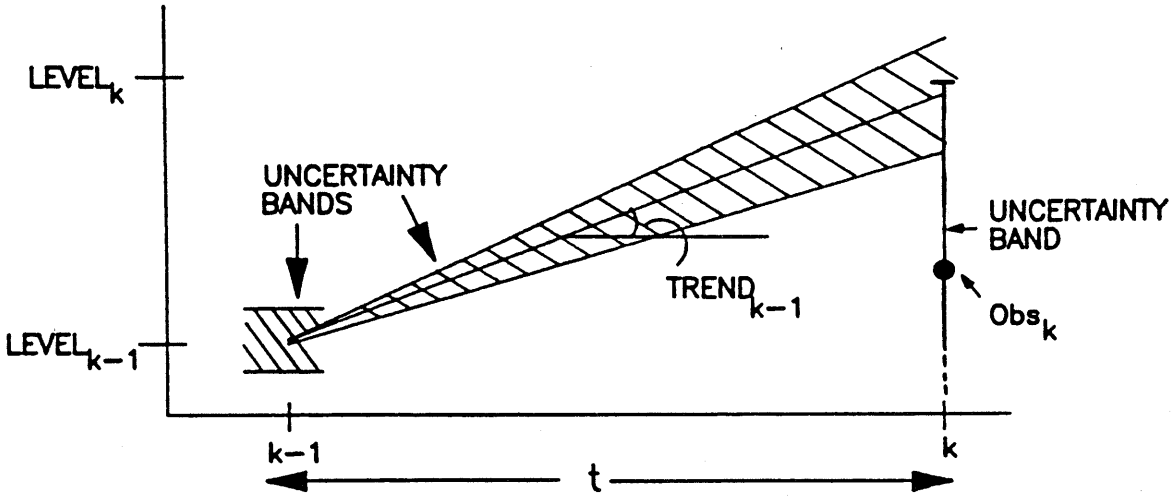

Figure 33: Diagrammatic representation of time series model

For reasons that will become apparent later, the equations above can be written in the following matrix forms:

1) $$\begin{pmatrix}\text{Level}\\ \text{Trend}\end{pmatrix}_k = \begin{pmatrix}1 & t\\ 0 & 1\end{pmatrix} \bullet \begin{pmatrix}\text{Level}\\ \text{Trend}\end{pmatrix}_{k-1} + \begin{pmatrix}1 & t\\ 0 & 1\end{pmatrix} \bullet \begin{pmatrix}wl\\ wt\end{pmatrix}_{k-1}$$

where $$\begin{pmatrix}wl\\ wt\end{pmatrix} = N\left(\begin{pmatrix}0\\ 0\end{pmatrix}, \begin{pmatrix}q_{11} & q_{12}\\ q_{12} & q_{22}\end{pmatrix}\right)$$

2) $$Obs_k = (1,0) \bullet \begin{pmatrix}\text{Level}\\ \text{Trend}\end{pmatrix}_k + v_k$$

where $v = N(0,r)$

5.2 Derivation of Smoothing/Trending Equations

The situation described above, in which one known (the observation) is used to estimate two unknowns (level and trend) is ideally suited to the application of Kalman Filter techniques. Before this can be done, the equations derived in the previous chapter need to be extended to their recursive form (References 40 and 41).

1) $\underline{\hat{x}}_k = \underline{A} \bullet \underline{\hat{x}}_{k-1} + \underline{K} \bullet (\underline{Y}_k - \underline{C} \bullet \underline{A} \bullet \underline{\hat{x}}_{k-1})$

2) $\underline{K} = \underline{P}' \bullet \underline{C}^T \bullet (\underline{C} \bullet \underline{P}' \bullet \underline{C}^T + \underline{R})^{-1}$

3) $\underline{P}' = \underline{A} \bullet \underline{P}_{k-1} \bullet \underline{A}^T + \underline{Q}$

4) $\underline{P}_k = (\underline{I} - \underline{K} \bullet \underline{C}) \bullet \underline{P}'$

where:

$\underline{\hat{x}}$ = best estimate of system state vector;

$\underline{Y}$ = vector of observations;

$\underline{C}$ = System Matrix: ideally:

$$\underline{Y} = \underline{C} \bullet \underline{x};$$

$\underline{K}$ = Kalman Gain Matrix: the weighting matrix used to update state estimates from observations;

$\underline{Q}$ = system covariance matrix: the uncertainties in the system are assumed to be normally distributed, with mean $\underline{0}$ and covariance $\underline{Q}$;

$\underline{R}$ = measurement repeatability covariance matrix: the random errors in the measurements are assumed to be normally distributed, with mean $\underline{0}$ and covariance $\underline{R}$;

$\underline{A}$ = matrix defining how $\underline{x}$ varies over time: ideally

$$\underline{x}_k = \underline{A} \bullet \underline{x}_{k-1} ;$$

$\underline{P}'$= covariance update;

$\underline{P}$ = covariance matrix of $\underline{\hat{x}}$; the errors in the estimate $\underline{\hat{x}}$ are assumed to be normally distributed, with mean $\underline{0}$ and covariance $\underline{P}$;

$\underline{I}$ = unit matrix of appropriate dimension;

Subscripts k, k-1 denote current time and immediately previous time respectively;

Superscripts T, -1 denote matrix transpose and matrix inverse respectively.

For the smoothing/trending case:

$$\underline{\hat{x}} = \begin{pmatrix} \text{Level} \\ \text{Trend} \end{pmatrix}$$

$$\underline{y} = \text{Obs}$$

$$\underline{A} = \begin{pmatrix} 1 & t \\ 0 & 1 \end{pmatrix}$$

$$\underline{C} = (1,0)$$

$$\underline{Q} = \begin{pmatrix} q_{11} & q_{12} \\ q_{12} & q_{22} \end{pmatrix}$$

$$\underline{R} = r$$

We can manipulate the above matrix equations for the level and trend into equations involving scalar quantities only, as follows:

1) $$\underline{P}' = \begin{pmatrix} p_{11}' & p_{12}' \\ p_{12}' & p_{22}' \end{pmatrix} = \begin{pmatrix} 1 & t \\ 0 & 1 \end{pmatrix} \bullet \begin{pmatrix} p_{11} & p_{12} \\ p_{12} & p_{22} \end{pmatrix}_{k-1} \bullet \begin{pmatrix} 1 & 0 \\ t & 1 \end{pmatrix} + \begin{pmatrix} 1 & t \\ 0 & 1 \end{pmatrix} \bullet \begin{pmatrix} q_{11} & q_{12} \\ q_{12} & q_{22} \end{pmatrix} \bullet \begin{pmatrix} 1 & 0 \\ t & 1 \end{pmatrix}$$

$$\Rightarrow p_{11}' = (p_{11,k-1} + q_{11}) + 2 \bullet t \bullet (p_{12,k-1} + q_{12}) + t^2 \bullet (p_{22,k-1} + q_{22})$$

$$p_{12}' = (p_{12,k-1} + q_{12}) + t \bullet (p_{22,k-1} + q_{22})$$

$$p_{22}' = (p_{22,k-1} + q_{22})$$

2) $$\underline{P}' \bullet \underline{C}^T = \begin{pmatrix} p_{11}' & p_{12}' \\ p_{12}' & p_{22}' \end{pmatrix} \bullet \begin{pmatrix} 1 \\ 0 \end{pmatrix} = \begin{pmatrix} p_{11}' \\ p_{12}' \end{pmatrix}$$

$$(\underline{C} \bullet \underline{P}' \bullet \underline{C}^T + \underline{R})^{-1} = \left((1,0) \bullet \begin{pmatrix} p_{11}' \\ p_{12}' \end{pmatrix} + r \right)^{-1}$$

$$= (p_{11}' + r)^{-1}$$

$$\Rightarrow \underline{K} = \begin{pmatrix} k_1 \\ k_2 \end{pmatrix} = \begin{pmatrix} p_{11}' \\ p_{12}' \end{pmatrix} \bullet (p_{11}' + r)^{-1}$$

$$\Rightarrow k_1 = p_{11}' \div (p_{11}' + r)$$

$$k_2 = p_{12}' \div (p_{11}' + r)$$

3) $$\underline{y}_k - \underline{C} \bullet \underline{A} \bullet \underline{x}_{k-1} = \text{Obs}_k - (1,0) \bullet \begin{pmatrix} 1 & t \\ 0 & 1 \end{pmatrix} \bullet \begin{pmatrix} \text{Level} \\ \text{Trend} \end{pmatrix}_{k-1}$$

$$= Obs_k - (1,t) \bullet \begin{pmatrix} Lev\hat{e}l \\ Tr\hat{e}nd \end{pmatrix}_{k-1}$$

$$= Obs_k - (Lev\hat{e}l_{k-1} + t \bullet Tr\hat{e}nd_{k-1})$$

This term, the difference between the actual observation at time k and the predicted observation based on estimates at time k-1, is sufficiently important to be given its own name, $Delta_k$:

$$Delta_k = Obs_k - (Lev\hat{e}l_{k-1} + t \bullet Tr\hat{e}nd_{k-1})$$

4) $$\underline{\hat{x}}_k = \begin{pmatrix} Lev\hat{e}l \\ Tr\hat{e}nd \end{pmatrix}_k = \begin{pmatrix} 1 & t \\ 0 & 1 \end{pmatrix} \bullet \begin{pmatrix} Lev\hat{e}l \\ Tr\hat{e}nd \end{pmatrix}_{k-1} + \begin{pmatrix} k_1 \\ k_2 \end{pmatrix} \bullet Delta_k$$

$$\Rightarrow Lev\hat{e}l_k = Lev\hat{e}l_{k-1} + t \bullet Tr\hat{e}nd_{k-1} + (p_{11}' \div (p_{11}' + r)) \bullet Delta_k$$

$$Tr\hat{e}nd_k = Tr\hat{e}nd_{k-1} + (p_{12}' \div (p_{11}' + r)) \bullet Delta_k$$

5) $$\underline{P}_k = \begin{pmatrix} p_{11} & p_{12} \\ p_{12} & p_{22} \end{pmatrix}_k = \left(\begin{pmatrix} 1 & 0 \\ 0 & 1 \end{pmatrix} - \begin{pmatrix} k_1 \\ k_2 \end{pmatrix} \bullet (1,0) \right) \bullet \begin{pmatrix} p_{11}' & p_{12}' \\ p_{12}' & p_{22}' \end{pmatrix}$$

$$= \begin{pmatrix} 1-k1 & 0 \\ -k2 & 1 \end{pmatrix} \bullet \begin{pmatrix} p_{11}' & p_{12}' \\ p_{12}' & p_{22}' \end{pmatrix}$$

$$\Rightarrow \quad p_{11,k} = (1-k_1) \bullet p_{11}'$$

$$p_{12,k} = (1-k_1) \bullet p_{12}' = p_{12}' - k_2 \bullet p_{11}'$$

$$p_{22,k} = p_{22}' - k_2 \bullet p_{12}'$$

If the equations for p_{11}', p_{12}', p_{22}', p_{11}, p_{12}, p_{22}, as well as q_{11}, q_{12}, q_{22}, are divided by r, we arrive at the following scalar relationships:

1) $$p_{11}' \div r = s_1 = (p_{11,k-1} \div r + q_{11} \div r) + 2 \bullet t \bullet (p_{12,k-1} \div r + q_{12} \div r) + t^2 \bullet (p_{22,k-1} \div r + q_{22} \div r)$$

$$p_{12}' \div r = s_2 = (p_{12,k-1} \div r + q_{12} \div r) + t \bullet (p_{22,k-1} \div r + q_{22} \div r)$$

$$p_{22}' \div r = s_3 = (p_{22,k-1} \div r + q_{22} \div r)$$

2) $$Delta_k = Obs_k - (Lev\hat{e}l_{k-1} + t \bullet Tr\hat{e}nd_{k-1})$$

$$Lev\hat{e}l_k = Lev\hat{e}l_{k-1} + t \bullet Tr\hat{e}nd_{k-1} + (s_1 \div (s_1+1)) \bullet Delta_k$$

$$Tr\hat{e}nd_k = Tr\hat{e}nd_{k-1} + (s_2 \div (s_1 + 1)) \bullet Delta_k$$

3) $p_{11,k} \div r = s_1 \div (s_1 + 1)$

$p_{12,k} \div r = s_2 \div (s_1 + 1)$

$p_{22,k} \div r = s_3 - s_2^2 \div (s_1 + 1)$

The above relationships define the Kalman Filter as applied to smoothing and trending. To start the algorithm off (ie for k = 1), the following relationships are used:

$\hat{Level}_0 = Obs_1$)
) or specified by user; see below
$\hat{Trend}_0 = 0$)

$p_{11,0} \div r = q_{11} \div r + 2 \bullet q_{12} \div r + q_{22} \div r$

$p_{12,0} \div r = q_{12} \div r + q_{22} \div r$

$p_{22,0} \div r = q_{22} \div r$

The algorithm is used in a recursive fashion, as shown diagrammatically in Figure 34.

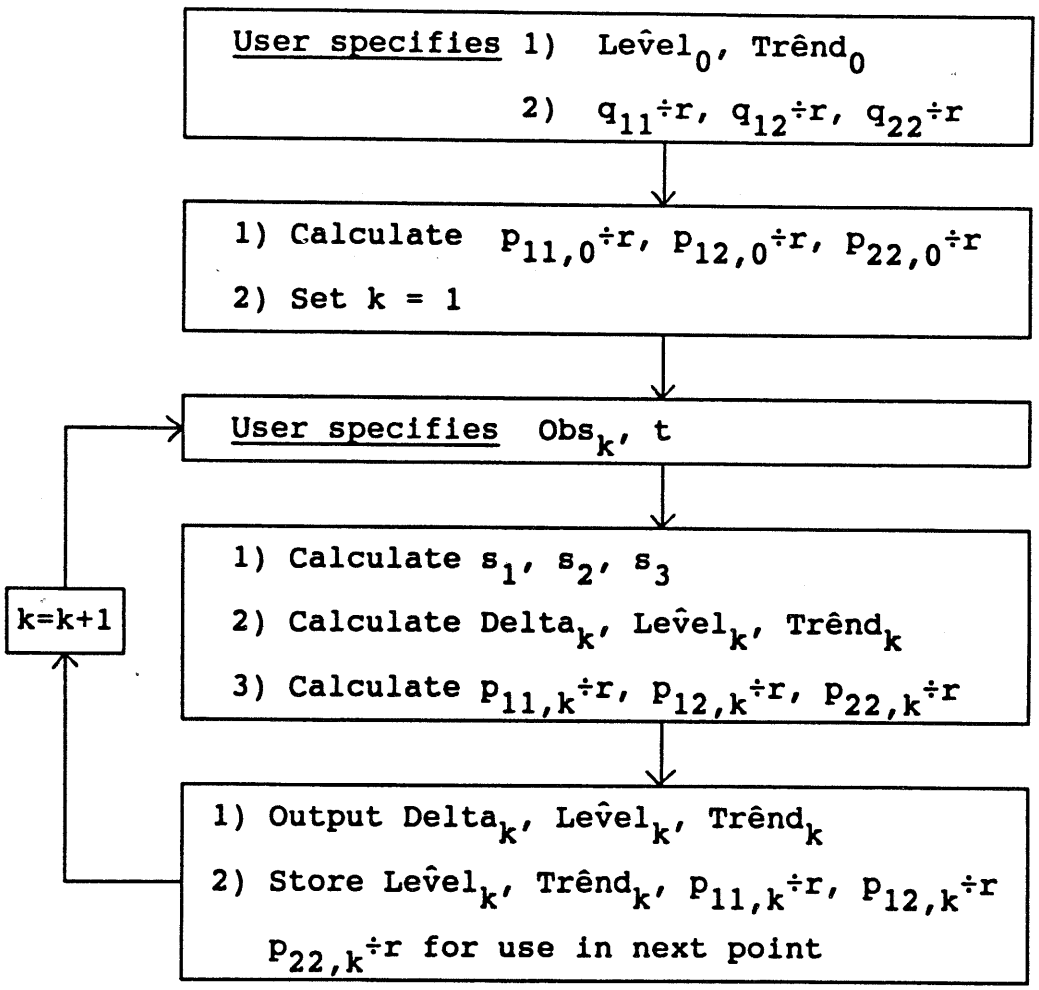

Figure 34: Calculation procedure for smoothing/trending

5.3 Meaning of Results

It is instructive to re-state some of the above equations in words, in order to understand what they mean.

The group $(\hat{Level}_{k-1} + t \bullet \hat{Trend}_{k-1})$, which appears twice in the equations, can be considered as a predicted level at time k before the observation is taken.

$Delta_k = Obs_k - (\hat{Level}_{k-1} + t \bullet \hat{Trend}_{k-1})$ is the difference between the actual observation at time k and the predicted level discussed above. It is a useful quantity for detecting sudden jumps in the series.

The equations:

$$\hat{Level}_k = \hat{Level}_{k-1} + t \bullet \hat{Trend}_{k-1} + (s_1 \div (s_1+1)) \bullet Delta_k$$

and:

$$\hat{Trend}_k = \hat{Trend}_{k-1} + (s_2 \div (s_1 + 1)) \bullet Delta_k$$

can be re-stated as:

> Estimated level after observation taken
> = Predicted level before observation taken plus level estimate gain multiplied by the difference between observation and predicted level;

and:

> Estimated trend after observation taken
> = Predicted trend before observation taken plus trend estimate gain multiplied by the difference between observation and predicted level;

The estimates of level and trend are modified, depending on the gains (which may be thought of as weighting factors), to take account of the differences between actual and predicted observations.

The terms:

$$\text{Level estimate gain} = s_1 \div (s_1 + 1) = p_{11,k} \div r$$

and:

$$\text{Trend estimate gain} = s_2 \div (s_1 + 1) = p_{12,k} \div r$$

can be re-stated as:

$$p_{11,k} \div r = \frac{\text{uncertainty in level estimate}}{\text{uncertainty in observation}}$$

and:

$$p_{12,k} \div r = \frac{\text{uncertainty in level-trend correlation}}{\text{uncertainty in observation}}$$

respectively.

It is seen that, if the uncertainty in the observations is low relative to the uncertainty in the level estimate and/or level-trend correlation, the level and/or trend estimate gains will be high, and the level and/or trend estimates will be adjusted to reflect the information carried in the observations. Conversely, if the uncertainty in the observations is high relative to the uncertainty in the level estimate and/or level-trend correlation, the level and/or trend estimate gains will be low, and the level and/or trend estimates will only respond slowly to the information in the observations.

Note that:

1) these gains vary from point to point as t varies: if, however, t is constant from point to point, they tend to converge to constant values as k increases.

2) these gains are independent of the observations: they are functions of $q_{11} \div r$, $q_{12} \div r$, $q_{22} \div r$ and t only.

5.4 Input Required

In order to use the algorithm, the user needs to supply:

1) level and trend estimates at the start of the time series. The level estimate can be either the theoretical expected level of the series, the first observation or the average value of the first few points. Usually, the trend estimate at the start of the time series is zero;

2) Values of $q_{11} \div r$, $q_{12} \div r$ and $q_{22} \div r$, which define how the algorithm will respond to the data. Usually, $q_{12} \div r$, the level-trend covariance/observation variance ratio, is set to zero: selecting values of $q_{11} \div r$ and $q_{22} \div r$ will be discussed later;

3) For each point in the series, values for the observation and the number of intervals between the current and previous observation. The interval units can be either time (eg hours, days, months) or discrete (eg cycle, point number): in all cases, the resulting units of trend will be level units/interval units.

5.5 Comparison with Moving Average and Exponential Smoothing

Two methods widely used for smoothing a time series are Moving Average and Exponential Smoothing. The methods of

generating smoothed level estimates using these techniques are as follows:

1) Moving Average

For a moving average of order n:

$$\hat{Level}_{k,n} = \frac{(Obs_k + Obs_{k-1} + \ldots + Obs_{k-n+1})}{n}$$

where n = number of points making up average

2) Exponential Smoothing

$$\hat{Level}_k = \hat{Level}_{k-1} + \alpha \bullet (Obs_k - \hat{Level}_{k-1})$$

where α = exponential smoothing constant ($0 < \alpha < 1$)

One of the problems with the Moving Average method is that it is not recursive, ie the calculations do not just depend on the current observation and immediately previous level estimates. The observation at time (k-n+1) has to be stored, ready to be subtracted from a running total when the observation at time (k+1) appears: this makes it very computationally inefficient.

The Exponential Smoothing method can be regarded as a limiting case of the Moving Average method: it is recursive, and it is very easy to implement. However, both of the above methods contain no trend estimate terms, which means that:

1) no estimates of trends are available;

2) time lags between the observations and the estimates are introduced, particularly when analysing a series in which a ramp is present.

Both methods also do not make proper allowance for different intervals between the observations. The Kalman Filter approach suffers from none of these drawbacks; the small increase in computational load over the Exponential Smoothing approach is more than justified by the extra information the Kalman Filter supplies.

5.6 Trend 'Concentration'

When smoothing/trending component changes and sensor biasses diagnosed using the methods discussed in the previous chapter, it is better to use the output from the basic Kalman Filter (the 'First Pass') as input to the Smoothing/Trending Algorithm discussed above instead of the 'Concentrator' output, in order to detect the onset of trends that, in their initial stages, produce levels that are too small for the 'Concentrator' to pick up. However,

this inevitably leads to 'smearing' of trend estimates, ie significant trends in a small number of component changes and/or sensor biasses are distributed, as smaller trends, over the whole set of component changes and sensor biasses being considered.

An alternative approach that avoids this problem and reduces the number of parameters that have to be stored for the time-series analysis of gas turbine component change and sensor bias diagnoses is as follows:

1) Process each measurement difference time series using the Smoothing/Trending Algorithm described above, making sure that the constants $q_{11} \div r$, $q_{12} \div r$ and $q_{22} \div r$ are identical for each series;

2) Create, from the outputs from the above process, three temporary 'pseudo-measurement' vectors for each point in the series:

   $\underline{Y}_{Level}$ = vector of measurement difference level estimates;

   $\underline{Y}_{Trend}$ = vector of measurement difference trend estimates;

   $\underline{Y}_{Delta}$ = vector of (actual - predicted) measurement differences;

3) Process each of these vectors through three separate 'Concentrator' algorithms, as discussed in the previous chapter, to produce:

   $\hat{\underline{x}}_{Level}$ = vector of component change and sensor bias level estimates;

   $\hat{\underline{x}}_{Trend}$ = vector of component change and sensor bias trend estimates;

   $\hat{\underline{x}}_{Delta}$ = vector of (actual - predicted) component changes and sensor biasses;

   for each point in the series. Note that, when processing the trend estimate vectors, the threshold for rejection in the final step of the 'Concentrator' should be reduced (typically by a factor of 100) to allow for the smaller numerical values of the trend estimates. All the other inputs to each of the 'Concentrators' are identical.

The above process has a number of advantages:

1) The noise in the measurement differences is 'smoothed' before diagnosis of component changes and sensor biasses, thus reducing the variability in the estimation of these parameters;

2) Trends and sudden changes in component performance and sensor biasses are identified from the trends and sudden changes in the interconnected series of measurement differences: the interconnections are, of course, expressed in the elements of the System Matrix;

3) This method is more computationally efficient than processing the output from the basic Kalman Filter through the Smoothing/Trending Algorithm; fewer recursive calculations need to be done, because the number of measurement differences is less than the number of component changes and sensor biasses, so fewer numbers need to be stored for subsequent processing of data gathered in the future. This feature becomes important when large numbers of gas turbines are being monitored.

5.7 'Tuning' the Smoothing/Trending Algorithm

The major decision that has to be made when implementing any time series analysis is the balance between 'sensitive' response to genuine changes (steps and ramps) in the series (which may lead to spurious results due to over-response to noise in the observations) and 'slugged' response to noise in the observations (which may lead to slow response to genuine changes in the series). The balance between these two effects has to be decided by the user, based on knowledge of the 'character' of the series (signal/noise ratio) and the requirements of the analysis.

When using the Moving Average and Exponential Smoothing algorithms discussed earlier, the user decides this balance by choice of the order of the Moving Average (n) or Exponential Smoothing Constant (α) respectively; the response is 'tuned' from high to low sensitivity by increasing n or reducing α, until a satisfactory level of smoothing is obtained. The user of the Smoothing/Trending Algorithm discussed above has the choice of three constants to vary:

1) $q_{11} \div r$, the ratio of level variance to observation repeatability variance;

2) $q_{12} \div r$, the ratio of level-trend covariance to observation repeatability variance;

3) $q_{22} \div r$, the ratio of trend variance to observation repeatability variance;

The number of intervals between points in the time series (t) and the position of the point in the time series (k) also affect the calculations.

If $q_{12} \div r$ is assumed to be zero (implying no correlation

between level and trend) then, for fixed values of t and k, a plot showing how the level and trend estimate gains vary with $q_{11} \div r$ and $q_{22} \div r$ can be produced. Figure 35 shows the form of such a relationship, indicating regions of 'sensitive' and 'sluggish' response. The Figure also shows a region where certain combinations of level and trend estimate gains are invalid, because they would require negative variance ratios to calculate them; in simple terms, it is impossible to imply a degree of certainty in the trend (implied by the value of the trend estimate gain) without implying a minimum degree of certainty in the level (implied by the value of the level estimate gain). These combinations are in the region in Figure 35 bounded by cross-hatching.

5.8 Examples

Figures 36 to 41 show the Smoothing/Trending Algorithm in operation, producing estimates of level and trend for a typical step, ramp and outlier, both with and without random noise. In all the Figures, 'sensitive' and 'sluggish' implementations of the algorithm are shown for comparison.

Figure 36 shows responses to a typical step in observations with no random noise, while Figure 37 shows responses to the same step with normally-distributed random noise added to the observations. Points to note are:

1) The 'overshoot' of level estimates in the no-noise case, caused by the large trend (1.0 units/time interval) when the series steps up to the new level at time interval 10. This overshoot dies away as information that the series is not rising further is gathered;

2) The value of Delta in both Figures at time interval 10 has risen sharply, before decaying to near zero as further information is gathered. This sharp rise can be used to warn the analyst that the series has changed its 'character';

3) The rise of trend estimates when the series steps up to its new level, followed by a fall to near zero as information is gathered that indicates that the series is not rising further.

Figure 38 shows responses to a typical ramp in observations with no random noise, while Figure 39 shows responses to the same ramp with normally-distributed random noise added to the observations. Points to note are:

1) The very close agreement between the observations and

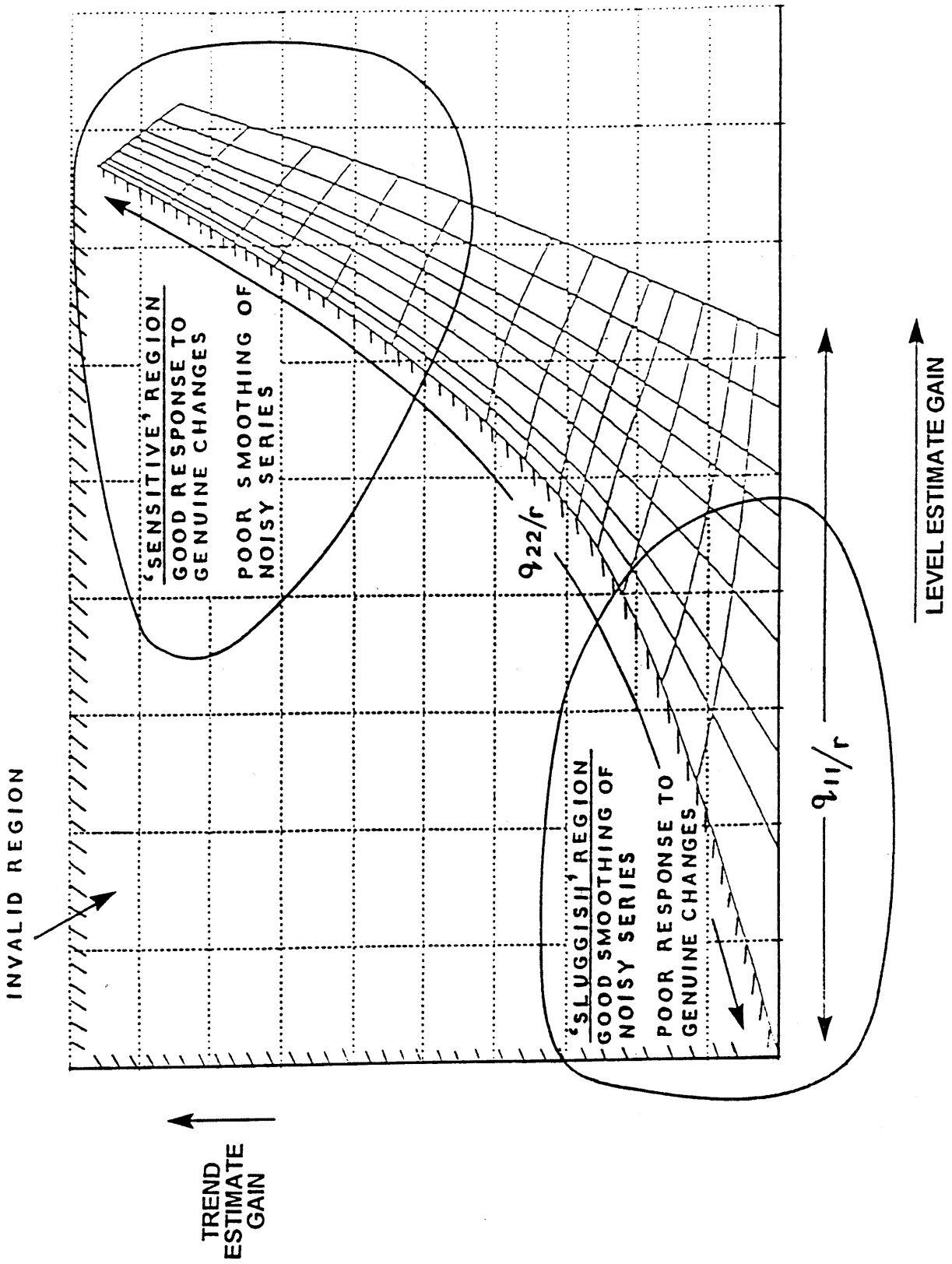

Figure 35: Typical relationship of level and trend estimate gains with $q_{11} \div r$, $q_{22} \div r$

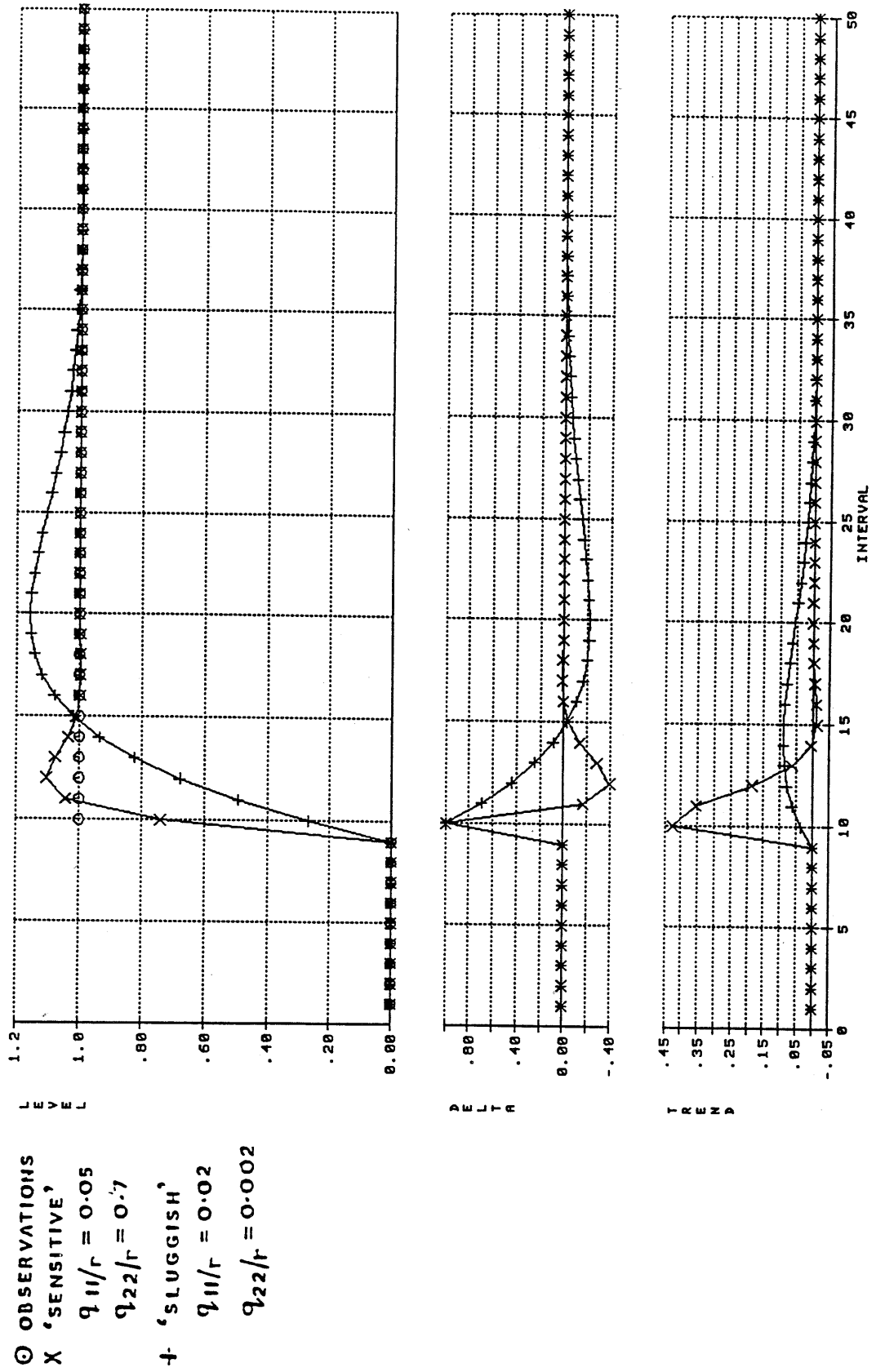

Figure 36: Smoothing/trending of step: no noise

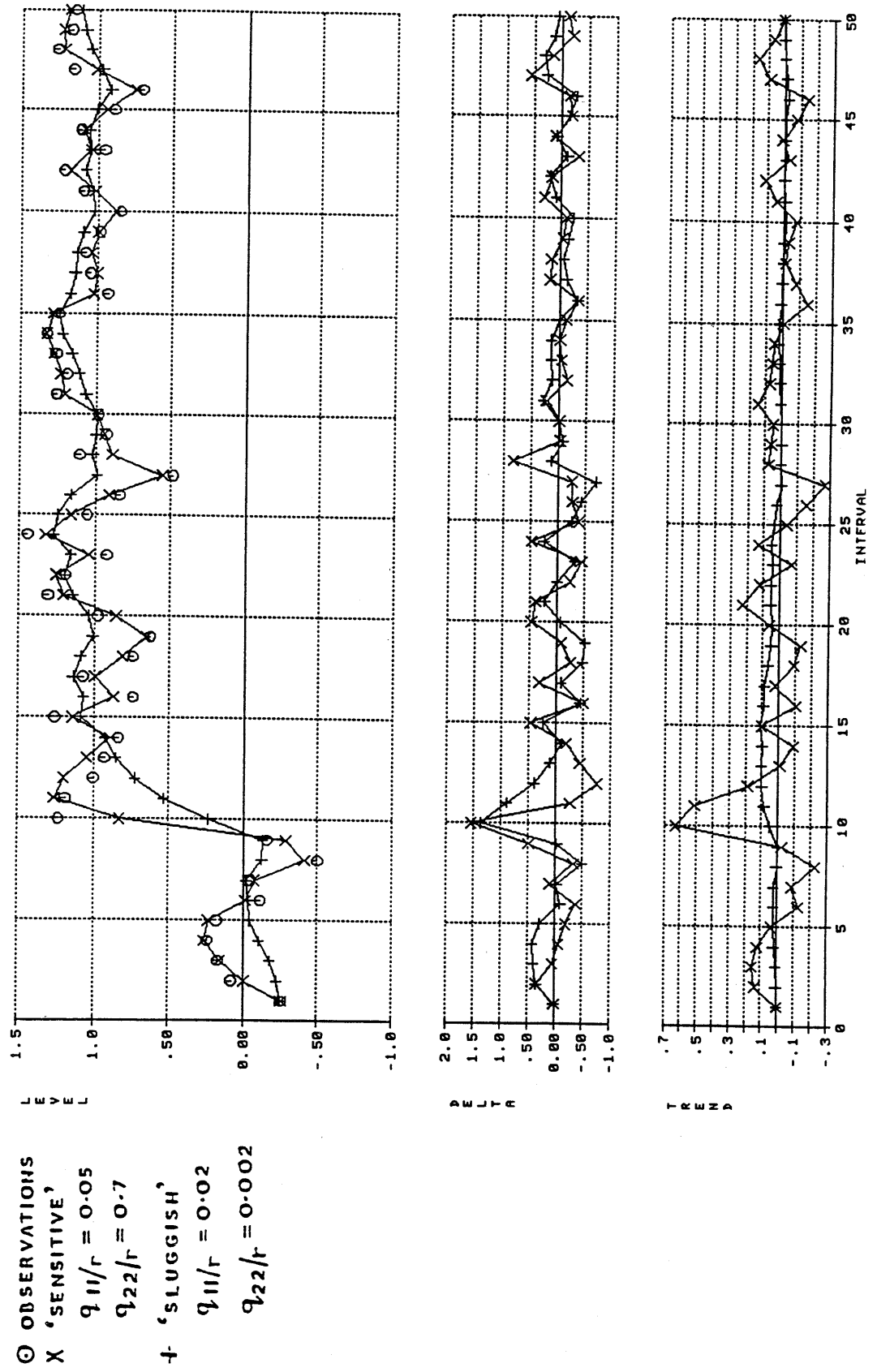

Figure 37: Smoothing/trending of step: noise in series

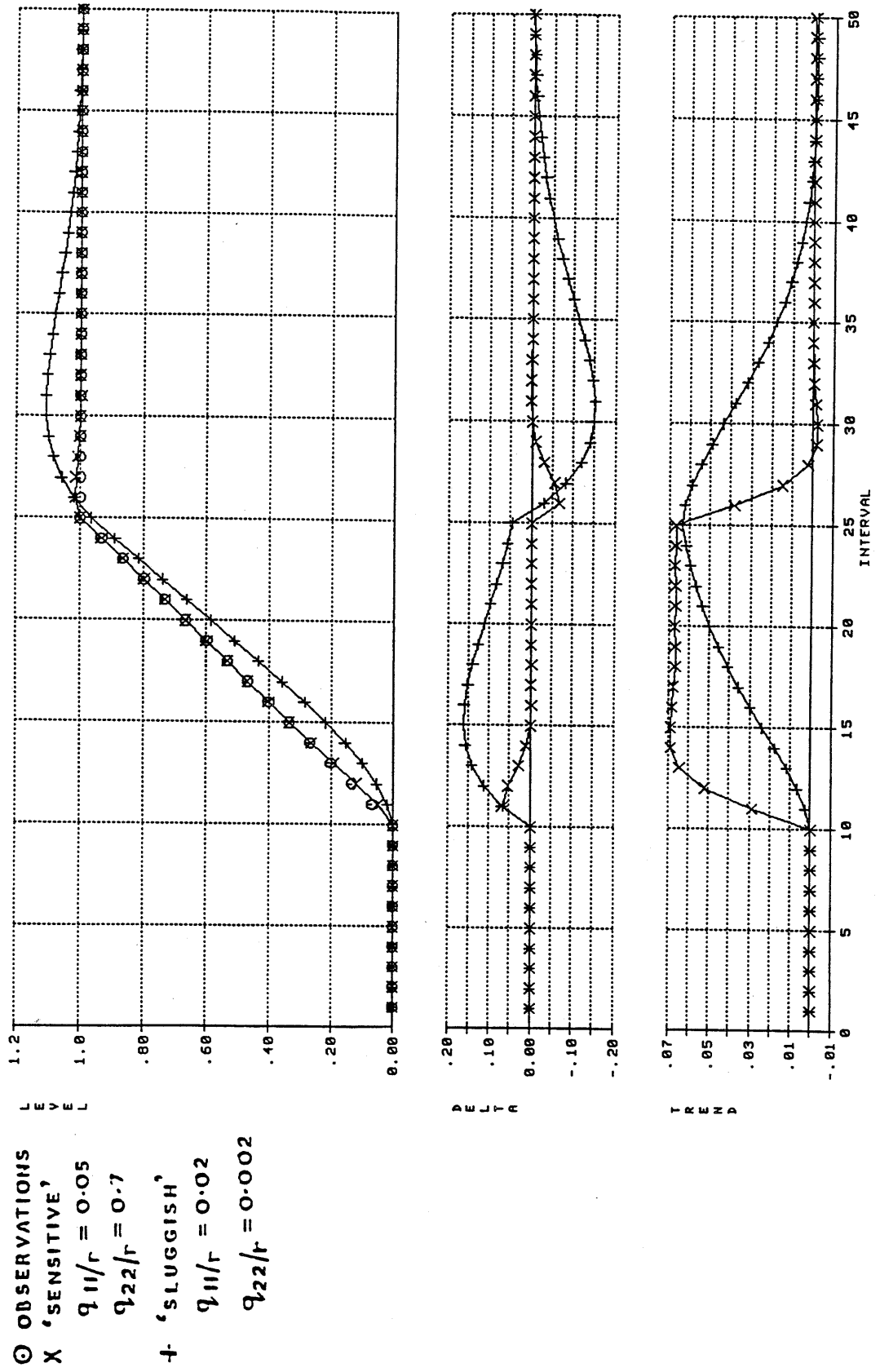

Figure 38: Smoothing/trending of ramp: no noise

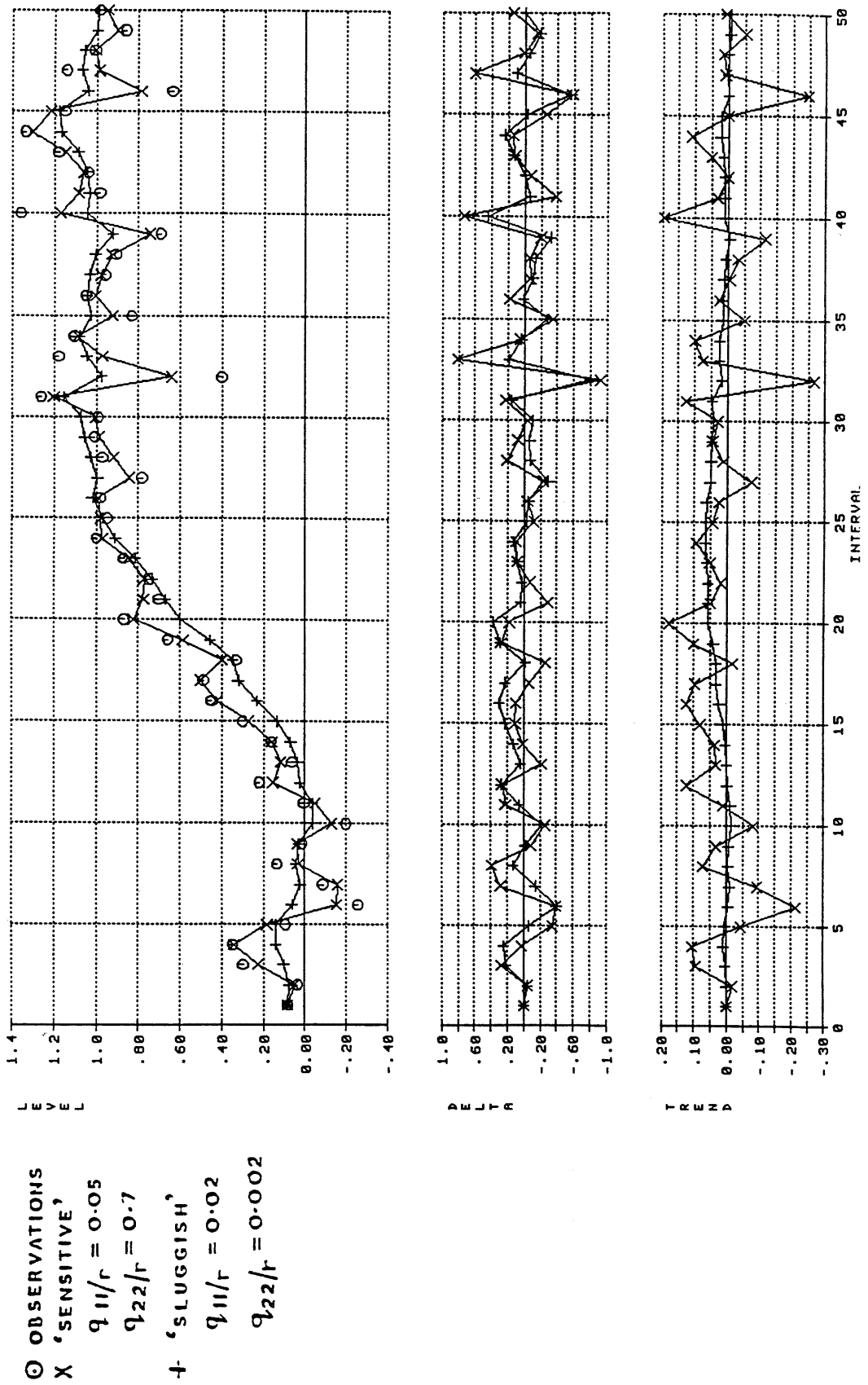

Figure 39: Smoothing/trending of ramp: noise in series

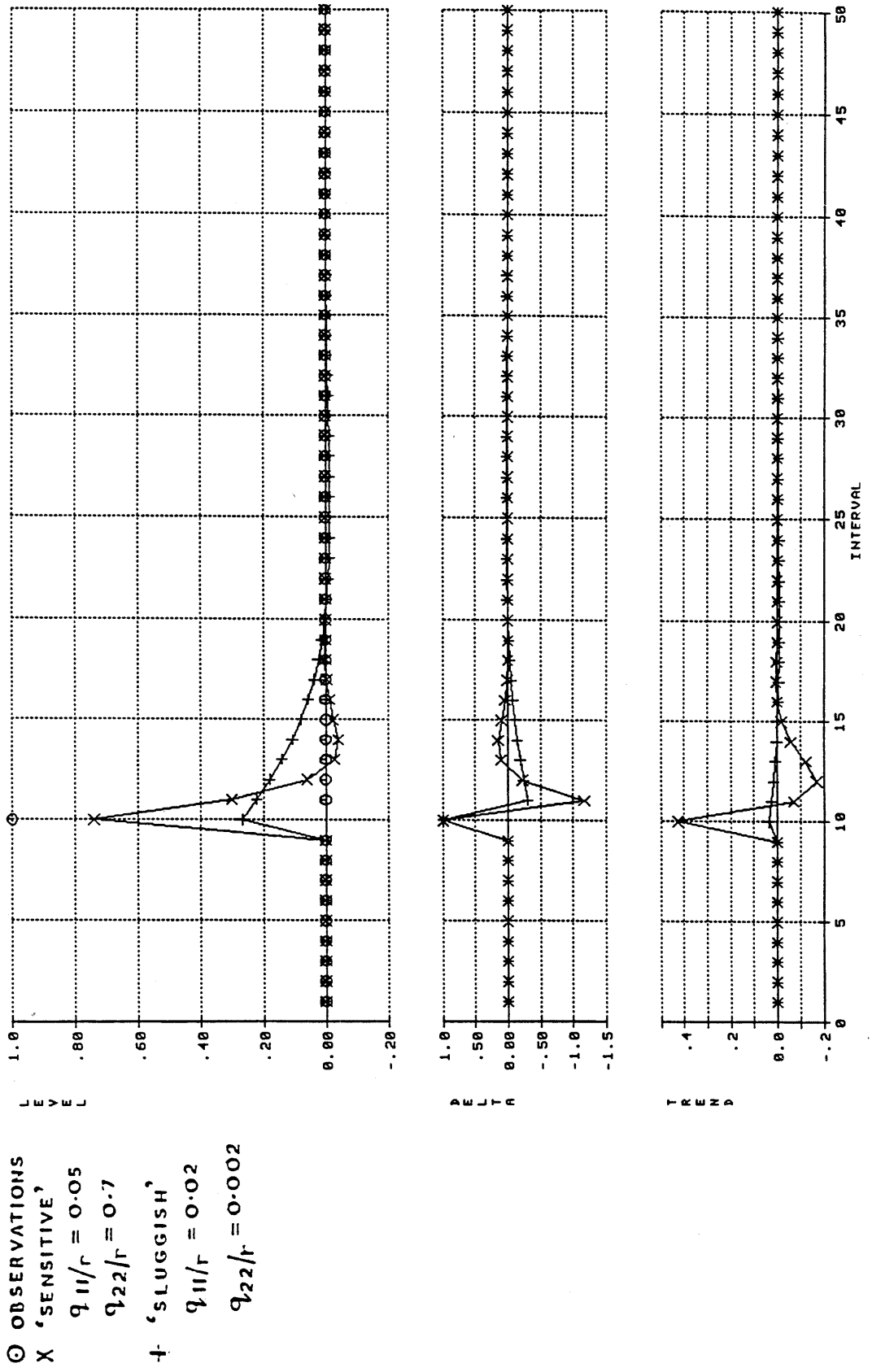

Figure 40: Smoothing/trending of outlier: no noise

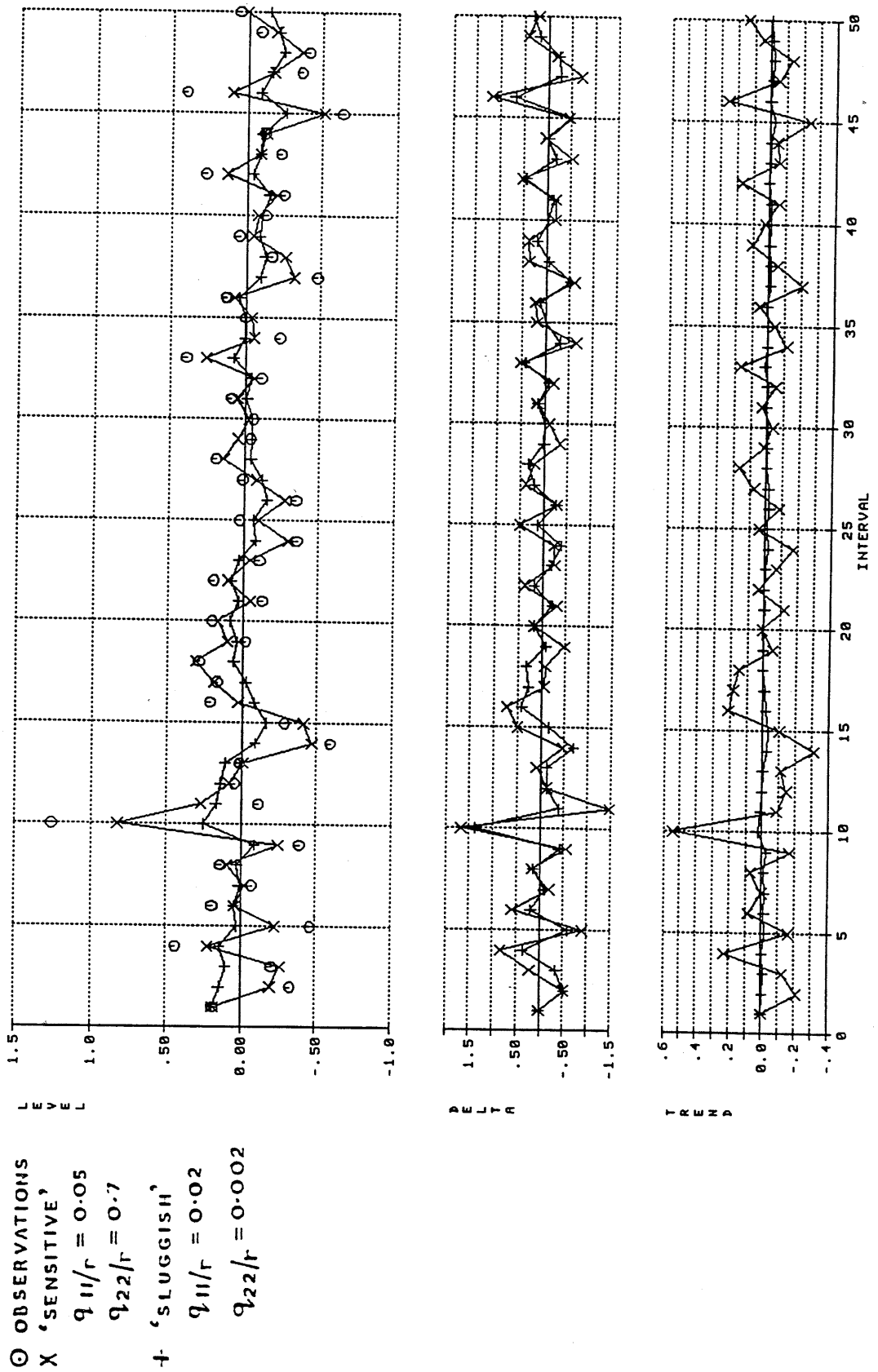

Figure 41: Smoothing/trending of outlier: noise in series

the estimates from the 'sensitive' implementation in the no-noise case; the 'lag' seen when Moving Average and Exponential Smoothing algorithms are used is not present;

2) The estimate of trend from the 'sensitive' implementation in the no-noise case is exact (1.0 units/15 time intervals = 0.06667) 6 to 7 observations after the ramp starts. The 'sluggish' implementation estimates the trend after 14 to 15 observations in both cases;

3) The value of Delta stays near zero, because there are no sudden changes in the series, except when the magnitudes of the noise terms are large.

Figure 40 shows responses to a typical outlier in observations with no random noise, while Figure 41 shows responses to the same outlier with normally-distributed random noise added to the observations. Points to note are:

1) The sharp rise in the value of Delta at time interval 10, followed by the sharp fall at time interval 11, in the 'sensitive implementation: this latter effect is due to the interpretation of observation 11 as an outlier, which it would be if observation 10 marked the beginning of a step;

2) The rapid decay of the over-estimates of level and trend in the no-noise case, as information is gathered confirming that observation 10 was really an outlier.

All the Figures show the better performance of the 'sensitive' implementation with no noise in the series, and the better performance of the 'sluggish' implementation when noise is present.

CHAPTER 6: EXAMPLES

This chapter presents a number of examples of the operation of the Kalman Filter and 'Concentrator, the Smoothing/Trending Algorithm and Trend 'Concentration'. Simulated gas turbine component changes and sensor biasses were used in these demonstrations, for two reasons:

1) data gathered from gas turbines by manufacturers during development and production testing, and by users during service operation, is proprietary;

2) it is extremely costly to deliberately introduce genuine component changes into a gas turbine, then run tests to see if the changes introduced can be detected analytically;

Detection of single component changes and sensor biasses (both with and without normally-distributed sensor non-repeatabilities added to the simulated sensor readings) by the 'Concentrator' is demonstrated, followed by detection of pairs of component changes and/or sensor biasses without sensor non-repeatability. To demonstrate the Smoothing/Trending Algorithm, fuel consumption figures gathered over six years of operation of the author's car have been used, demonstrating the universal applicability of the technique. Simulated gas turbine time series data (both with and without the addition of sensor non-repeatability) has been used to demonstrate all the Kalman Filter based analysis techniques discussed in this thesis, including Trend 'Concentration'. All the matrices used as input to the Kalman Filter and 'Concentrator' are identical to those used in previous chapters; note, however, that the $\underline{Q}$ matrix elements are those used to produce the 'Auto-Tuned' analysis given in Table 1. The component change and sensor bias standard deviations used to generate this $\underline{Q}$ matrix are listed for reference in Table 2; they replace those given in the column labelled SYSTM SD in Figure 31.

FAN ETA	0.606%	WFE bias	0.399%
FAN CAP	0.396%	P26 bias	0.273%
LPC ETA	0.880%	T26 bias	0.125%
HPC ETA	0.368%	P3 bias	0.391%
HPC CAP	0.524%	T3 bias	0.270%
HPT ETA	0.278%	T49 bias	0.369%
HPT CAP	0.412%	P13 bias	0.125%
LPT ETA	0.453%	FN bias	0.228%
		W1A bias	0.149%
EPR bias	0.137%		
P2 bias	0.168%		
T2 bias	0.133%		

Table 2: Square Roots of Diagonal Elements of $\underline{Q}$ Matrix

The Kalman Gain Matrix on the first pass, the first pass

analysis matrix and the (Normalised analysis ÷ Normalised analysis of input change or bias) matrix calculated using this Q matrix are given for reference in Figures 42, 43 and 44 respectively: they are equivalent to those presented in Figures 26, 27 and 29 respectively.

** KALMAN GAIN MATRIX ON FIRST PASS **

	WFE	P26	T26	P3	T3	T49	P13	XNL	XNH
FAN ETA	-0.2896	-0.1128	0.5305	-0.1367	0.0896	0.1404	0.0701	-1.0264	-0.2682
FAN CAP	0.1194	-0.0355	0.1836	-0.0861	0.0308	-0.0432	0.0036	-1.3714	0.2574
LPC ETA	-0.0477	1.0455	-0.0481	0.2296	-0.1467	-0.2976	-0.5364	-0.6722	-0.0851
HPC ETA	-0.0356	-0.1877	0.0962	0.0759	-0.4140	-0.1324	0.0428	0.2050	0.0958
HPC CAP	0.0430	-0.4994	0.3816	0.2424	0.2528	-0.1206	0.1107	0.3781	-2.4936
HPT ETA	-0.0650	-0.0006	-0.1500	-0.0294	0.1861	-0.1387	0.0006	-0.0142	0.4026
HPT CAP	0.1105	-0.0556	-0.0642	-0.3600	-0.2483	-0.0521	0.1163	0.2356	0.1829
LPT ETA	-0.1259	-0.0357	0.1648	-0.1007	0.0987	-0.1359	0.1529	0.0833	-0.5616
EPR	-0.0519	0.0159	0.1206	-0.0278	0.0239	-0.0076	0.0618	-0.1757	-0.1309
P2	-0.0300	-0.0880	-0.0895	-0.0254	0.0188	0.0139	-0.3813	0.3198	-0.1044
T2	0.0190	-0.0344	-0.3763	0.0165	-0.0144	-0.0887	-0.0598	0.0356	-0.2032
WFE	0.4812	-0.0337	0.1646	-0.0703	-0.0478	-0.3410	-0.1928	-0.3572	-0.0806
P26	-0.0158	0.5081	-0.0236	-0.0562	-0.0085	0.0099	-0.2093	-0.4113	0.7547
T26	0.0162	-0.0050	0.6280	0.0331	-0.0347	-0.0402	-0.0742	-0.2988	-0.0935
P3	-0.0675	-0.1152	0.3257	0.4700	-0.1242	0.0804	-0.0807	-0.0440	-0.7761
T3	-0.0219	-0.0084	-0.1617	-0.0592	0.5752	-0.0962	0.0077	-0.0337	-0.3334
T49	-0.2916	0.0180	-0.3501	0.0716	-0.1797	0.5868	-0.0028	0.3033	0.4208
P13	-0.0189	-0.0439	-0.0742	-0.0082	0.0017	-0.0083	0.5830	0.0639	-0.0333
FN	-0.0250	0.0208	0.0126	0.0000	-0.0056	-0.0148	-0.2193	-0.2933	-0.0165
M1A	0.0088	-0.0060	0.1075	-0.0101	0.0133	0.0291	-0.3340	-0.0382	0.0391

	FN	M1A
FAN ETA	0.4174	0.6725
FAN CAP	0.2651	0.0268
LPC ETA	0.1019	-0.3646
HPC ETA	-0.0061	-0.0219
HPC CAP	0.0208	-0.1002
HPT ETA	-0.0171	0.0545
HPT CAP	0.0182	-0.0018
LPT ETA	0.0475	0.1254
EPR	-0.0704	-0.0381
P2	0.0782	-0.0717
T2	-0.0052	0.1059
WFE	-0.0765	0.0631
P26	0.0298	-0.0200
T26	0.0038	0.0757
P3	-0.0001	-0.0695
T3	-0.0079	0.0437
T49	-0.0387	0.1783
P13	-0.0459	-0.2351
FN	0.4628	-0.3852
M1A	-0.1637	0.5607

** KALMAN GAIN MATRIX ANALYSIS **

** 4 MOST SIGNIFICANT MEASUREMENTS FOR DETERMINING COMPONENT CHANGES AND MEASUREMENT BIASSES LISTED **

FAN ETA	XNL	M1A	T26	FN
FAN CAP	XNL	FN	XNH	T26
LPC ETA	P26	XNH	XNL	P13
HPC ETA	T3	XNL	P26	T49
HPC CAP	XNH	P26	XNL	T26
HPT ETA	XNH	T3	T26	T49
HPT CAP	P3	T3	XNL	P13
LPT ETA	XNL	XNH	T26	P13
EPR	XNL	XNH	T26	FN
P2	P13	XNL	XNH	T26
T2	T26	XNH	M1A	P13
WFE	WFE	XNL	T49	P13
P26	XNH	P26	XNL	P13
T26	T26	XNL	XNH	M1A
P3	XNH	P3	T26	T3
T3	T3	XNH	T26	T49
T49	T49	XNH	T26	XNL
P13	P13	M1A	T26	FN
FN	FN	M1A	XNL	P13
M1A	M1A	P13	FN	T26

Figure 42: Kalman Gain Matrix on first pass: 'Auto-Tuned' Q Matrix

6.1 Single Component Changes and Sensor Biasses

For this demonstration, gas-path measurement difference vectors appropriate to +1% changes in each individual component change and sensor bias were simulated by taking each column of the System Matrix C in turn, to create 20 y vectors that were then input into the Kalman Filter and 'Concentrator'.

The results of the basic Kalman Filter analyses of each of these gas-path measurement difference vectors produced a matrix of answers that is identical to that given in Figure 43: this is to be expected, since the demonstration essentially reproduced, by different means, the process of post-multiplying the Kalman Gain Matrix K by the System Matrix C. The 'Concentrator' enhancement to the Kalman Filter produced the results summarised in Table 3.

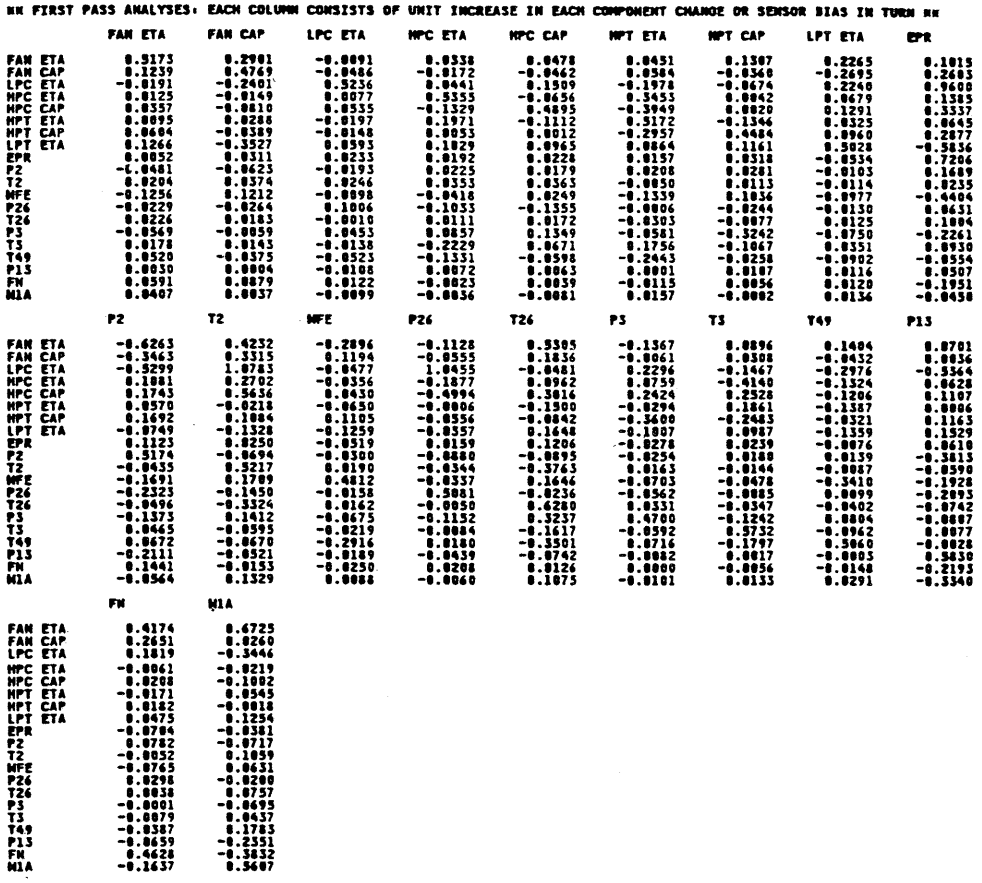

```
** FIRST PASS ANALYSES: EACH COLUMN CONSISTS OF UNIT INCREASE IN EACH COMPONENT CHANGE OR SENSOR BIAS IN TURN **

              FAN ETA    FAN CAP    LPC ETA    HPC ETA    HPC CAP    HPT ETA    HPT CAP    LPT ETA    EPR
FAN ETA        0.9173     0.2901    -0.0891     0.0538     0.0478     0.0431     0.1307     0.2265     0.1015
FAN CAP        0.1239     0.4769    -0.0486    -0.0172    -0.0462     0.0584    -0.0568    -0.2695     0.2483
LPC ETA       -0.0191    -0.2401     0.5236     0.0441     0.1509    -0.1978    -0.0674     0.2240     0.9600
HPC ETA        0.0125    -0.0149     0.0077     0.5355    -0.0656     0.5455     0.0042     0.0679     0.1385
HPC CAP        0.0357    -0.0810     0.0535    -0.1329     0.4895    -0.3949     0.0820     0.1291     0.3537
HPT ETA        0.0095     0.0288    -0.0197     0.1971    -0.1112     0.5172    -0.1346     0.0325     0.0645
HPT CAP        0.0684    -0.0389    -0.0148     0.0053     0.0012    -0.2957     0.4484     0.0960     0.2877
LPT ETA        0.1266    -0.3527     0.0593     0.1029     0.0965     0.0864     0.1161     0.5028    -0.5836
EPR            0.0052     0.0311     0.0233     0.0192     0.0228     0.0157     0.0518    -0.0534     0.7206
P2            -1.0481    -0.0623    -0.0193     0.0225     0.0179     0.0208     0.0281    -0.0103     0.1489
T2             0.0204     0.0374     0.0246     0.0353     0.0365    -0.0050     0.0113    -0.0114     0.0235
WFE           -0.1256     0.1212    -0.0098    -0.0418     0.0249    -0.1339     0.1036    -0.0977    -0.4404
P26           -0.0229    -0.0264     0.1006    -0.1033    -0.1355    -0.0006    -0.0244    -0.0130     0.0631
T26            0.0226     0.0183    -0.0010     0.0111     0.0172    -0.0303    -0.0077     0.0125     0.1004
P3            -0.0569    -0.0059     0.0453     0.0857     0.1349    -0.0581    -0.3242    -0.0750    -0.2261
T3             0.0178     0.0145    -0.0138    -0.2229     0.0671     0.1756    -0.1067     0.0551     0.0930
T49            0.0520    -0.0375    -0.0523    -0.1331    -0.0598    -0.2443    -0.0258    -0.0902    -0.0554
P13            0.0030     0.0004    -0.0108     0.0872     0.0863     0.0001     0.0187     0.0116     0.0307
FN             0.0591     0.0879     0.0122    -0.0023     0.0039    -0.0115     0.0056     0.0120    -0.1951
W1A            0.0407     0.0037    -0.0099    -0.0036    -0.0081     0.0157    -0.0002     0.0134    -0.0458

              P2         T2         WFE        P26        T26        P3         T3         T49        P13
FAN ETA       -0.6263     0.4232    -0.2896    -0.1128     0.9305    -0.1367     0.0896     0.1404     0.0701
FAN CAP       -0.3463     0.3315     0.1194    -0.0555     0.1836    -0.0061     0.0308    -0.0432     0.0036
LPC ETA       -0.5299     1.0783    -0.0477     1.0455    -0.0481     0.2296    -0.1467    -0.2976    -0.5364
HPC ETA        0.1081     0.2702    -0.0356    -0.1877     0.0962     0.0759    -0.0140    -0.1324     0.0428
HPC CAP        0.1743     0.5636     0.0430    -0.4994     0.3816     0.2424     0.2528    -0.1206     0.1107
HPT ETA        0.0570    -0.0218    -0.0650    -0.0006    -0.1500    -0.0294     0.1861    -0.1387     0.0006
HPT CAP        0.1692     0.1084     0.1105    -0.0556    -0.0842    -0.3600    -0.2483    -0.0521     0.1163
LPT ETA       -0.0749    -0.1328    -0.1259    -0.0357     0.1648    -0.1807     0.0987    -0.1359     0.1529
EPR            0.1123     0.0250    -0.0519     0.0159     0.1206    -0.0278     0.0239    -0.0076     0.0610
P2             0.5174    -0.0694    -0.0300    -0.0880    -0.0895    -0.0254     0.0188     0.0139    -0.3813
T2            -0.0455     0.5217     0.0190    -0.0344    -0.3765     0.0163    -0.0144    -0.0087    -0.0590
WFE           -0.1691     0.1709     0.4812    -0.0337     0.1646    -0.0703    -0.0478    -0.3418    -0.1928
P26           -0.2323    -0.1450    -0.0158     0.5081    -0.0236    -0.0562    -0.0885     0.0099    -0.2895
T26           -0.0496    -0.3324     0.0162    -0.0050     0.6280     0.0331    -0.0347    -0.0402    -0.0742
P3            -0.1373     0.1412    -0.0675    -0.1152     0.3237     0.4700    -0.1242     0.0804    -0.0807
T3             0.0465    -0.0595    -0.0219    -0.0084    -0.1617    -0.0592     0.5732    -0.0962     0.0077
T49            0.0672    -0.0670    -0.2916     0.0180    -0.3501     0.0716    -0.1797     0.5060    -0.0028
P13           -0.2111    -0.0521    -0.0189    -0.0439    -0.0742    -0.0082     0.0017    -0.0003     0.5830
FN             0.1441    -0.0153    -0.0250     0.0208     0.0126     0.0000    -0.0056    -0.0148    -0.2193
W1A           -0.0564     0.1329     0.0088    -0.0060     0.1075    -0.0101     0.0133     0.0291    -0.3340

              FN         W1A
FAN ETA        0.4174     0.6725
FAN CAP        0.2651     0.0260
LPC ETA        0.1819    -0.3446
HPC ETA       -0.0061    -0.0219
HPC CAP        0.0208    -0.1002
HPT ETA       -0.0171     0.0545
HPT CAP        0.0182    -0.0018
LPT ETA        0.0475     0.1254
EPR           -0.0704    -0.0381
P2             0.0782    -0.0717
T2            -0.0052     0.1059
WFE           -0.0765     0.0631
P26            0.0298    -0.0200
T26            0.0038     0.0757
P3            -0.0001    -0.0695
T3            -0.0079     0.0437
T49           -0.0387     0.1783
P13           -0.0659    -0.2351
FN             0.4628    -0.3832
W1A           -0.1637     0.5607
```

Figure 43: First pass analyses: 'Auto-Tuned' Q Matrix

Component Change or Sensor Bias	Simulated Change	Analysed Change	Other Changes Analysed
FAN ETA	+1%	+0.980%	None
FAN CAP	+1%	+0.995%	None
LPC ETA	+1%	+0.996%	None
HPC ETA	+1%	+0.999%	None
HPC CAP	+1%	+0.997%	None
HPT ETA	+1%	+1.000%	None
HPT CAP	+1%	+0.995%	None
LPT ETA	+1%	+0.998%	None
EPR bias	+1%	+0.949%	None
P2 bias	+1%	+0.954%	None
T2 bias	+1%	+0.970%	None
WFE bias	+1%	+0.939%	None
P26 bias	+1%	+0.978%	None
T26 bias	+1%	+0.971%	None
P3 bias	+1%	+0.935%	None
T3 bias	+1%	+0.911%	None
T49 bias	+1%	+0.999%	None
P13 bias	+1%	+0.925%	None
FN bias	+1%	+0.704%	None
W1A bias	+1%	+0.970%	None

Table 3: 'Concentrator' Results: Single Component Changes and Sensor Biasses

```
** FIRST PASS ANALYSES: AS ABOVE, BUT EACH COLUMN DIVIDED BY (ANALYSED CHANGE/S.D.) FOR CHANGE BEING ANALYSED **

          FAN ETA   FAN CAP   LPC ETA   HPC ETA   HPC CAP   HPT ETA   HPT CAP   LPT ETA   EPR
FAN ETA    1.0000    0.4138   -0.0249    0.0376    0.0868    0.0480    0.2118    0.3417    0.0242
FAN CAP    0.3520    1.0000   -0.1970   -0.0282   -0.1235    0.0762   -0.0856   -0.5977    0.0913
LPC ETA   -0.0256   -0.2374    1.0000    0.0340    0.1901   -0.1216   -0.0757    0.2342    0.1588
HPC ETA    0.0405   -0.0356    0.0357    1.0000   -0.1999    0.5142    0.0114    0.1719    0.0555
HPC CAP    0.0776   -0.1299    0.1658   -0.1663    1.0000   -0.3940    0.0036    0.2190    0.0896
HPT ETA    0.0400    0.0895   -0.1186    0.4778   -0.4401    1.0000   -0.4756    0.1070    0.0335
HPT CAP    0.1607   -0.0764   -0.0560    0.0881    0.0831   -0.3609    1.0000    0.1993    0.0945
LPT ETA    0.3225   -0.6631    0.2156    0.1508    0.2310    0.1810    0.2480    1.0000   -0.1836
EPR        0.0583    0.2585    0.5728    0.1242    0.2489    0.0807    0.2997   -0.4682    1.0000
P2        -0.3357   -0.3208   -0.1920    0.0904    0.1174    0.0666    0.1645   -0.0561    0.1454
T2         0.1804    0.2442    0.5107    0.1797    0.3019   -0.0202    0.0838   -0.0791    0.0257
WFE       -0.3556    0.2533   -0.0396   -0.0681    0.0664   -0.1740    0.2460   -0.2159   -0.1540
P26       -0.0973   -0.0827    0.6097   -0.2527   -0.5414   -0.0011   -0.0869   -0.0430    0.0331
T26        0.2410    0.1441   -0.0148    0.0682    0.1722   -0.1486   -0.0693    0.1045    0.1324
P3        -0.1627   -0.0125    0.1847    0.1410    0.3626   -0.0762   -0.7773   -0.1674   -0.0798
T3         0.0820    0.0488   -0.0908   -0.5918    0.2910    0.3718   -0.4126    0.1265    0.0530
T49        0.1633   -0.0868   -0.2341   -0.2404   -0.1763   -0.3518   -0.0678   -0.2208   -0.0215
P13        0.0301    0.0027   -0.1556    0.0421    0.0597    0.0885    0.0905    0.0916    0.0632
FN         0.2878    0.3158    0.0848   -0.0065    0.0180   -0.0257    0.0228    0.0457   -0.1173
M1A        0.3351    0.0224   -0.1161   -0.0171   -0.0627    0.0592   -0.0816    0.0873   -0.0458

AV ABS()   0.2174    0.2219    0.2189    0.1862    0.2342    0.1992    0.2217    0.2288    0.1301
RANK          1.0       1.0       1.0       1.0       1.0       2.0       1.0       1.0       1.0
NO GT AV      8.0       9.0       6.0       5.0       7.0       6.0       7.0       5.0       6.0

             P2        T2       WFE       P26       T26        P3        T3       T49       P13
FAN ETA   -0.3356    0.1772   -0.4189   -0.1010    0.1330   -0.1966    0.0655    0.1709    0.0231
FAN CAP   -0.2727    0.2041    0.2490   -0.0750    0.0778   -0.0128    0.0331   -0.0772    0.0017
LPC ETA   -0.1968    0.3130   -0.0469    0.6487   -0.0096    0.2289   -0.0743   -0.2511   -0.1223
HPC ETA    0.0973    0.1899   -0.0847   -0.2821    0.0466    0.1832   -0.5079   -0.2705    0.0347
HPC CAP    0.1050    0.2654    0.0686   -0.5027    0.0978    0.3920    0.2077   -0.1650    0.0410
HPT ETA    0.0665   -0.0199   -0.2009   -0.0012   -0.0943   -0.0921    0.2965   -0.3679    0.0804
HPT CAP    0.1247    0.0624    0.2156   -0.0684   -0.0356   -0.7126   -0.2497   -0.0538    0.0526
LPT ETA   -0.0529   -0.0733   -0.2555   -0.0421    0.0626   -0.1989    0.0951   -0.2180    0.0663
EPR        0.3498    0.0688   -0.4282    0.0827    0.2022   -0.2322    0.1017   -0.0541    0.1166
P2         1.0000   -0.1048   -0.1534   -0.2841   -0.0931   -0.1316    0.0474    0.0611   -0.4524
T2        -0.1066    1.0000    0.1233   -0.1410   -0.4967    0.1076   -0.0483   -0.0485   -0.0888
WFE       -0.1327    0.1048    1.0000   -0.0442    0.0695   -0.1481   -0.0512   -0.6081   -0.0929
P26       -0.2737   -0.1335   -0.0492    1.0000   -0.0150   -0.1777   -0.0137    0.0264   -0.1514
T26       -0.1467   -0.7687    0.1265   -0.0245    1.0000    0.2628   -0.1399   -0.2701   -0.1347
P3        -0.1088    0.0874   -0.1416   -0.1526    0.1381    1.0000   -0.1343    0.1448   -0.0393
T3         0.0594   -0.0595   -0.0741   -0.0178   -0.1113   -0.2034    1.0000   -0.2795    0.0061
T49        0.0584   -0.0456   -0.6716    0.0262   -0.1639    0.1673   -0.2132    1.0000   -0.0015
P13       -0.5899   -0.1138   -0.1400   -0.2049   -0.1115   -0.0619    0.0063   -0.0020    1.0000
FN         0.1945   -0.0162   -0.0895    0.0468    0.0091   -0.0001   -0.0104   -0.0454   -0.1817
M1A       -0.1289    0.2372    0.0532   -0.0227    0.1322   -0.0619    0.0415    0.1509   -0.4684

AV ABS()   0.2200    0.2019    0.2281    0.1883    0.1559    0.2282    0.1669    0.2133    0.1538
RANK          1.0       1.0       1.0       1.0       1.0       1.0       1.0       1.0       1.0
NO GT AV      6.0       6.0       6.0       6.0       4.0       6.0       6.0       8.0       4.0

             FN       M1A
FAN ETA   0.3580    0.2813
FAN CAP   0.3341    0.0160
LPC ETA   0.1881   -0.0999
HPC ETA  -0.0087   -0.0154
HPC CAP   0.0201   -0.0471
HPT ETA  -0.0329    0.0497
HPT CAP   0.0215   -0.0018
LPT ETA   0.0537    0.0691
EPR      -0.3512   -0.0926
P2        0.2420   -0.1882
T2       -0.0205    0.2027
WFE      -0.0961    0.0387
P26       0.0561   -0.0184
T26       0.0179    0.1749
P3       -0.0001   -0.0430
T3       -0.0161    0.0437
T49      -0.0539    0.1211
P13      -0.2948   -0.5129
FN        1.0000   -0.4039
M1A      -0.5984    1.0000

AV ABS()  0.1842    0.1678
RANK         1.0       1.0
NO GT AV     7.0       6.0

** POSSIBLE ANALYSIS DIFFICULTIES **

** WARNING ** LPT ETA  MAY BE ANALYSED INSTEAD OF FAN CAP : RATIO= -0.6631
** WARNING ** P26      MAY BE ANALYSED INSTEAD OF LPC ETA : RATIO=  0.6097
** WARNING ** P3       MAY BE ANALYSED INSTEAD OF HPT CAP : RATIO= -0.7773
** WARNING ** T26      MAY BE ANALYSED INSTEAD OF T2      : RATIO= -0.7687
** WARNING ** T49      MAY BE ANALYSED INSTEAD OF WFE     : RATIO= -0.6716
** WARNING ** LPC ETA  MAY BE ANALYSED INSTEAD OF P26     : RATIO=  0.6487
** WARNING ** HPT CAP  MAY BE ANALYSED INSTEAD OF P3      : RATIO= -0.7126
** WARNING ** WFE      MAY BE ANALYSED INSTEAD OF T49     : RATIO= -0.6081
```

Figure 44: Normalised analysis : Normalised analysis of input change or bias 'Auto-Tuned' Q Matrix

Table 3 indicates that the 'Concentrator' has behaved as expected: analysed component changes and sensor biasses are close to those simulated, with no component changes or sensor biasses other than those being simulated appearing in each analysis. The low value of analysed net thrust bias (FN bias) is due to the relatively poor repeatability

of this measurement, seen in the column labelled INST SD in Figure 31; this low value forced the Kalman Filter to give less 'weight' to the net thrust reading, even when it was the only non-zero gas-path measurement difference.

6.2 Single Component Changes and Sensor Biasses with Normally-Distributed Sensor Non-Repeatability

For this demonstration, gas-path measurement difference vectors appropriate to +1% changes in each individual component change and sensor bias were simulated by taking each column of the System Matrix $\underline{C}$ in turn to create 20 $\underline{y}$ vectors; this was repeated 100 times, with each of the gas-path measurement differences having normally-distributed random noise added. The noise terms had a mean of zero and standard deviations as shown in the column labelled INST SD in Figure 31, which are the inputs into the calculation of the measurement repeatability covariance matrix $\underline{R}$. Note that the effects of environmental sensor non-repeatability were also included. These $\underline{y}$ vectors (2000 in all) were then input into the Kalman Filter and 'Concentrator'.

The results of the 'Concentrator' outputs from each of these analyses are summarised in Figures 45 to 64: these figures show, for each simulated component change and sensor bias in turn, histograms of the amounts of each simulated change and bias analysed by the 'Concentrator'. The results of Table 3 have been added to each Figure for reference.

Points to note are:

1) the median of each distribution lies close to the 'no-noise' analysis of each component change and sensor bias given in Table 3;

2) failures to analyse the simulated component change or sensor bias can be generally explained by;

   - high noise levels in the measurements: gas-path measurements with large repeatability standard deviations tend to have a wider distribution of sensor bias analyses;

   - correlations between component changes and/or sensor biasses calculated by the System Correlation Matrix (Figure 14);

   - possible analysis difficulties indicated by the (Normalised analysis ÷ Normalised analysis of input change or bias) matrix in Figure 44.

Of particular note are:

1) the spreads of Fan Tip efficiency analyses (Figure 45),

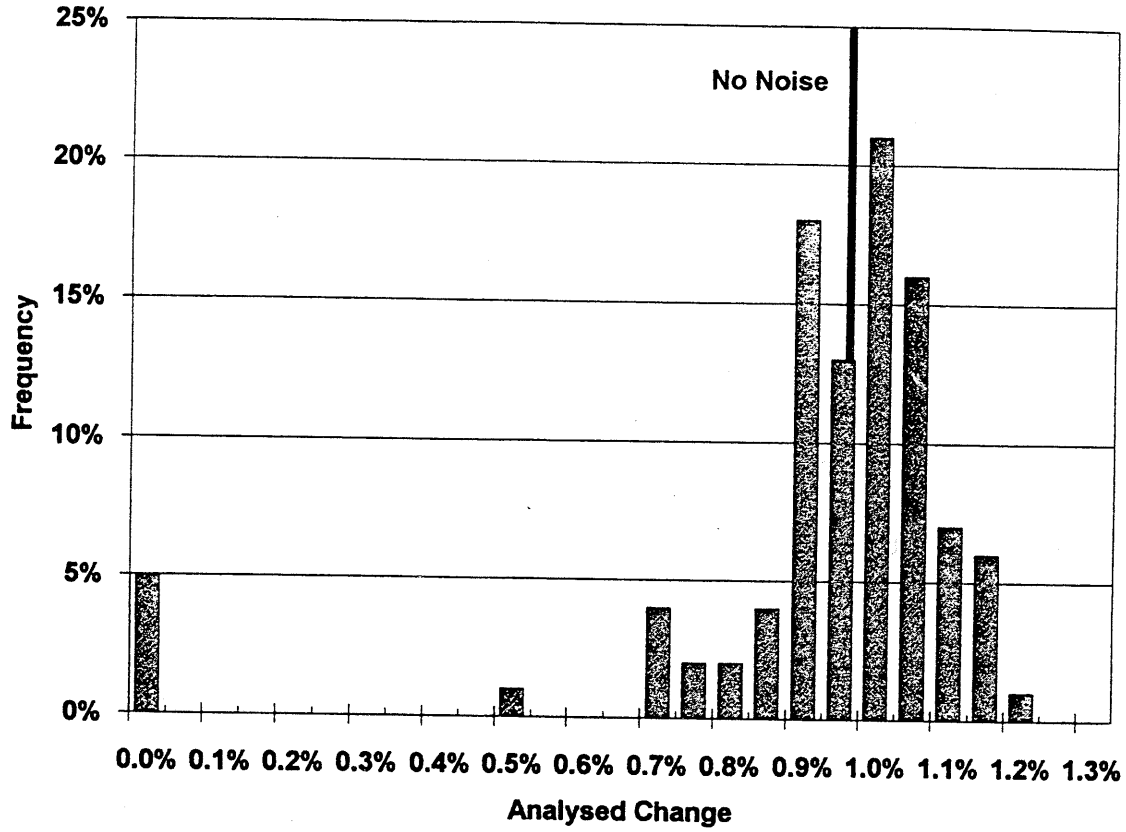

Figure 45: Fan Tip Efficiency Analysis Distribution

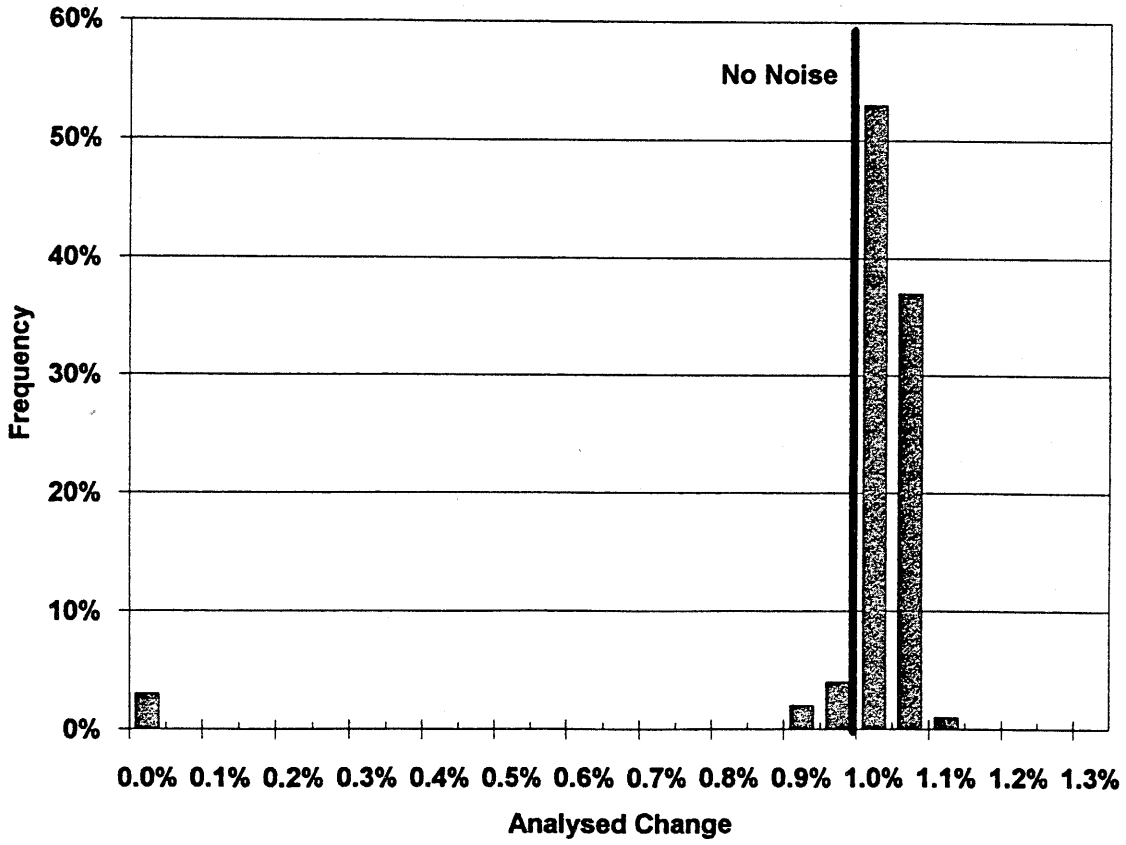

Figure 46: Fan Tip Capacity Analysis Distribution

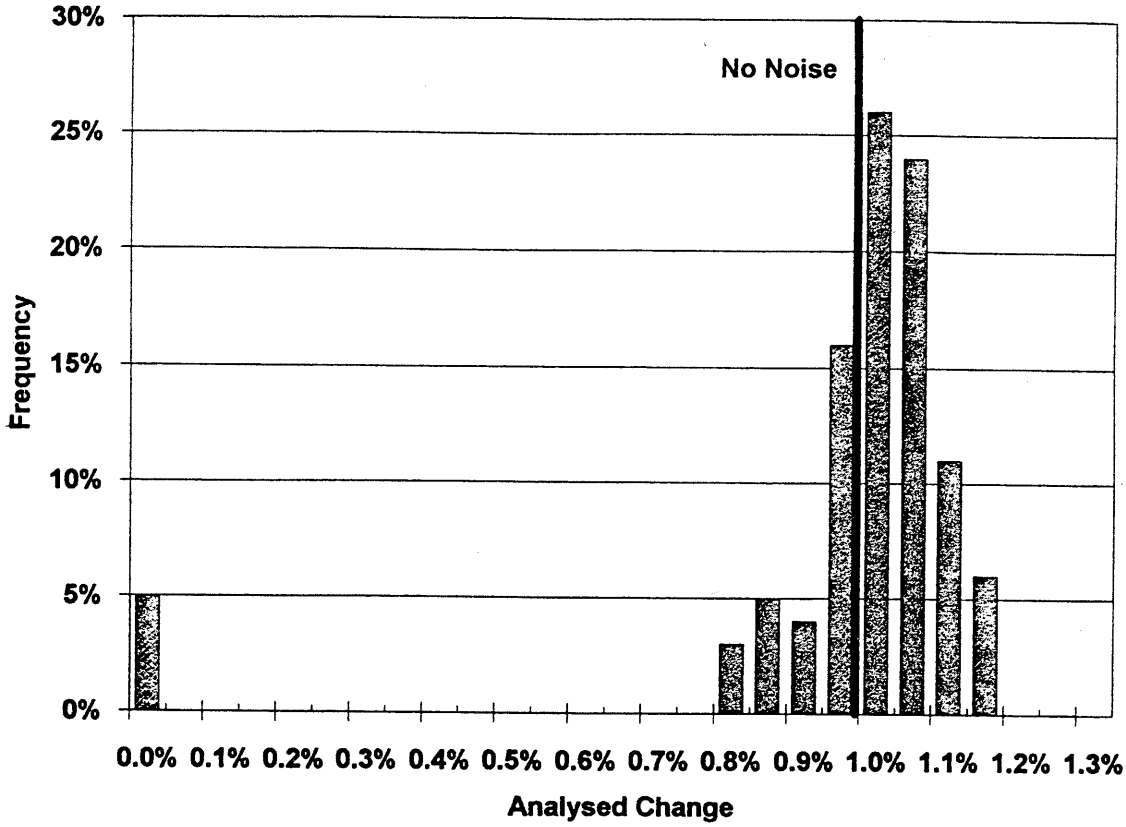

Figure 47: LP Compressor Efficiency Analysis Distribution

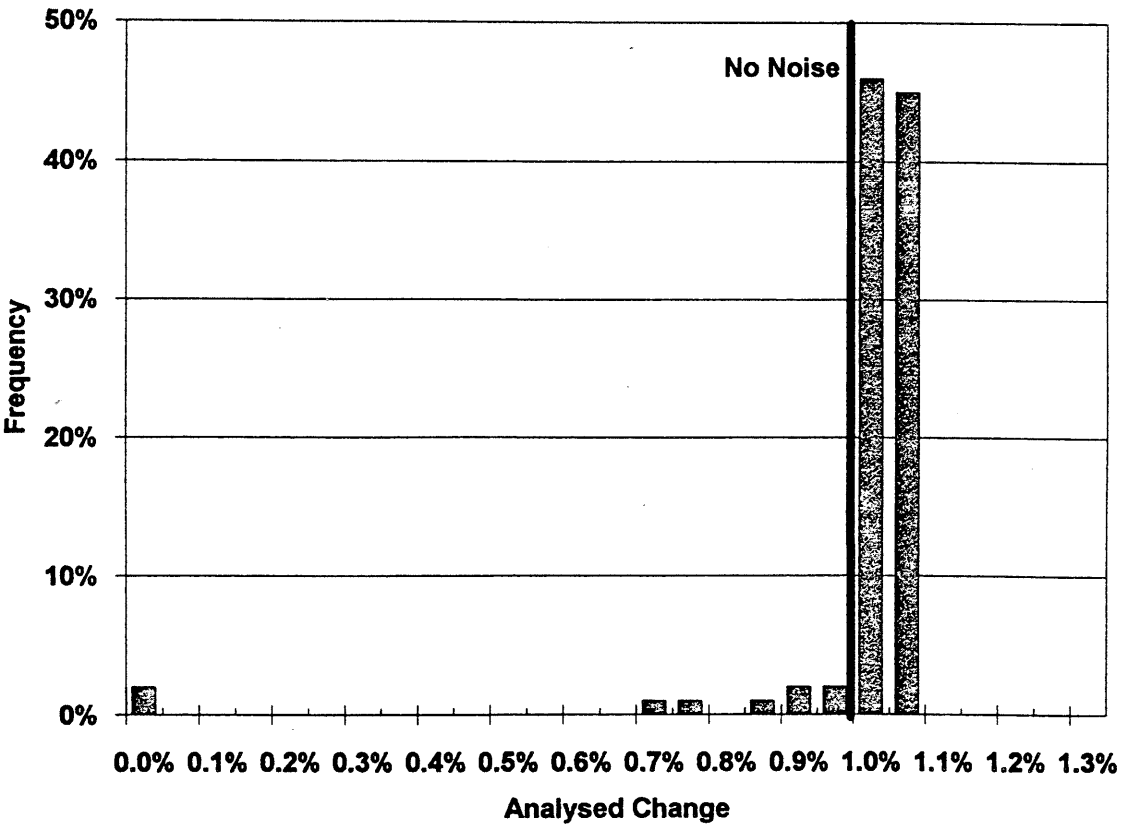

Figure 48: HP Compressor Efficiency Analysis Distribution

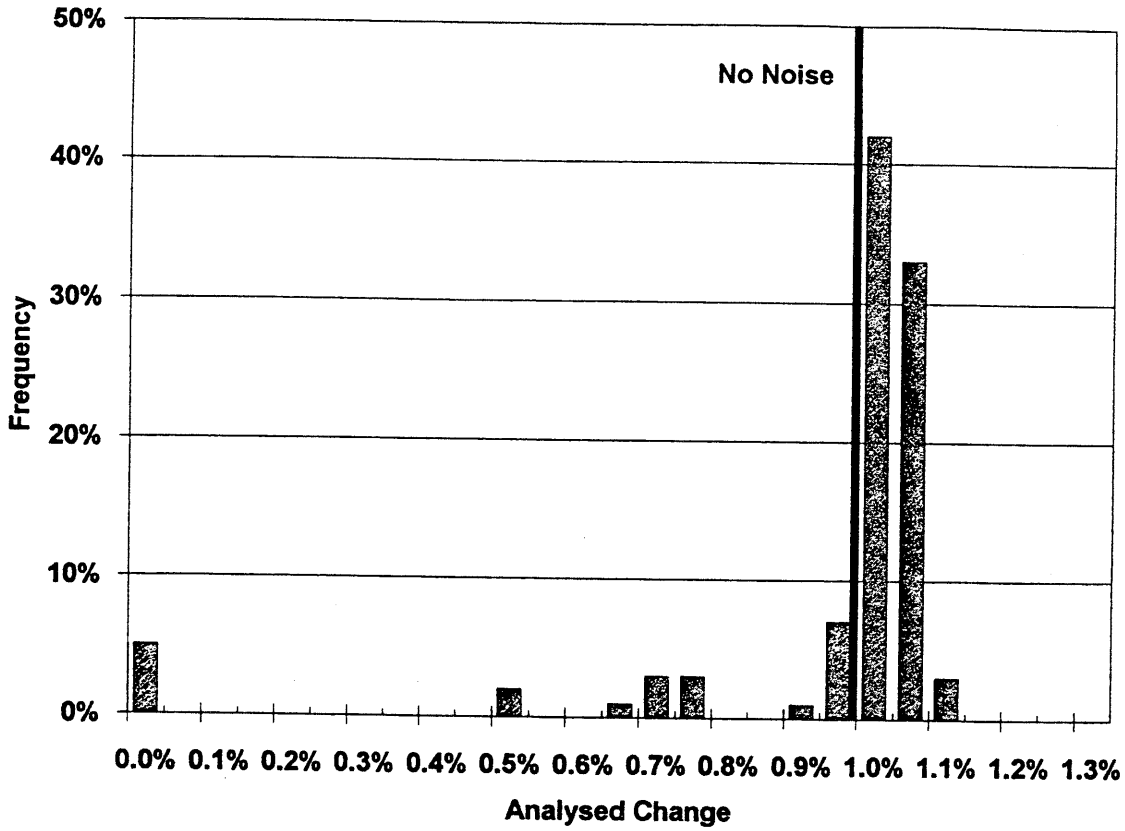

Figure 49: HP Compressor Capacity Analysis Distribution

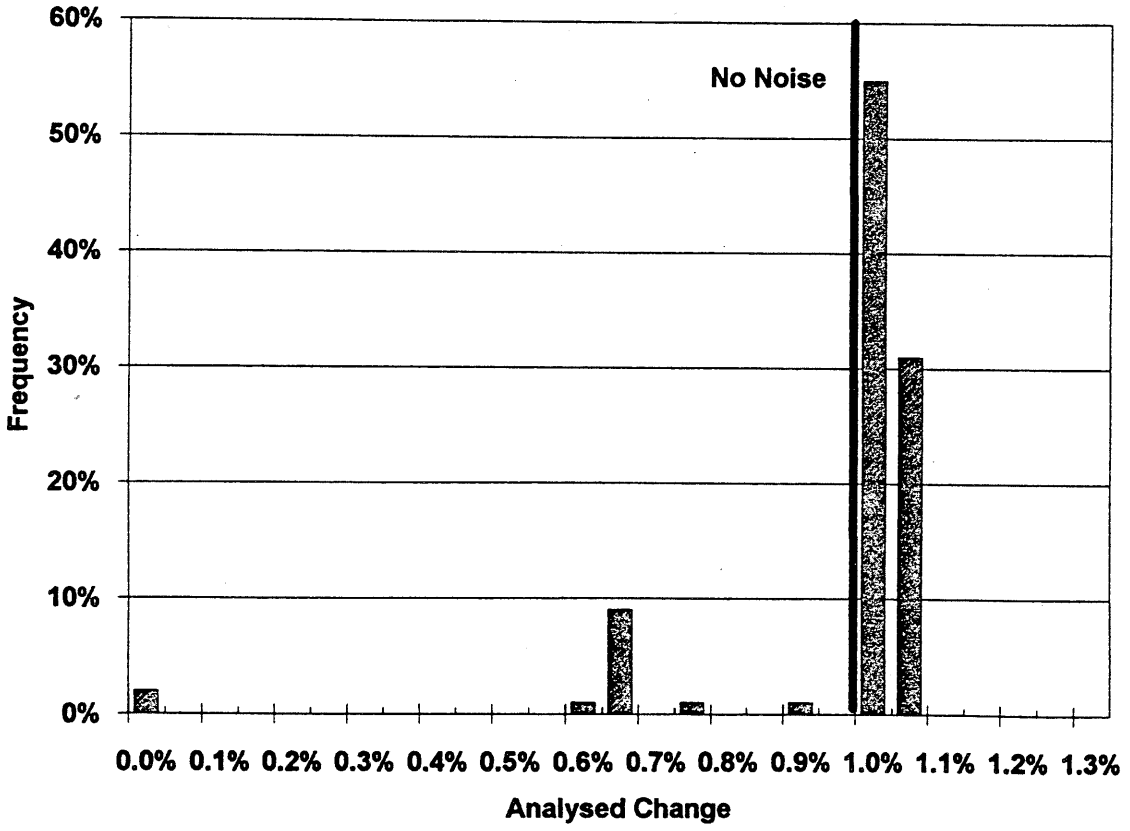

Figure 50: HP Turbine Efficiency Analysis Distribution

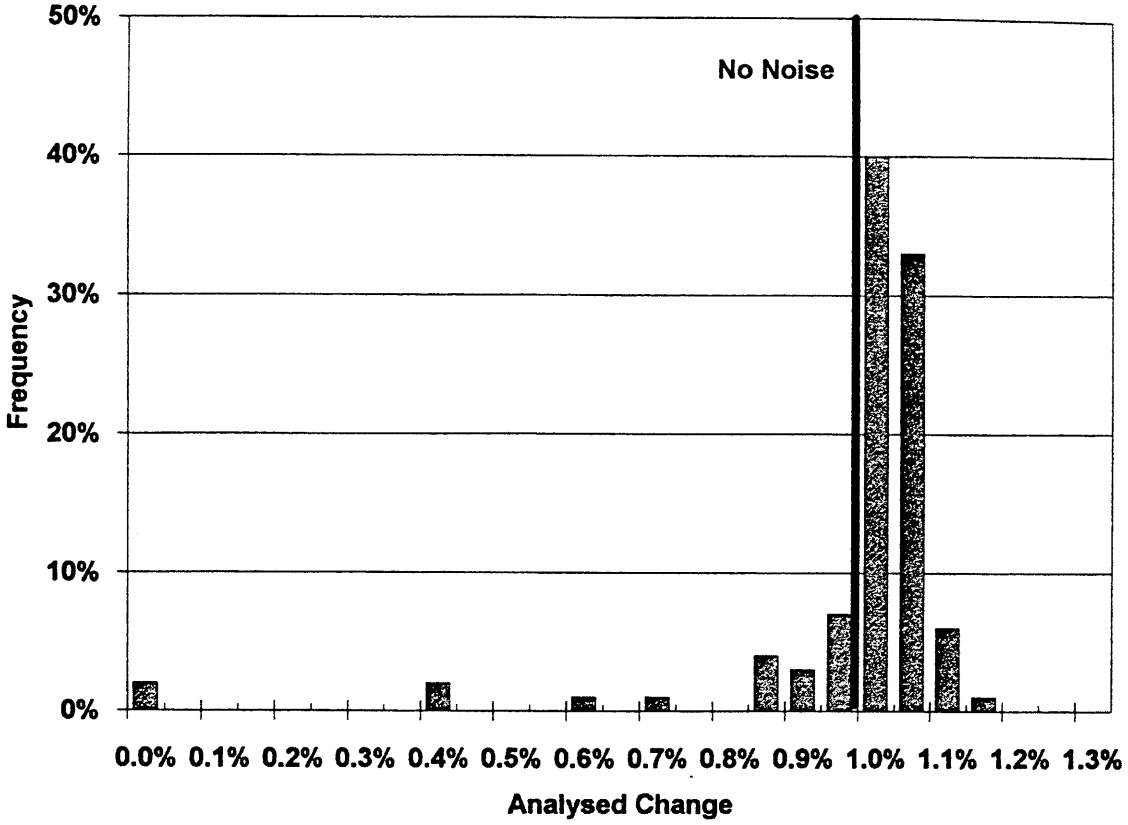

Figure 51: HP Turbine Capacity Analysis Distribution

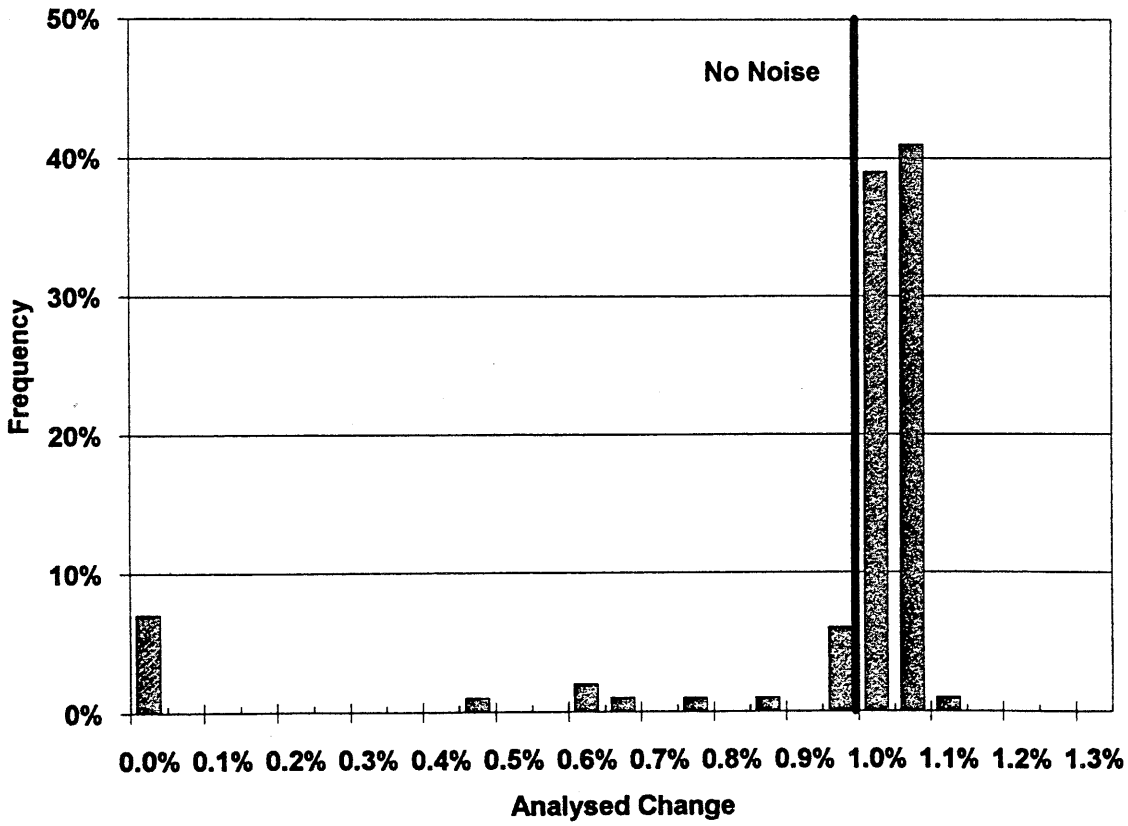

Figure 52: LP Turbine Efficiency Analysis Distribution

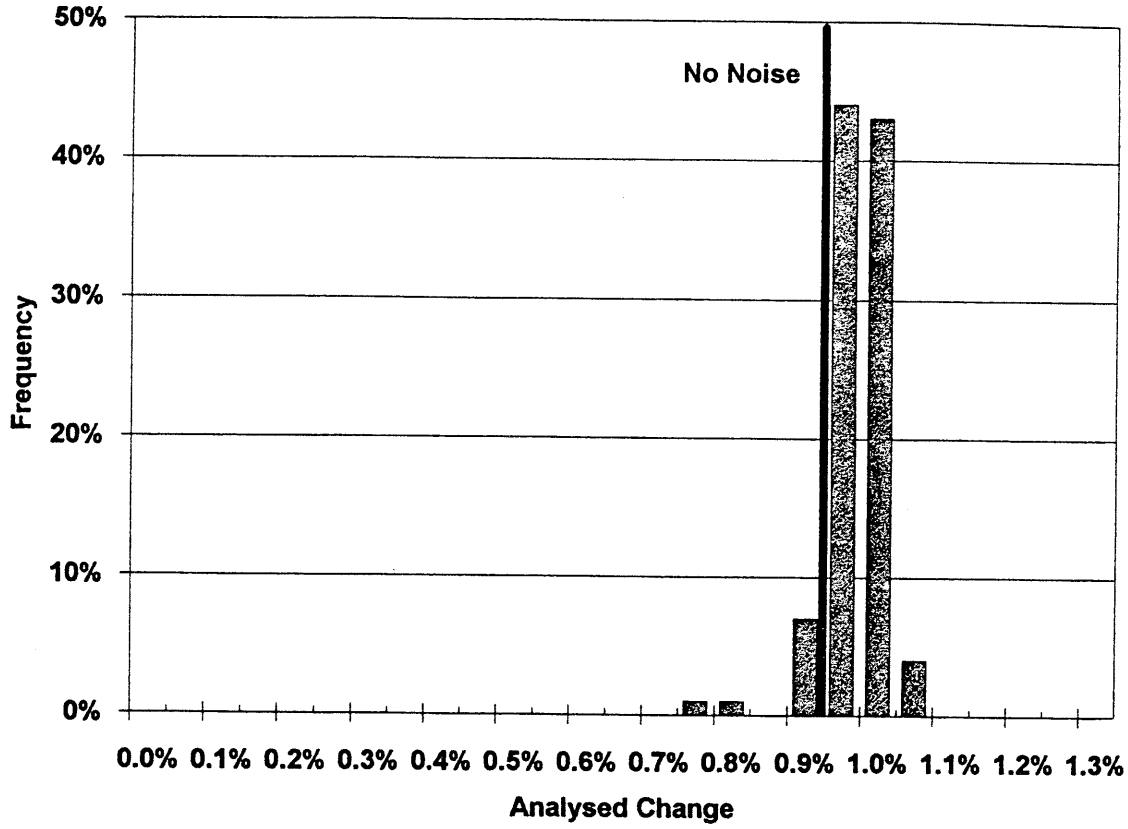

Figure 53: EPR Bias Analysis Distribution

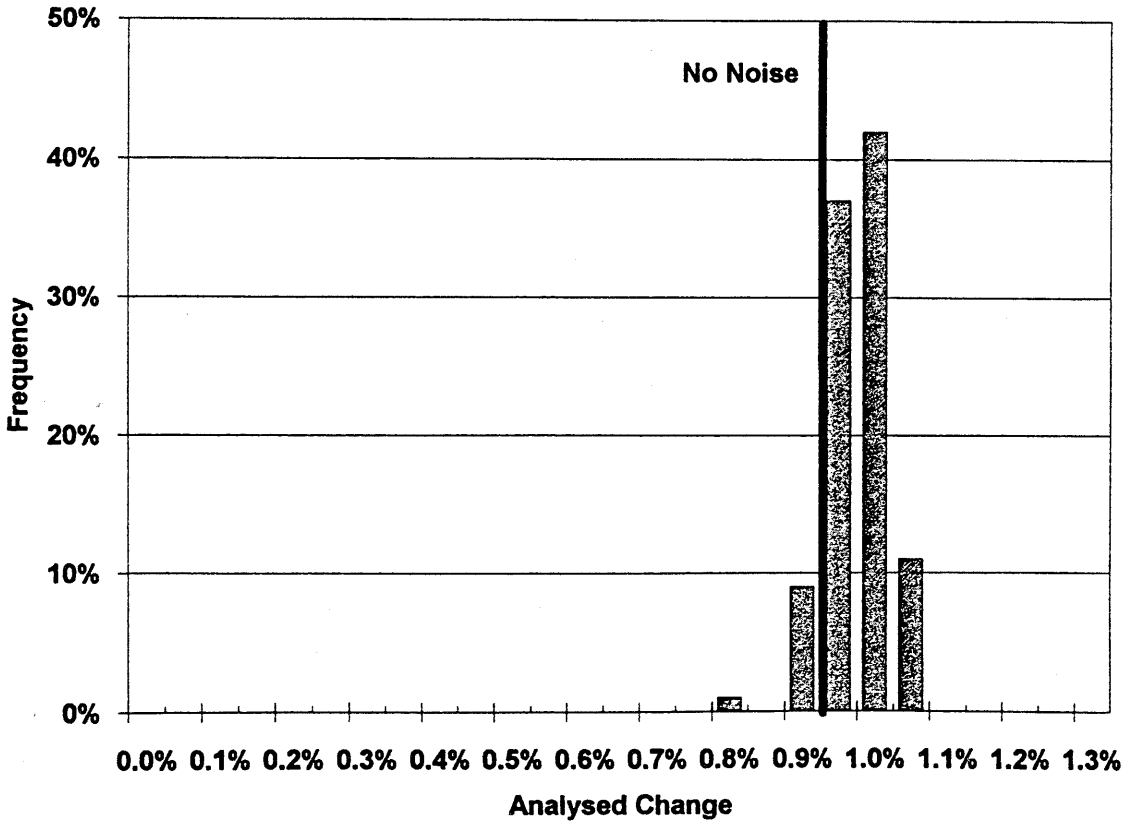

Figure 54: Inlet Pressure Bias Analysis Distribution

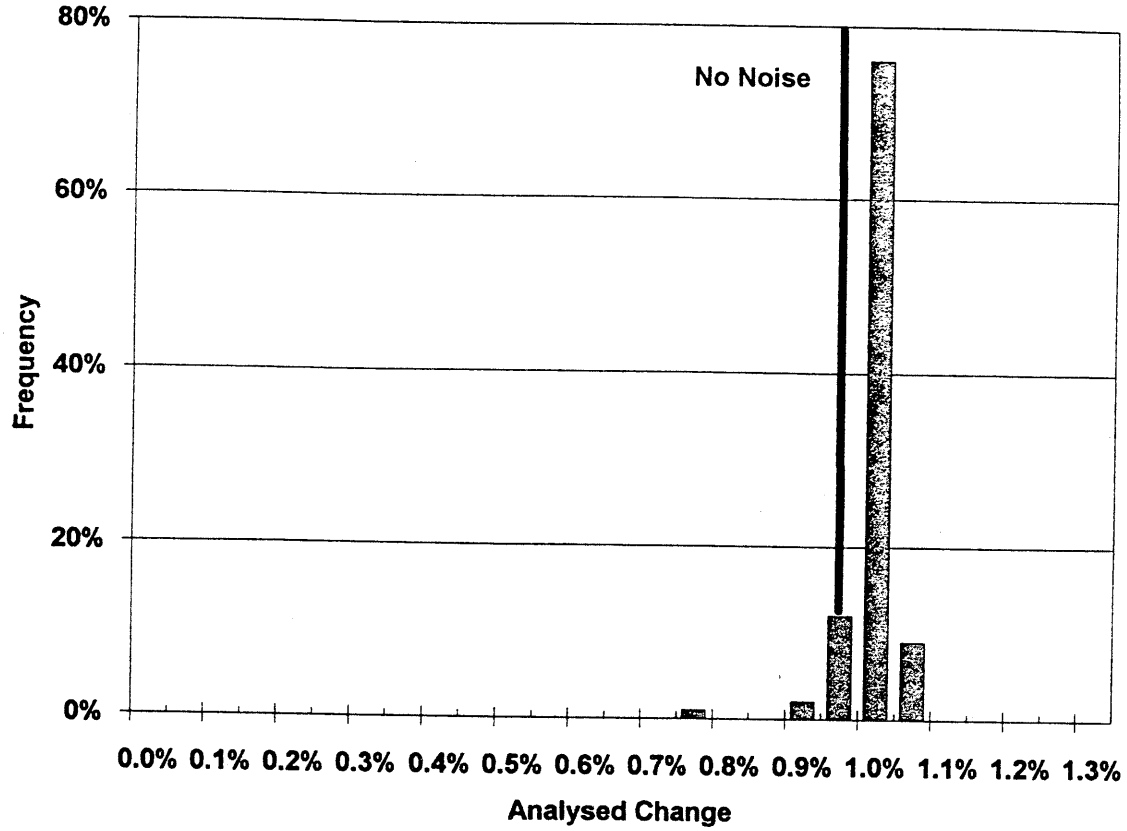

Figure 55: Inlet Temperature Bias Analysis Distribution

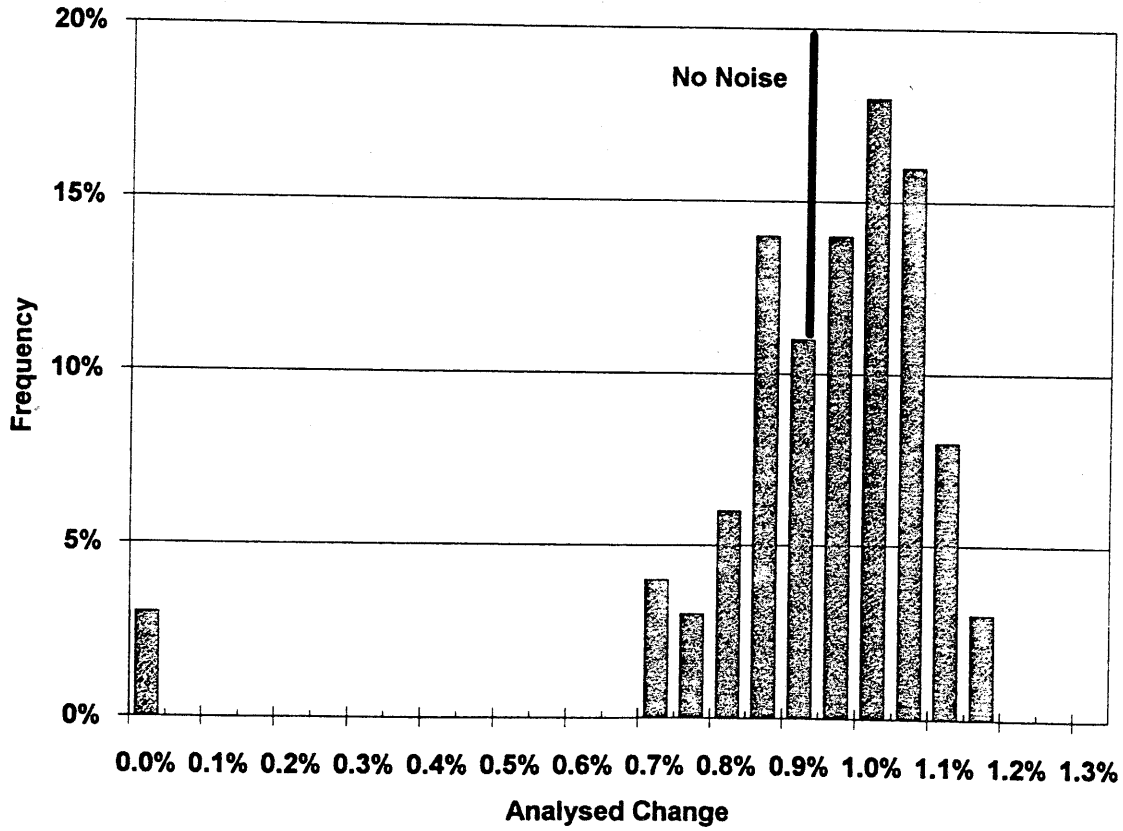

Figure 56: Fuel Flow Bias Analysis Distribution

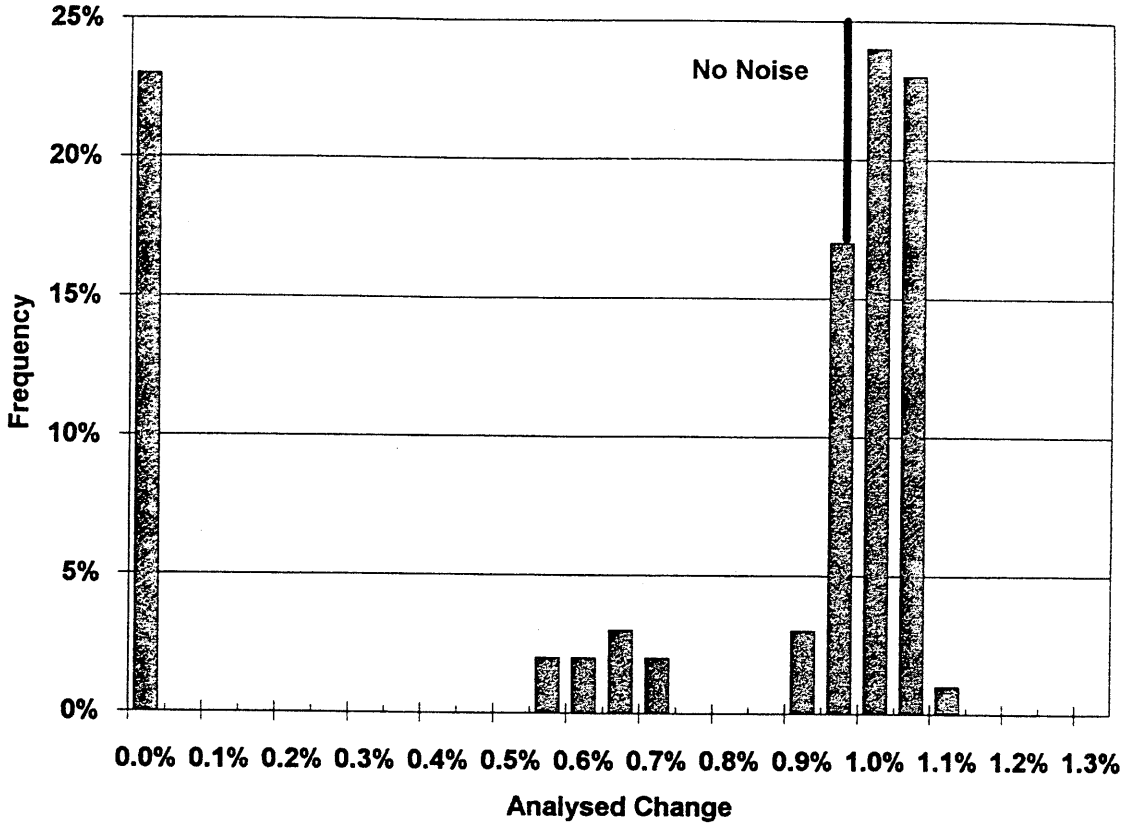

Figure 57: HPC Entry Pressure Bias Analysis Distribution

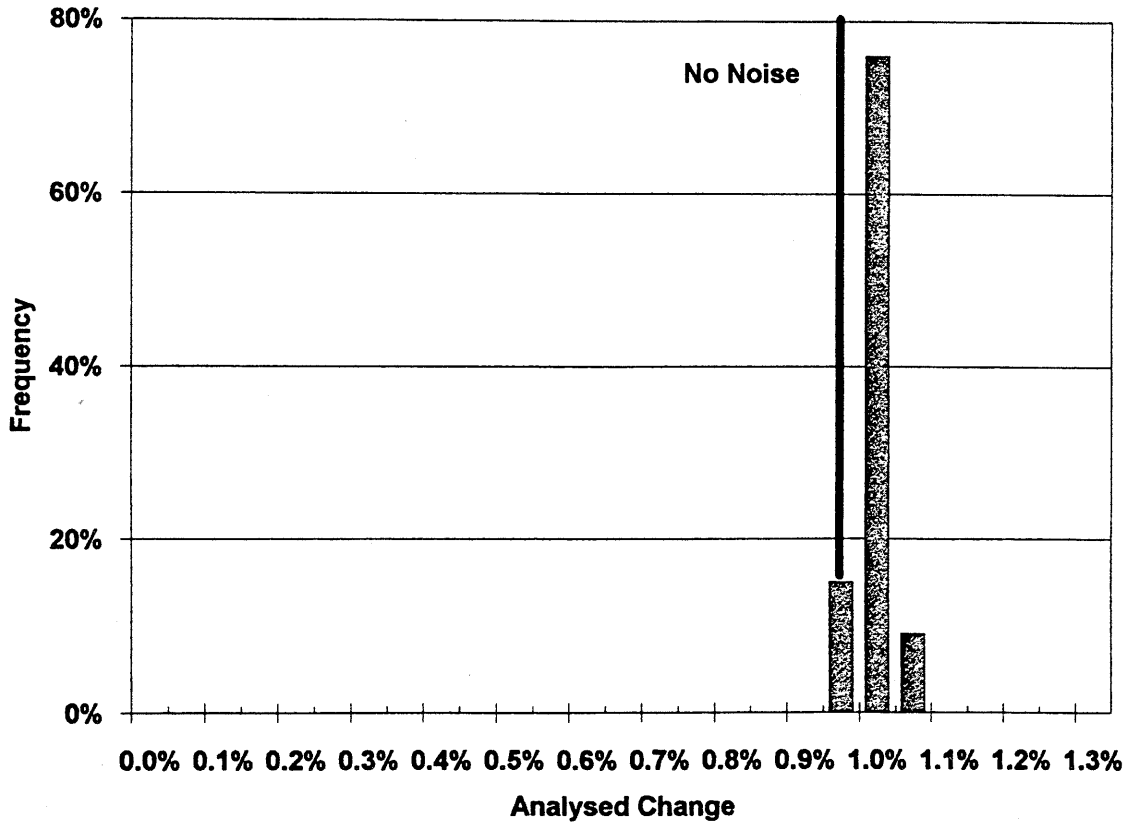

Figure 58: HPC Entry Temperature Bias Analysis Distribution

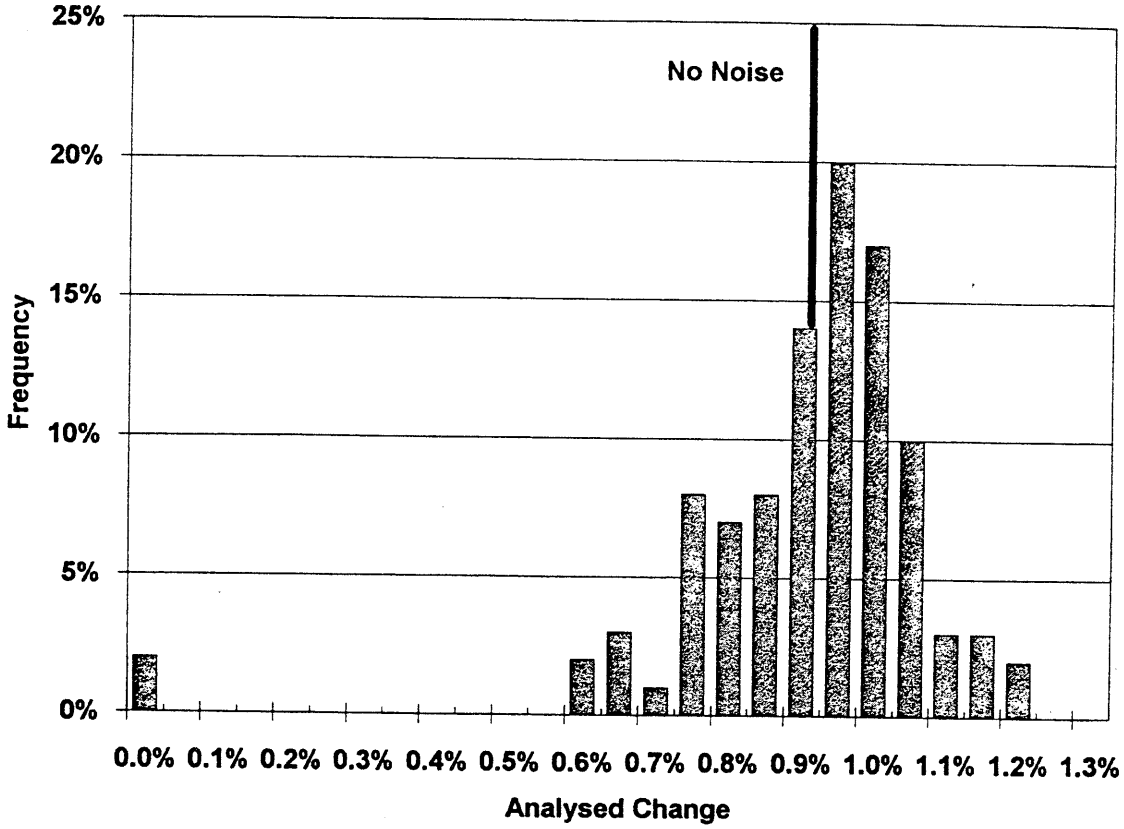

Figure 59: HPC Exit Pressure Bias Analysis Distribution

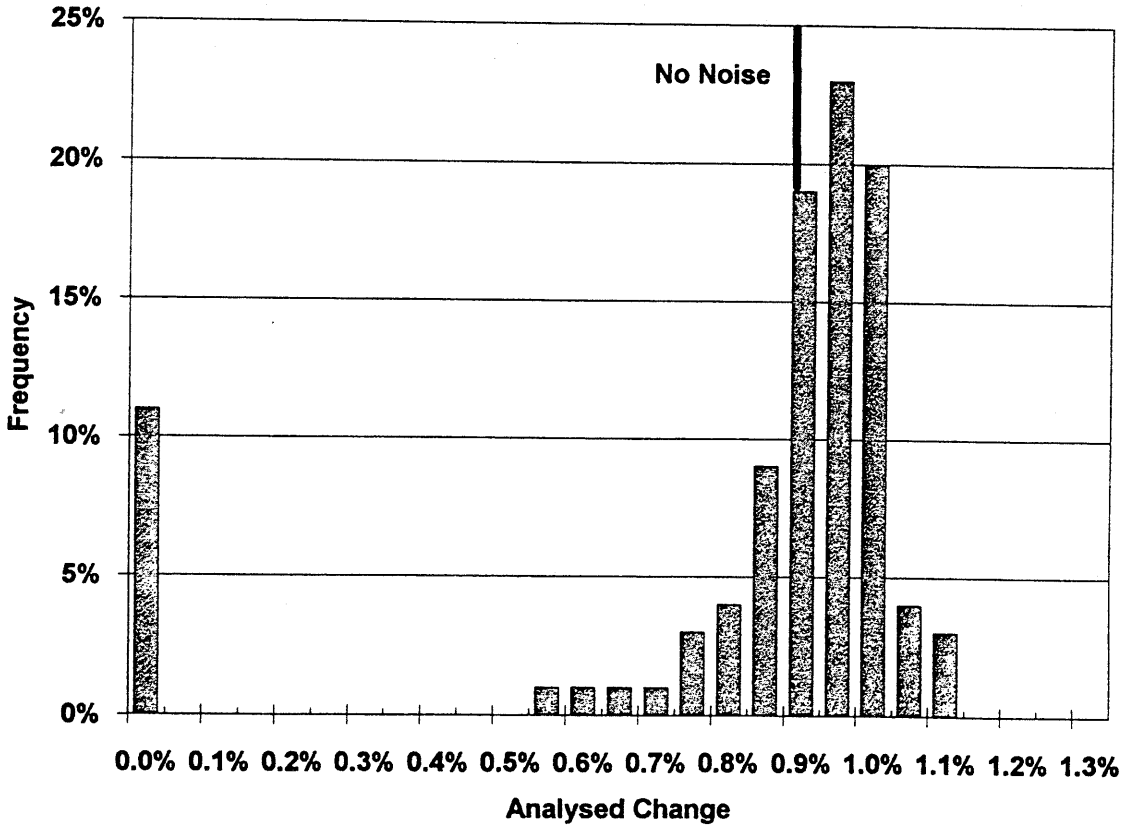

Figure 60: HPC Exit Temperature Bias Analysis Distribution

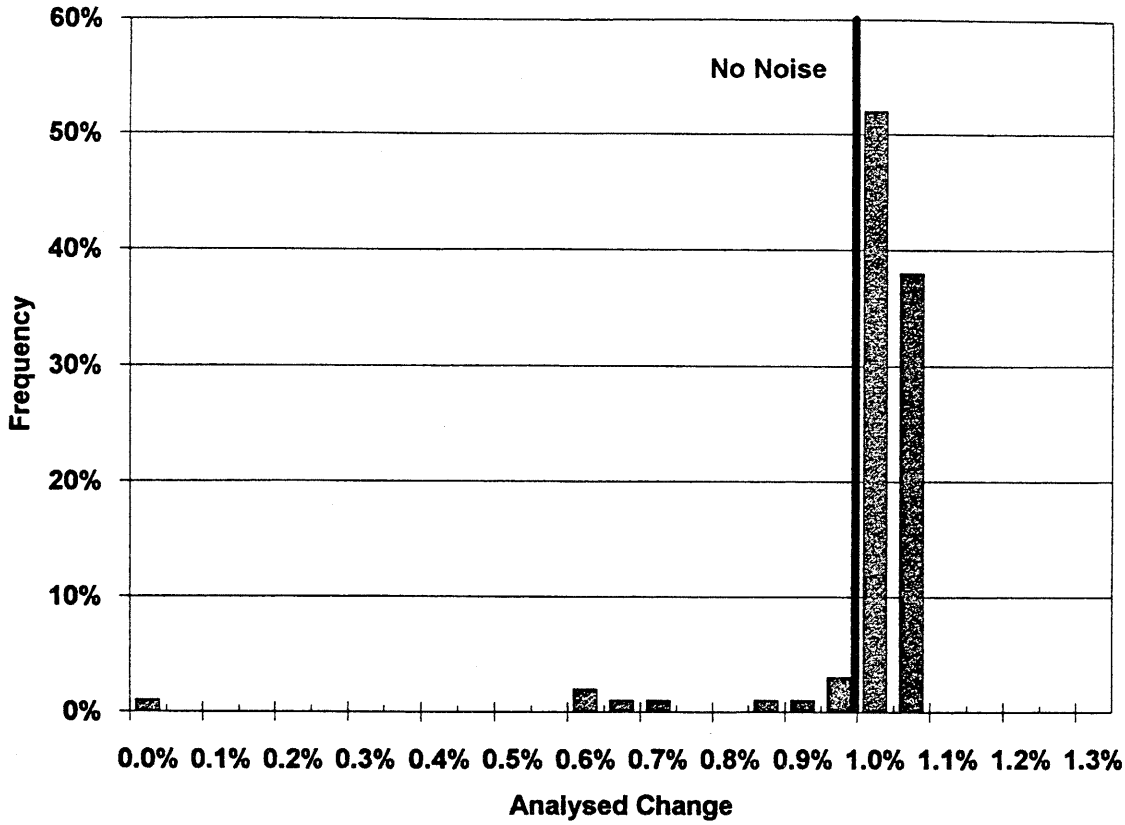

Figure 61: LPT Exit Temperature Bias Analysis Distribution

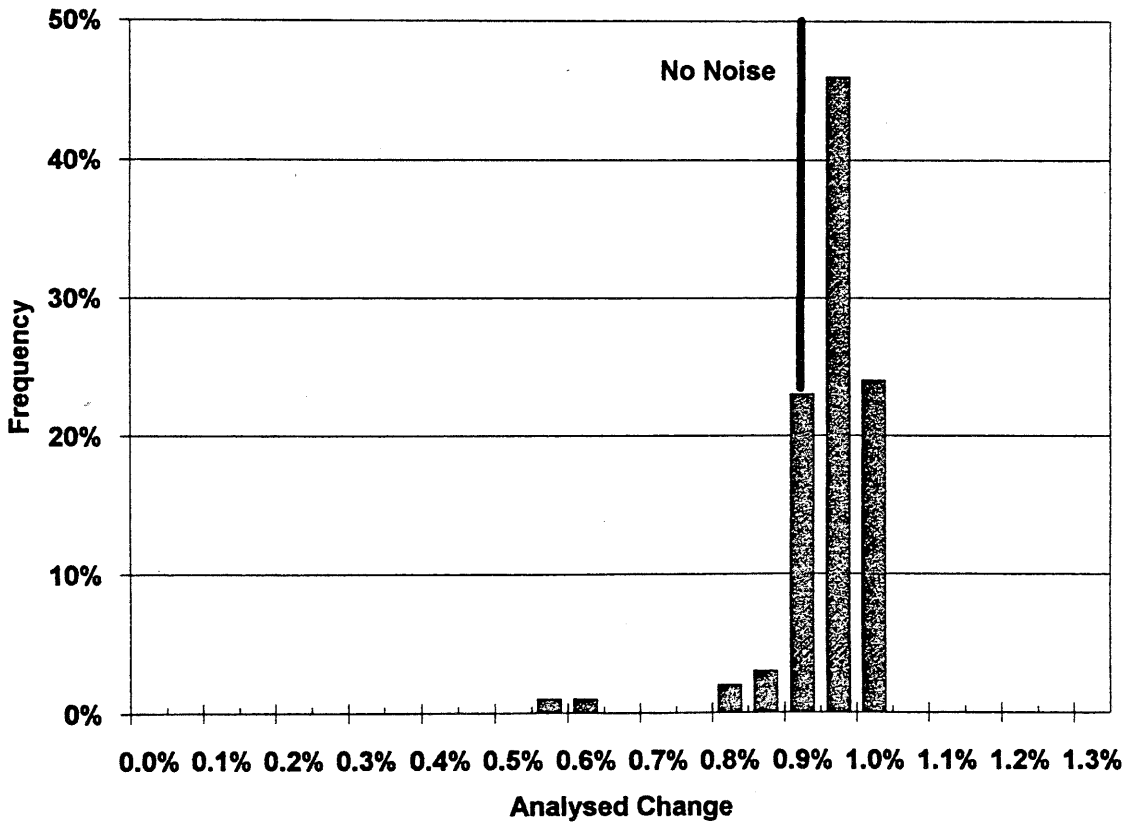

Figure 62: Fan Tip Exit Pressure Bias Analysis Distribution

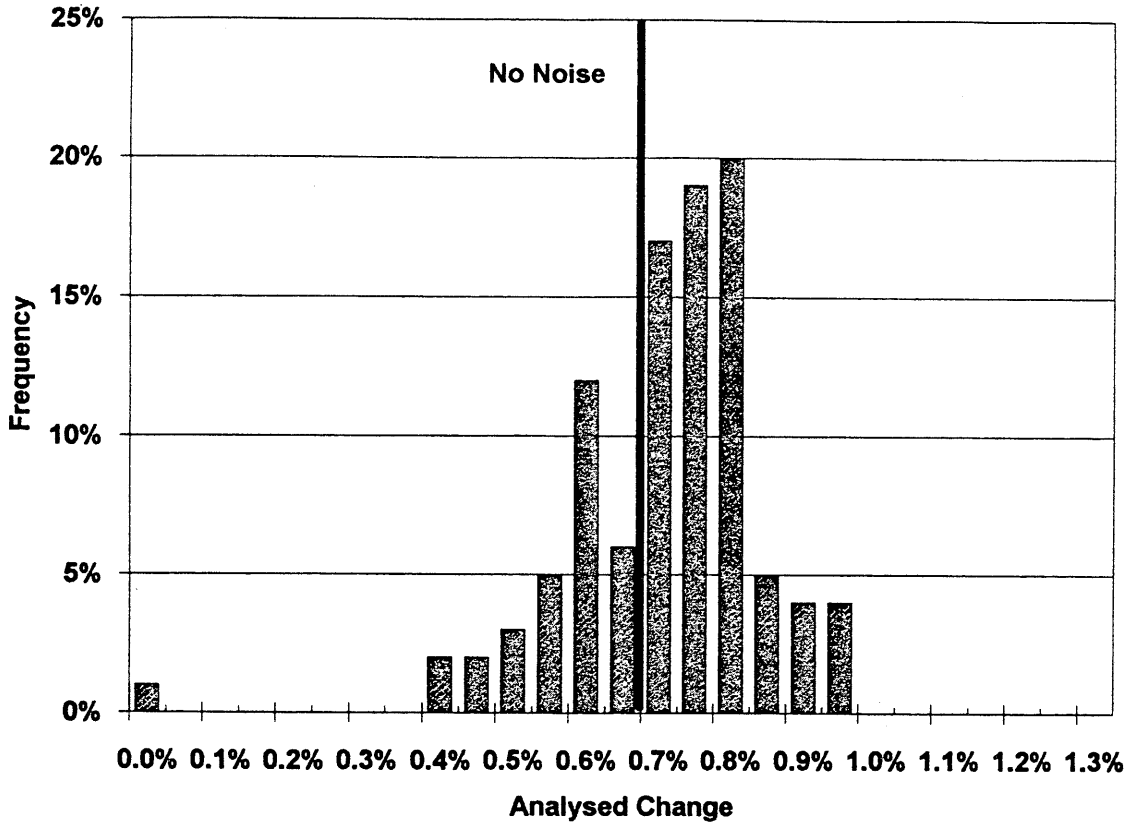

Figure 63: Net Thrust Bias Analysis Distribution

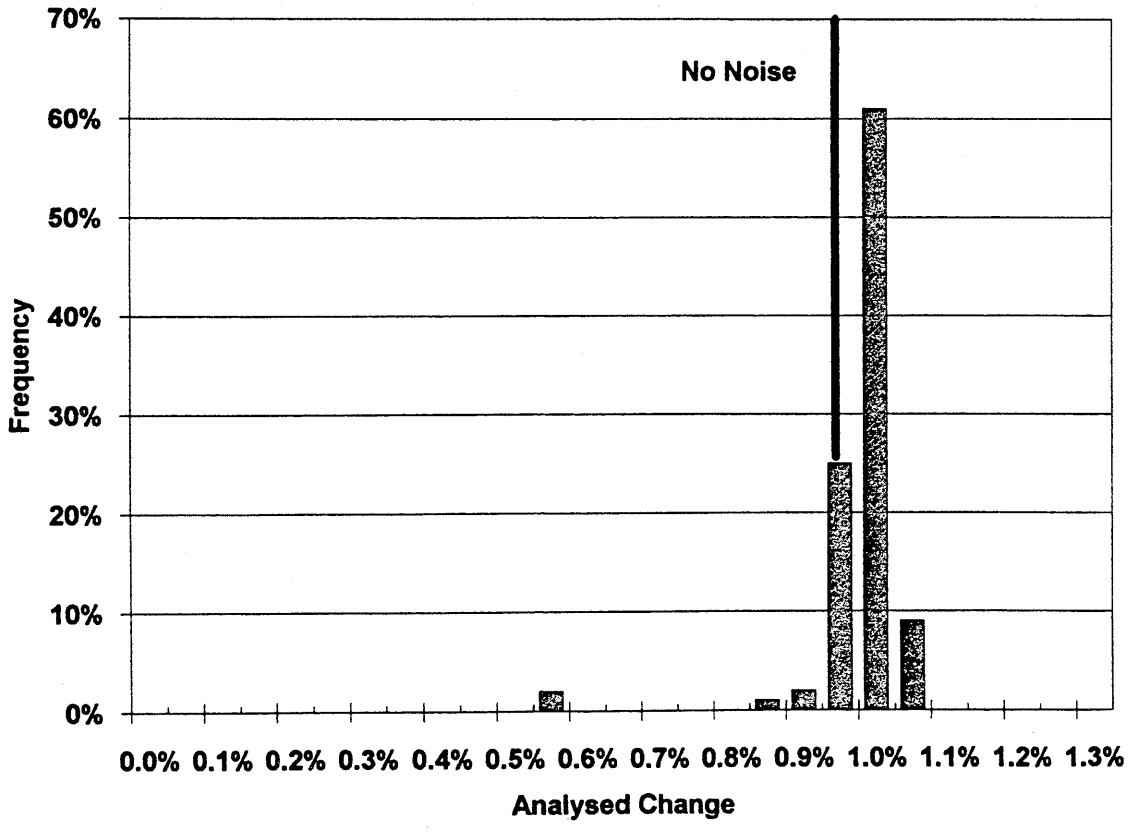

Figure 64: Total Inlet Airflow Bias Analysis Distribution

Fan Tip capacity analyses (Figure 46) and LP Turbine efficiency analyses (Figure 52);

2) the spreads of LP Compressor efficiency analyses (Figure 47), and HP Compressor entry total pressure (P26) bias analyses (Figure 57);

3) the spreads of HP Compressor efficiency analyses (Figure 48) and HP Turbine efficiency analyses (Figure 50);

4) the spreads of HP Turbine capacity analyses (Figure 51) and HP Compressor exit total pressure (P3) bias analyses (Figure 59);

5) the spreads of fuel flow (WFE) bias analyses (Figure 56) and LP Turbine exit total temperature (T49) bias analyses (Figure 61).

In the light of the known correlations between component changes and/or sensor biasses and the known analysis difficulties, all caused by the structure of the System Matrix $\underline{C}$, the above results are to be expected.

6.3 Pairs of Component Changes and/or Sensor Biasses

For this demonstration, gas-path measurement difference vectors appropriate to +1% changes in each possible component change and/or sensor bias pair were simulated by taking appropriate pairs of columns of the System Matrix $\underline{C}$ in turn, then adding each of the possible column pairs together to produce a set of 190 $\underline{y}$ vectors that were then input into the Kalman Filter and 'Concentrator'.

Of the 190 analyses produced by the 'Concentrator', 161 (85%) correctly diagnosed the simulated component change/sensor bias pair. The 29 failures (defined by analyses of component changes and/or sensor biasses different to those simulated and/or significant differences in the magnitudes of the analyses of one or both of the pair from those given in Table 3) are listed in Table 4.

This demonstration was then repeated with the sign changed for one of each of the pairs, to produce gas-path measurement difference vectors appropriate to +1% changes in one component change or sensor bias and -1% changes in the other component change or sensor bias. This new set of 190 $\underline{y}$ vectors were then input into the Kalman Filter and 'Concentrator'.

Of the 190 analyses produced by the 'Concentrator', 152 (80%) correctly diagnosed the simulated component change/sensor bias pair. The 38 failures, defined as above, are listed in Table 5.

FAN ETA & P2 bias	FAN ETA & T3 bias
FAN CAP & P2 bias	LPC ETA & HPT ETA
LPC ETA & LPT ETA	LPC ETA & P2 bias
LPC ETA & P26 bias	LPC ETA & T26 bias
LPC ETA & T49 bias	LPC ETA & P13 bias
LPC ETA & W1A bias	HPC ETA & T3 bias
HPC CAP & HPT ETA	HPC CAP & P26 bias
HPC CAP & W1A bias	HPT ETA & HPT CAP
HPT ETA & T49 bias	HPT CAP & T26 bias
HPT CAP & P3 bias	LPT ETA & EPR bias
LPT ETA & T2 bias	EPR bias & WFE bias
EPR bias & P3 bias	P2 bias & P13 bias
WFE bias & P13 bias	P26 bias & T3 bias
T26 bias & T49 bias	P3 bias & T3 bias
FN bias & W1A bias	

Table 4: Failures of +1%/+1% Component Change and/or Sensor Bias Pairs

FAN ETA & EPR bias	FAN ETA & T2 bias
FAN ETA & T26 bias	FAN ETA & T49 bias
FAN ETA & P13 bias	FAN ETA & FN bias
FAN ETA & W1A bias	FAN CAP & EPR bias
FAN CAP & T2 bias	FAN CAP & WFE bias
FAN CAP & T26 bias	LPC ETA & EPR bias
LPC ETA & T2 bias	LPC ETA & P26 bias
LPC ETA & T26 bias	LPC ETA & P3 bias
LPC ETA & FN bias	HPC ETA & T2 bias
HPC CAP & EPR bias	HPC CAP & P2 bias
HPC CAP & T2 bias	HPC CAP & T26 bias
HPC CAP & P13 bias	HPT ETA & HPT CAP
HPT ETA & P26 bias	HPT ETA & T3 bias
HPT CAP & EPR bias	HPT CAP & P2 bias
HPT CAP & T2 bias	HPT CAP & P13 bias
LPT ETA & T26 bias	LPT ETA & P3 bias
LPT ETA & P13 bias	T2 bias & WFE bias
T2 bias & P3 bias	WFE bias & T26 bias
P26 bias & FN bias	T26 bias & P3 bias

Table 5: Failures of -1%/+1% Component Change and/or Sensor Bias Pairs

The following comments on these results can be made:

1) the only pairs that appear in both Tables are;

   - LP Compressor efficiency and HP Compressor entry total pressure (P26) bias;
   - LP Compressor efficiency and HP Compressor entry total temperature (T26) bias;
   - HP Turbine efficiency and HP Turbine capacity;

2) LP Compressor efficiency changes appear difficult to analyse when combined with other component changes and

sensor biasses, possibly because of the small magnitudes of the elements in the LPC ETA column of the System Matrix C (Figure 8);

3) environmental measurement biasses (EPR, P2 and T2) are also difficult to analyse when combined with other component changes and sensor biasses, possibly because of the large magnitudes of most of the elements in the Environmental Exchange Rate Table section of the System Matrix C (Figure 8);

4) the reasons for failures to analyse single component changes or sensor biasses when sensor non-repeatability was added to the gas-path measurement differences also apply when pairs of component changes and/or sensor biasses are being sought.

Given the difficulties mentioned in the Introduction that 'traditional' analysis techniques have in detecting multiple component changes and/or sensor biasses, the performance of the 'Concentrator' demonstrated above is considered to be very good. The structure of the System Matrix C, which determines the ability of any analysis technique to successfully discriminate between individual component changes and sensor biasses, makes many combinations of component changes and/or sensor biasses difficult or impossible to analyse correctly.

6.4 Smoothing/Trending Algorithm Demonstration

For this demonstration, fuel consumption figures (expressed in Imperial Units of miles per gallon) calculated each time the author's car fuel tank was filled with petrol were arranged as a time series and input into the Smoothing/Trending Algorithm. The results are shown in Figure 65, which uses a format similar to that used in Figures 36 to 41; note that:

1) all three graphs use a common x scale, labelled FUEL TANK FILL-UP NUMBER on the bottom graph, as the time axis;

2) the top graph, with a y scale labelled FUEL CONSUMPTION (MPG), shows:

   - the recorded miles per gallon as circles, with filled-in circles indicating that long journeys were undertaken prior to those recordings;

   - the miles per gallon level estimates output from the Smoothing/Trending Algorithm, as a line without symbols;

   - the official urban cycle, 56 miles/hour and 75 miles/hour fuel consumption figures as horizontal dashed lines;

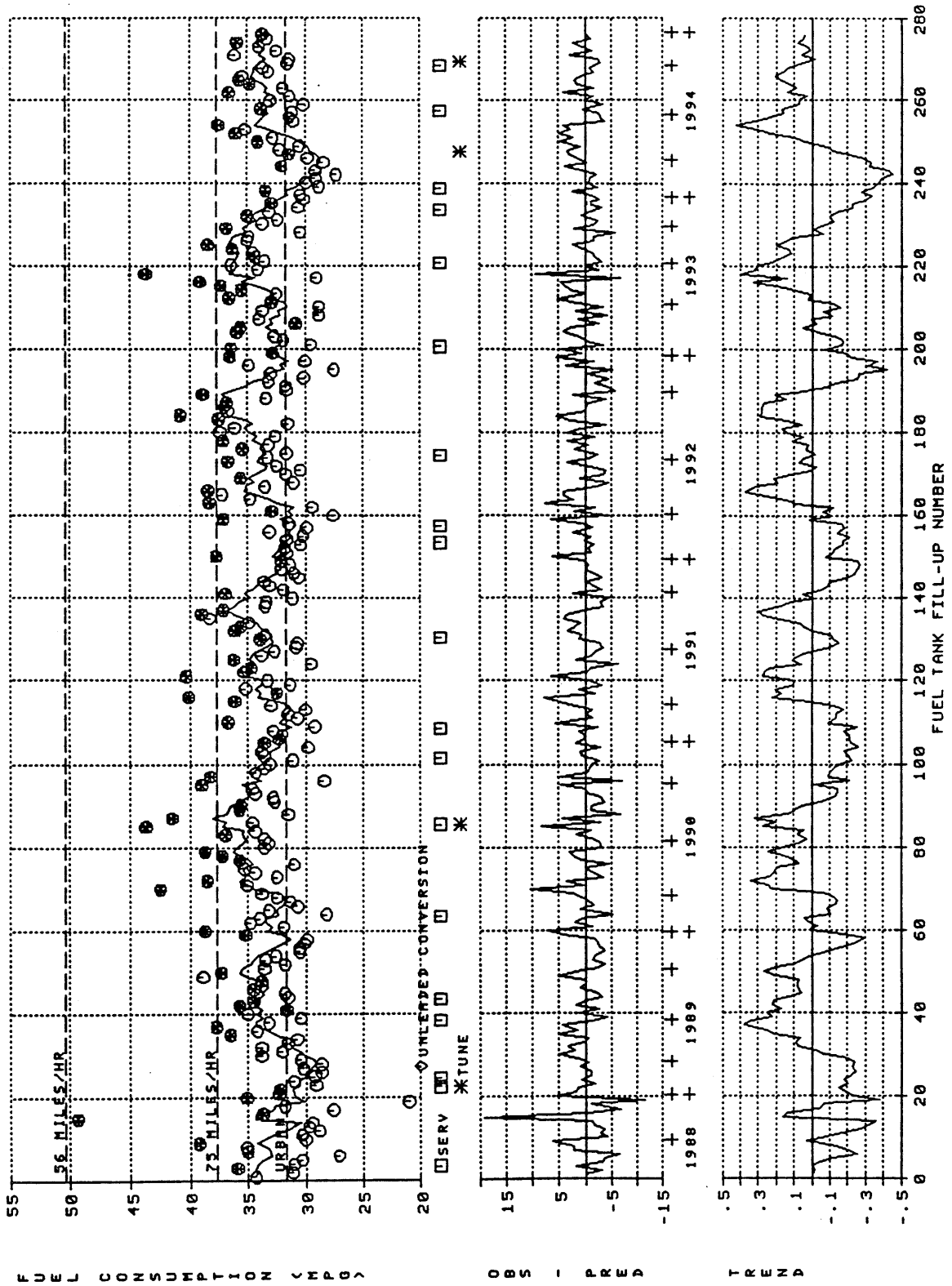

Figure 65: Smoothing/Trending of Car Fuel Consumption Records

3) the middle graph, with a y scale labelled OBS - PRED, shows the differences between the observed fuel consumption and the fuel consumption predicted from the level and trend estimates for the immediately previous points: this is output from the Smoothing/Trending Algorithm;

4) the bottom graph, with a y scale labelled TREND, shows the miles per gallon trend estimates output from the Smoothing/Trending Algorithm;

5) an approximate date scale, with each year divided into quarters, is shown between the middle and bottom graphs;

6) regular servicing and other repairs are indicated by square event markers between the top and middle graphs; also shown here are asterisks marking when engine tuning took place and a diamond marking when the engine was re-tuned to accept unleaded petrol;

7) values of $q_{11} \div r$ and $q_{12} \div r$ of zero were used, with $q_{22} \div r$ set to 0.001.

The top graph shows the fuel consumption varying seasonally between the urban and 75 miles/hour 'tramlines', with good fuel consumption being recorded in the summer months (possibly because the number of long journeys is higher) and poorer fuel consumption being recorded in the winter months. The consistently poor fuel consumption figures recorded from the middle of 1988 to early 1989 and during the early part of 1994 are probably due to major road works introducing significant delays in the author's journeys into work. It is interesting to note that the change to unleaded petrol did not, as one would normally expect, worsen the fuel consumption, and that the car's fuel consumption has remained remarkably consistent over more than 70,000 miles of motoring, possibly due to the author's diligent use of petrol additive. Tuning the engine appears to have made no noticeable difference to the pattern of fuel consumption. The bottom graph confirms the rising trends in miles per gallon in summer and the the falling trends in winter seen in the top graph, while the middle graph confirms the sudden changes in fuel consumption when a long journey has followed a spate of short journeys (note particularly observation 15, taken after a long cruise near 56 miles/hour forced by traffic and weather conditions) or vice-versa (note observation 19, which was taken after many very short journeys).

This demonstration, while not using gas turbine data, clearly demonstrates the usefulness and wide applicability of the Smoothing/Trending Algorithm. Note that the level and trend estimate outputs from the Smoothing/Trending Algorithm could be automatically compared with appropriate

limits by a computer program, to give warnings when the level and/or trend of the parameter being monitored exceeded desirable limits, while the difference between the observed and predicted level could be compared with another set of limits to give warnings when significant sudden changes had taken place in the 'character' of the time series. These warnings would focus the user's attention on significant events, enabling many parameters to be effectively monitored without the necessity for continuous visual checking of each time series.

6.5 Trend 'Concentration'

For this demonstration, a time series of gas-path measurement difference vectors appropriate to a simulated time series of HP Compressor changes was created by taking the HPC ETA column of the System Matrix $\underline{C}$, then multiplying each element by the amount of HP Compressor efficiency change being simulated at each point in the time series (according to the schedule in Table 6) to produce a set of 30 $\underline{y}$ vectors that were then input into the Kalman Filter and 'Concentrator', the Smoothing/ Trending Algorithm and the Trend 'Concentration' logic. The relationships between these analytical techniques are shown diagrammatically in Figure 66.

Time	Amount of HP Compressor Efficiency Change	
1 to 5	0.0%	
6	-0.2%)	
7	-0.4%)	
8	-0.6%)	
.	.)	
.	.)	-0.2% per time interval
18	.)	
19	-2.8%)	
20	-3.0%)	
21 to 30	-3.0%	

Table 6: Time Series of Simulated HP Compressor Efficiency Changes

Because no sensor non-repeatability was simulated, the Smoothing/Trending Algorithm was 'tuned' to be very sensitive to changes in the time series, with $q_{11} \div r$ and $q_{12} \div r$ both set to zero and $q_{22} \div r$ set to 0.3.

The results of this demonstration were very voluminous (as indicated by the structure of Figure 66), containing the following outputs:

1) 11 time series of actual gas-path measurement differences, together with level estimates, trend estimates and (observed - predicted) values;

2) 20 time series of 'Concentrator' analyses of component

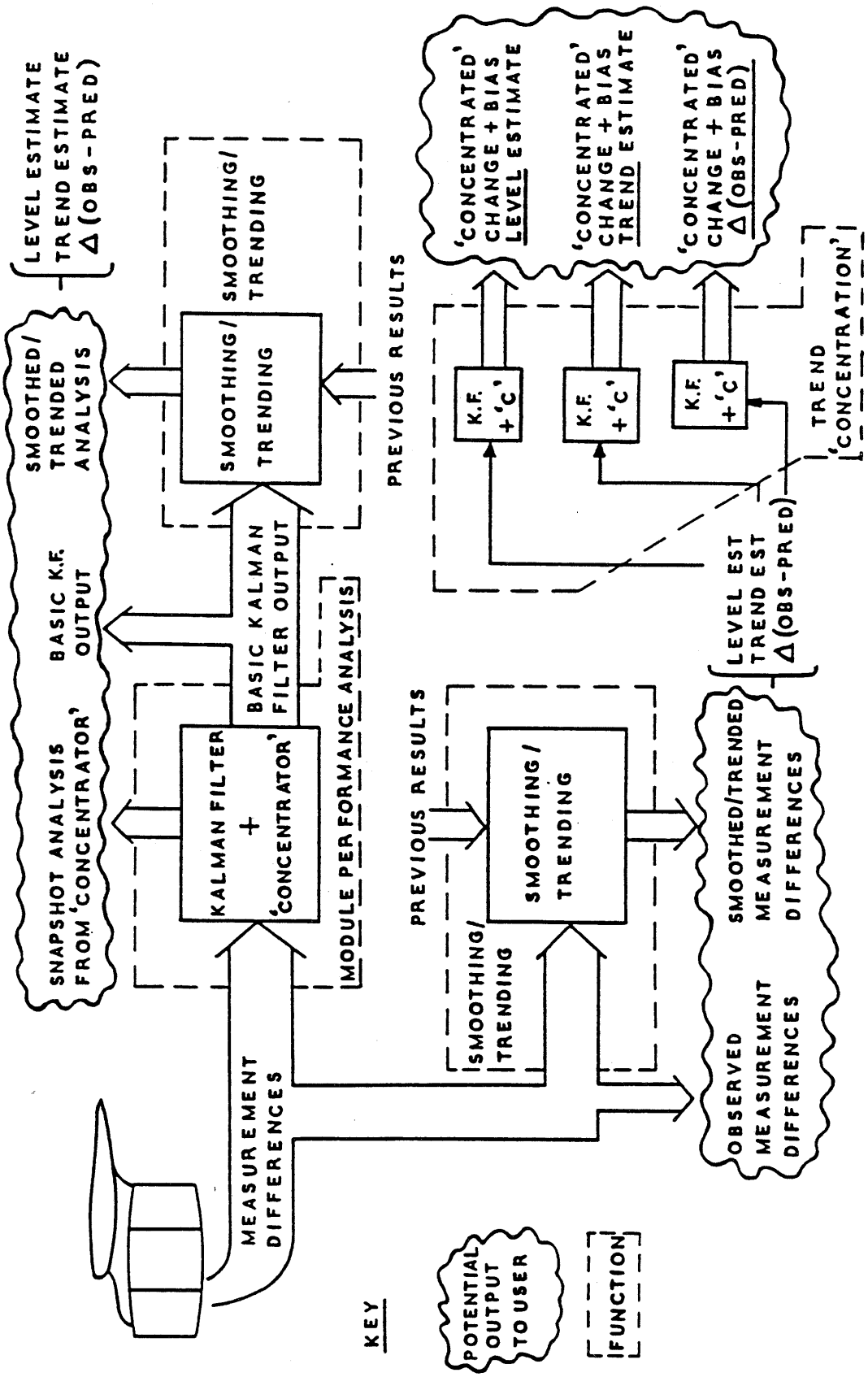

Figure 66: Relationships between Kalman Filter and 'Concentrator', Smoothing/Trending and Trend 'Concentration'

changes and sensor biasses;

3) 20 time series of basic Kalman Filter analyses of component changes and sensor biasses, together with level estimates, trend estimates and (observed - predicted) values;

4) 20 time series of level estimates, trend estimates and (observed - predicted) values for analysed component changes and sensor biasses output from the Trend 'Concentration' process.

However, the results can be summarised as follows:

1) because of the 'sensitive' tuning of the Smoothing/ Trending Algorithm, all the gas-path measurement difference level estimates closely followed the simulated values, with the trend estimates quickly reaching the simulated rates of change of each gas-path measurement difference and the (observed - predicted) gas-path measurement difference values staying close to zero because of the absence of sudden large changes in all of the time series;

2) the 'Concentrator' analyses of each set of gas-path measurement differences correctly diagnosed the HP Compressor efficiency changes given in Table 6;

3) the basic Kalman Filter analyses of each set of gas-path measurement differences produced the 'smearing' effect shown in Figure 43, which the 'Concentrator' is intended to remove;

4) because of the 'sensitive' tuning of the Smoothing/ Trending Algorithm, all the basic Kalman Filter analysed component change and sensor bias level estimates closely followed the values discussed in 3), with the trend estimates quickly reaching the appropriate rates of change of each analysed component change and sensor bias and the (observed - predicted) analysed component change and sensor bias values staying close to zero because of the absence of sudden large changes in all of the time series;

5) because of the 'sensitive' tuning of the Smoothing/ Trending Algorithm, the Trend 'Concentration' logic produced HP Compressor efficiency level estimates that closely followed those shown in Table 6, and HP Compressor efficiency trend estimates that quickly reached the trends in HP Compressor efficiency indicated in Table 6. HP Compressor efficiency (observed - predicted) values stayed close to zero because of the absence of sudden large changes in all of the time series;

6) The Trend 'Concentration' logic did not analyse any

other component changes or sensor biasses.

This demonstration was then repeated, except that normally-distributed random noise was added to all the previously generated gas-path measurement difference time series (as detailed in the section describing the testing of the 'Concentrator' when analysing single component changes and sensor biasses with sensor noise) to produce a new set of 30 $\underline{y}$ vectors that were then input into the Kalman Filter and 'Concentrator', the Smoothing/Trending Algorithm and the Trend 'Concentration' logic. Because sensor non-repeatability was simulated, the Smoothing/ Trending Algorithm was 'tuned' to be somewhat less sensitive to changes in the time series, with $q_{11} \div r$ and $q_{12} \div r$ both set to zero and $q_{22} \div r$ set to 0.01.

Because the addition of sensor non-repeatability makes the output more difficult to concisely summarise and more worthy of closer study, the full results of this demonstration are presented graphically in Figures 67 to 97. Figures 67 to 77 show the 11 time series of actual gas-path measurement differences, together with level estimates, trend estimates and (observed - predicted) values, laid out in a similar format to Figure 65, with:

1) all three graphs in each Figure using a common x scale, labelled OBSERVATION on the bottom graph, as the time axis;

2) the top graph in each Figure, with a y scale labelled ACTUAL & LEVEL, showing:

   - the simulated gas-path measurement differences as circles;

   - the level estimates of the simulated gas-path measurement differences output from the Smoothing/ Trending Algorithm, as a line without symbols;

3) the middle graph in each Figure, with a y scale labelled OBS - PRED, showing the differences between the simulated gas-path measurement differences and the gas-path measurement differences predicted from the level and trend estimates for the immediately previous points: this is output from the Smoothing/Trending Algorithm;

4) the bottom graph in each Figure, with a y scale labelled TREND, showing the simulated gas-path measurement difference trend estimates output from the Smoothing/Trending Algorithm;

Figures 78 to 97 show the 20 time series of Kalman Filter, 'Concentrator' and Trend 'Concentration' analyses for each component change and sensor bias being sought, laid out as follows:

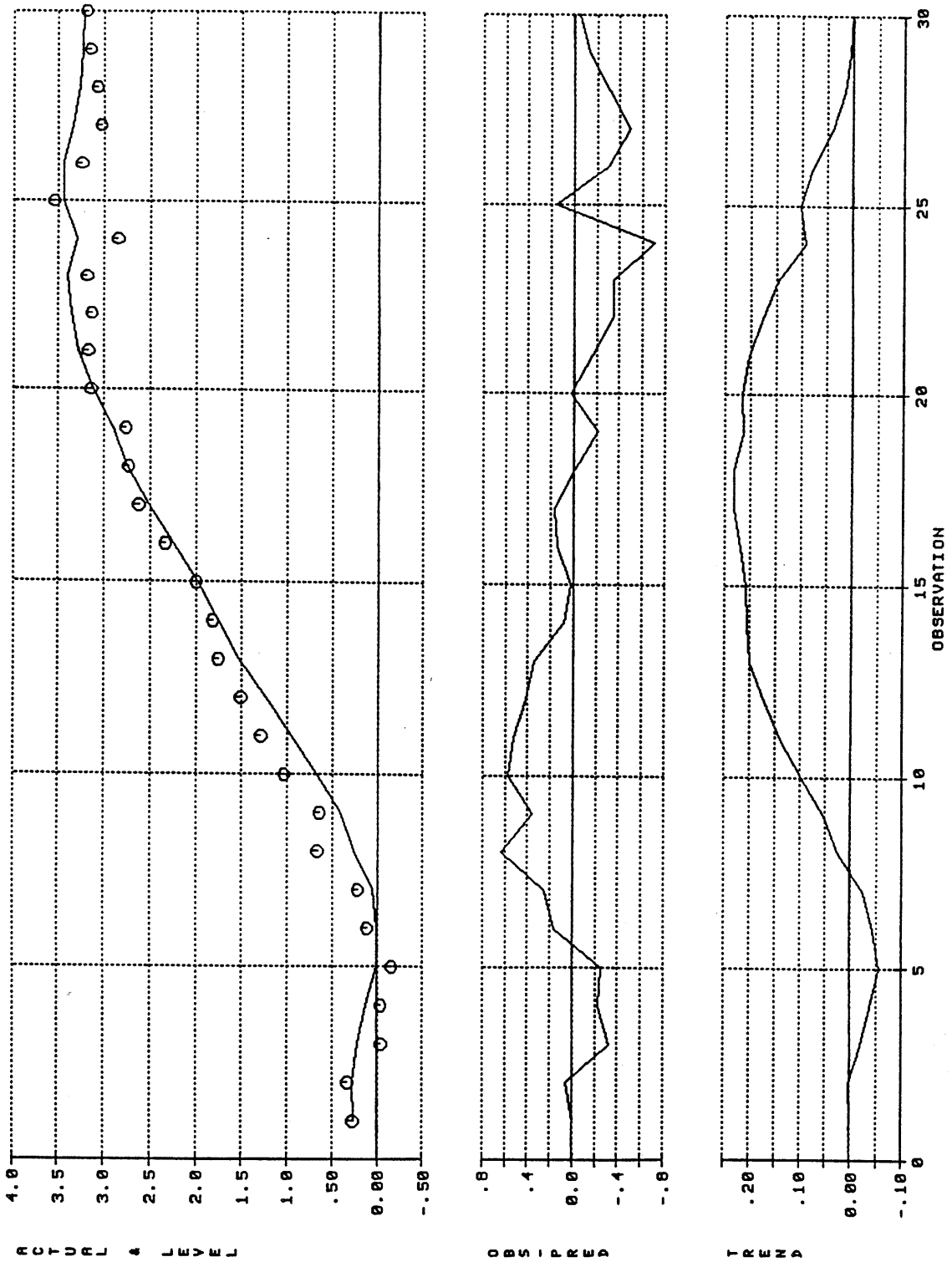

Figure 67: Fuel Flow Measurement Differences

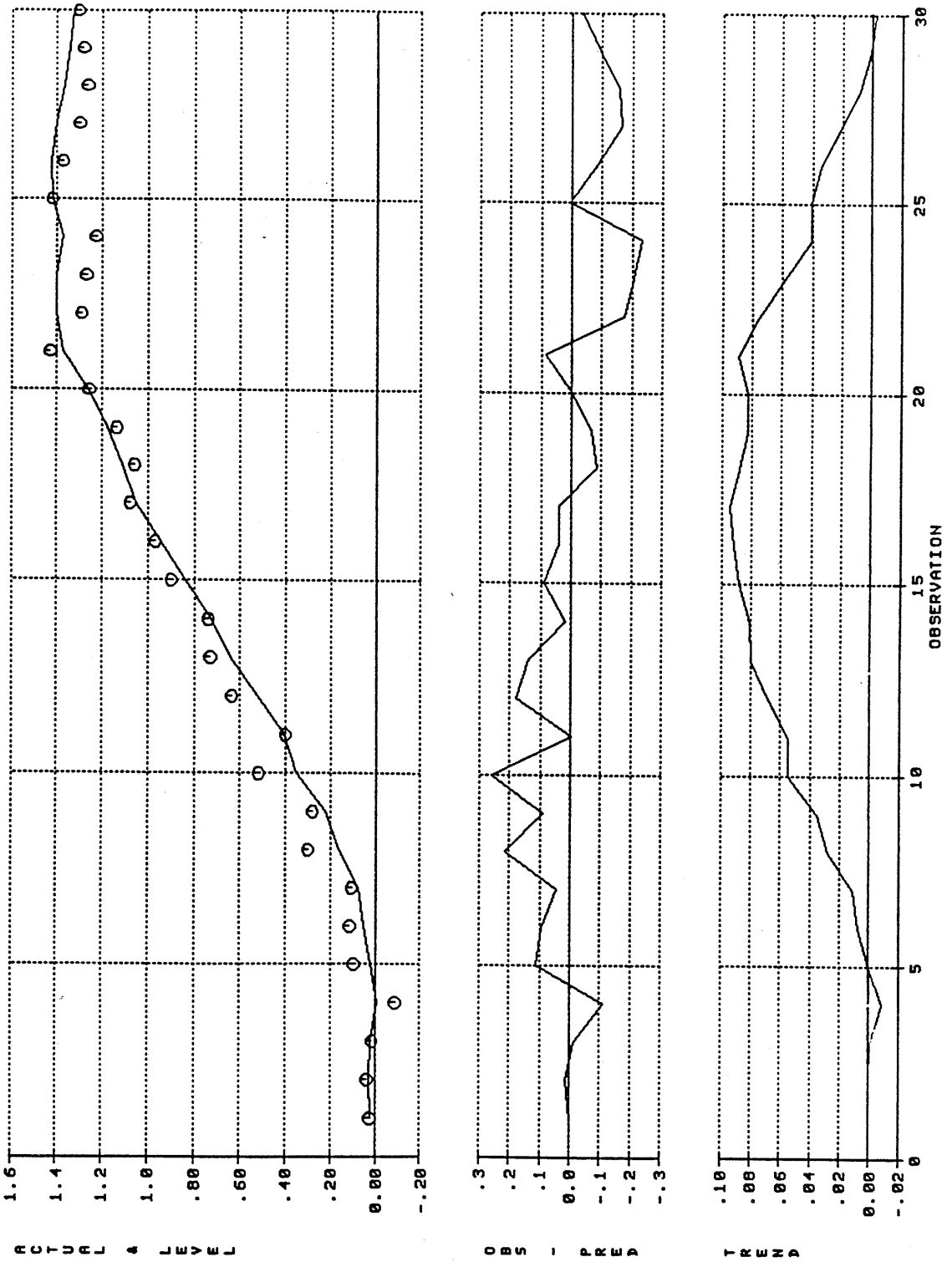

Figure 68: HPC Entry Total Pressure Measurement Differences

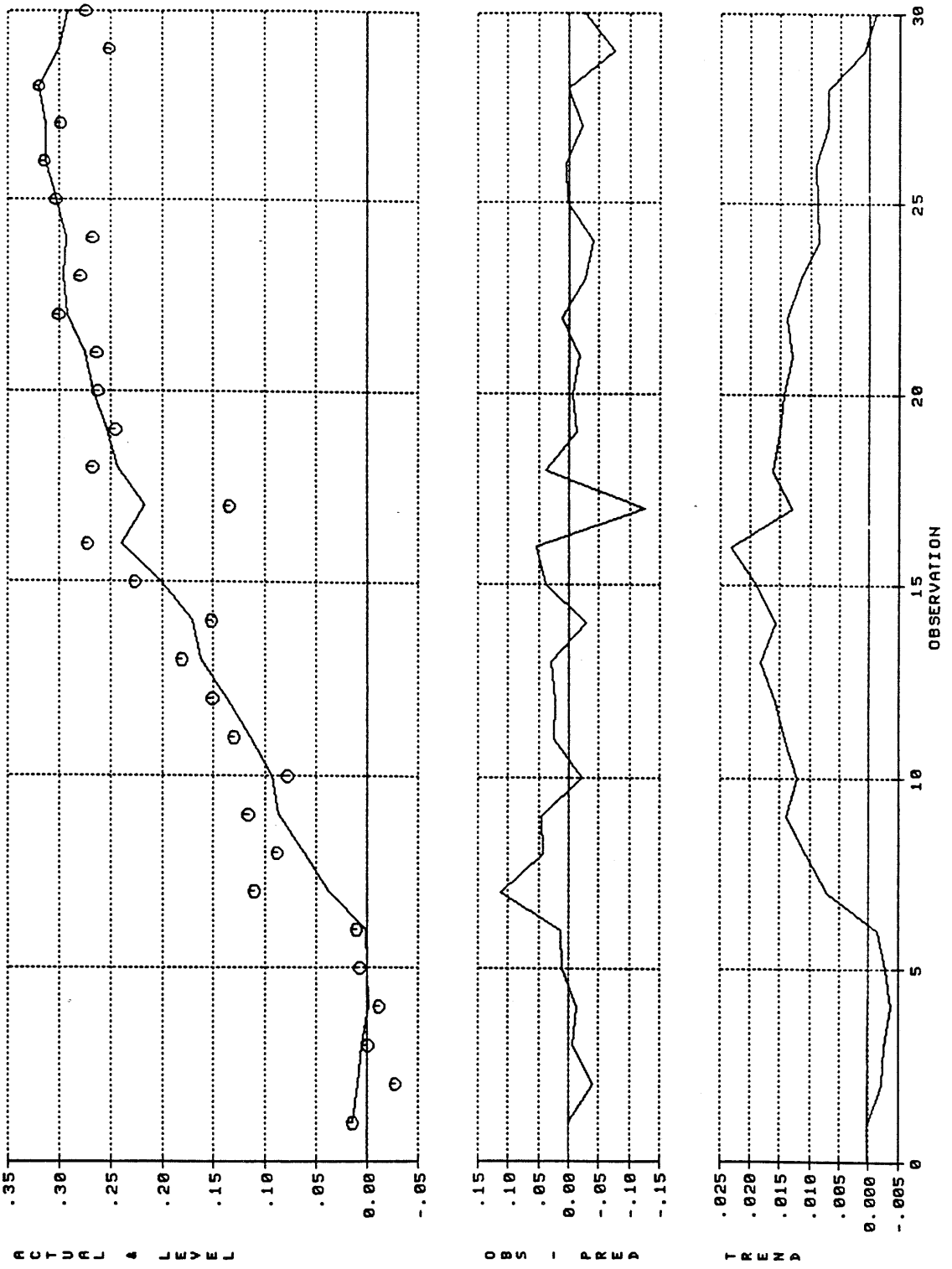

Figure 69: HPC Entry Total Temperature Measurement Differences

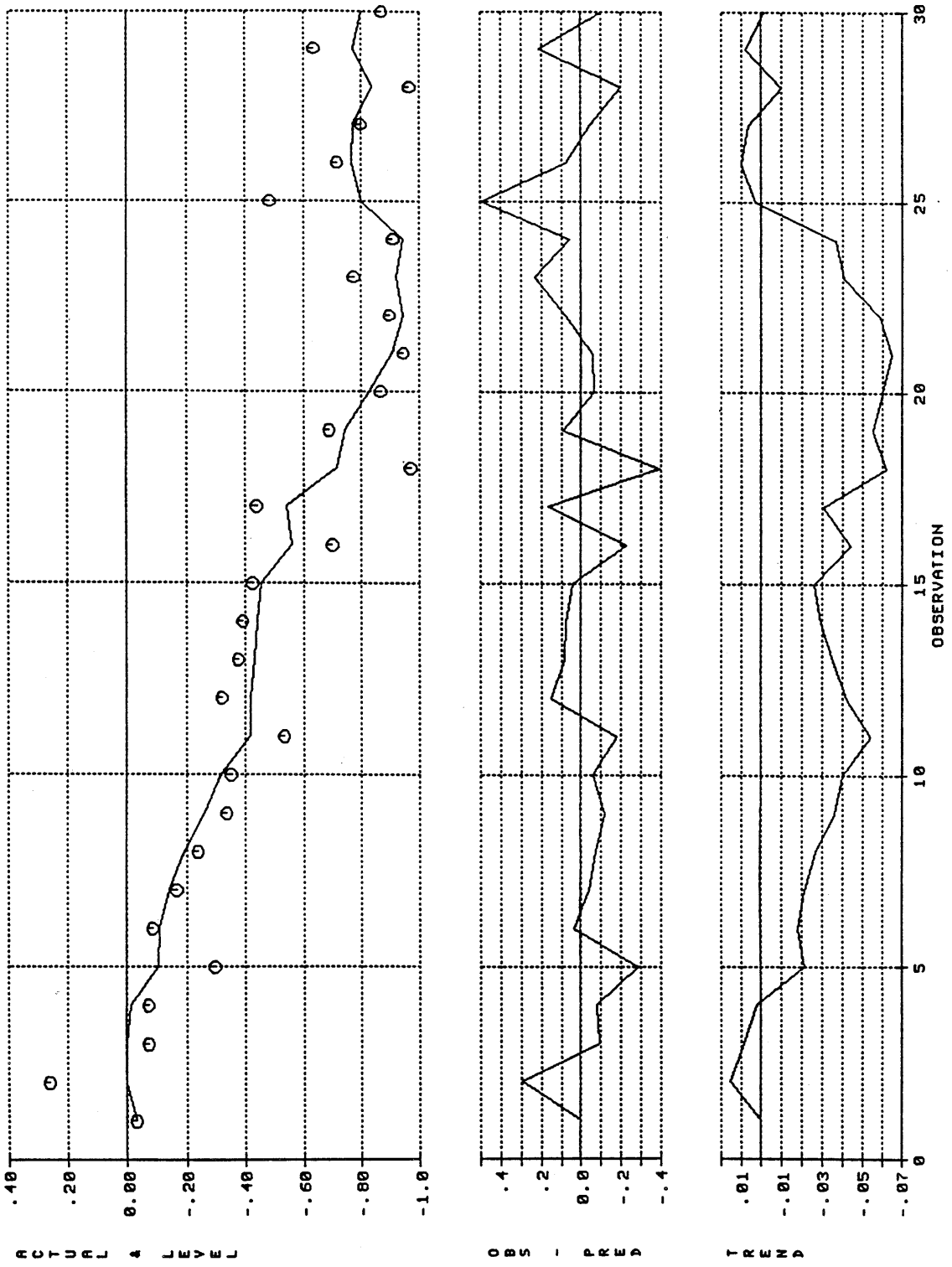

Figure 70: HPC Exit Total Pressure Measurement Differences

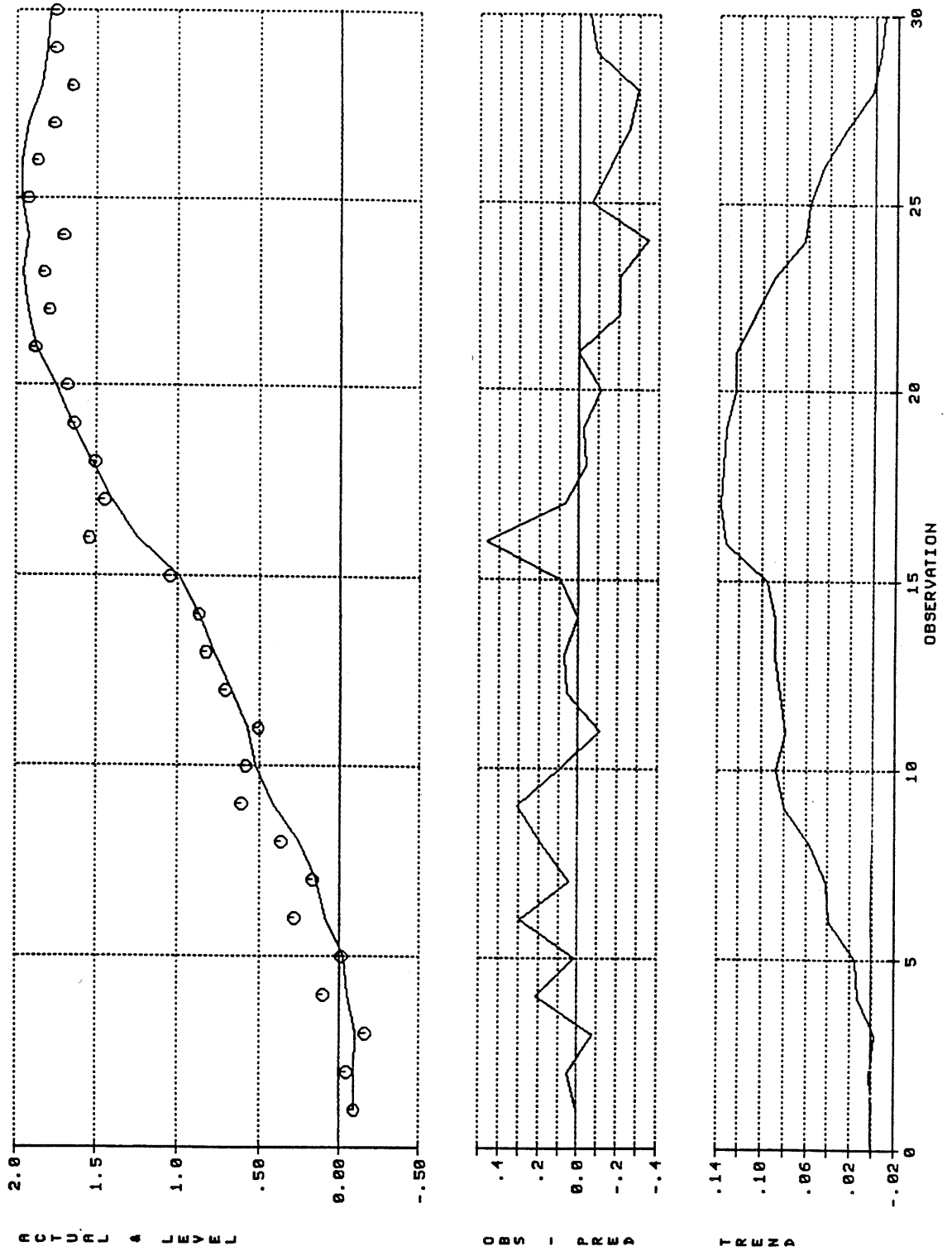

Figure 71: HPC Exit Total Temperature Measurement Differences

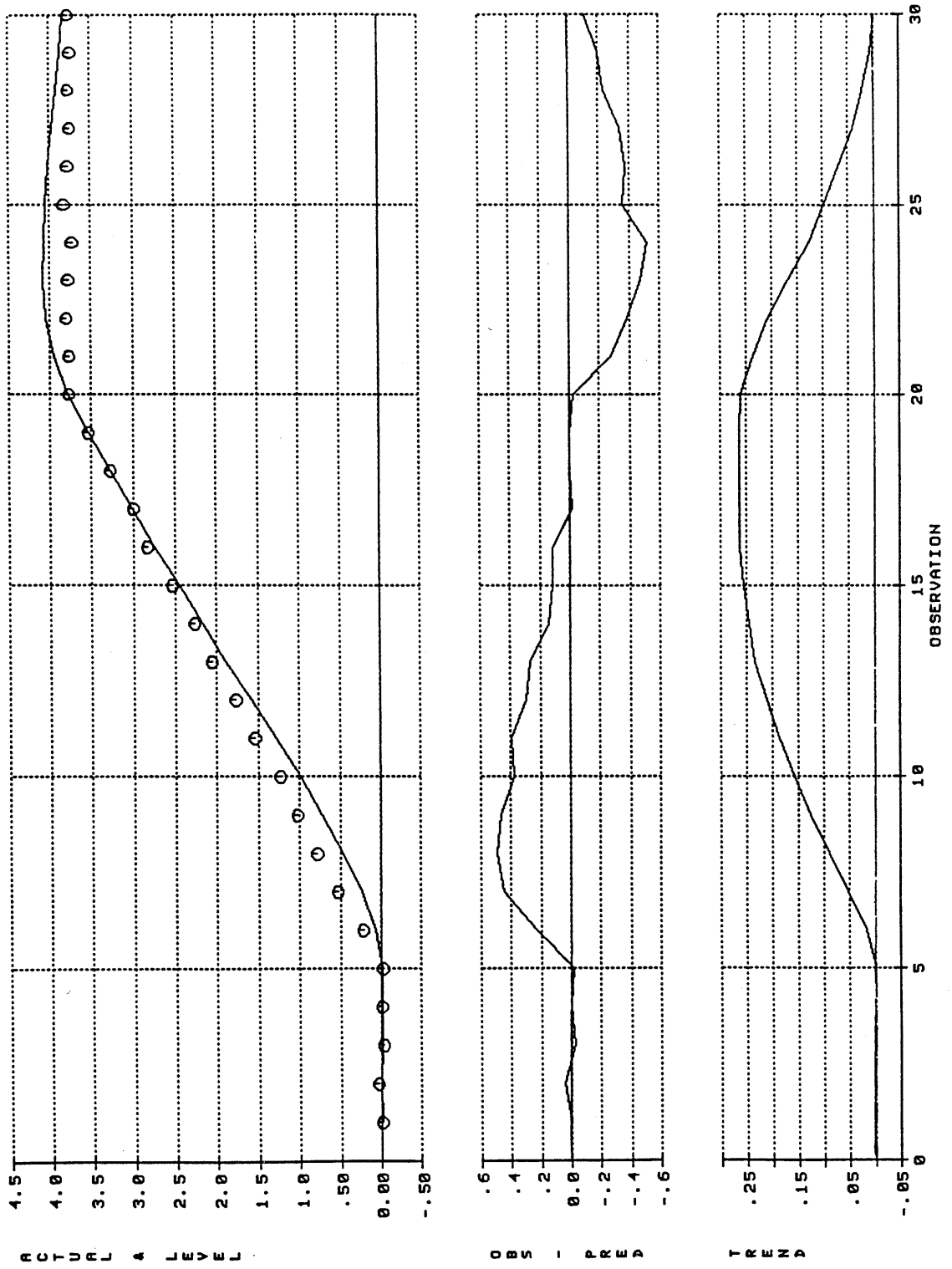

Figure 72: LPT Exit Total Temperature Measurement Differences

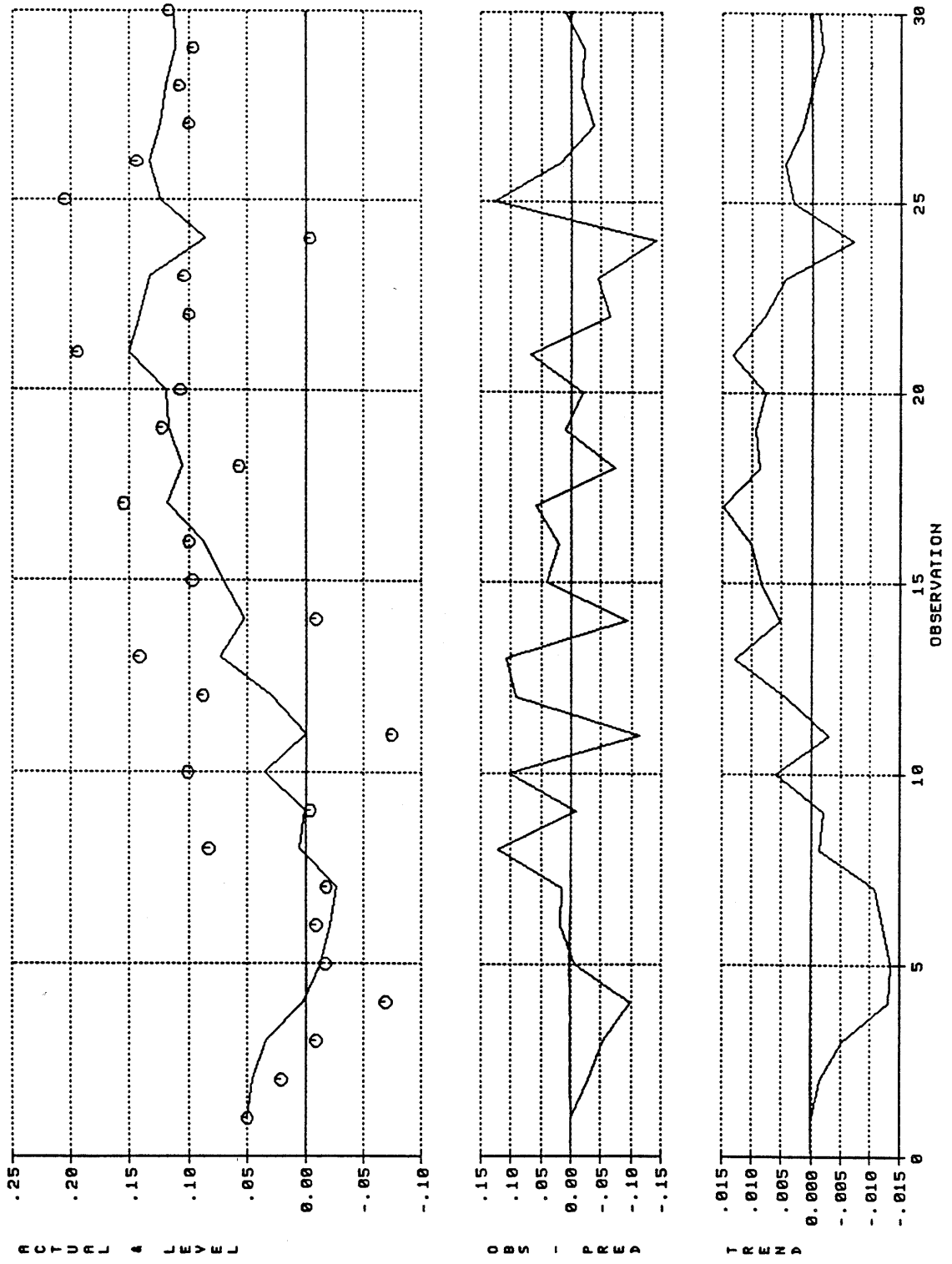

Figure 73: Fan Tip Exit Total Pressure Measurement Differences

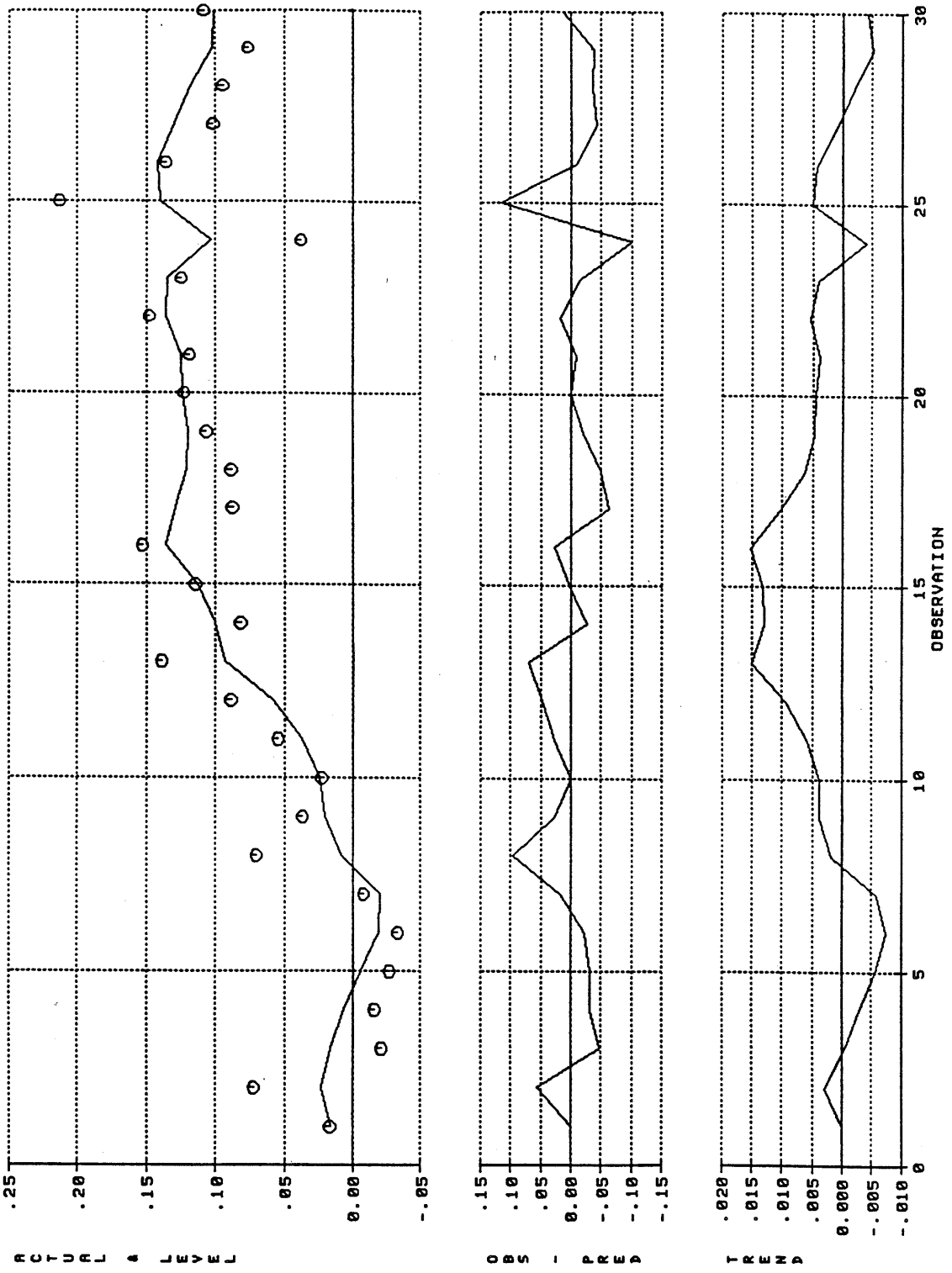

Figure 74: LP Speed Measurement Differences

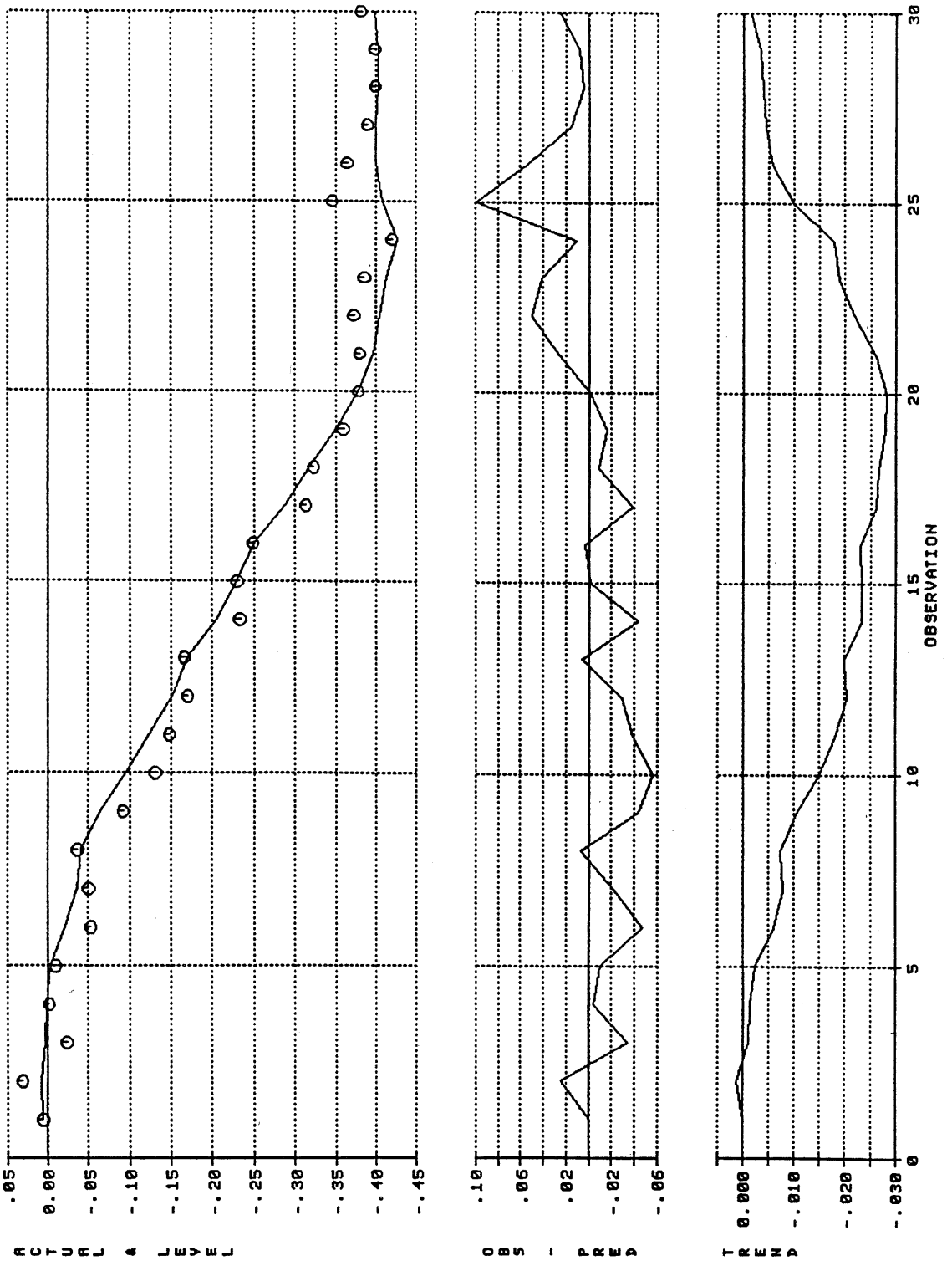

Figure 75: HP Speed Measurement Differences

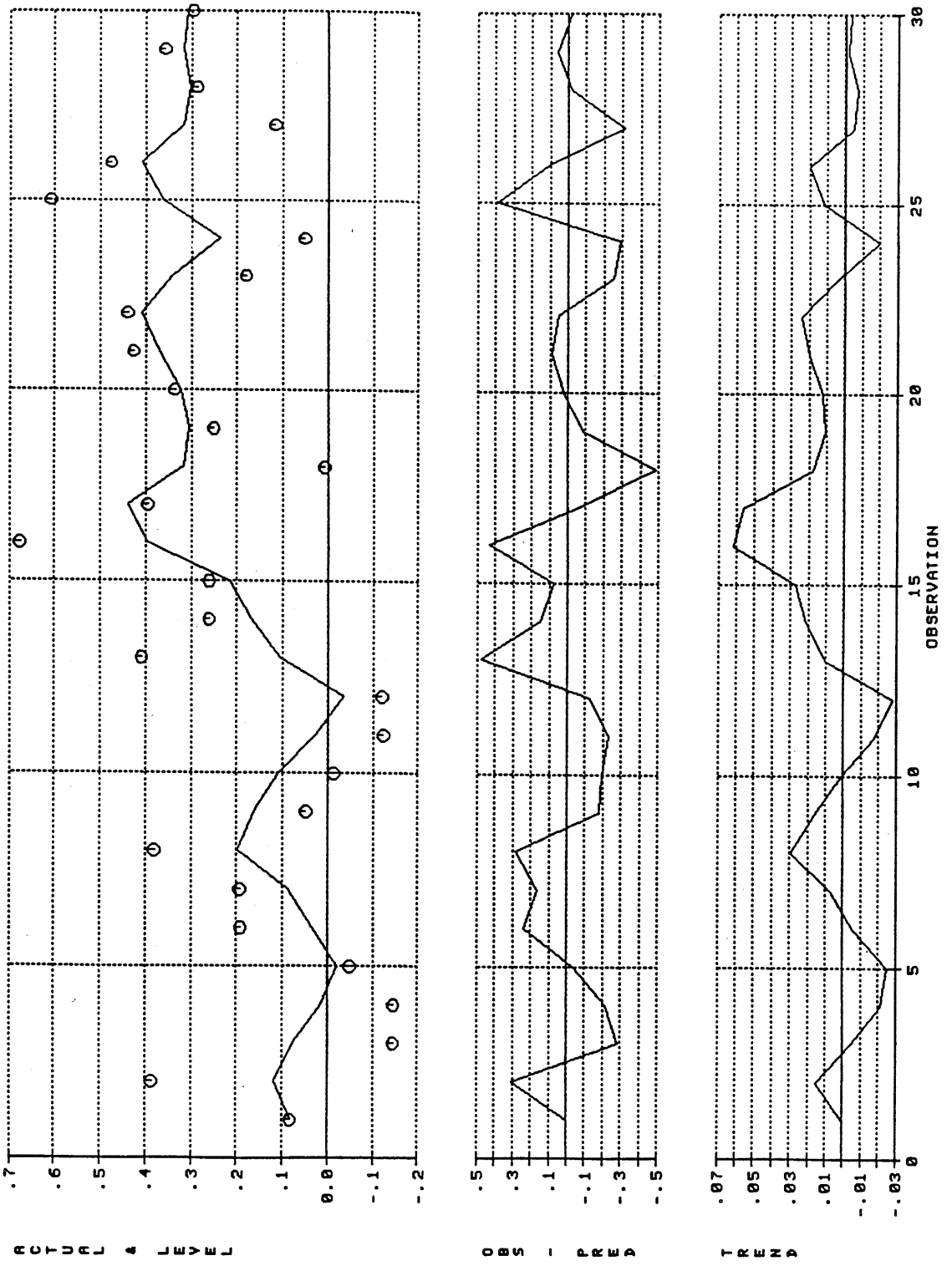

Figure 76: Net Thrust Measurement Differences

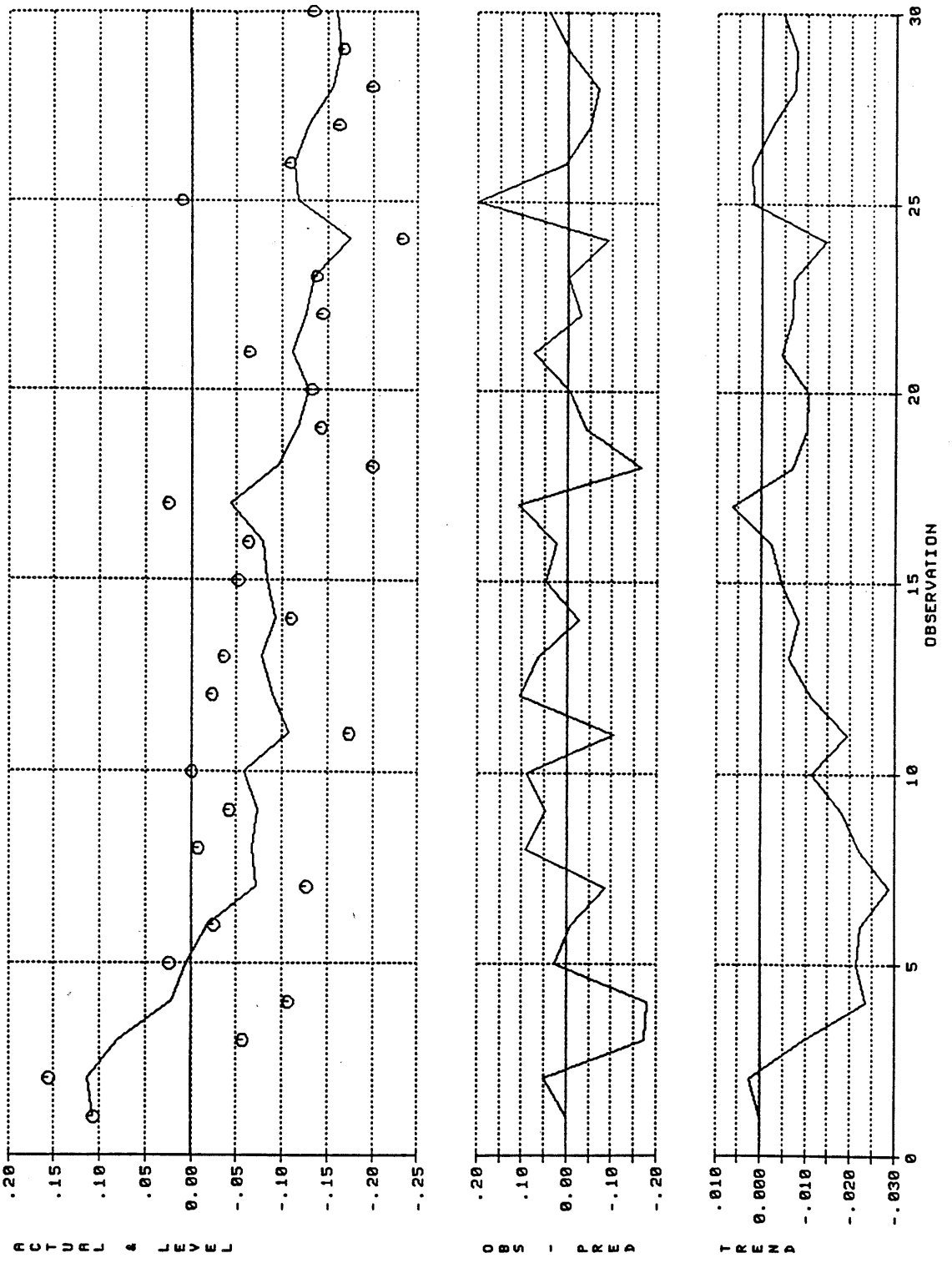

Figure 77: Total Inlet Airflow Measurement Differences

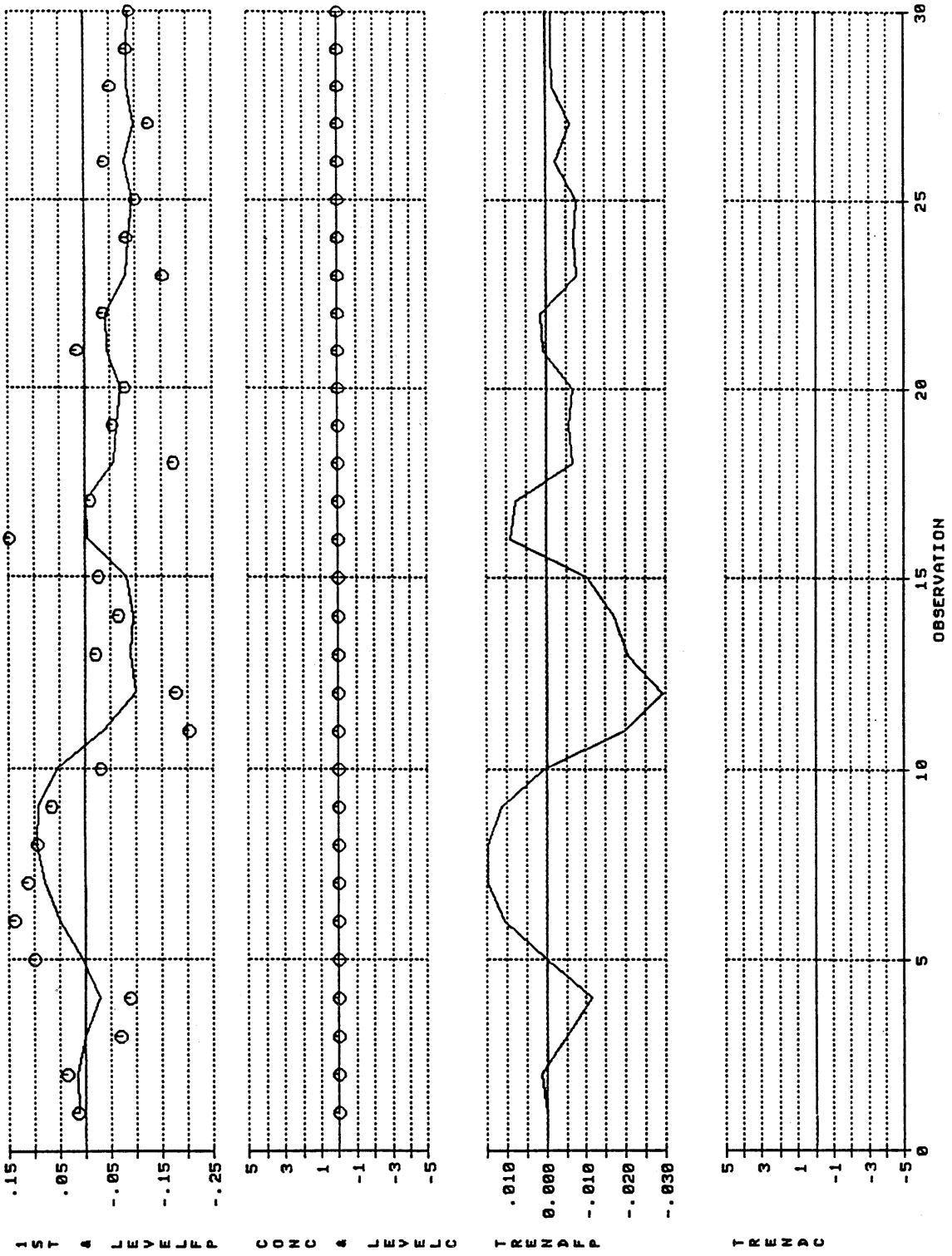

Figure 78: Fan Tip Efficiency Analyses

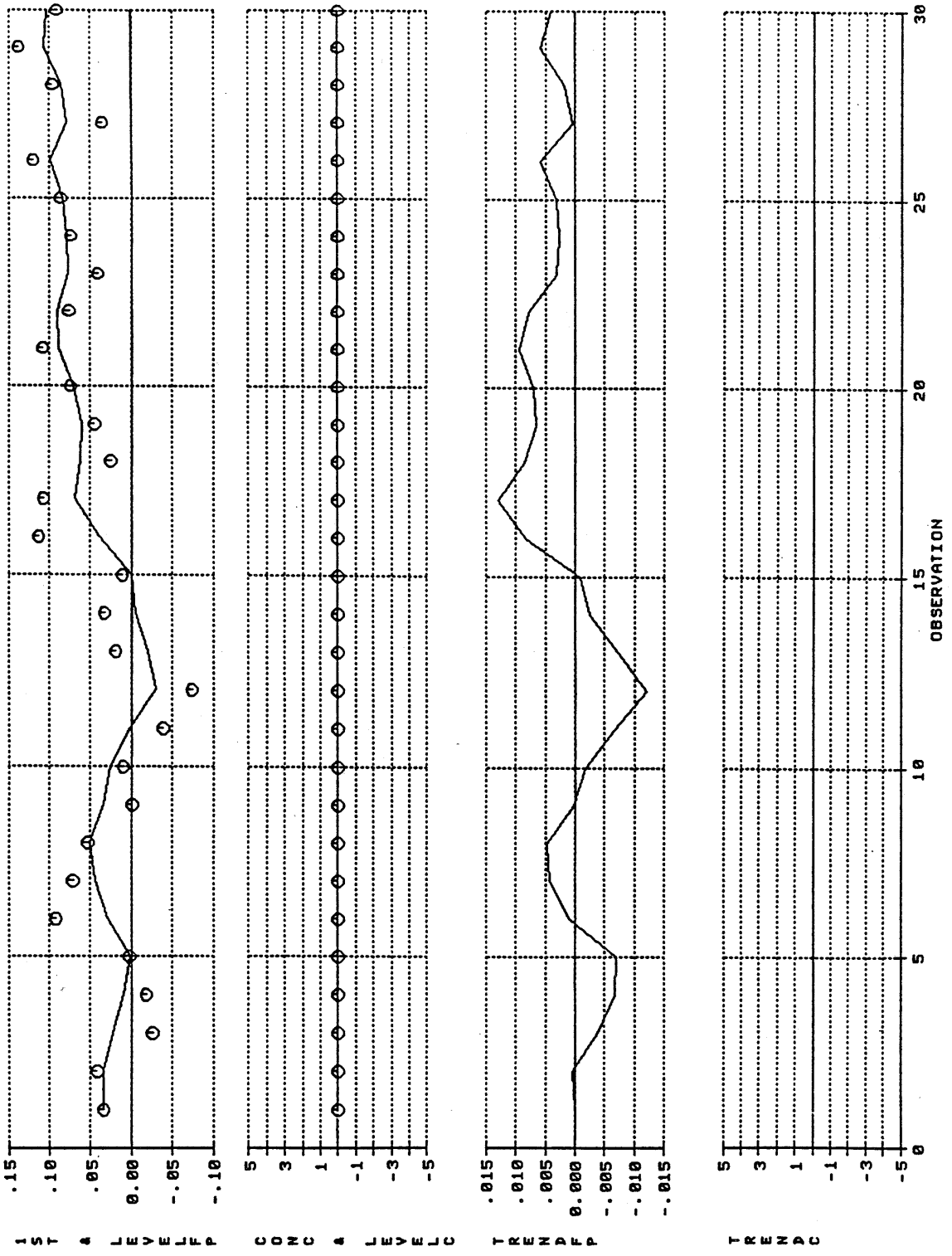

Figure 79: Fan Tip Capacity Analyses

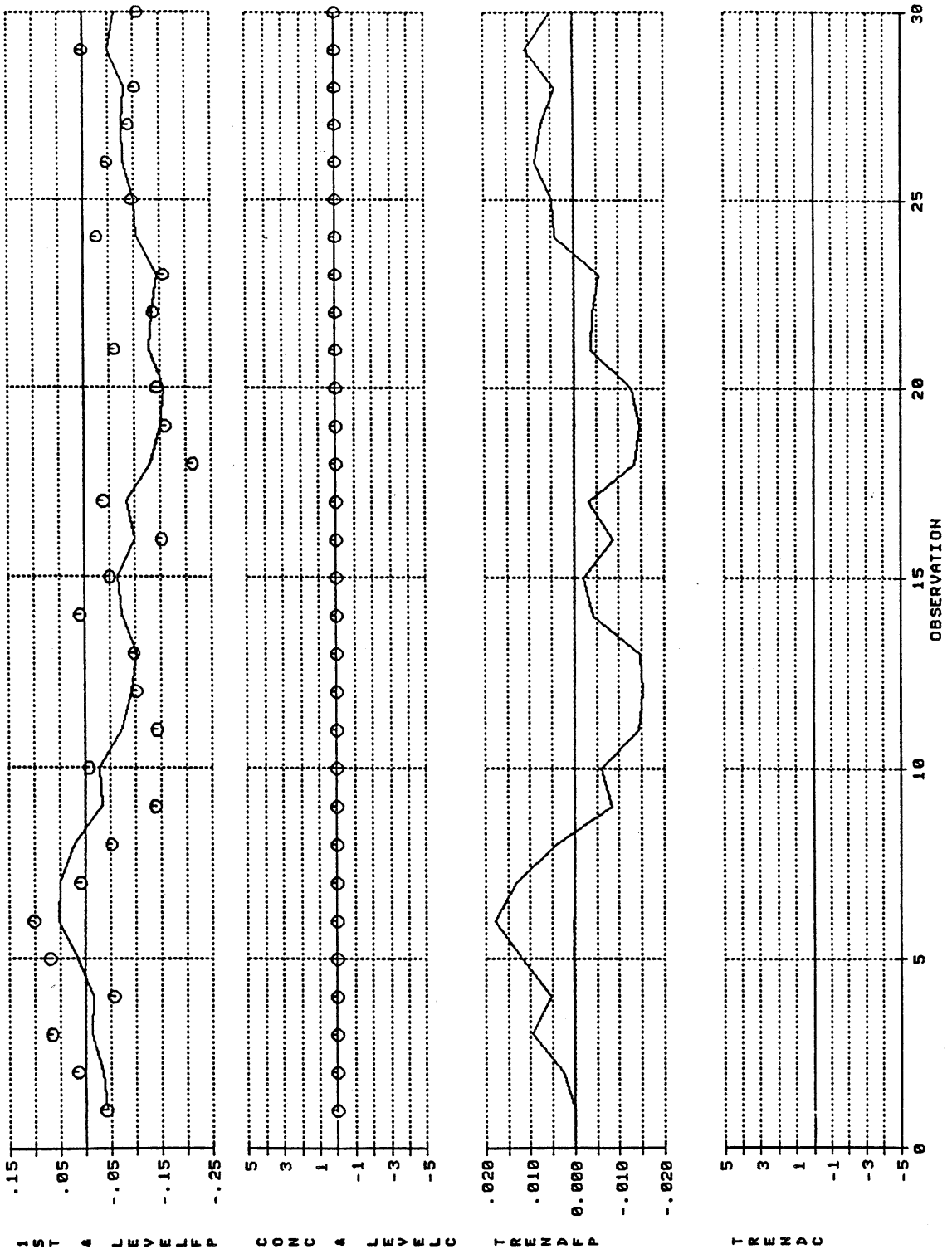

Figure 80: LP Compressor Efficiency Analyses

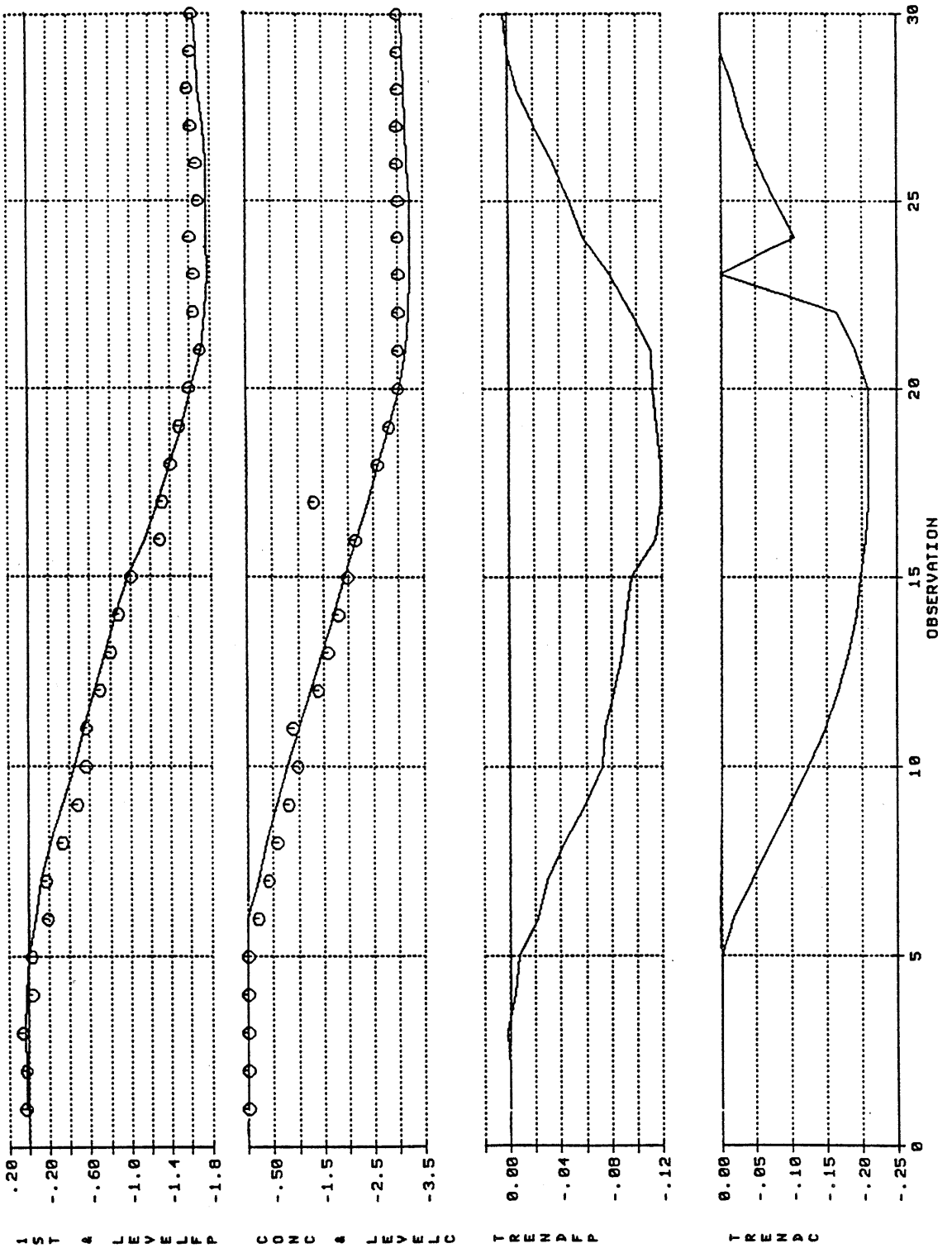

Figure 81: HP Compressor Efficiency Analyses

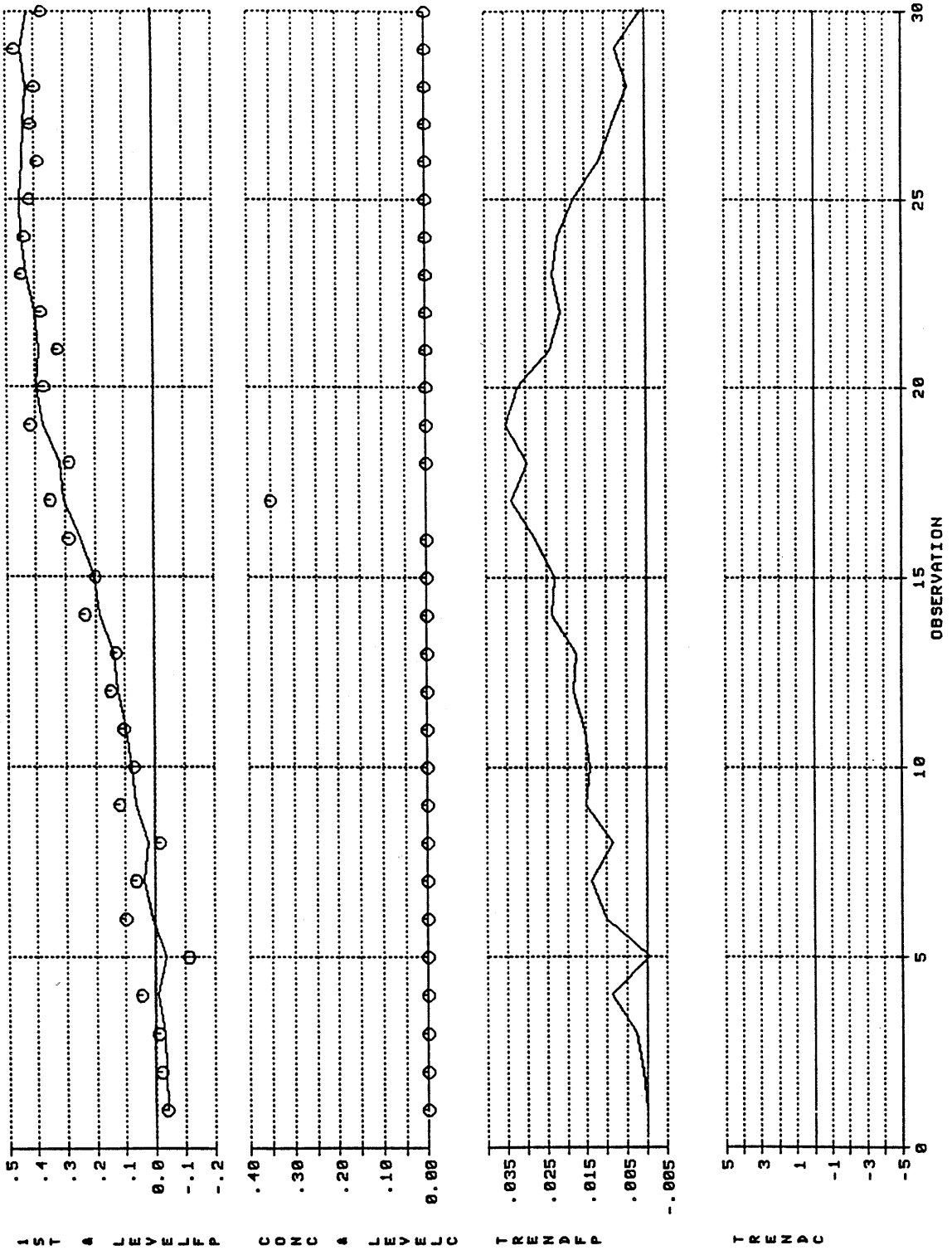

Figure 82: HP Compressor Capacity Analyses

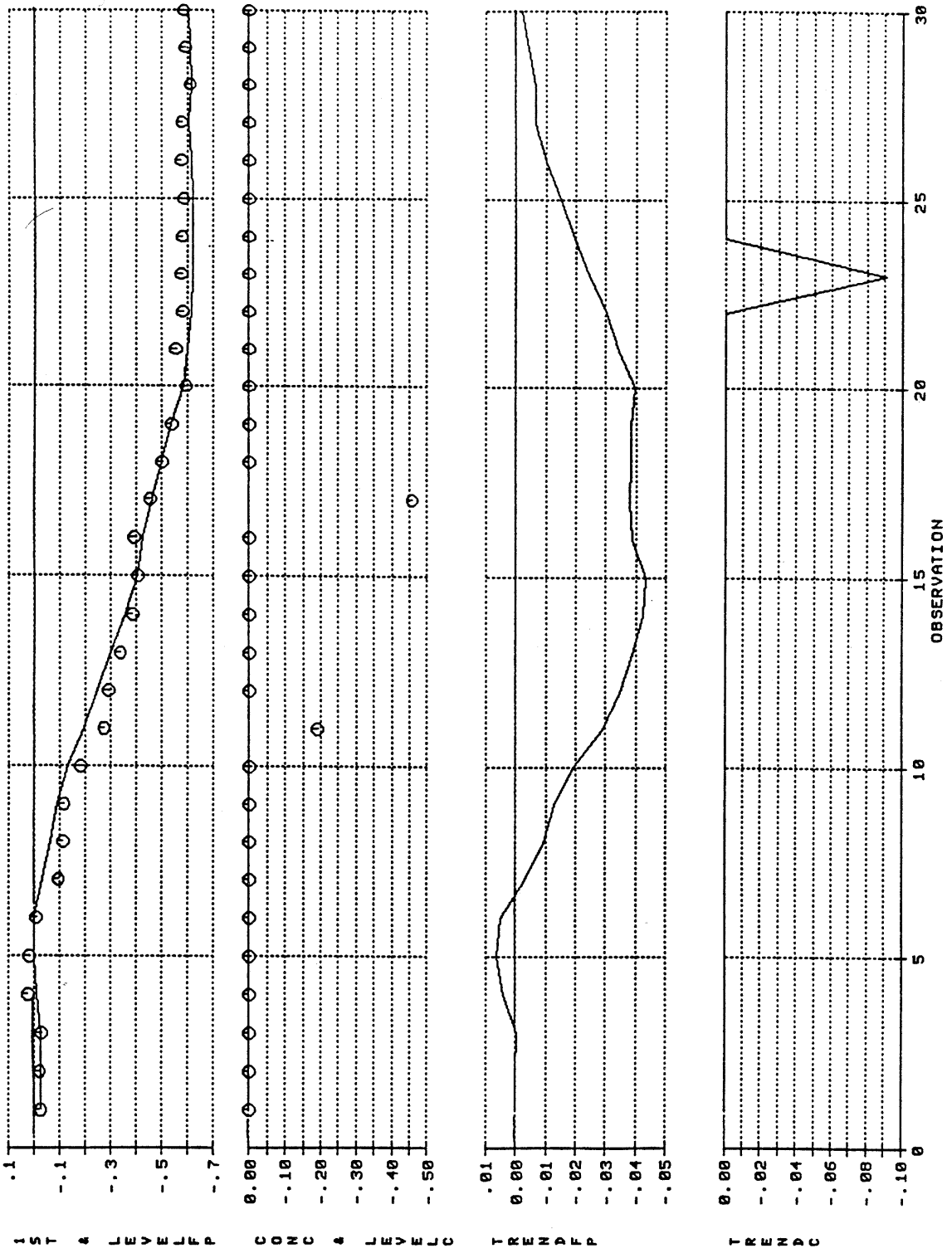

Figure 83: HP Turbine Efficiency Analyses

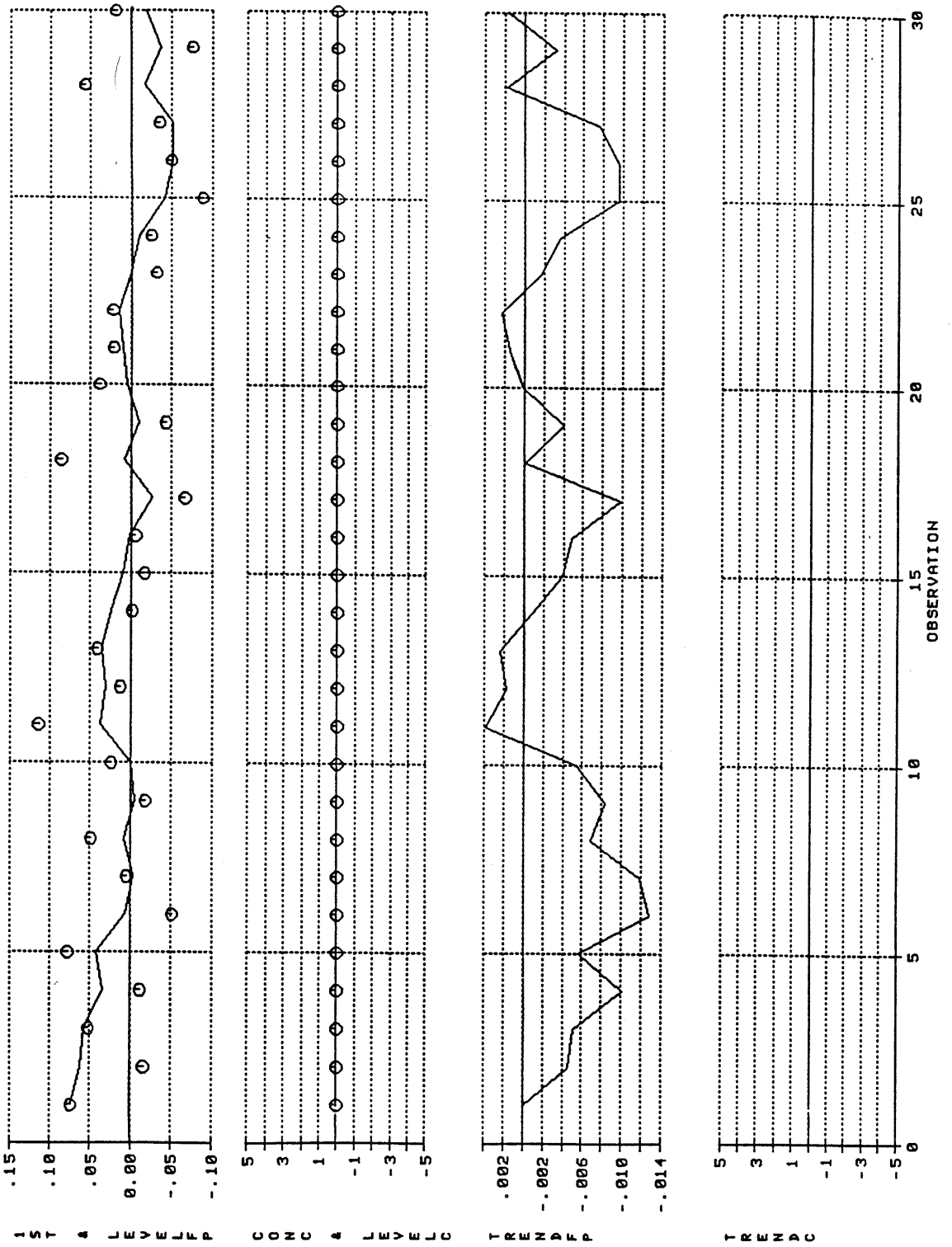

Figure 84: HP Turbine Capacity Analyses

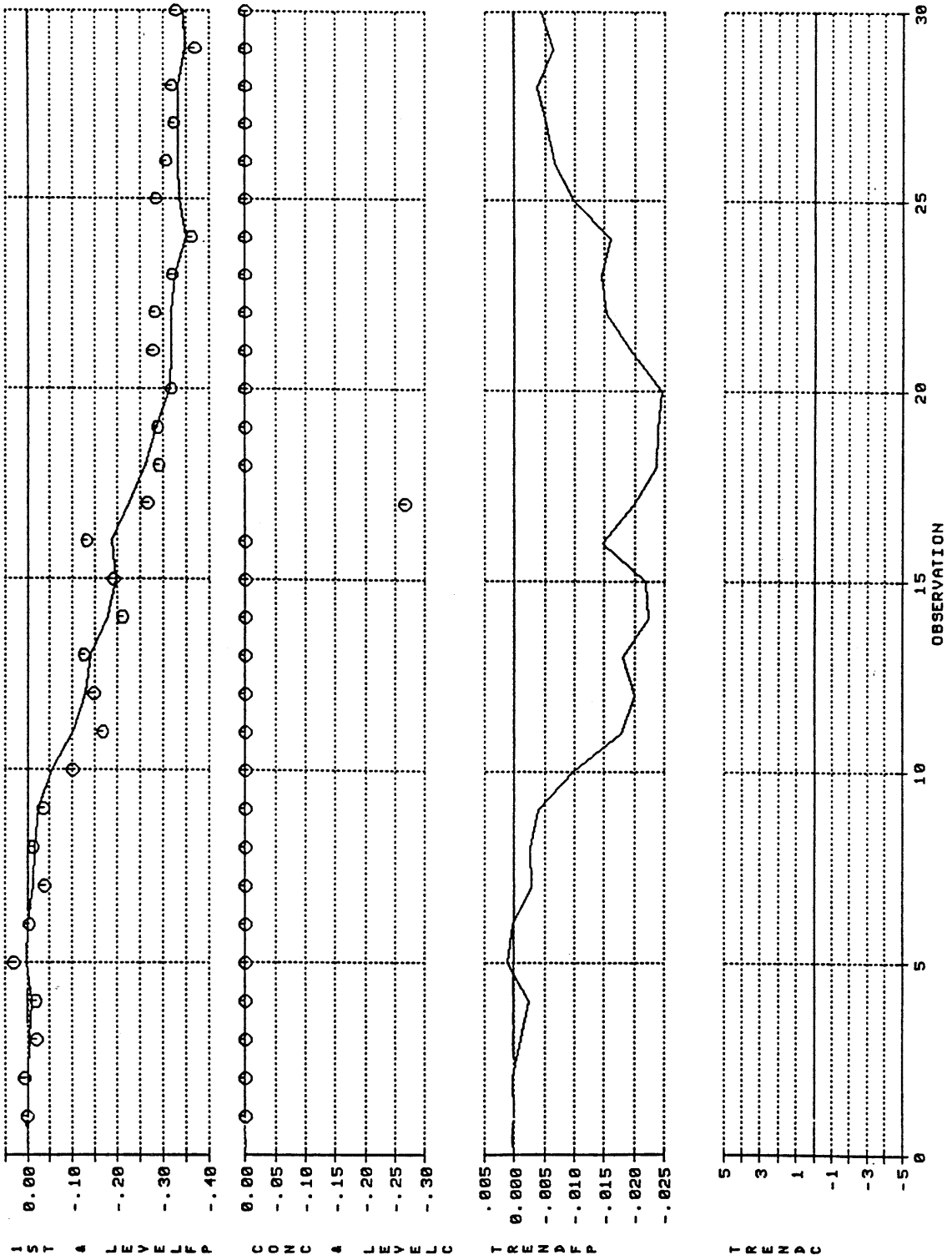

Figure 85: LP Turbine Efficiency Analyses

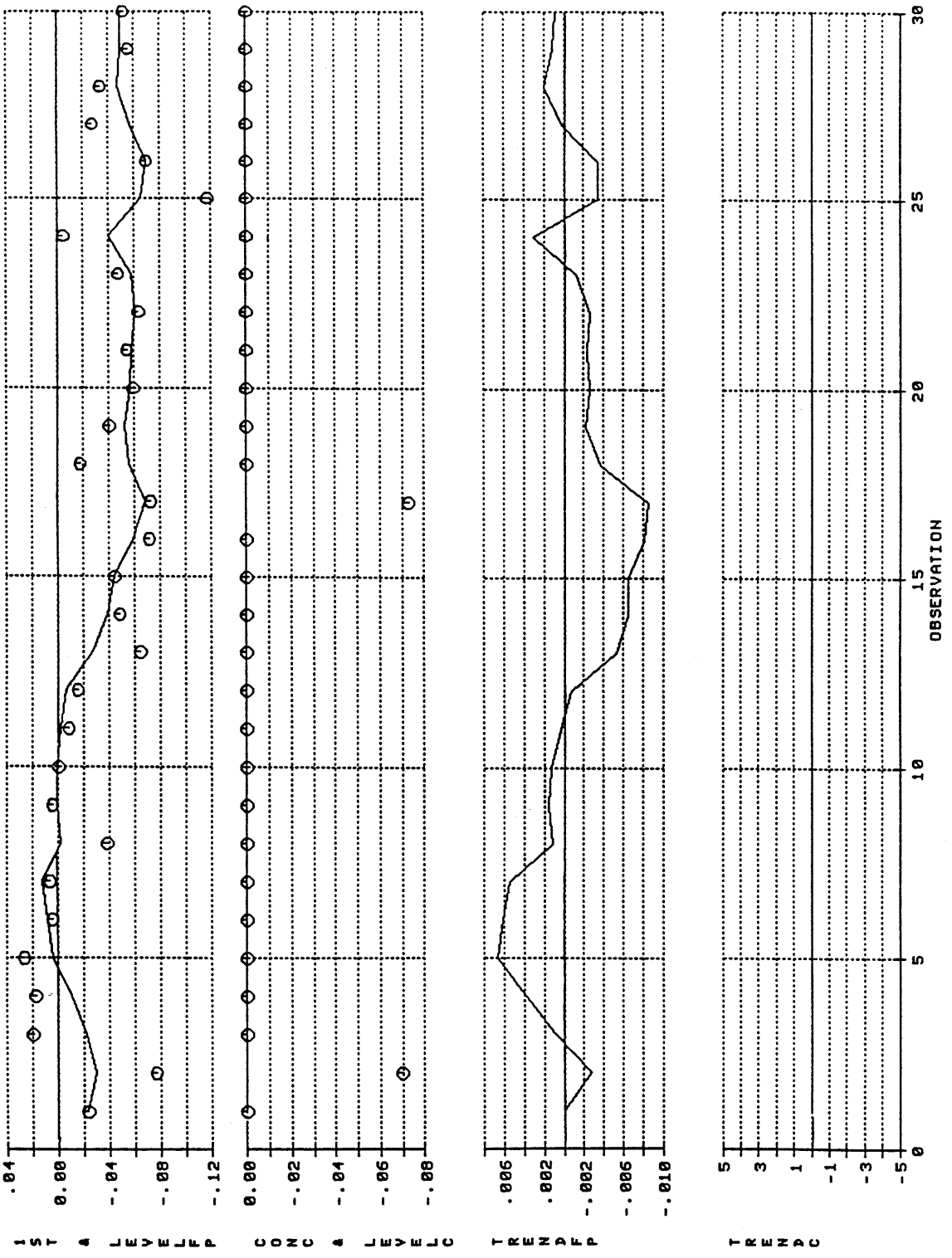

Figure 86: EPR Sensor Bias Analyses

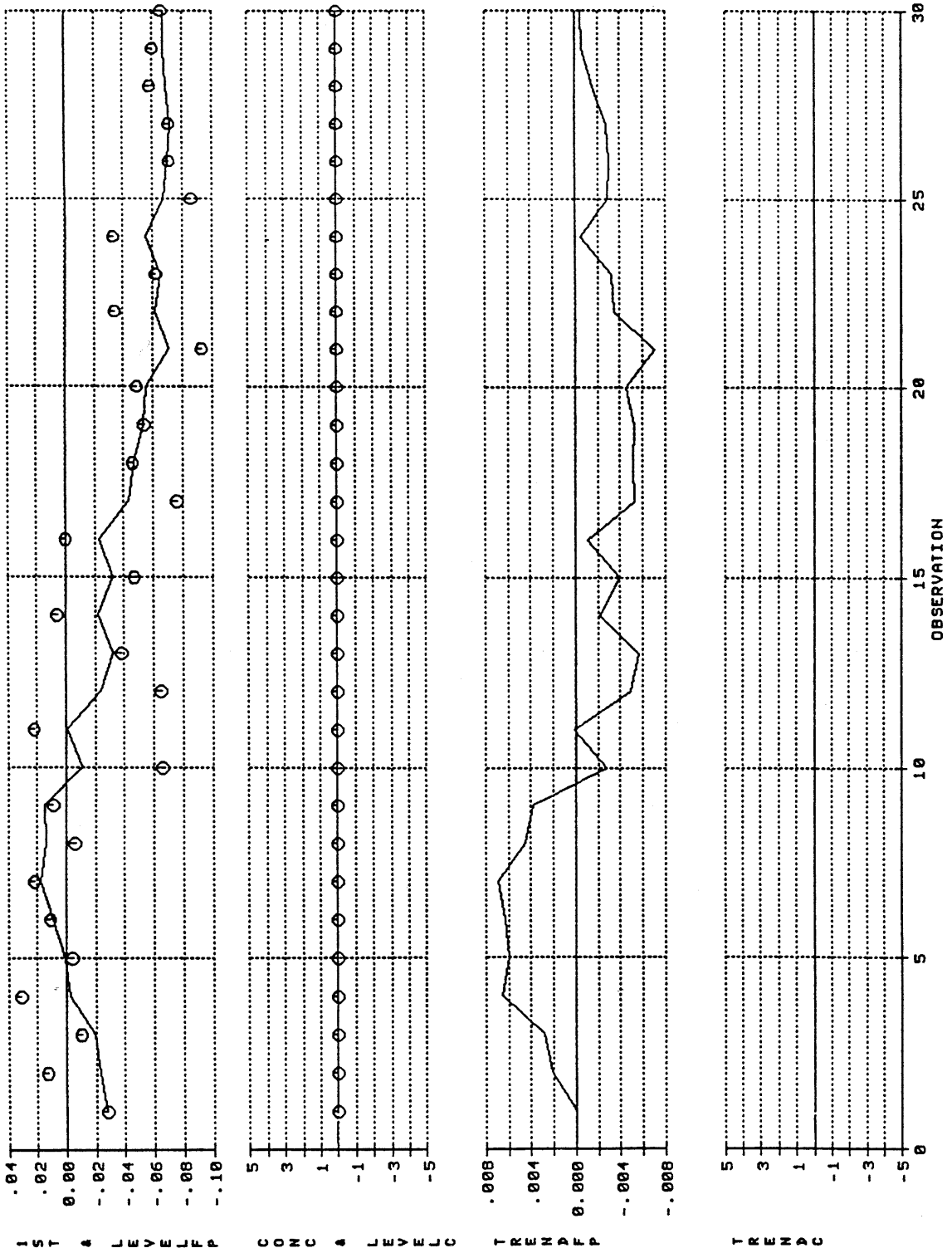

Figure 87: Inlet Total Pressure Sensor Bias Analyses

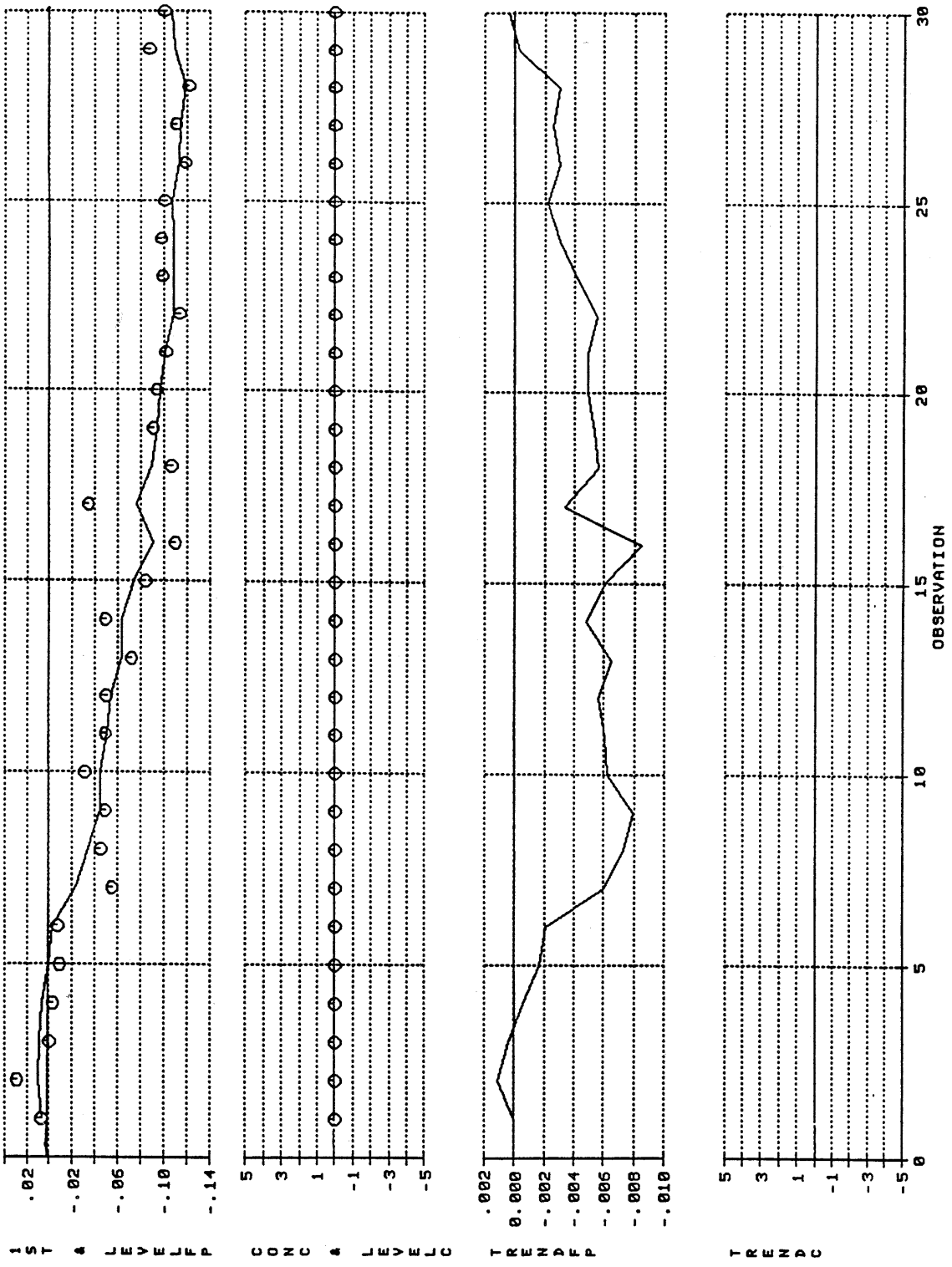

Figure 88: Inlet Total Temperature Sensor Bias Analyses

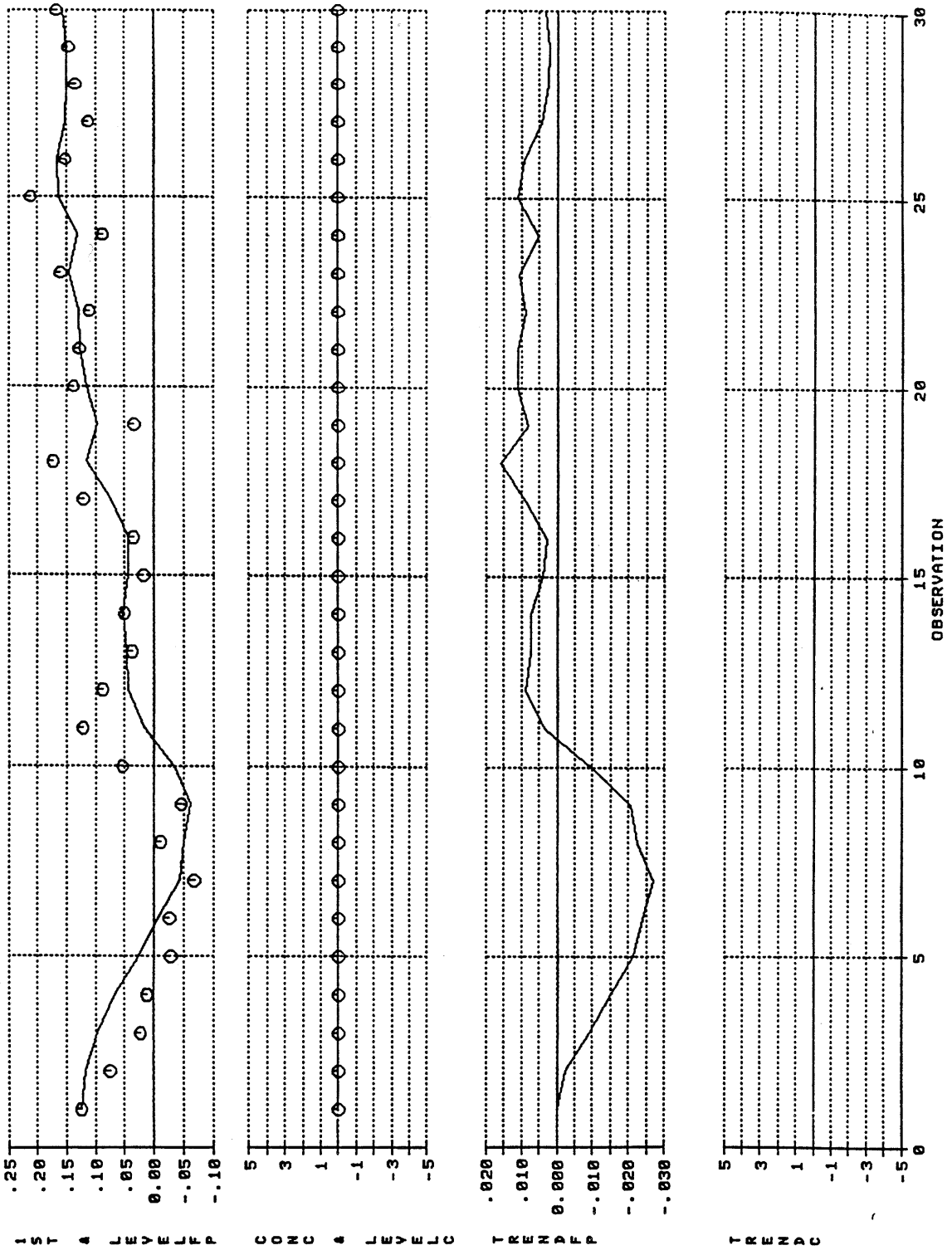

Figure 89: Fuel Flow Sensor Bias Analyses

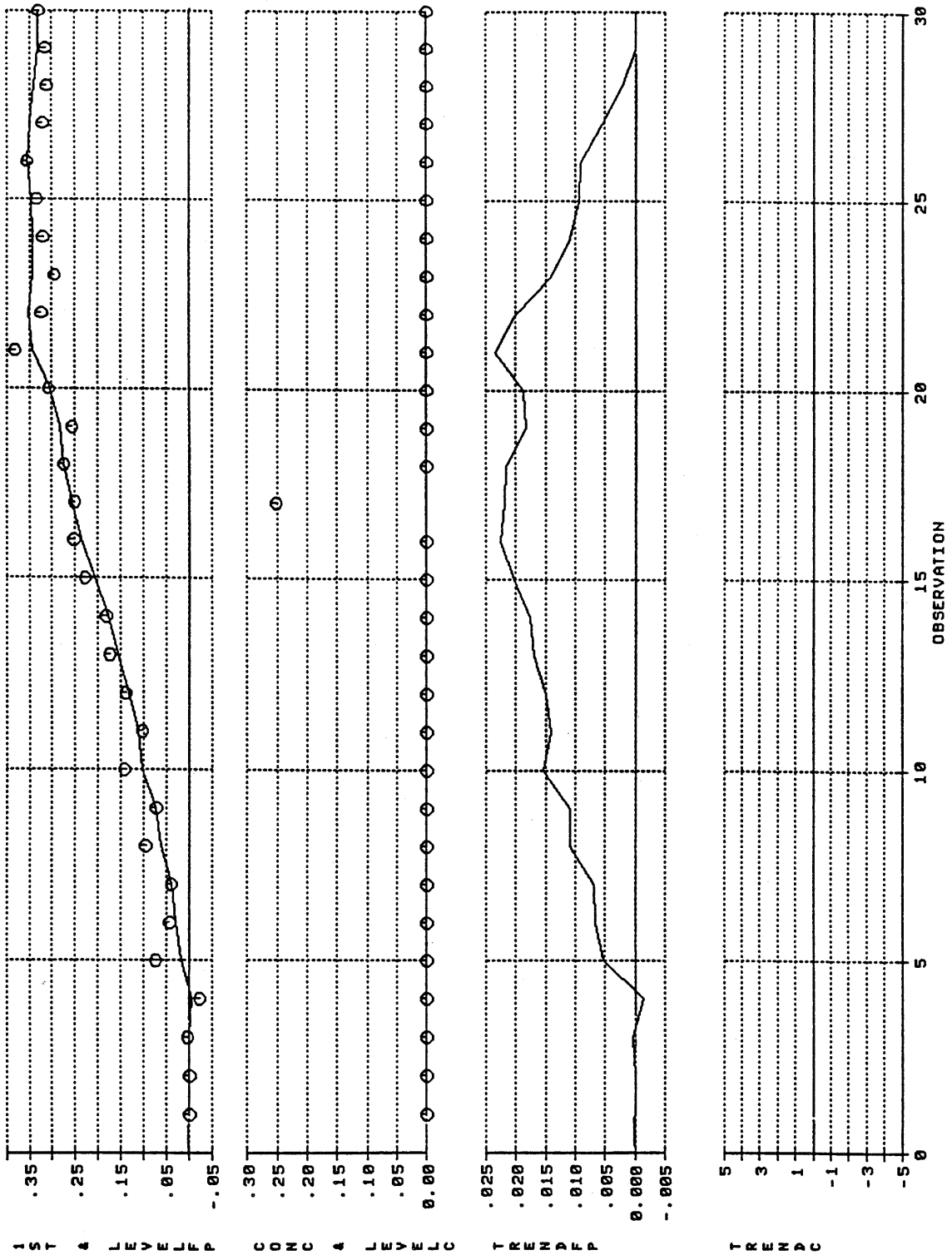

Figure 90: HPC Entry Total Pressure Sensor Bias Analyses

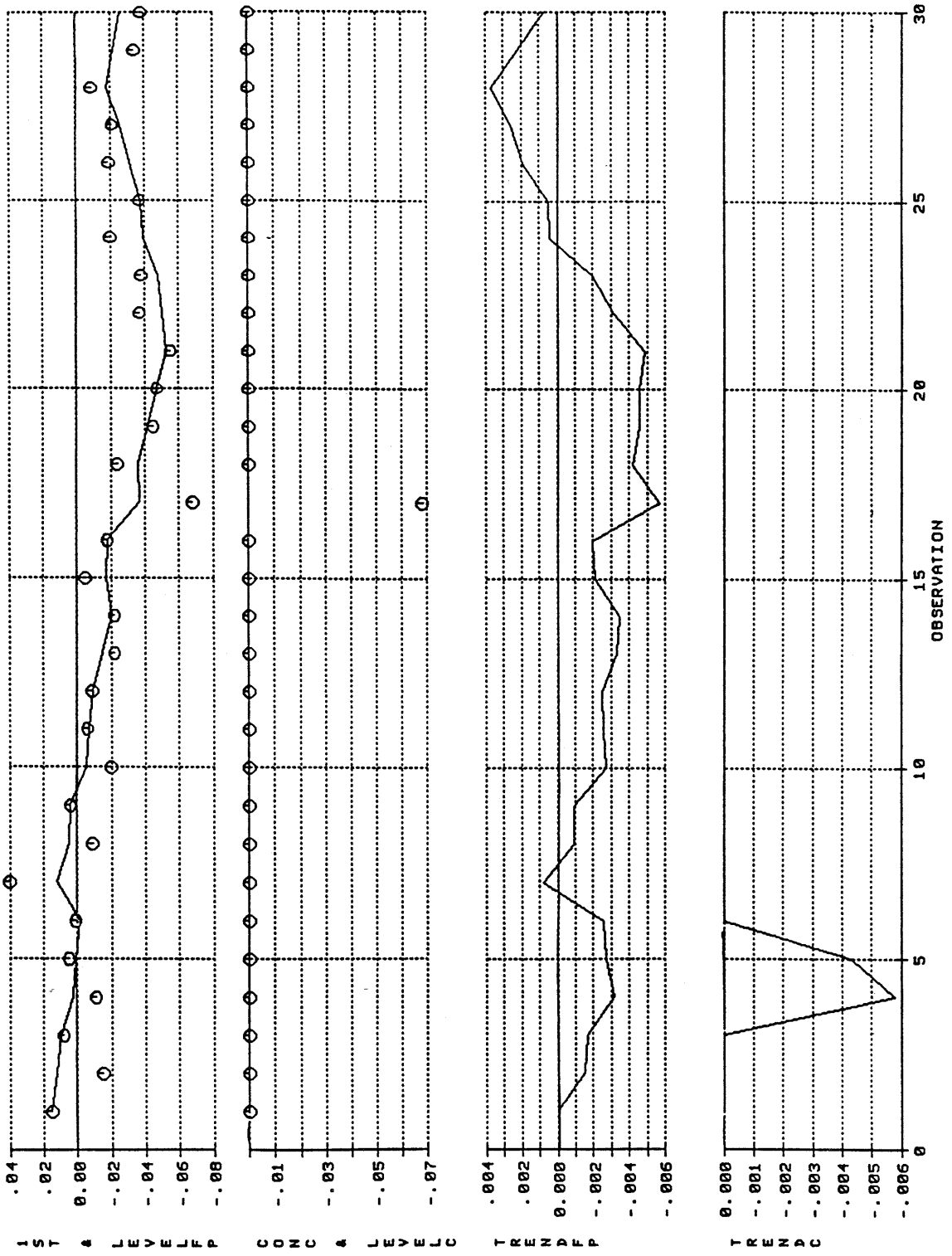

Figure 91: HPC Entry Total Temperature Sensor Bias Analyses

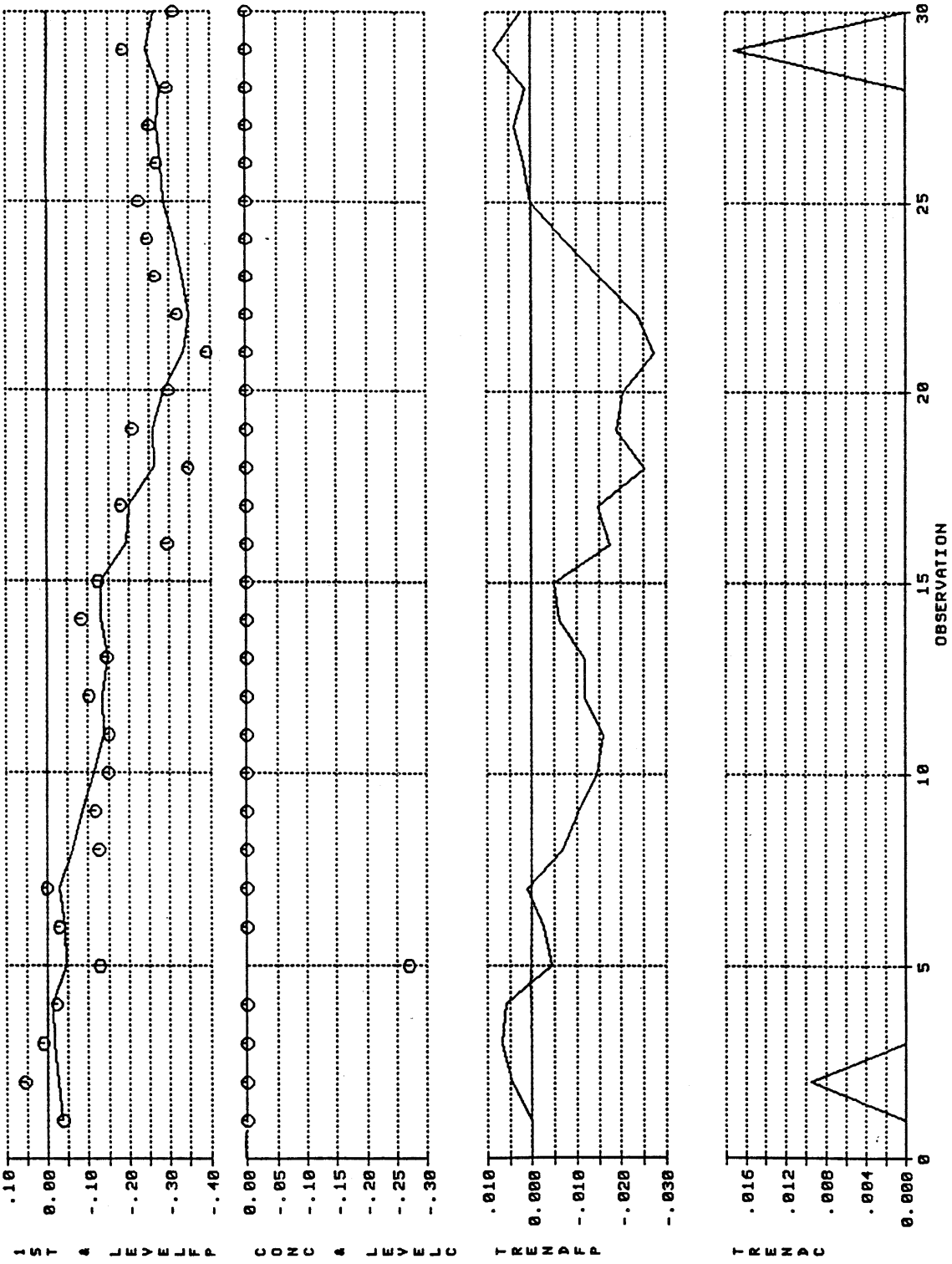

Figure 92: HPC Exit Total Pressure Sensor Bias Analyses

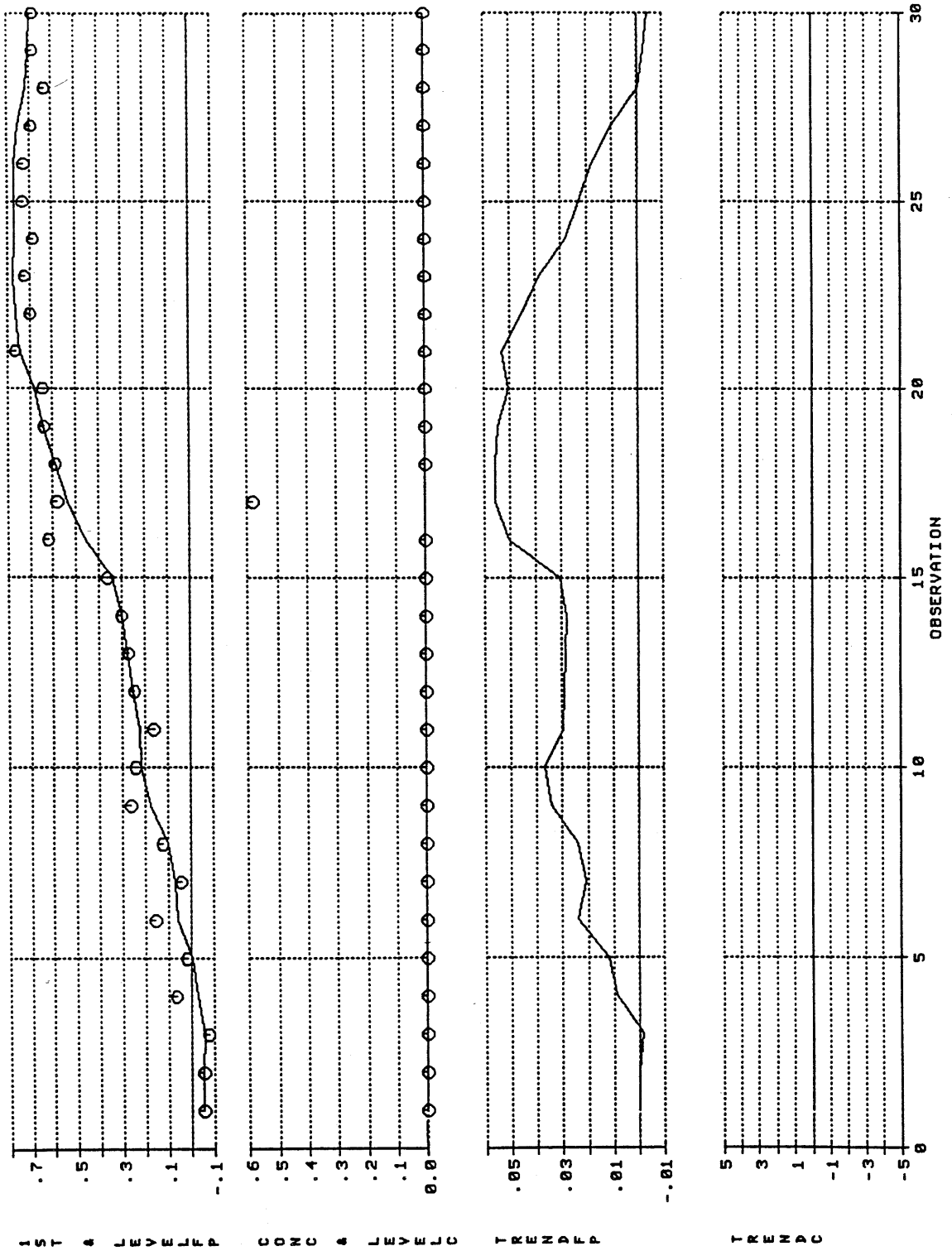

Figure 93: HPC Exit Total Temperature Sensor Bias Analyses

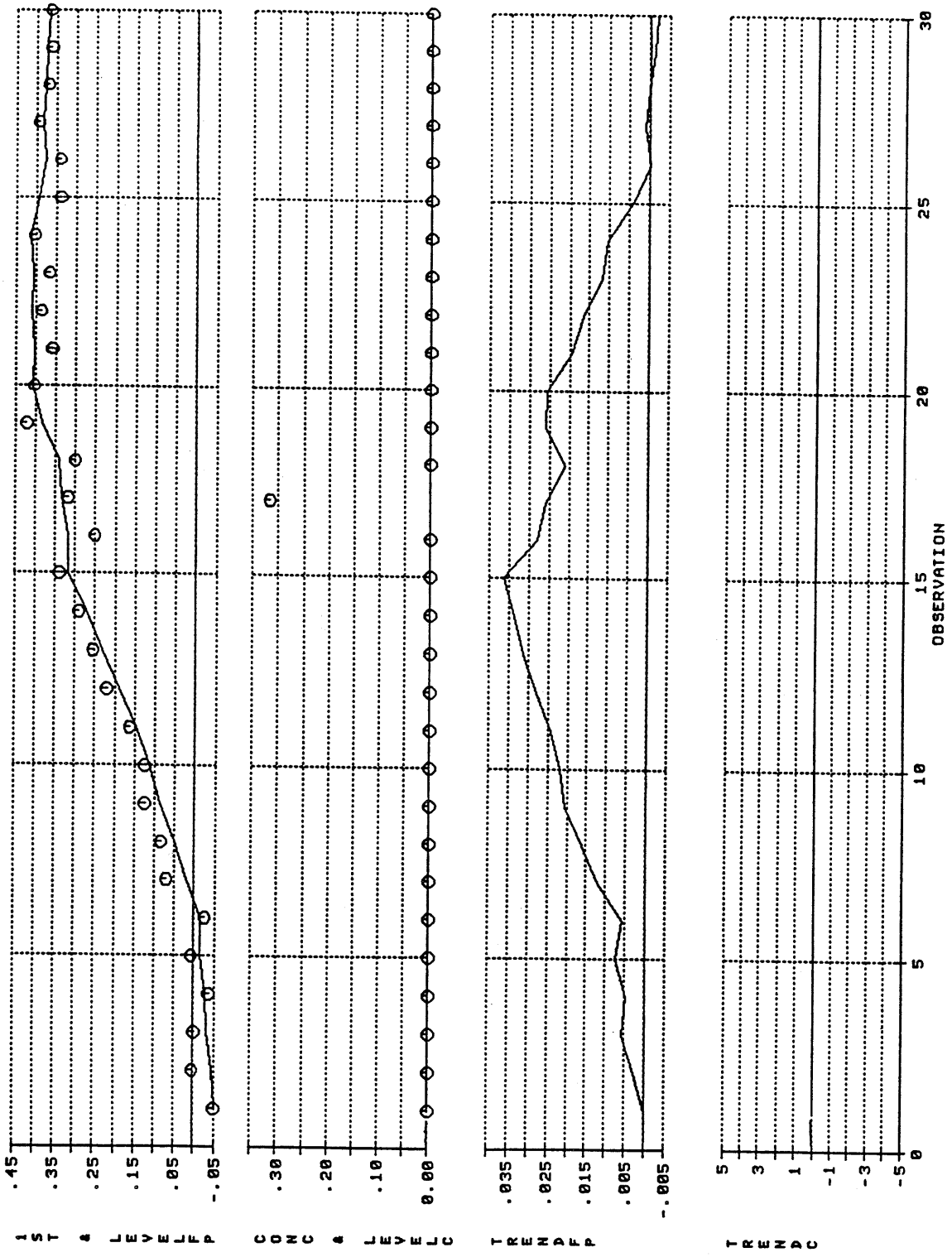

Figure 94: LPT Exit Total Temperature Sensor Bias Analyses

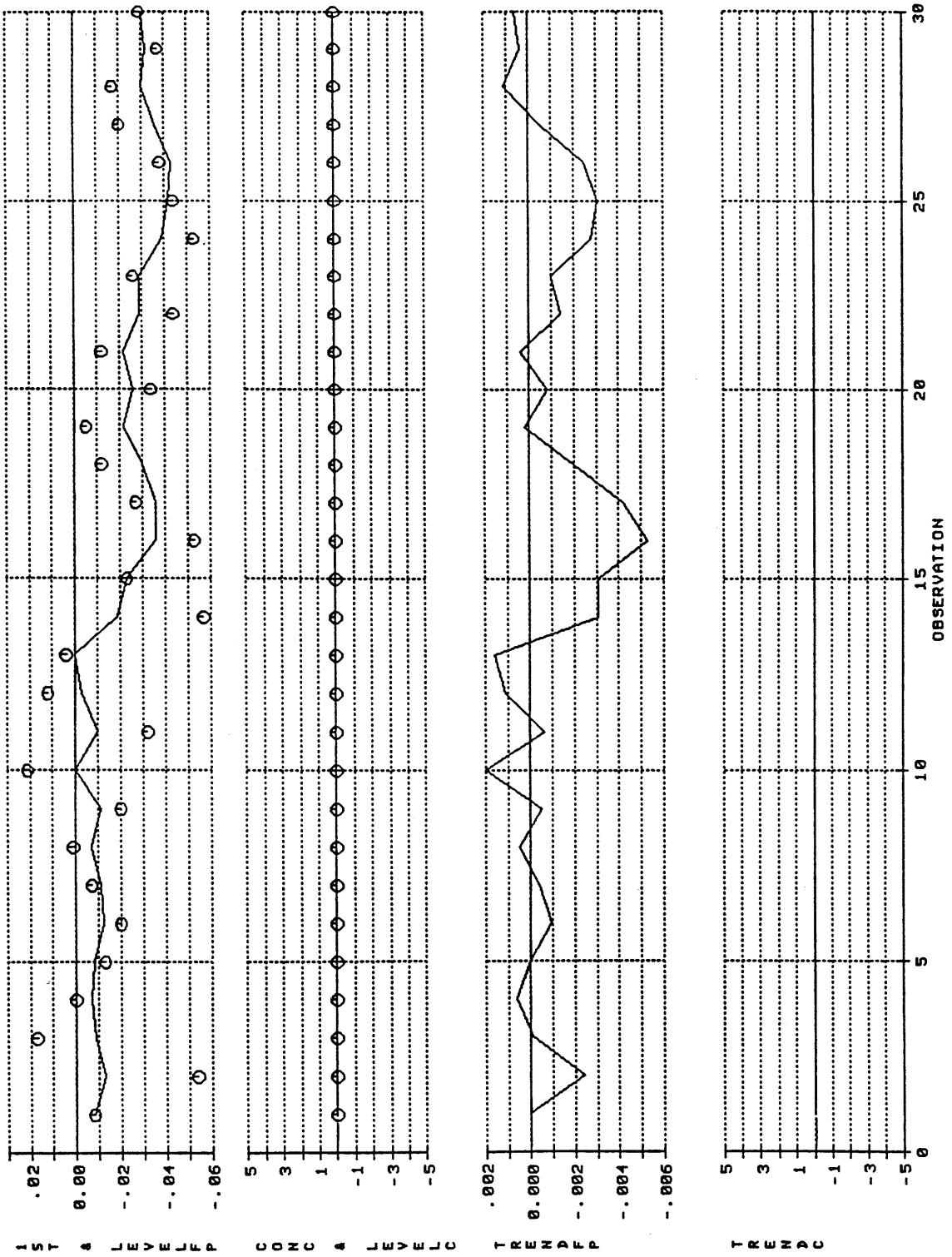

Figure 95: Fan Tip Exit Total Pressure Sensor Bias Analyses

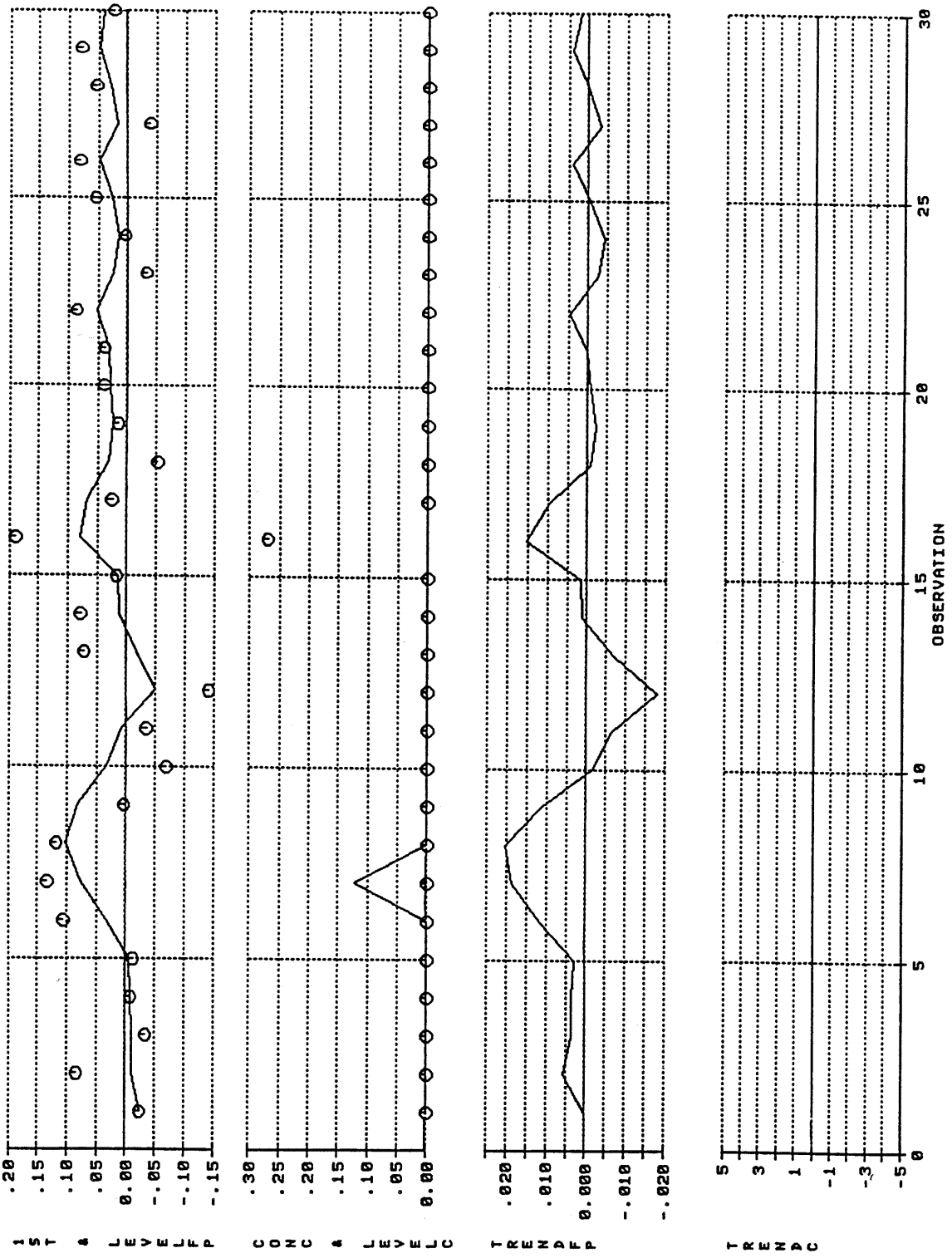

Figure 96: Net Thrust Sensor Bias Analyses

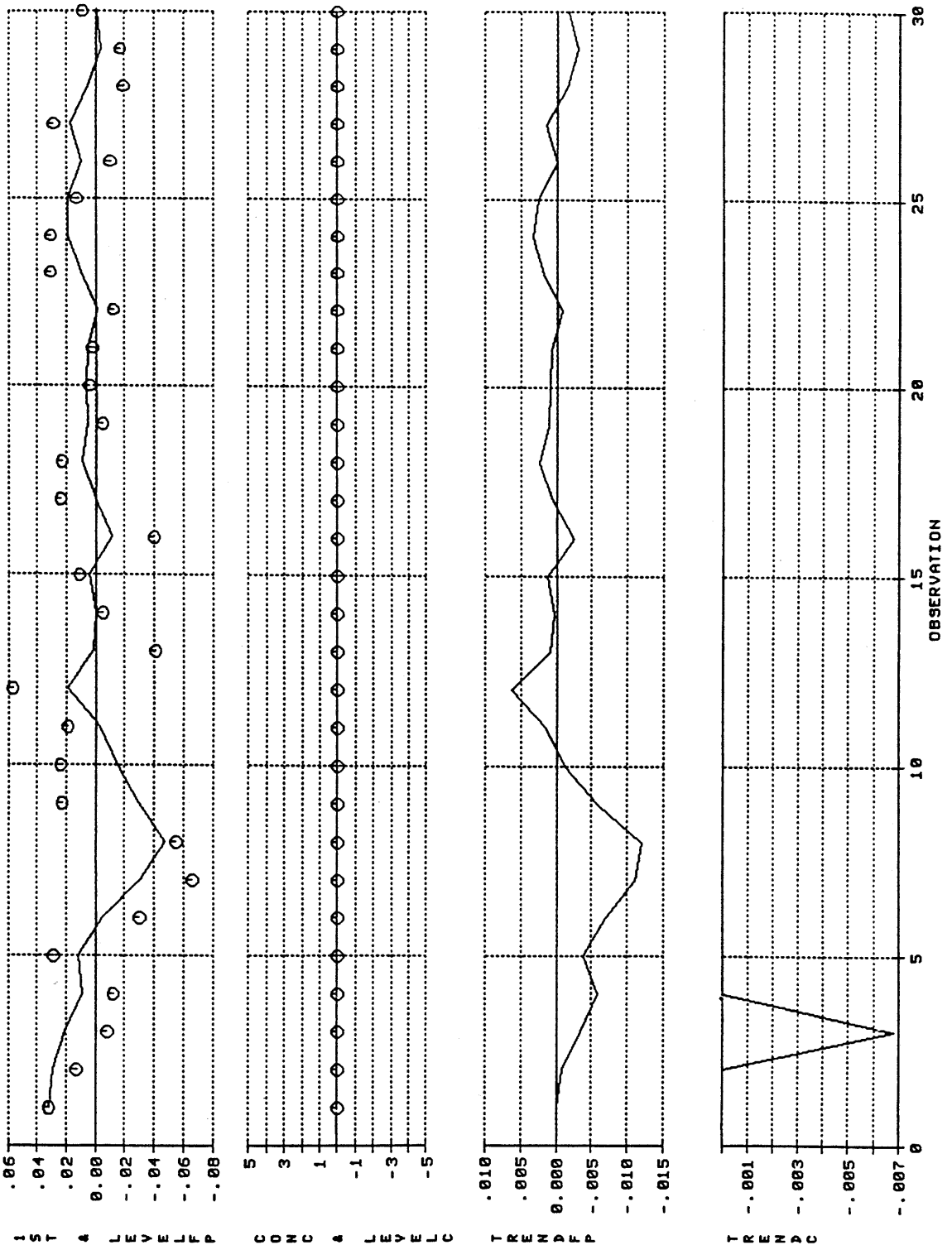

Figure 97: Total Inlet Airflow Sensor Bias Analyses

1) all four graphs in each Figure use a common x scale, labelled OBSERVATION on the bottom graph, as the time axis;

2) the top graph in each Figure, with a y scale labelled 1ST & LEVELFP, shows:

   - the basic Kalman Filter analyses of the component change or sensor bias as circles;

   - the level estimates of the basic Kalman Filter analyses of the component change or sensor bias output from the Smoothing/Trending Algorithm, as a line without symbols;

3) the second graph in each Figure, with a y scale labelled CONC & LEVELC, shows:

   - the 'Concentrator' analyses of the component change or sensor bias as circles;

   - the level estimates of the component change or sensor bias output from the Trend 'Concentration' logic, as a line without symbols;

4) the third graph in each Figure, with a y scale labelled TRENDFP, shows the trend estimates of the basic Kalman Filter analyses of the component change or sensor bias output from the Smoothing/Trending Algorithm;

5) the fourth graph in each Figure, with a y scale labelled TRENDC, shows the trend estimates of the component change or sensor bias output from the Trend 'Concentration' logic.

For space reasons, the (observed-predicted) outputs from both the Smoothing/Trending Algorithm and the Trend 'Concentration' logic (equivalent to the middle graphs in Figures 67 to 77) have been omitted from Figures 68 to 97: because there were no sudden changes in any of the time series, these values were either small or, in the case of the Trend 'Concentration' logic, almost all zero.

Note that the software used to plot Figures 67 to 97 has chosen different y scales for each graph, depending on the values being plotted: this should be borne in mind when interpreting the results.

The following comments on these results can be made:

1) the level estimates for the gas-path measurement differences in Figures 67 to 77 follow the noisy simulated gas-path measurement differences reasonably closely, 'smoothing' out the noise in the process. Because of the 'sluggish' tuning, however, the level

estimates lag the simulated values at the beginning of the ramp (after observation 5) and at the beginning of the plateau (after observation 20) for some of the gas-path measurement differences: this effect is less obvious for others because of the effects of the sensor non-repeatability;

2) the trend estimates for the gas-path measurement differences in Figures 67 to 77 reach values close to those calculated in the 'no-noise' demonstration within 7 to 10 observations of the start of the ramp, and return to values near zero within 7 to 10 observations of the start of the plateau;

3) the differences between the simulated gas-path measurement differences and the gas-path measurement differences predicted from the level and trend estimates for the immediately previous points (the middle graphs in Figures 67 to 77) fluctuate because of noise in the sensor readings; however, they are consistently high or low when lags develop between the level estimates and the simulated values;

4) the basic Kalman Filter analyses of the component changes and sensor biasses in Figures 78 to 97 are not only very sensitive to sensor non-repeatability (the level estimates produced by the Smoothing/Trending Algorithm 'smoothing' out the noise to some extent), but are also 'smeared' across all the possible component changes and sensor biasses;

5) the 'Concentrator' analyses of the component changes and sensor biasses are also affected by the sensor non-repeatability to some extent, with incorrect diagnoses (according to the criteria laid down in the discussion of the analyses of single component changes and sensor biasses given above) for five of the 30 sets of simulated gas-path measurement differences;

6) the level estimates of the component changes and sensor biasses from the Trend 'Concentration' logic are hardly affected by sensor non-repeatability: this is to be expected, since the inputs to this process are the level estimates of the gas-path measurement differences (Figures 67 to 77), which have 'smoothed' out the sensor noise;

7) the combination of sensor non-repeatability and the 'smearing' effect of the basic Kalman Filter renders the trend estimates of the component changes and sensor biasses produced by the Smoothing/Trending Algorithm from the results of the basic Kalman Filter analyses virtually meaningless;

8) the trend estimates of the component changes and sensor biasses from the Trend 'Concentration' logic are also

hardly affected by sensor non-repeatability: again, this is to be expected, since the inputs to this process are the trend estimates of the gas-path measurement differences (Figures 67 to 77);

9) Figure 81 shows that the Trend 'Concentration' logic has correctly diagnosed both the level of HP Compressor efficiency given in the schedule in Table 6 (with some lags at the beginnings of the ramp and the plateau, highlighted in the Figures by the presence of the 'Concentrator' output) and the trend of HP Compressor efficiency given in Table 6 within 10 observations.

The exercises described in this chapter are considered to have successfully demonstrated all the Kalman Filter based analysis techniques discussed in this thesis.

CHAPTER 7: DISCUSSION

As stated in the Introduction, gas turbine analysis is inherently more difficult than gas turbine modelling (also known as synthesis) because of the presence of measurement error. 'Traditional' analysis techniques, as outlined in Appendix A, do not recognise the possibility of measurement error explicitly: this makes the output from such techniques potentially misleading, since incorrect component performance parameter calculations caused by measurement errors will lead to fruitless searching for non-existent implied hardware faults in some parts of the gas turbine being analysed, leaving other genuine faults undetected. Even the most experienced performance analysts find situations with more than one measurement error present difficult to resolve satisfactorily, particularly when the measurements are being influenced by genuine component changes as well. The work described in this thesis was motivated by the need to speed up an inefficient, time-consuming and demoralising process, carried out because of its great importance to the understanding of the behaviour of gas turbines. Such understanding is vital both when developing gas turbines, because of its importance in guiding the process of redesigning components whose performance is poorer than expected, and also when using them in service, where guidance is needed to pinpoint sub-standard components which require repair or overhaul.

An alternative approach to gas turbine analysis recognises that the differences between observed measurements and measurements expected if the gas turbine was behaving correctly (of more interest than the absolute measurement levels themselves, as explained in the Introduction) can be caused by:

1) genuine component performance changes;

2) biasses (shifts of calibration) in the measurements used to define the expected performance of the gas turbine (flight condition and power-setting measurements);

3) biasses (shifts of calibration) in the gas-path measurements added to the gas turbine for diagnostic purposes;

4) random scatter in all of the measurements.

The effects of component changes and sensor biasses on the observed measurement differences can be expressed in a matrix (conventionally called the System Matrix), with each column giving the effects of unit change in each of the component changes and sensor biasses being sought on each of the gas-path measurement differences. The System Matrix is generally built up from three sub-matrices:

1) a Component Exchange Rate Table (also called a Synthesis Exchange Rate Table), which shows the effects on the gas-path measurements of unit changes (generally 1%) in each of the component performance parameters (efficiency, flow capacity, cooling bleed, etc) in turn;

2) an Environmental Exchange Rate Table (also called a Slope Table), which shows the effects on the gas-path measurements of sensor biasses in each of the flight condition and power-setting measurements in turn;

3) a unit matrix, showing the effects of sensor biasses on each of the gas-path measurements in turn.

It is important to separate out the measurement bias errors from those due to random scatter, because bias errors can be corrected by repair and/or recalibration of the affected sensors, whereas errors due to random effects cannot be 'repaired': they are part of the imperfect world we live in, and cannot be eliminated completely.

Because the number of unknown component changes and sensor biasses is generally much greater than the number of known measurement differences from expectation, optimal estimation techniques (which are able to proceed in situations where the number of unknowns in a problem is not always equal to the number of knowns) have to be used. The most famous of such techniques is known as the Kalman Filter, after the man who, in the 1960's, first formulated a set of optimal estimation equations that were both easy to understand (in comparison to previous work) and ideally suited to computer implementation. Indeed, Kalman Filters have been used to analyse measurements taken from gas turbines since the mid-1970's: however, the problem of the Kalman Filter calculating shifts in all the component changes and sensor biasses being considered in an analysis, even when it is known that the gas-path measurement differences are due to a small subset of component changes and/or sensor biasses, has not been addressed, except by very crude means such as choosing the largest component change or sensor bias as being the only fault worth investigating.

This deficiency has been addressed by an enhancement to the basic Kalman Filter, called the 'Concentrator', which selectively removes component changes and/or sensor biasses from the analysis until a small subset of possible component changes and/or sensor biasses is left which successfully accounts for the observed measurement differences. The 'Concentrator' works without introducing assumptions about either the number or magnitude of any significant component changes and/or sensor biasses, thus making it capable of detecting multiple component and/or sensor faults.

The Kalman Filter requires the following prior knowledge about the gas turbine being analysed and its gas-path measurement set:

1) the System Matrix, which expresses the basic relationships between component changes, sensor biasses and gas-path measurement differences;

2) statistical knowledge about the sensor non-repeatabilities, expressed as standard deviations;

3) statistical knowledge about the relative probabilities of occurrence (expressed as standard deviations) of component changes and sensor biasses.

These latter probabilities are very difficult to obtain from gas turbine data, since the long production runs of identical gas turbines necessary to build up a complete picture of the way component changes and sensor biasses are distributed are rarely achieved because of competitive pressures to continuously change and improve the hardware. This thesis describes several methods for obtaining these standard deviations, using the results of analytical techniques devised to determine the sensitivity of the Kalman Filter to its statistical inputs. A minimisation technique is also described which further adjusts the component change and sensor bias standard deviations to optimise the ability of the 'Concentrator' to achieve the required analysis capability.

Before any analysis technique, no matter how sophisticated, can proceed, the performance analyst must be certain that the gas-path measurements added to the gas turbine for diagnostic purposes are capable of providing the information required to detect the component changes and sensor biasses of interest. Ideally, each of the gas-path measurements must react to each of the possible component changes and sensor biasses being considered in a different way, thus giving each component change and sensor bias a unique 'signature' which cannot be confused with other changes or biasses. However, the temptation to over-specify gas-path measurement sets must be avoided, since the provision and maintenance of sensors can be extremely costly. A related question the performance analyst needs to ask is whether there are sets of component changes and/or sensor biasses which would be difficult to detect because their net effects on all of the gas-path measurements add up to zero; even if several important changes have occurred, have their effects 'self-cancelled', making them non-observable?

These questions can be answered by methods described in this thesis for calculating the cosines of the angles between all the possible pairs of rows or columns of the System Matrix (or one of its sub-matrices), the values of which give an indication of whether these pairs of rows or

columns are nearly parallel or nearly perpendicular to one another. Developments in Observability Theory are also presented, which can be used to show which sets of component changes and/or sensor biasses are not observable with a given gas-path measurement set. The thesis also presents a very simple method of calculating and expressing the invertibility or otherwise of the System Matrix (or one of its sub-matrices), which is another test of the 'distinguishability' of each of its rows and columns. All of these methods are extremely powerful tools for justifying the addition of diagnostic gas-path measurements to a gas turbine, understanding the levels of information they provide and appreciating their limitations. This is an aspect of gas turbine analysis which has received very little attention in the literature, but is nevertheless vital to the success of both 'Traditional' and Kalman-Filter based analysis techniques.

Analysis of time series data taken from gas turbines either during endurance testing undertaken as part of a development programme or during in-service operation is an important aspect of gas turbine analysis. The performance analyst requires a tool that, with the minimum amount of historical data and computational effort, gives:

1) a best estimate of the level of the underlying process generating the observations, recognising that the observations may have been corrupted by random noise;

2) a best estimate of the trend (rate of change) of the underlying process generating the observations, again recognising that the observations may have been corrupted by random noise.

Ideally, these estimates should be in a form that can be compared with appropriate limits by a computer program, enabling warnings to be given when the level and/or trend of the parameter(s) being monitored exceed(s) desirable values. By focusing the analyst's attention on significant events, many parameters can be effectively monitored without the necessity of continuous visual checking of each time series.

These thesis presents a Kalman Filter based algorithm, called the Smoothing/Trending Algorithm, which meets the above requirements in a recursive and computationally-efficient fashion. An additional output from the algorithm is the difference between the observed value of a parameter and the value predicted from the level and trend estimates produced from the previous point; this value is an ideal indicator of the presence of sudden changes in the character of the time series. This method represents a clear advance over more traditional techniques, such as Moving Average or Exponential Smoothing, which do not give a direct indication of trend and whose outputs tend to lag

the observations when a ramp is present in the time series.

A final technique presented in this thesis combines the Smoothing/Trending Algorithm and the 'Concentrator' to reduce the effects of sensor non-repeatability on the analysis of component changes and sensor biasses from time series data of gas-path measurement differences. This logic, called Trend 'Concentration', uses the outputs from the Smoothing/Trending Algorithm (operating on all the gas-path measurement time series as a set) as inputs to the 'Concentrator', to convert level estimates, trend estimates and (observed - predicted) differences of gas-path measurement differences into level estimates, trend estimates and (observed - predicted) differences of component changes and sensor biasses. This technique is also more computationally efficient than using the Smoothing/Trending Algorithm on analysed component changes and/or sensor biasses, since less data needs to be carried forward from point to point.

All of the methods described in this thesis appear to offer significant advances in the 'state of the art' of gas turbine performance analysis, by addressing the fundamental requirements of:

1) analysing component changes in the presence of both sensor bias and sensor non-repeatability;

2) determining the information content of the gas-path measurements;

3) analysing time series in a way that produces information that the analyst can use directly.

CHAPTER 8: CONCLUSIONS

The work described in this thesis has achieved the following objectives:

1) Methods have been developed for determining the gas-path measurements in a gas turbine that are needed to enable the required analysis of gas turbine component changes and sensor biasses to be performed, including:

   - determination of possible gas-path measurement redundancy;

   - determination of the ability of any analysis technique to successfully distinguish between all the component changes and sensor biasses being sought, for a given set of gas-path measurements;

   - determination of the combinations of component changes and/or sensor biasses that are not observable with a given set of gas-path measurements;

2) An enhancement to the Kalman Filter (called the 'Concentrator') has been developed which overcomes the tendency of the basic Kalman Filter to 'smear' the effects of changes in a small number of component changes and/or sensor biasses over the whole set of possible component changes and sensor biasses. Unlike some techniques developed to address this problem, the 'Concentrator' does not assume either numbers or magnitudes of component changes and/or sensor biasses when determining the significant component changes and/or sensor biasses that have occurred;

3) Analytical methods have been developed for determining the sensitivity of the Kalman Filter to its various statistical inputs;

4) Methods have been developed to optimise some of the statistical inputs to the Kalman Filter to improve the ability of the 'Concentrator' enhancement to carry out the required analysis;

5) Kalman Filter theory has been used to develop a recursive algorithm for the analysis of time series data (called the Smoothing/Trending Algorithm), which produces the following information each time an observation is gathered:

   - a best estimate of the level of the underlying process generating the observations, recognising that the observations may have been corrupted by random noise;

   - a best estimate of the trend (rate of change) of

the underlying process generating the observation, again recognising that the observations may be corrupted by random noise;

- a difference between the actual and predicted observation, which may be used as an indicator of sudden changes in the character of the time series;

6) A method of combining the Smoothing/Trending Algorithm and the 'Concentrator' (called Trend 'Concentration') has been developed to:

   - reduce the effects of sensor non-repeatability on the analysis of component changes and/or sensor biasses from time series data of gas-path measurement differences;

   - increase the computational efficiency of this analysis process;

7) The methods described above have been successfully demonstrated on simulated gas turbine gas-path measurement data and, for the Smoothing/Trending Algorithm in isolation, fuel consumption data from the author's car.

The methods described in this thesis have applications beyond the field of gas turbine analysis: they can be used in any situation where a matrix can be derived that relates the response of a set of measurements to changes in a set of variables that cannot be observed directly, particularly where measurement non-repeatability is a serious concern and the possibility of sensor bias corrupting the measurements needs to be considered. Many types of prime movers and process plant could be effectively analysed using the techniques described in this thesis. The Smoothing/Trending Algorithm can be used to analyse any time series, both within and outside engineering.

CHAPTER 9: RECOMMENDATIONS FOR FURTHER WORK

1) The large tables of observability Eigenvalues and Eigenvectors produced by the observability analysis (an example of such a table is given in Figure 20) could be further processed to make the non-observable combinations of component changes and/or sensor biasses more easily identifiable. This would involve devising methods of adding together combinations of multiples of the various non-observable Eigenvectors to isolate small sets of component changes and/or sensor biasses that cannot be observed with the gas-path measurement set used.

2) Careful correlation of the analysed component changes and sensor biasses produced by the Kalman Filter and 'Concentrator' with the state of gas turbine hardware determined during maintenance, followed by adjustments to the inputs to the Kalman Filter, is needed to ensure that future analyses are meaningful. This exercise may also provide information to calculate some or all of the elements of the System Matrix, thus reducing reliance on gas turbine modelling. This work should be done when a large database of experience in using the techniques described in this thesis has been established.

3) Throughout this thesis, it has been assumed that the effects of component changes and sensor biasses on the gas-path measurement differences from expectation (expressed in the System Matrix) are linear. This assumption is reasonable for small changes, but becomes progressively less satisfactory as the magnitudes of component changes increase and the operating points on the gas turbine components move in response. Some theoretical investigations into non-linear filtering theory may produce methods to better cope with these effects.

4) The software developed to implement the methods described in this thesis is currently mainframe-based: transfer to a personal computer environment, preferably with a Windows-type user interface, would be desirable.

5) Integration of the methods discussed in this thesis with other computer techniques such as neural nets, expert systems, relational databases and hypertext would produce a system combining the best features of all these techniques. A possible system architecture is shown in Figure 98, which shows the outputs from the methods discussed in this thesis being combined with signals from other gas-turbine monitoring techniques (oil analysis, vibration analysis, etc) before being fed into a neural net, trained to detect the presence of faults. Having detected a fault, the neural net would activate an expert system, which would contain

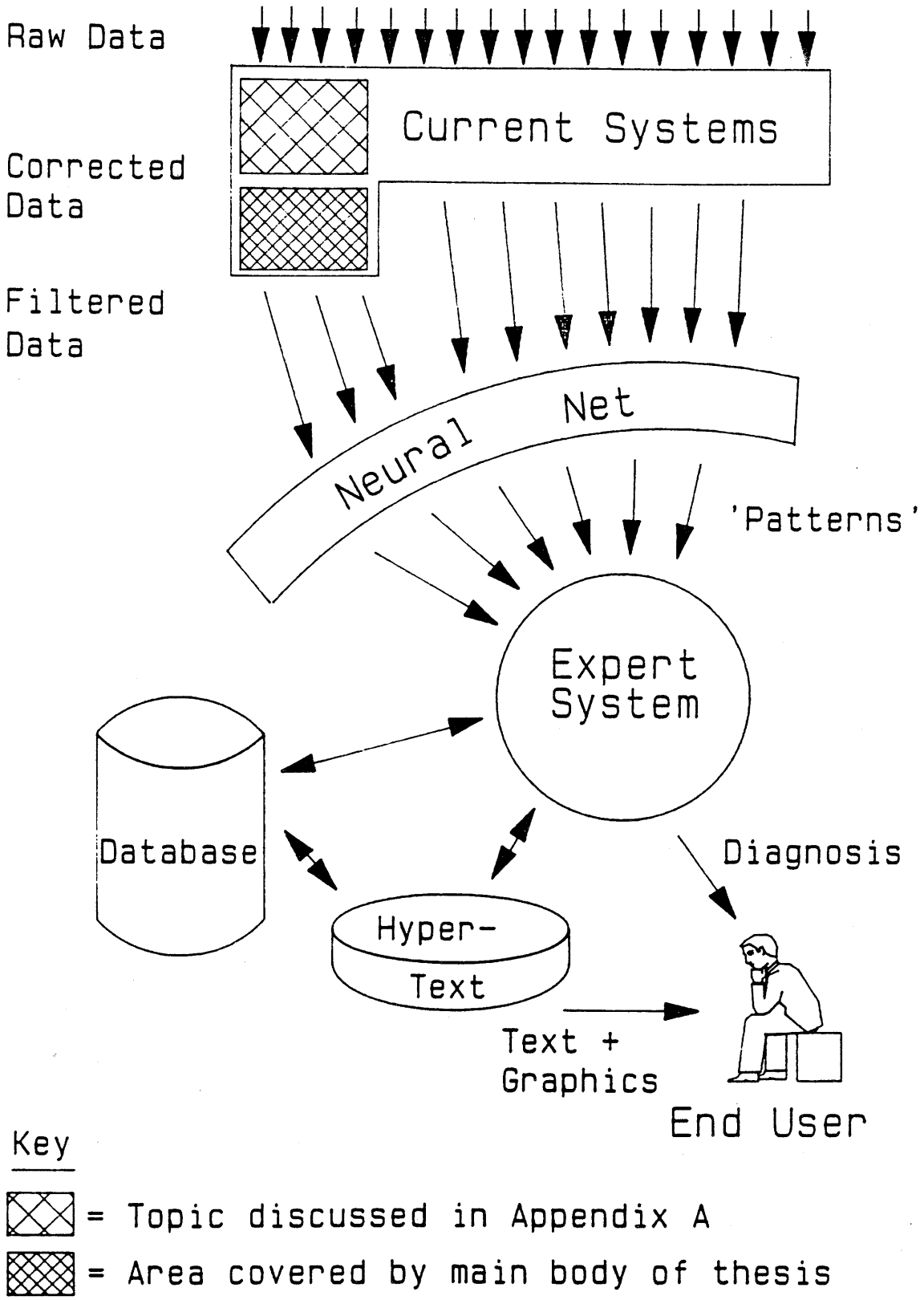

Figure 98: System Architecture for Enhancements to Kalman Filter Based Analysis Methods

rules that:

- presented the user with a detailed diagnosis of the fault;

- interacted with a database of past diagnoses to both add this diagnosis to its knowledge base and make the user aware of any history that may be relevant;

- interacted with a hypertext package to present the user with any textual and graphical data that he needs to fix the fault.

CHAPTER 10: REFERENCES

1) ROLLS-ROYCE PLC — The Jet Engine. 4th Edition, Rolls-Royce plc, 1986.

2) WALTER J BOYNE & DONALD S LOPEZ (Ed) — The Jet Age: Forty Years of Jet Aviation. Smithsonian Institution, 1979.

3) JOHN GOLLEY & Sir FRANK WHITTLE OM KBE CB (Ed BILL GUNSTON) — Whittle: The True Story. Airlife, 1987.

4) Dr ALLAN J VOLPONI — Gas Path Analysis: An Approach to Engine Diagnostics. 35th Symposium, Mechanical Failures Prevention Group, Gaithersburg, Maryland April 20-22 1982.

5) H W SORENSEN — Least-Squares Estimation: from Gauss to Kalman. IEEE Spectrum, July 1970, pp 63-68.

6) R E KALMAN — A New Approach to Linear Filtering and Prediction Problems. ASME Journal of Basic Engineering, March 1960, pp 35-46.

7) LOUIS A URBAN — Gas Path Analysis - A Tool for Engine Condition Monitoring. Paper presented at the 33rd Annual International Air Safety Seminar, Flight Safety Foundation Inc, Christchurch, New Zealand, September 15-18 1980.

8) LOUIS A URBAN — Gas Path Analysis of Commercial Aircraft Engines. 11th AIDS Symposium, DFVLR AIDS Study Group, Cologne, September 22-24 1981.

9) R J E DYSON & D L DOEL — CF6-80 Condition Monitoring: The Engine Manufacturer's Involvement in Data Acquisition and Analysis. AIAA paper 84-1412, presented at the AIAA/SAE/ASME 20th Joint Propulsion Conference, Cincinnati, Ohio, June 11-13 1984.

10) DAVID L DOEL — TEMPER - A Gas Path Analysis Tool for Commercial Jet Engines. ASME paper 92-GT-315, presented at the International Gas Turbine and Aeroengine Congress and Exposition, Cologne, June 1-4 1992.

11) M J BARWELL — COMPASS: Ground Based Engine Monitoring Program for General Application. SAE paper 87-1734, presented at the SAE Aerospace Technology Conference and Exposition, Long Beach, California, October 5-8 1987.

12) A GELB (Ed) — Applied Optimal Estimation. MIT Press, 1974.

13) S M BOZIC — Digital and Kalman Filtering. Edward Arnold, 1984.

14) A E BRYSON & Y C HO — Applied Optimal Control. Halstead Press, 1975.

15) O L R JACOBS — Introduction to Control Theory. Oxford University Press, 1974.

16) P EYKHOFF — System Identification. J Wiley and Sons, 1974.

17) IAN B RHODES — A Tutorial Introduction to Estimation and Filtering. IEEE Transactions on Automatic Control, Vol AC-16 No 6, December 1971, pp688-706.

18) M HEALEY — A Working Man's Guide to Kalman Filters. Unpublished notes, Nottingham University.

19) J L LEMAY & W L BROGAN — Kalman Filtering I (2 Volumes) and Kalman Filtering II: Lecture Notes for 5-Day Short Courses. St Joseph Sciences Inc, 1984.

20) C T LEONDES (Ed) — Theory and Applications of Kalman Filtering. AGARDograph 139, February 1970.

21) CYRUS B MEHER-HOMJI & JIM P CULLEN — Integration of Condition Monitoring Technologies for the Health Monitoring of Gas Turbines.

ASME paper 92-GT-52, presented at the International Gas Turbine and Aeroengine Congress and Exposition, Cologne, June 1-4 1992.

22) S G DANIELSSON & S G DIENGER — A European View on Gas Turbine Engine Monitoring on Current and Future Civil Aircraft. SAE paper 79-1200, presented at the AIAA/SAE/ASME 15th Joint Propulsion Conference, Las Vegas, Nevada, June 18-20 1979.

23) GERWIN DIENGER — 'The Airborne Engine on Test' - Condition Monitoring for the Lufthansa A310 Aircraft. Paper presented at the Annual Conference of the Deutsche Gesellschaft fur Luft und Raumfahrt (DGLR), Hamburg, October 1-3 1984.

24) SVEN-GÖRAN DANIELSSON — Gas Path Analysis Applied to Pre- and Post-Overhaul Testing of the JT9D Turbofan Engine. SAE paper 77-0993, presented at the Aerospace Meeting, Airport Sheraton Inn, Los Angeles, California, November 14-17 1977.

25) WILLEM J SCHRÖDER & HARMEN LANSER — Introduction and Application of a Modular Turbine Engine Performance Analysis System within KLM Royal Dutch Airlines. ASME paper 89-GT-317, presented at the Gas Turbine and Aeroengine Congress and Exposition, Toronto, Ontario, June 4-8 1989.

26) R LUNDERSTÄDT & K FIEDLER — Diagnostic Procedures for Jet Engines. ASME paper 85-IGT-5, presented at the Beijing International Gas Turbine Symposium and Exposition, Beijing, September 1-7 1985.

27) GURBUX S ALAG & GLENN B GILYARD — A Proposed Kalman Filter Algorithm for Estimation of Unmeasured Output Variables for an F100 Turbofan Engine. NASA Technical Memorandum 4234, 1990.

28) G W GALLOPS, F D GASS & M H KENNEDY — On-Board Condition Management for Aircraft Gas Turbines.

ASME paper 92-GT-416, presented at the International Gas Turbine and Aeroengine Congress and Exposition, Cologne, June 1-4 1992.

29) JOHN C DELAAT & WALTER C MERRILL — A Real-Time Implementation of an Advanced Sensor Failure Detection, Isolation and Accommodation Algorithm. NASA Technical Memorandum 83533, prepared for the AIAA 22nd Aerospace Sciences Meeting, Reno, Nevada, January 9-12 1984.

30) WALTER C MERRILL — Sensor Failure Detection for Jet Engines Using Analytical Redundancy. AIAA paper 84-1452, presented at the AIAA/SAE/ASME 20th Joint Propulsion Conference, Cincinnati, Ohio, June 11-13 1984.

31) WALTER C MERRILL & JOHN C DELAAT — A Real-Time Simulation Evaluation of an Advanced Detection, Isolation and Accommodation Algorithm for Sensor Failures in Turbine Engines. NASA Technical Memorandum 87289, prepared for the 1986 American Control Conference, Seattle, Washington, June 18-20 1986.

32) JOHN C DELAAT & WALTER C MERRILL — Advanced Detection, Isolation and Accommodation of Sensor Failures in Turbofan Engines. NASA Technical Paper 2925, February 1990.

33) CYRUS B MEHER-HOMJI — A Feasibility Study of the Application of Artificial Intelligence Techniques for Turbomachinery Diagnostics. ASME paper 85-GT-102, presented at the Gas Turbine Conference and Exhibition, Houston, Texas, March 18-21 1985.

34) DAVID L DOEL — The Role of Expert Systems in Commercial Gas Turbine Engine Monitoring. ASME paper 90-GT-374, presented at the Gas Turbine and Aeroengine Congress and Exposition, Brussels, June 11-14 1990.

35) L A URBAN — Parameter Selection for Multiple Fault Diagnostics of Gas Turbine Engines. ASME Paper 74-GT-62, presented at the Gas Turbine Conference, Zurich, March 31-April 4 1974.

36) R G BROWN — Not Just Observable, but How Observable? Proceedings of the National Electronics Conference, Vol 22, 1966, pp 709-714.

37) F M HAM — Determination of the Degree of Observability in Linear Control Systems. PhD Dissertation, Iowa State University, Ames, 1980.

38) M ROESNICK — Eine Systemtheoretische Lösung des Fehlerdiagnoseproblems am Beispiel eines Flugtriebwerkes. (A System Theory Solution to the Defect Diagnosis Problem using the Example of an Aircraft Engine). PhD Thesis, Hochschule der Bundeswehr, Hamburg, 1984.

39) WILLIAM H PRESS, BRIAN P FLANNERY, SAUL A TEUKOLSKY & WILLIAM T VETTERLING — Numerical Recipes: The Art of Scientific Computing. Cambridge University Press, 1986.

40) P J HARRISON & C F STEVENS — Bayesian Forecasting. Journal of the Royal Statistical Society, No 3, 1976, pp 205-247.

41) P J HARRISON & C F STEVENS — A Bayesian Approach to Short-Term Forecasting. Operational Research Quarterly, Vol 22, No 4, 1971, pp 341-362.

APPENDIX A: GAS TURBINE MEASUREMENTS AND 'TRADITIONAL' ANALYSIS TECHNIQUES

A1 Measurements

The following sections describe current Rolls-Royce practice for measurements on high-bypass ratio civil engines; other engine types will have measurement systems that are broadly similar.

A2 Thrust

Figure 99 shows a typical arrangement for measuring the force produced by an engine, on both indoor and outdoor test beds. The system consists of an outer fixed steel frame (shown shaded) which supports an inner moveable frame (thrust cradle) on four diaphragms which can support the dead weight of the cradle and attached engine plus airmeter, but offer minimum resistance to axial forces. Such axial forces are resisted by four load cells which are interposed between the frame and the cradle in two pairs, one on each side of the frame. In principle, one cell in each pair measures forward thrust, the other reverse; in practice, some preload is applied (of the order of 80 kN) to all four cells to make the whole cradle assembly resemble a stiff spring. The net forward thrust can be calculated by adding the two forward load cell readings and then subtracting the two rearward cell readings. The combined output from the load cells is fed to a voltage-to-frequency converter; during a data scan, the resulting pulse train is integrated and an average pulse rate/second determined, which can be converted to thrust via an appropriate calibration. The whole assembly is carefully designed to minimise sensitivity to thermal expansion effects, and facilities are provided to fit calibration load cells (traceable to National Physical Laboratory standards).

The performance of an engine is usually quoted as if it were operating in an infinite atmosphere, ie with no adjacent structures/surfaces constraining the flows into and out of the engine. An open air (outdoor) test bed gives a sufficiently close approximation to infinite atmosphere performance, provided corrections are made for wind forces on the bed structure ('sail effects') and inlet momentum drag induced by the wind; however, outdoor testing on a day-to-day basis is impractical because of noise and lack of protection from the weather. Most testing is therefore done indoors, in an enclosed bed in which the air is constrained to enter through sound-attenuating 'splitters' in the front of the bed and leave through a 'detuner' which further reduces noise. This constrained flow (Figure 100) introduces an 'approach momentum' of the inlet air, which results in an apparent thrust loss: the forces registered on the thrust cradle are less than the thrust actually being produced by the

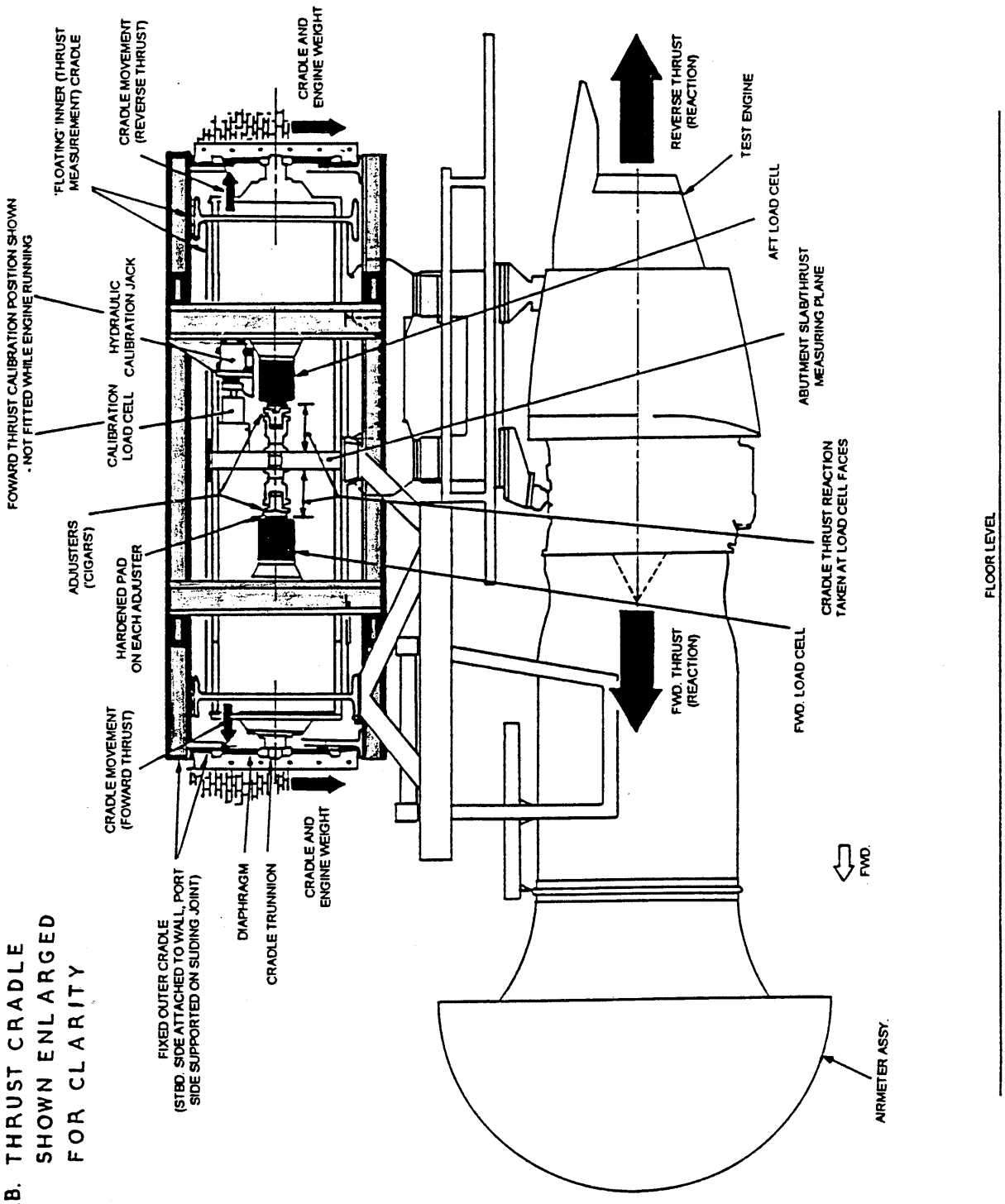

Figure 99: Engine thrust measurement system

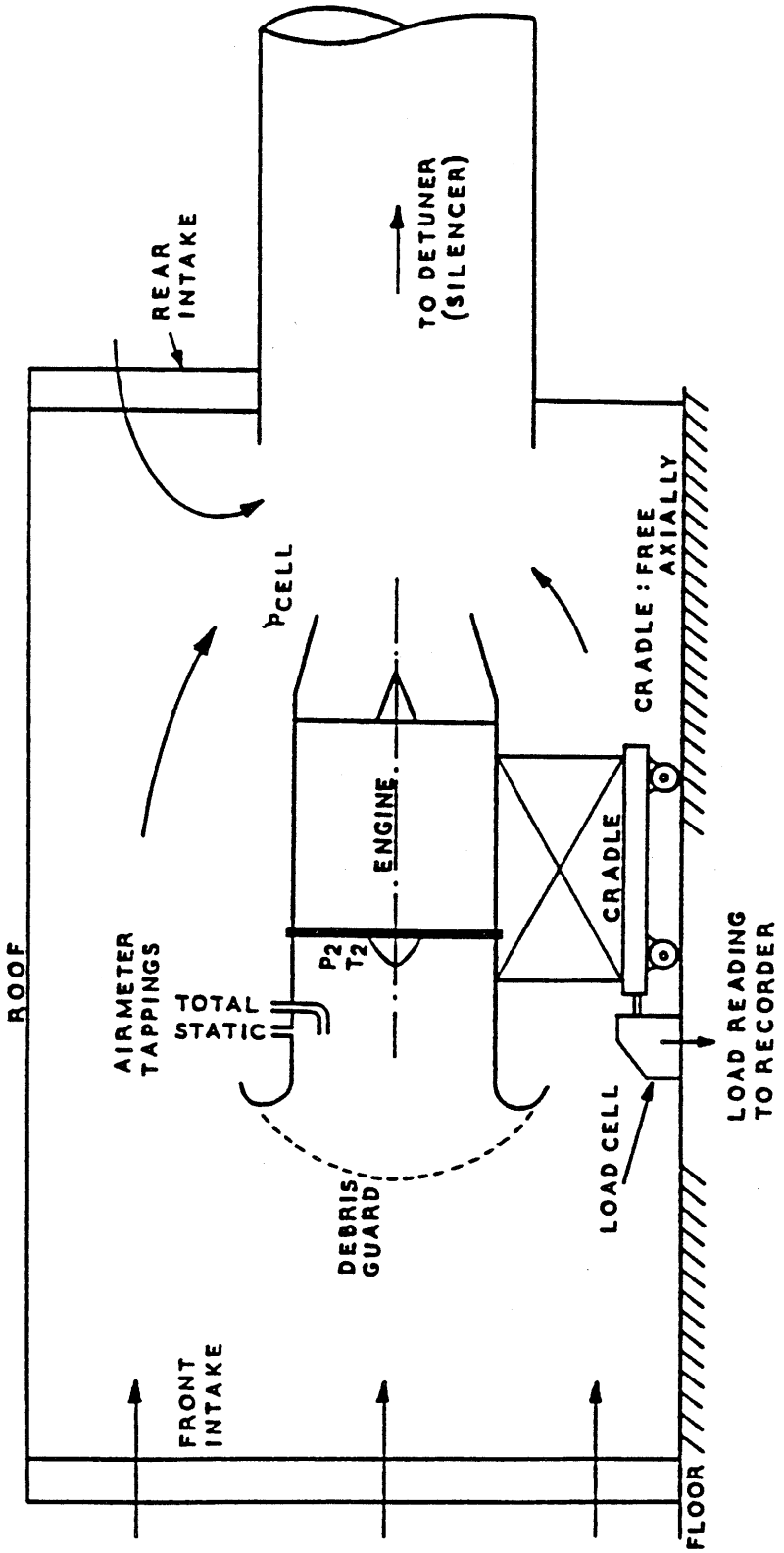

Figure 100: Diagram of indoor test bed

engine. Typically, this thrust loss (usually determined by calibration of a specific indoor bed against the outdoor bed by running one or more engines on both beds and comparing the thrust readings) is of the order of 5%. However, it is very sensitive to bed configuration, with even trivial changes in the position of test bed equipment (ladders, access platforms, etc) and splitter/detuner configurations producing large effects on this thrust loss. Since this thrust loss appears as an equal and opposite pressure force on the test bed walls, floor and ceiling, it is possible to correlate it with the readings of exceedingly sensitive pressure measurements taken at strategic places in the bed: changes in these readings indicate that changes in the test bed aerodynamics have taken place, and indicate that either the bed configuration has been inadvertently altered (and should be returned to its 'datum' state) or a re-calibration against the outdoor bed is required.

A3 Fuel Flow

Two basic ways of measuring fuel flow are used:

1) Positive displacement meters, which measure a fixed volume of fuel in a single revolution, which can be timed (Figure 101);

2) Turbine flow meters, which, as their name implies, derive fuel flow rate from the rotational speed of a small turbine rotor placed in a straight section of fuel pipe.

Both of the above types measure fuel volume flow rate; mass flow rate has to be determined by multiplying by fuel density (or fuel specific gravity multiplied by the density of water), determined at the time of the test, with corrections applied to density for fuel temperature and pressure measured at the meter. A third type, which determines fuel mass flow rate directly (by imparting some angular momentum to the fuel and then measuring the torque required to remove it) is usually used only in measurements for aircraft cockpit displays.

Positive displacement meters, an example of which is shown in Figure 101, work by using the pressure of the fuel to drive a series of carefully-machined pistons (connected to a common crankshaft) running in interconnected bores; in a single revolution of the crankshaft, the pistons sweep through a known fixed volume, and hence let through a known fixed volume of fuel. The time taken for a single revolution therefore indicates the rate of fuel flow.

Positive displacement meters are used for measurement of fuel flow during steady-state running; they cannot be used for transient measurements, or in situations where space is at a premium (such as in flight), where turbine

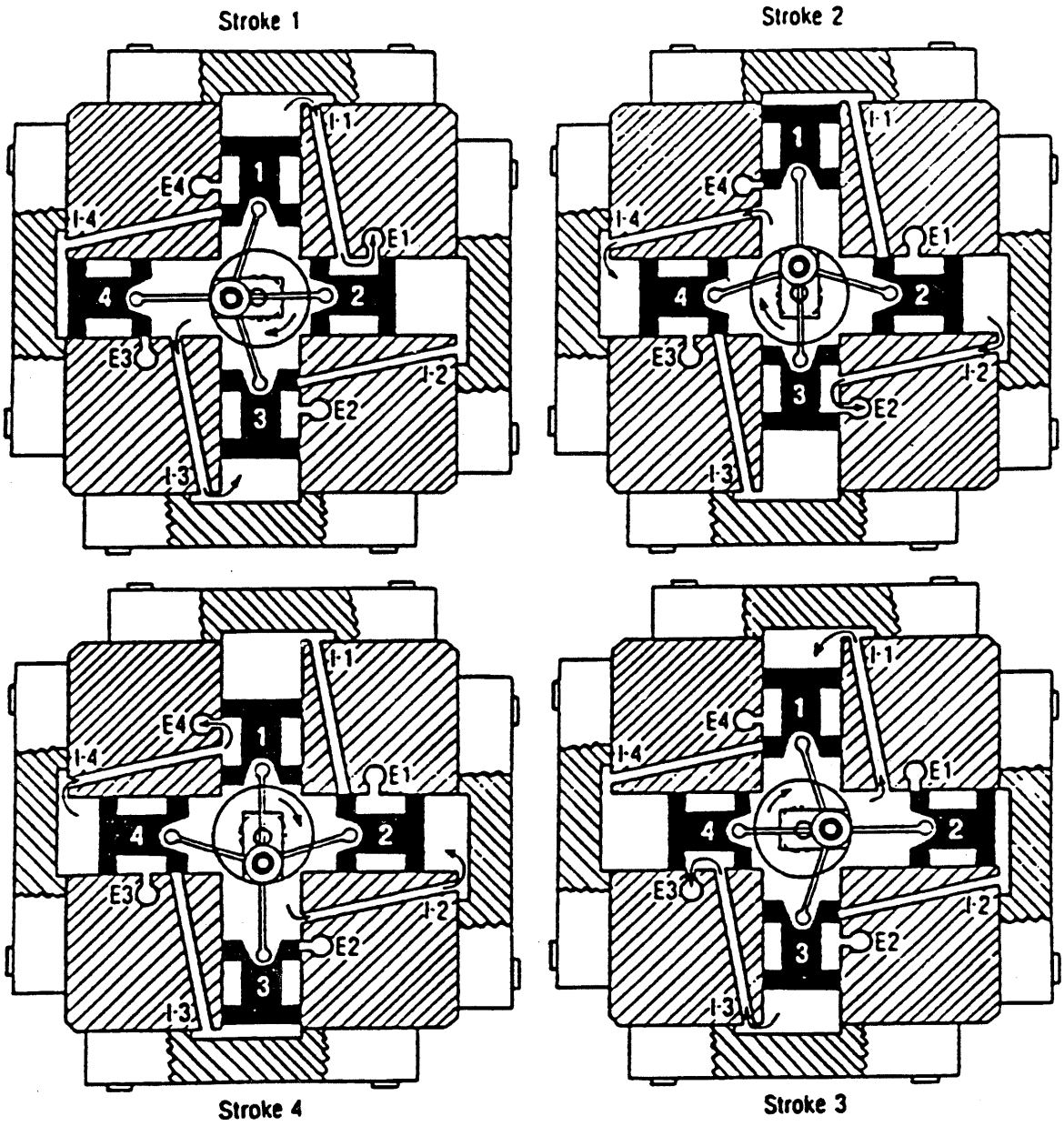

Figure 101: Typical positive displacement flow meter

flowmeters have to be used instead.

It must not be forgotten that fuel flow is an energy flow as well as a mass flow. Fuel calorific value is an important parameter, which is determined with either a standard 'bomb' calorimeter or from correlations with hydrogen/carbon ratio; this is determined using nuclear magnetic resonance (NMR).

A4 Pressures

Engine pressure measurements are made in a variety of ways, depending on the following considerations:

1) The room available in the annulus for inserting pressure probes, as well as room on the engine carcass for instrumentation bosses;

2) The accuracy and coverage required;

3) Whether total pressure is required, or whether derivation of total pressure from a cheaper and less intrusive wall static is acceptable;

4) The temperature of the gas;

5) The instrumentation fitted to component rigs.

The most desirable pressure measurements are those made with instrumentation that is identical to that used in component rigs; this ensures, as far as possible, that calculations using these measurements (eg efficiencies) are to a similar aero-thermal standard, thus enabling engine and rig results to be directly compared. Typically, these measurements will be made by inserting a number of 'rakes' into the annulus in the stations between major components; at each station, a number of rakes would be placed at various circumferential positions. The number of tappings on each rake and the number of rakes at each station will depend on the coverage required and the room available in the annulus; Figures 102, 103 and 104 show various typical pressure rake configurations. Some of the rakes fitted may not in fact be used for whole engine performance analysis, but by component specialists to assess such details as wake profiles and boundary layer losses that are accounted indirectly in performance synthesis and analysis work.

Each pressure tapping consists of a small-diameter open tube (carefully made to ensure that no 'burrs' or other imperfections exist on the end) known as a Pitot head, mounted on the rake to point into the local flow direction. The tube is usually surrounded by a concentric shroud known as a Kiel head, which is fitted to make the pressure reading less sensitive to variations in flow direction. The sensed total pressure is usually fed via small-diameter nylon tubes to a device known as a Scanivalve (Figure 105). The Scanivalve basically consists of two circular plates, one on top of the other; one of the plates is fixed, and contains a number of holes (up to 48) near its circumference to which tubes connected to engine pressure tappings are attached, while the other, which is arranged to rotate, contains one hole fitted with a pressure transducer. When a data scan is taken, this plate is rotated, and the pressure transducer senses each of the connected pressures in turn, converting the pressures into voltages which can be read by computer. Usually, some of the fixed tappings are connected to known calibration pressures, thus re-calibrating the pressure transducer on each scan.

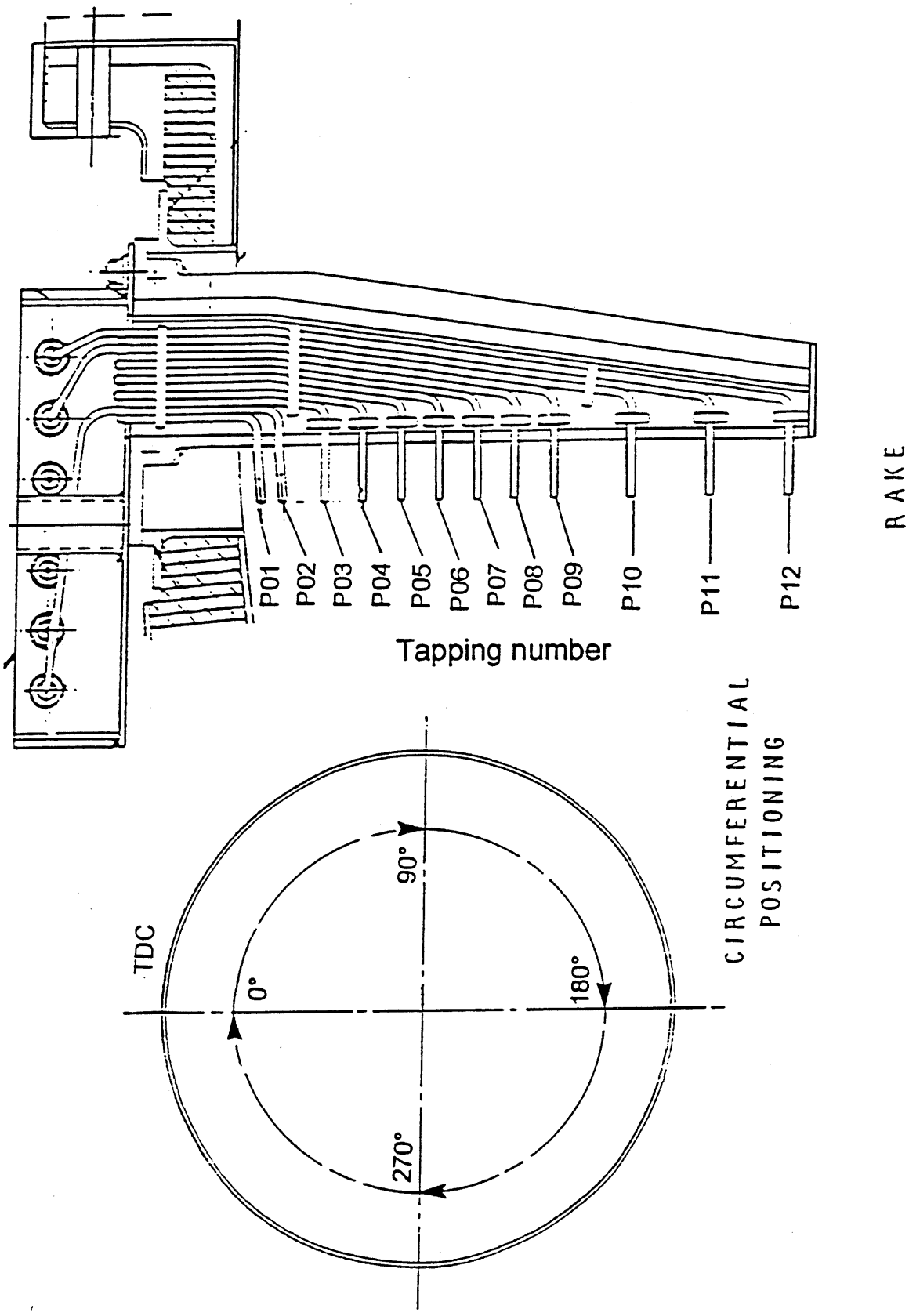

Figure 102: Typical pressure rake (1)

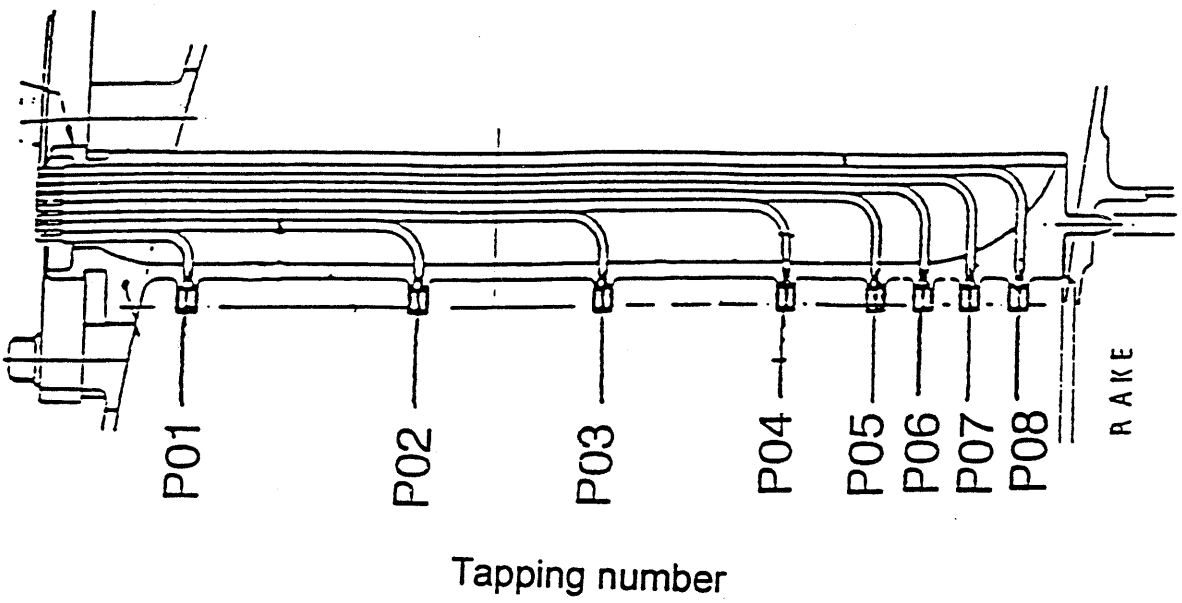

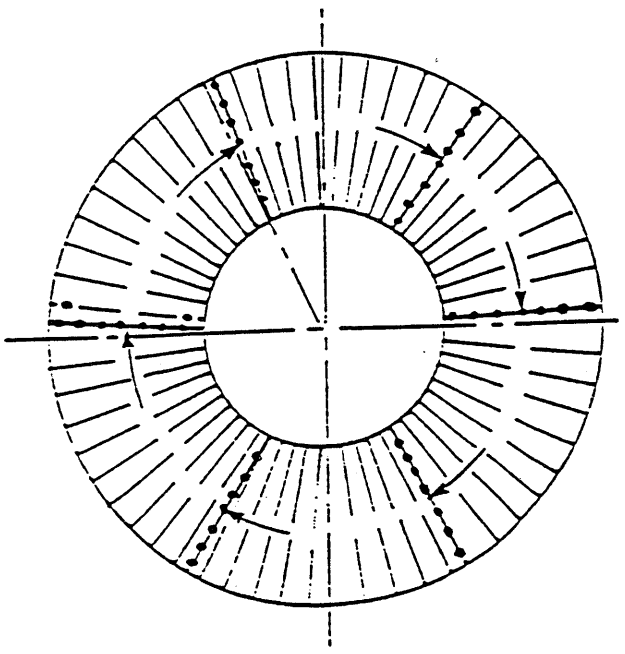

Figure 103: Typical pressure rake (2)

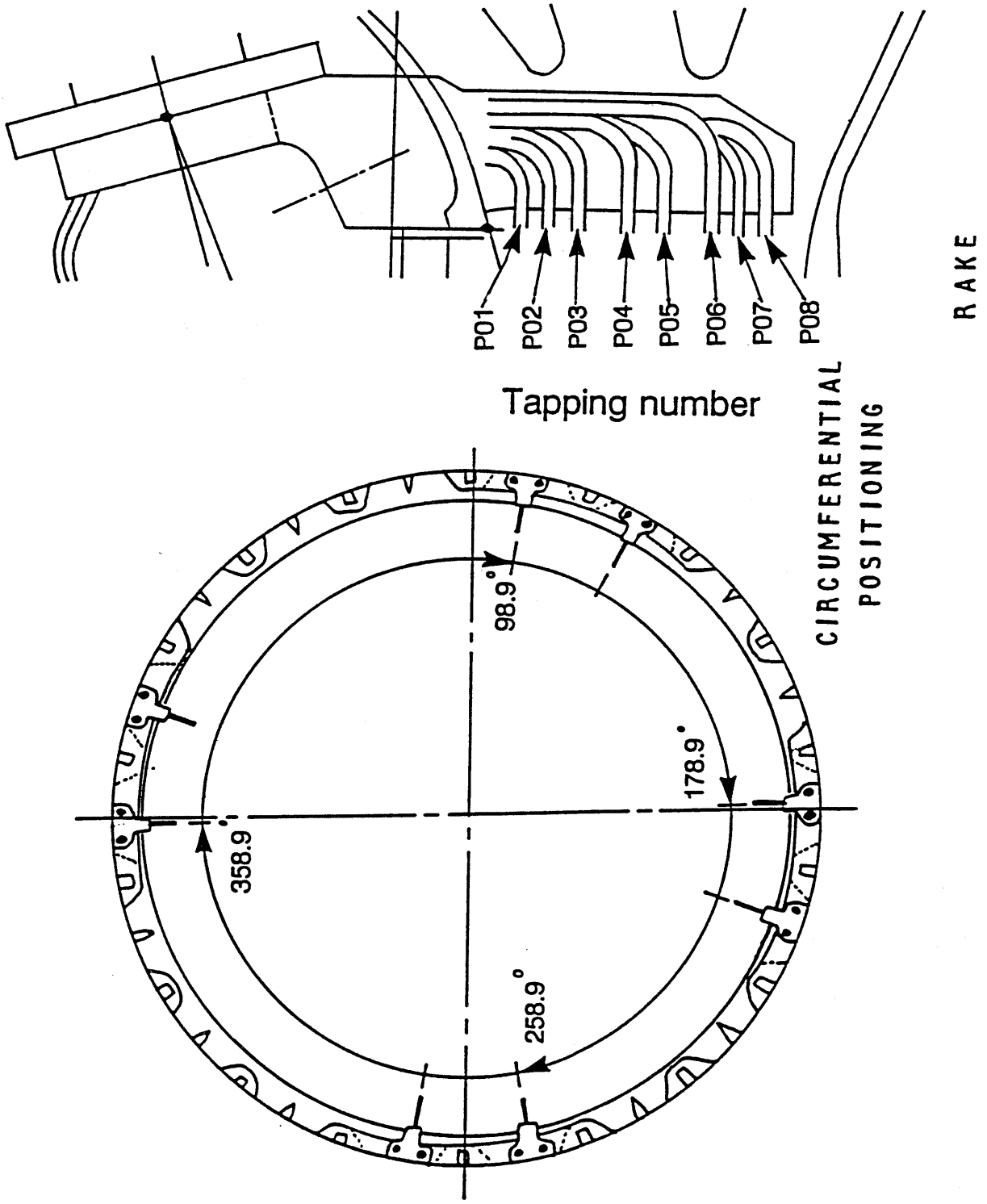

Figure 104: Typical pressure rake (3)

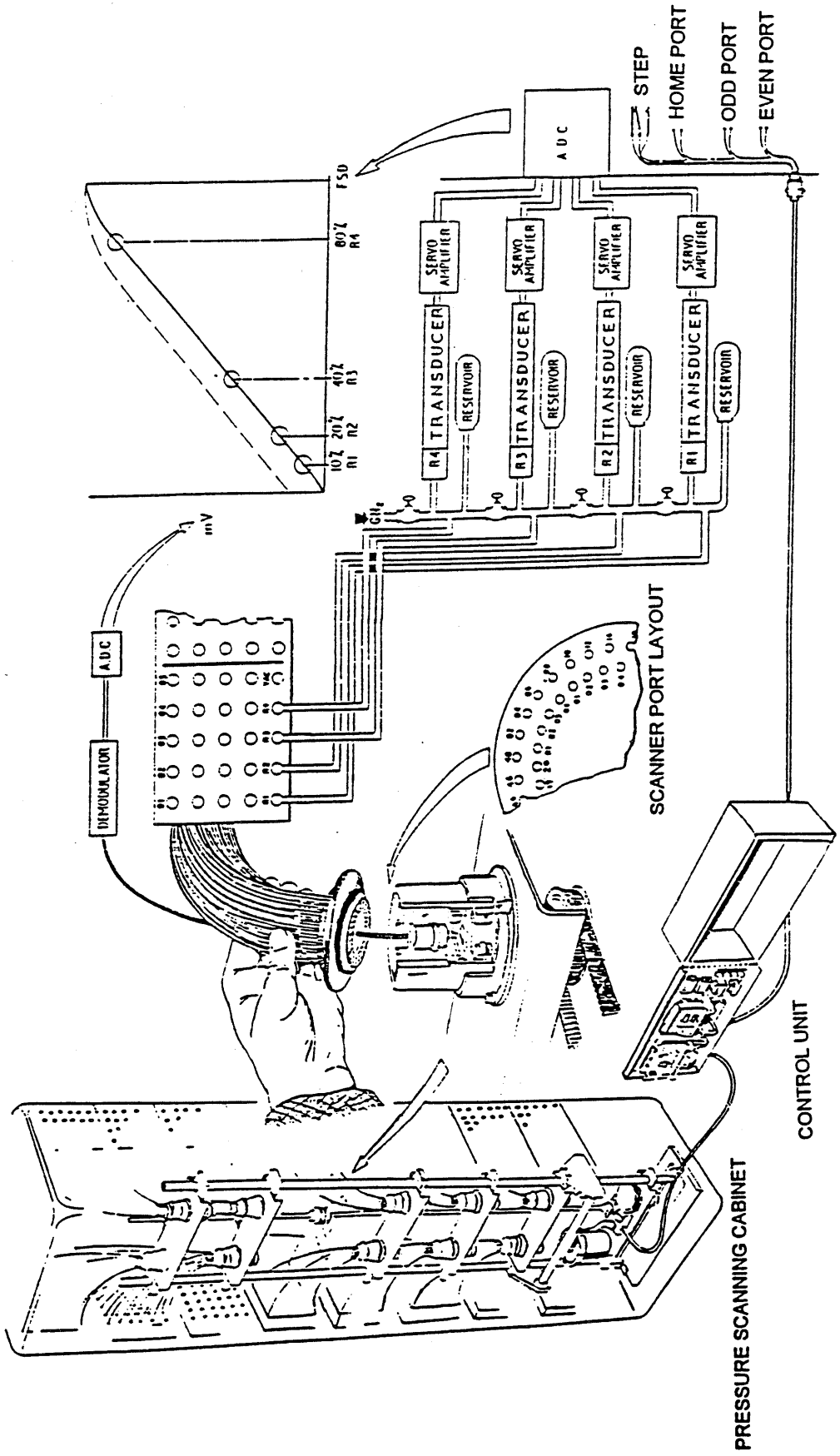

Figure 105: Typical Scanivalve arrangement

The presence of multiple Pitot heads improves reliability and, if the rakes are positioned correctly, gives a good average pressure where there may be profiles induced by upstream hardware. Sometimes the individual tappings at a station are 'ganged' together by feeding them to a plenum chamber which pneumatically means the pressure before feeding it to the pressure transducer; this is done in situations such as flight testing where the number of transducers has to be minimised.

If it is impractical or too costly to fit multiple rakes, either a single rake (which may have temperature tappings mounted on it as well) or a wall static is fitted, and a calibration factor, derived from engine testing, is applied to get from the observed readings to the values that would have been seen had the full set of rakes been fitted.

Measuring pressures in the hottest parts of the engine (above 1000°C) is difficult and expensive, because the instruments have to be cooled; it is therefore rare to do this, except for special one-off tests. Pressures in these regions therefore have to be calculated; see later.

Cell static pressure is normally measured using 'pepperpot' tappings on the cell walls in the plane of the final nozzle, while engine face total pressure is normally derived from a calibration against cell pressure and inlet airflow (ie a pseudo intake pressure 'loss'); measuring engine face pressure using rakes is not practical on a day-to-day basis because of the fan stresses introduced by the wakes shed from these (potentially very large) pieces of hardware in the intake, and the real danger of substantial engine damage should one of these rakes break off during engine running.

A5 Temperatures

Engine temperature measurements are made in a very similar way to pressure measurements, using hardware that is almost identical (Figures 106 and 107); the Pitot head is, of course, replaced by a thermocouple bead, which generates a voltage that can be read by computer. Chromel/Alumel is used for temperature measurements up to 1000°C, while Platinum/Rhodium is used above that temperature.

Most of the considerations affecting pressure measurements mentioned above also apply to temperatures. Note that a 'static' temperature measurement is not a true static (since the temperature sensor is not moving along with the gas!), and can only be used if a calibration factor to get to a total temperature value is available. Usually, calibration factors are also applied to correct from measured component outlet temperatures to temperatures derived from shaft power measurements on component rigs;

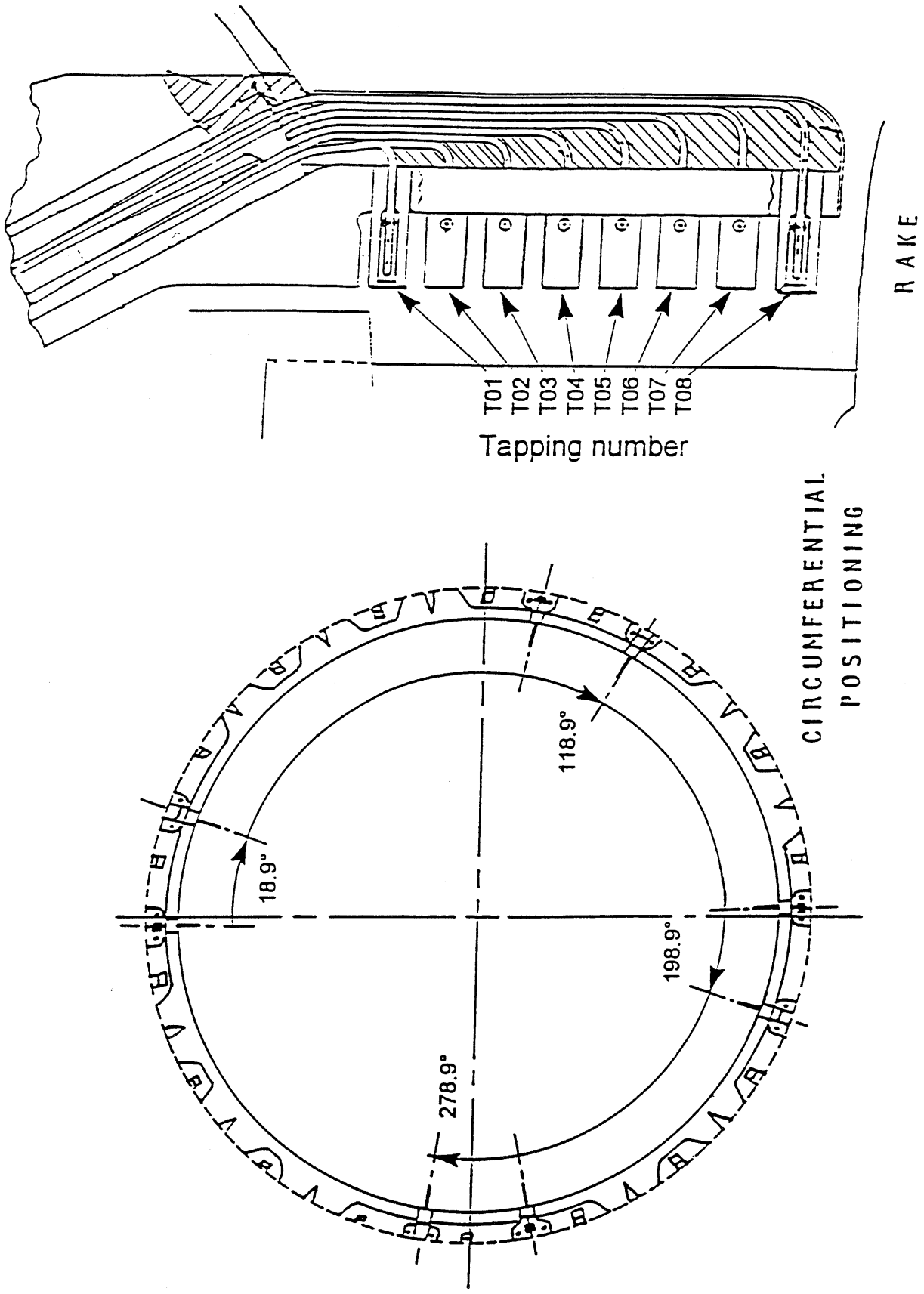

Figure 106: Typical temperature rake (1)

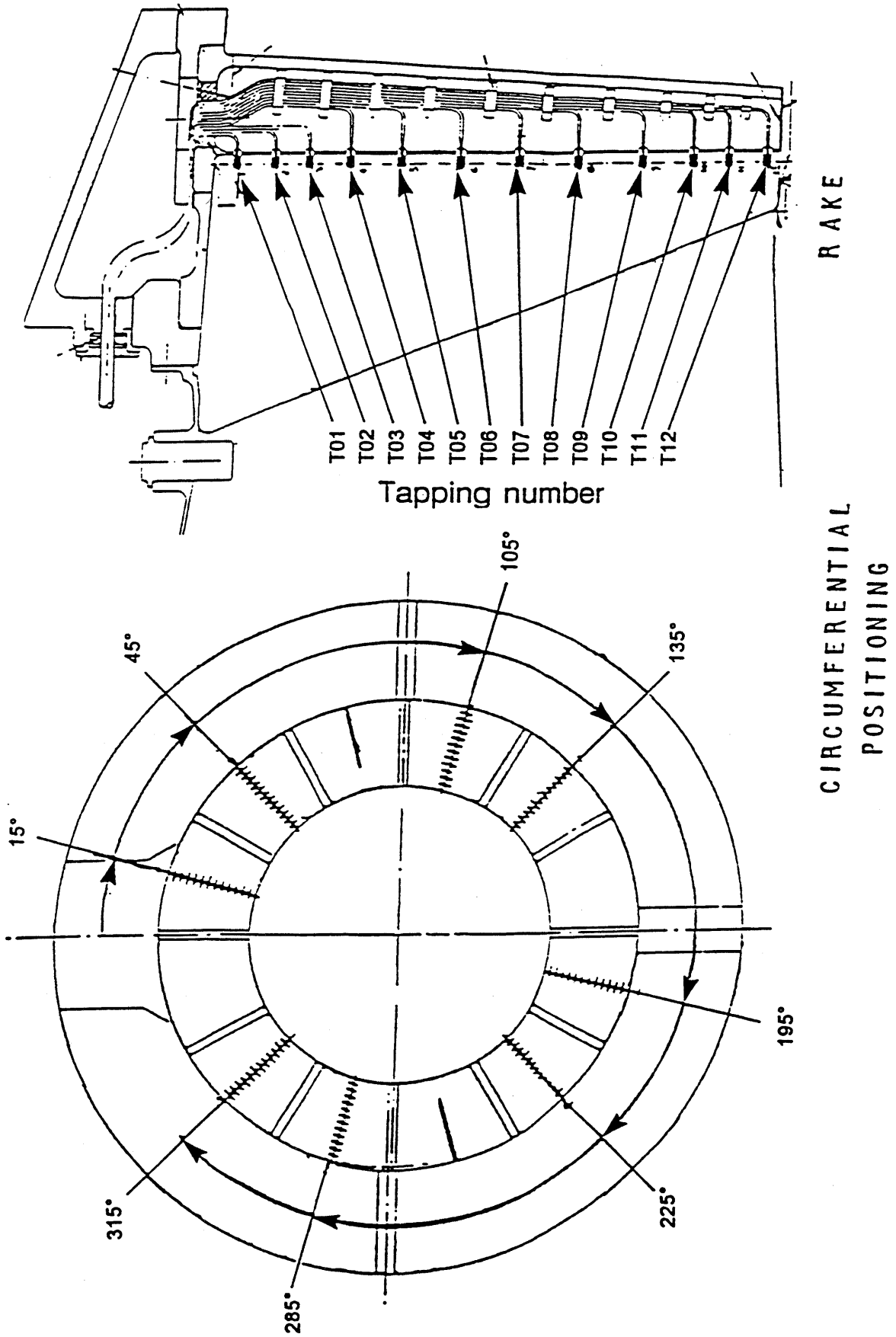

Figure 107: Typical temperature rake (2)

this removes temperature outlet profile effects, since the calculation from shaft power automatically 'averages' the outlet temperature.

Temperature measurements downstream of the Combustion Chamber should be read on multiple probes (ideally 'verniered' relative to the burner pitch) to average out hot spots; see Figure 108.

Like pressures, temperatures are difficult to measure in the hottest parts of the engine, and most of them have to be calculated; see later.

Engine inlet temperature is usually measured by thermocouples or resistance bulb thermometers strung over the debris guard.

Care must be taken when using thermocouples to ensure that:

1) the cold junction temperature is at a known stable value. To improve temperature measuring accuracy, the cold junctions of a number of thermocouples can be embedded in a conducting block placed in an insulated container, which also has a platinum resistance thermometer embedded in it; this arrangement is called a Uniform Temperature Reference (UTR) box;

2) the number of connections in the thermocouple wires is minimised, to reduce the possibility of spurious thermal EMF's;

3) for really accurate temperature measurements, the thermocouple wires used are calibrated specially, rather than relying on published thermal EMF characteristics; this process is known as Batch Wire Calibration. Calibration of individual rakes after manufacture also improves accuracy;

4) proper account is taken of 'ageing' of the thermocouple wire (ie a change of calibration as time passes) due to long periods of exposure to high temperatures (above 600°C).

Temperature rake design is usually a compromise between mechanical integrity (implying thick wires and small shrouds) and minimising errors due to conduction and radiation heat transfers (implying thin wires and shrouds large enough to screen hot surfaces from the thermocouple bead).

Pressure and temperature tappings can be combined onto a single rake for convenience (Figure 109). Figures 110 and 111 show composite pictures of the various possible rakes and other pressure/temperature tappings that can be fitted (not all at once, though!) to a typical civil engine.

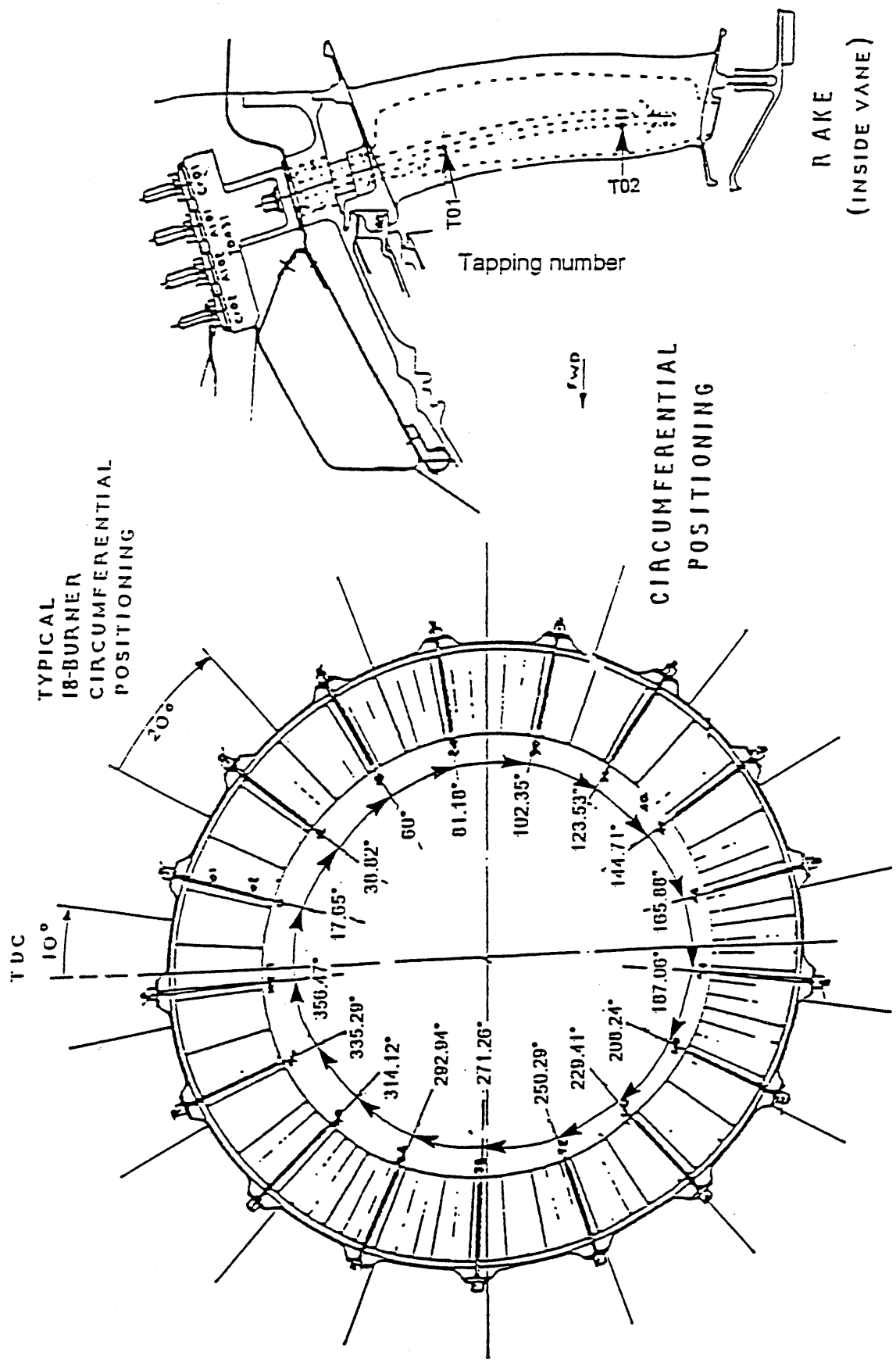

Figure 108: Typical 'verniered' temperature rakes

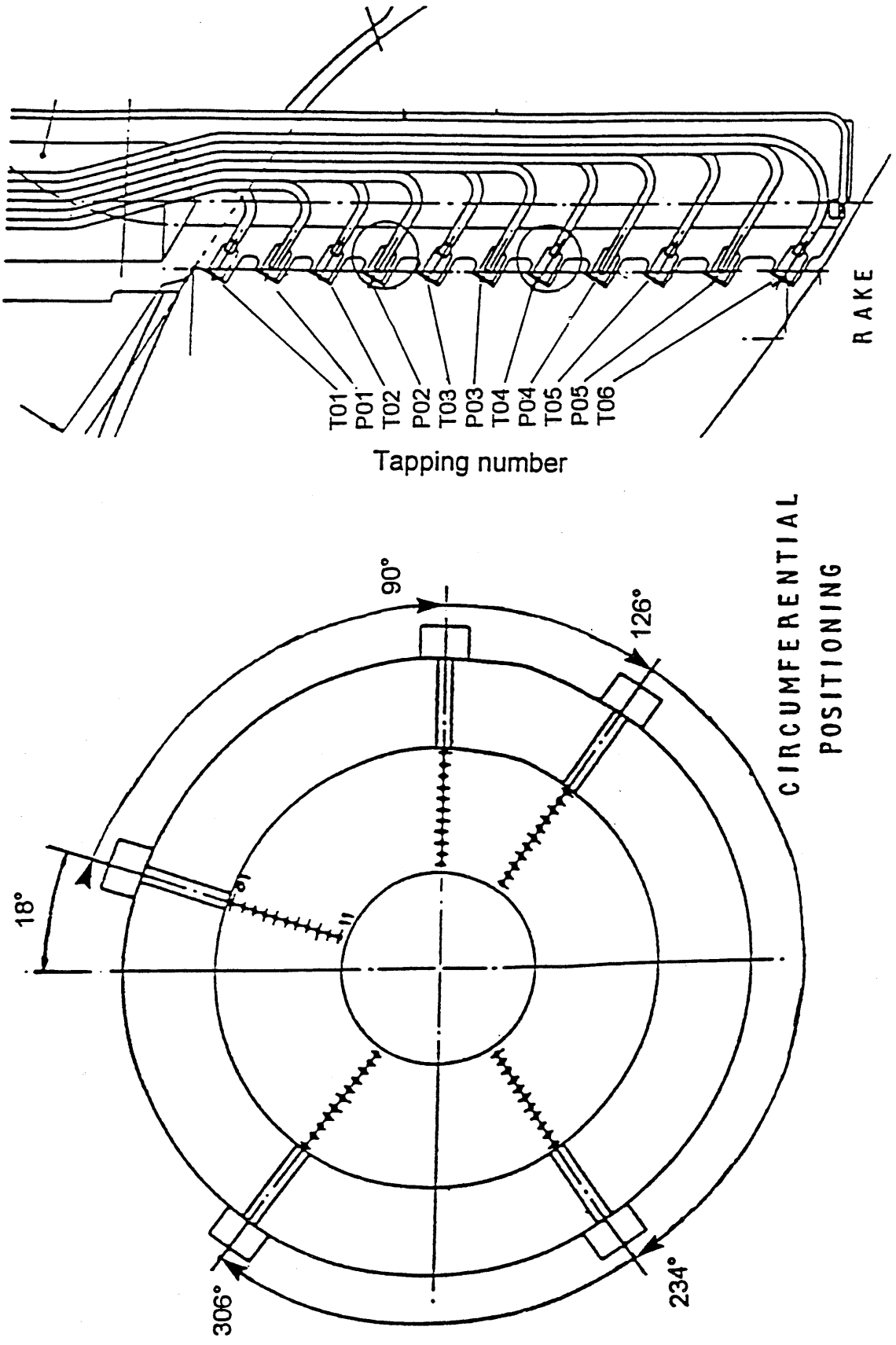

Figure 109: Typical combined pressure and temperature rake

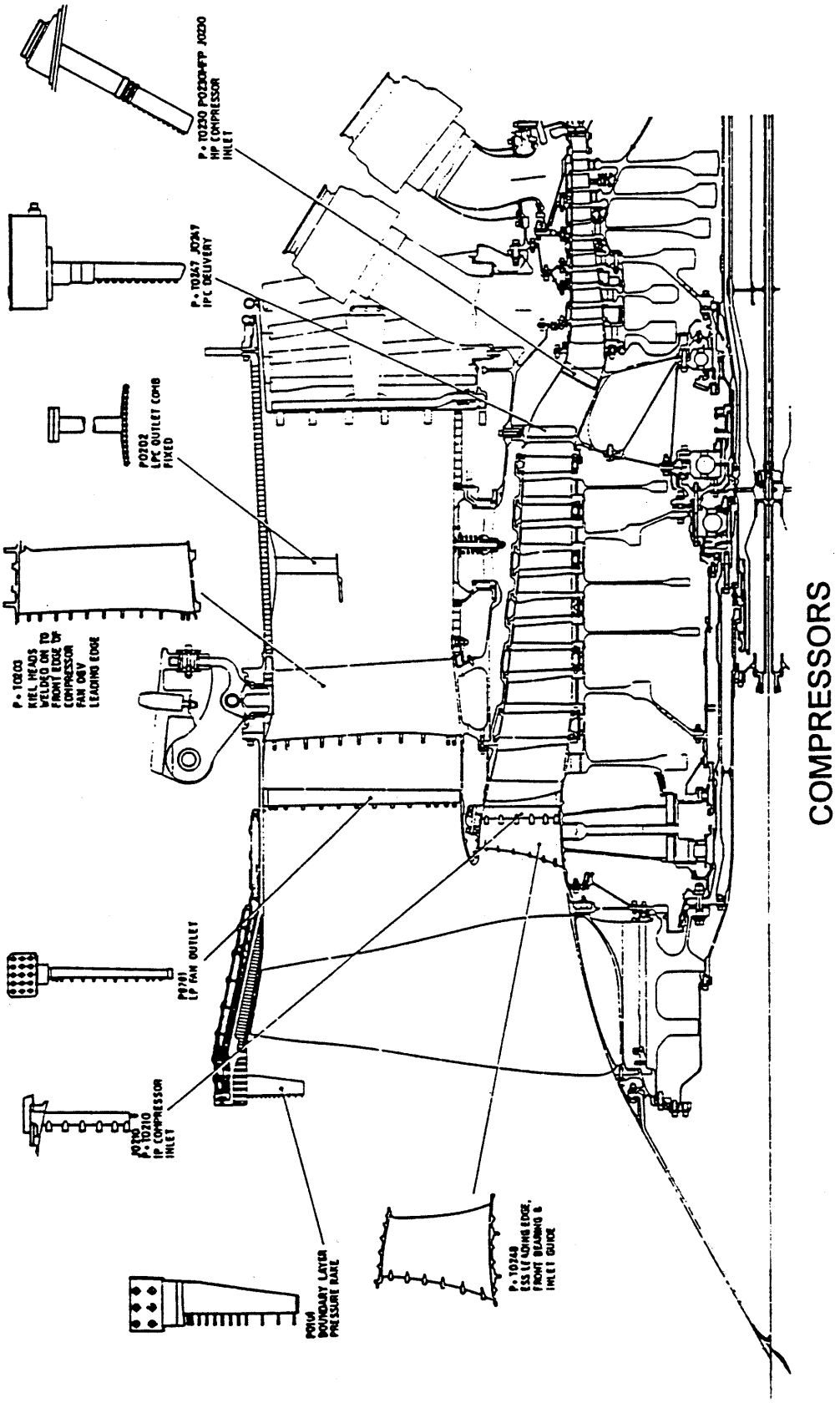

Figure 110: Composite picture of typical pressure and temperature measurements in compressor section of engine

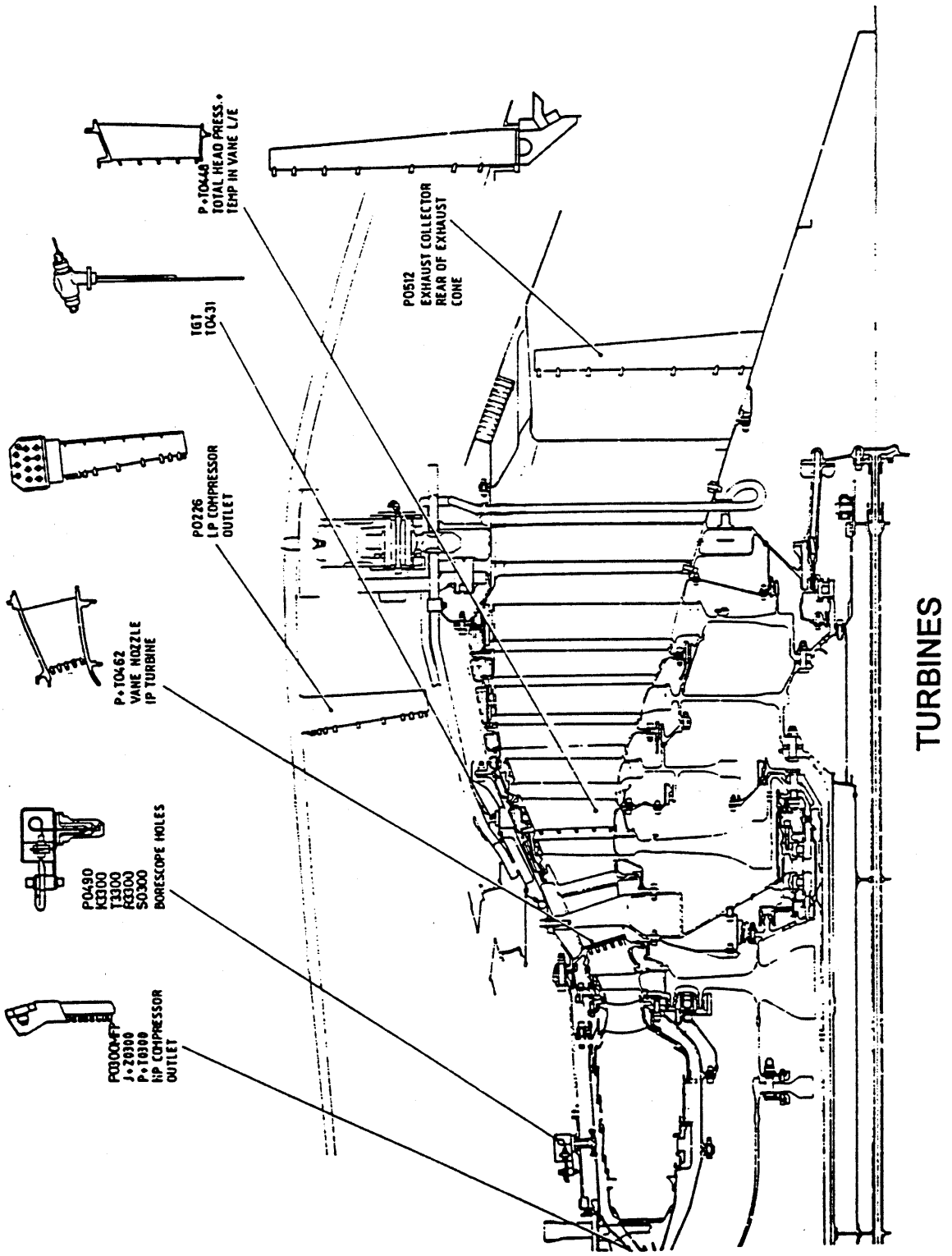

Figure 111: Composite picture of typical pressure and temperature measurements in turbine section of engine

A6 Airflow

Total inlet airflow is the only airflow that can be measured on a high-bypass turbofan. It is calculated from total and static pressure measurements made in a parallel section of inlet between the inlet scroll/debris guard assembly and the engine face; this whole assembly is called an airmeter (see Figure 100). From the ratio of total to static pressures, the non-dimensional group $W\sqrt{T}\div AP$ can be worked out from the compressible flow relationships; knowing the total inlet temperature, the total pressure and the airmeter cross-sectional area (factored to take account of boundary layer growth and instrument position errors by a discharge coefficient that is determined by calibration on a suction rig), the air mass flow rate can then be calculated.

Great care must be taken with the maintenance of the airmeter and its instrumentation; significant errors can be introduced if the airmeter is allowed to get dirty and/or the static pressure tapping hole shapes are distorted. Like thrust, airflow can also be affected by the aerodynamics of an indoor bed, so airflow calibration is also carried out when an indoor/outdoor thrust calibration exercise is carried out.

Airflows at the other stations in the engine has to be calculated; see later.

A7 Shaft Speeds

Shaft rotational speeds are measured using two methods:

1) A toothed wheel on the shaft (known as a phonic wheel) running next to an electrical coil. As each tooth passes the coil, the change of magnetic reluctance induces a pulse; the frequency of the resulting series of pulses is proportional to shaft speed;

2) A tachometer (essentially a small electrical generator) driven by the shaft produces a voltage output that is proportional to shaft speed.

A8 Engine Geometry

Engine controlling areas, such as turbine nozzle guide vane (NGV) throats, turbine rotor blade throats and final nozzle areas are also required for performance analysis. These are measured by a variety of methods, depending on what the geometry is; from simple diameter measurements (using a 'long' micrometer) in the case of circular final nozzles to computer-controlled probes that deduce 3-dimensional NGV throat area changes from nominal from sensed vane profile changes. Complications can arise in the case of cold stream nozzles on a separate-jets bypass engine and chute areas on a mixed engine due to the

presence of mounting struts, relative movement of outer and inner skins and the precise definition of exactly where the controlling area is; various ad-hoc methods involving pieces of shaped plywood, etc are evolved to suit particular situations. If final nozzles happen to be convergent-divergent (con-di), the both throat and exit areas are required.

A9 Correction of Measurements to 'true' values

The above descriptions briefly mentioned in several places the fact that the actual pressure and temperature measurements recorded from probes in the engine very rarely equal the 'true' thermodynamic average values at the various stations, for several reasons:

1) The 'true' thermodynamic values may be defined using instruments that cannot be fitted to the engine for space or cost reasons, or, in the case of temperatures, defined by a calculation process that uses parameters such as shaft power that cannot be measured on an engine;

2) Particular engine builds may only have a partial set of instrumentation rakes fitted, or some of the tappings on a rake set may be unserviceable; both of these problems reduce the coverage of the annulus from that originally designed for;

3) Pressure tappings may be placed in positions that do not pick up wakes, boundary layers, etc; they therefore record a higher average pressure at that station than is thermodynamically correct, with the result that the wake and boundary layer losses are allocated to the downstream components;

4) The conversion of kinetic energy to thermal energy in a total temperature tapping (known as the dynamic temperature 'recovery') is not isentropic; this means that the total temperature recorded is less than the total temperature of the gas;

5) As indicated previously, conduction and radiation effects may further influence temperature readings.

For all of the above reasons, it is necessary to apply correction factors to each pressure and temperature measurement to get from the value that is recorded to what is considered to be the 'true' value at that plane. Usually, the 'truth' is defined as the value recorded or derived from component rig testing at that plane, and used in the calculation of efficiencies, etc that are declared by the specialist component technology areas. If necessary, several correction factors may be applied to take account of several effects that may apply to a single instrument. These correction factors may come from rig

testing, in which engine instruments are calibrated against the corresponding declared rig values, or engine testing, in which one rake or static tapping is calibrated against the full engine instrumentation at that station. Usually, these factors vary with local aerodynamic conditions, and hence engine power setting; more sophisticated analysis methods have to take this into account. While the values of correction factors are usually quite small (less than 1% for most effects, but up to 5% for correction from static to total), they can have a large influence on subsequent analysis.

A10 Calculation of Unmeasured Parameters

As indicated previously, there are many flows, pressures and temperatures in the engine that either cannot be measured for a number of reasons:

1) The difficulty and expense of fitting a sufficient number of tappings in the engine, particularly in the turbines;

2) The fact that certain parameters may not be measured with sufficient accuracy to produce meaningful analysis. Temperatures downstream of a single-stage fan fall into this category for most engine testing; special high-accuracy 'one-off' instrumentation has to be made (which can cause so much blockage in the bypass duct that the engine performance is seriously degraded) and care taken to ensure the engine is run on low-humidity days (to avoid spurious temperature readings due to condensation/evaporation of water vapour);

3) The physical impossibility of measuring some parameters directly, such as mass flows downstream of the intake, because of the absence of parallel ducts between components.

Fortunately, there are a number of techniques available to calculate these parameters. The calculation of two of the most important ones, Turbine Entry Temperature (TET) and core mass flow in a bypass engine, will be discussed here; the calculation of others, which follow on from the calculations of these, will be discussed later.

A11 Calculation of TET from HP Turbine Capacity ($W\sqrt{T}\div P$)

Calculation of TET is an iterative procedure, relying on the knowledge of four items:

1) Combustion Chamber entry pressure (P3);

2) Combustion Chamber entry temperature (T3);

3) Fuel flow into the Combustion Chamber (WFE);

4) The capacity (semi-dimensional flow function $W\sqrt{T}\div P$) of the HP Turbine (immediately downstream of the Combustion Chamber, at Station 4 ($W4\sqrt{T4}\div P4$)

The procedure is as follows:

1) Guess the flow at entry to the Combustion Chamber (W3);

2) From P3 and the Combustion Chamber pressure loss (which may depend on W3), calculate the Combustion Chamber exit pressure (P4);

3) From T3, fuel/air ratio (= WFE÷W3), combustion efficiency and the temperature rise charts (for the correct fuel calorific value), calculate the Combustion Chamber exit temperature (T4);

4) The Combustion Chamber exit flow (W4) is, of course, equal to W3 + WFE;

5) Does $W4 \bullet \sqrt{T4} \div P4$ equal the known HP Turbine capacity $W\sqrt{T}\div P$ (within a small tolerance)?

   - if YES, iteration has converged, with W3, W4, T4 and P4 now known;

   - if NO, update guess of W3 and re-calculate.

Knowing W4 and T4, the TET is easily derived from heat balance calculations, using assumed cooling bleed flows between Station 4 (NGV throat) and the HP Turbine rotor entry plane (where TET is defined). Other airflows in the core can now be calculated, by adding in assumed cooling bleed flows at the appropriate points, working both forward and backward from the Combustion Chamber.

A12 Calculation of Core Flow using a Heat Balance

If a temperature measurement exists at the station between the exit from the last core turbine and the entry to the LP Turbine driving the fan, then a control surface can be drawn enclosing the core (Figure 112), and an energy balance calculation can be done. Since all the core shaft works are included within the control surface:

Energy in = Energy out

Fuel Energy + Energy of air entering core	=	Energy of gas leaving core + Energy of any air/power offtake(s) crossing control surface

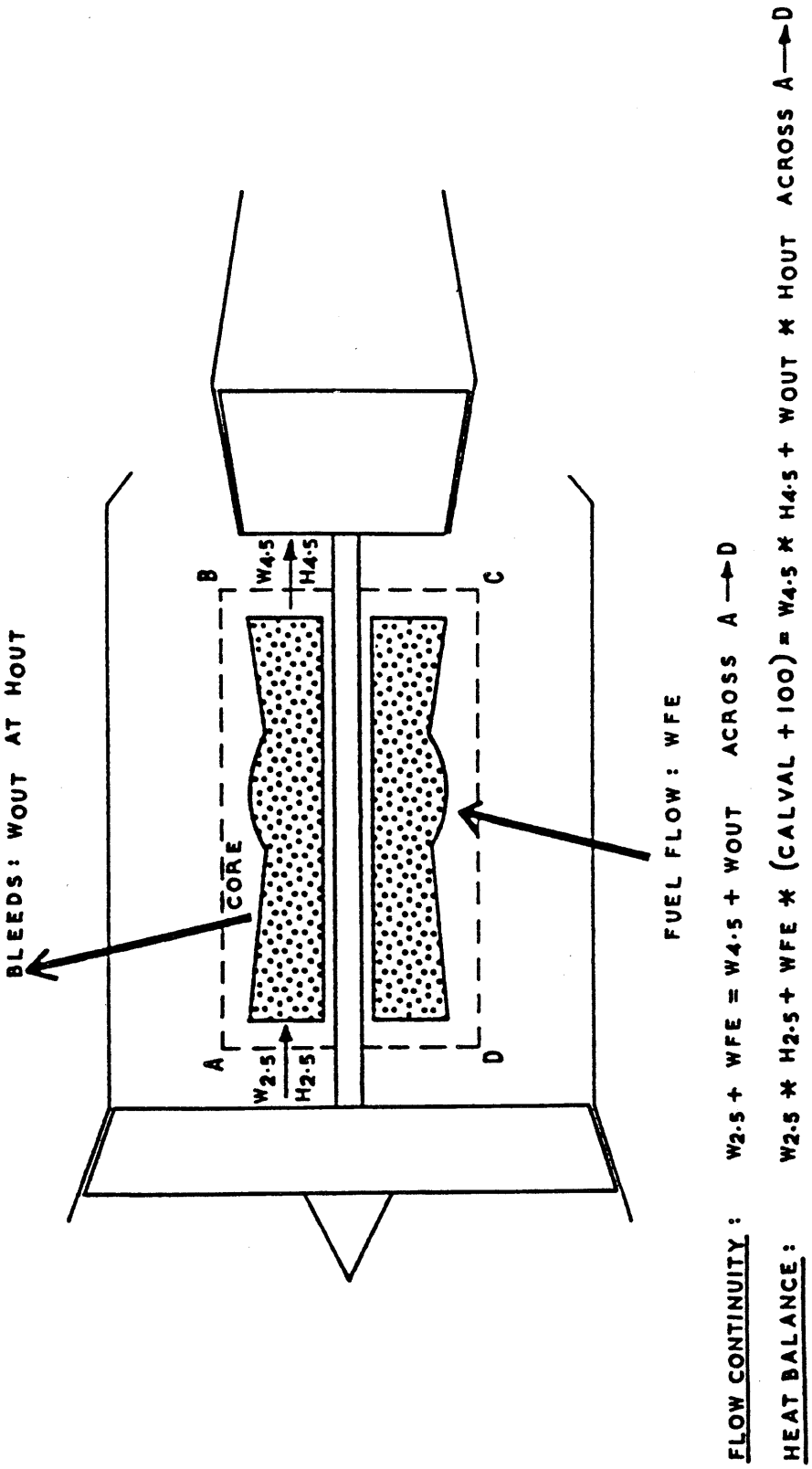

Figure 112: Core flow calculation using heat balance

Also:

Flow in = Flow out

Core inlet flow + Fuel flow	= Core outlet flow + Bleed offtake flow(s)

If bleed flow(s), engine fuel flow (WFE) and combustion efficiency are known, and the temperatures (and hence enthalpies) at inlet and exit from the control surface are also known, then core inlet flow can be calculated from the above relationships. The procedure is iterative, since the enthalpy at exit from the core is a function of fuel/air ratio at that station. In practice, for a low pressure ratio Fan Root, the calculation is fairly insensitive to core inlet temperature, so this can be assumed (from Fan Root characteristics, say) without unduly compromising the calculation.

Differences in the core flow calculated by both of the above methods can provide important information about both cooling bleed assumptions and possible measurement errors.

A13 Calculation of Other Unmeasured Parameters

Once core flow has been calculated, other unmeasured pressures, temperatures and flows can be calculated quite easily using the laws of conservation of energy and flow and assuming some component performance parameters, notably cooling and sealing bleeds and leakages, duct pressure losses and turbine capacities. The following relationships, shown diagrammatically in Figure 113, are used:

1) If core flow has been derived from HP Turbine capacity, then the flows at entry to and exit from the Combustion Chamber are known; airflows in the core compressors can be derived working forward from combustion entry, adding back in any assumed or measured air offtakes and cooling/sealing bleeds, while airflows in the turbines can be derived working rearward from combustion exit, adding in cooling/sealing bleeds at the appropriate bleed return stations;

2) If core flow has been derived from a heat balance, then the flows in the compressors, Combustion Chamber and turbines can be derived in a similar way; bleeds are subtracted from the compressors at the appropriate offtake positions, the fuel flow is added in the Combustion Chamber and the cooling/sealing bleeds are added back in at the appropriate turbine stations;

3) If core flow has been derived from both methods, any differences can usually be reconciled by adjusting one of the cooling bleed assumptions; the most common bleed to adjust, because it is usually the largest flow, is the bleed from the rear of the HP Compressor

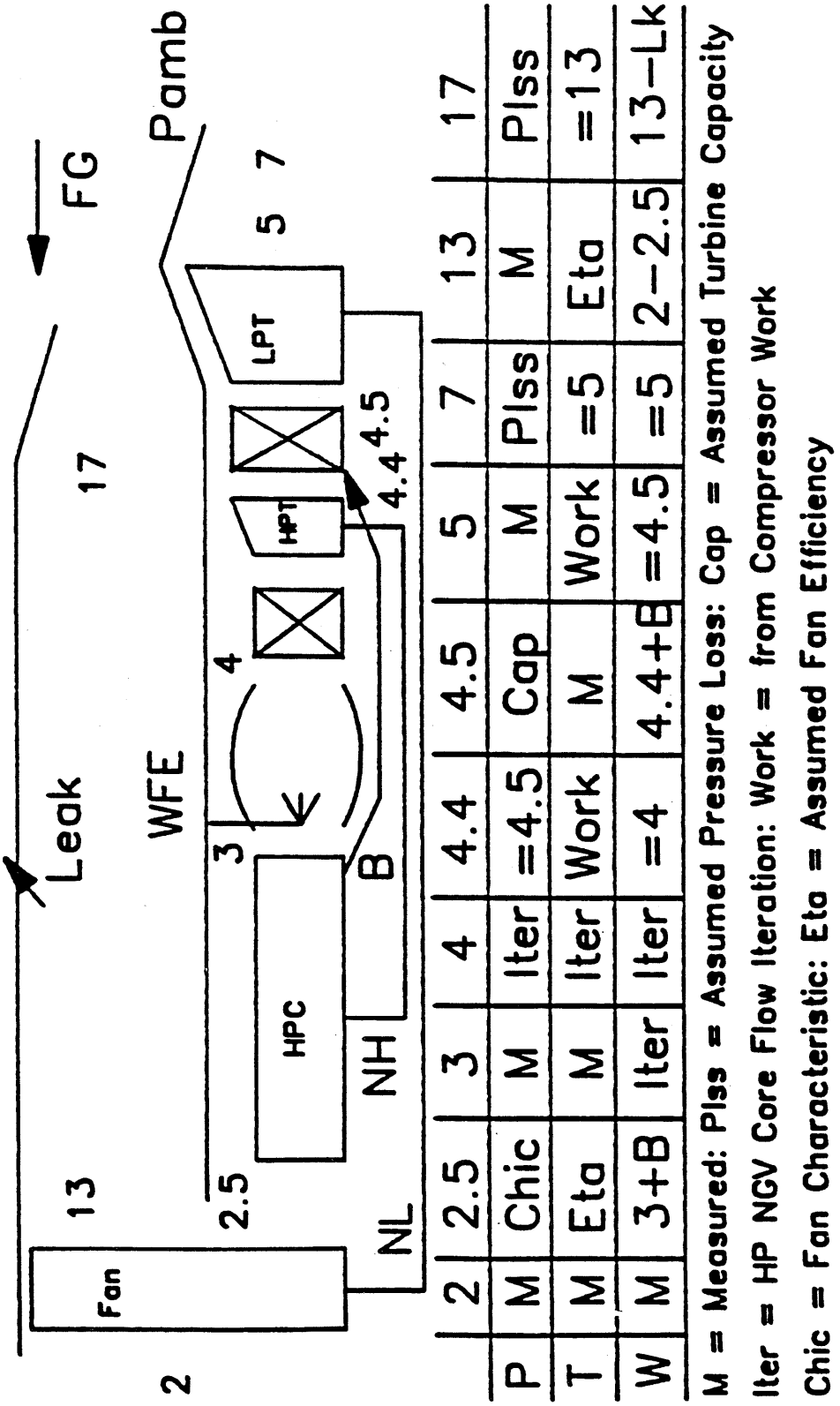

	2	2.5	3	4	4.4	4.5	5	7	13	17
P	M	Chic	M	Iter	=4.5	Cap	M	Plss	M	Plss
T	M	Eta	M	Iter	Work	M	Work	=5	Eta	=13
W	M	3+B	Iter	=4	4.4+B	=4.5	=5	=5	2–2.5	13–Lk

Figure 113: Two-shaft turbofan: summary of analysis

to the rear of the HP Turbine;

4) The flow at entry to the Bypass Duct is simply the measured total airflow less the derived core flow; flows down the Bypass Duct can be derived from this, subtracting assumed leakage and adding in handling bleed(s) (at low powers) at the appropriate station(s);

5) Any unmeasured pressures and temperatures in the compressor section (usually at Fan Tip and/or Root exit, where for reasons given above temperatures are particularly difficult to measure accurately and, in the case of the Fan Root, there may be difficulties in fitting any instrumentation at the exit station) can be derived from assumed efficiency and pressure rise characteristics, which are usually a function of non-dimensional speed (known from measurements) and flow (known from the core flow iteration);

6) Knowing the compressor flows and temperature rises, the compressor powers can be derived, so turbine power can be calculated from:

turbine power = compressor power + any assumed parasitic powers

The turbine airflows are known, therefore the turbine temperature drops and hence exit temperatures are known;

7) Heat balance calculations at the cooling/sealing bleed return stations (and handling bleed addition(s) in the bypass duct) give temperature drops (or rise) at the various bleed return points;

8) Assumed duct pressure losses can be used to derive pressures at exit from the Bypass Duct and Jet Pipe if upstream pressures are measured (or entry pressures if downstream ones are measured);

9) Inter-turbine pressures (and, on occasion, nozzle entry pressures), can be derived from assumed capacities ($W\sqrt{T}\div P$'s) (or nozzle areas, discharge coefficients and compressible flow equations, which give nozzle $W\sqrt{T}\div P$'s) and measured or derived flows and temperatures;

$$P = (W_{known} \bullet \sqrt{T}_{known}) \div (W\sqrt{T}\div P)_{assumed}$$

By appropriate use of relationships such as those given above, it is possible to derive the pressures, temperatures and flows at every station in the engine. Note that in many cases assumptions have been made about component performance or cooling/sealing bleed flows; it is important, therefore, to check the sensitivity of the calculations to these assumptions, and change them if necessary to produce a believable analysis.

A14 Correction of Measurements to Standard Day Conditions

The performance of the engine is usually declared at a standard flight condition, such as Sea Level Static ISA in the case of take-off performance or 35000ft 0.8 Mach No ISA for cruise performance. Since it is highly unlikely that the atmospheric conditions on the day will correspond to the standard condition, a procedure is needed to convert the measurements from their 'true' values at the test flight condition to the values that would have been seen had the test condition corresponded to the standard day condition. The basis for conversion is the relevant non- or semi-dimensional group, which will remain constant between the test and standard day conditions. Consider the following examples:

1) Engine Pressures

The non-dimensional group is $P \div P2$, where P2 is the engine face total pressure;

$$(P \div P2)_{test} = (P \div P2)_{corrected}$$

$$\Rightarrow P_{corrected} = P_{test} \bullet P2_{corrected} \div P2_{test}$$

$$= P_{test} \div (P2_{test} \div P2_{corrected})$$

$$= P_{test} \div \delta$$

where δ conventionally represents $P2_{test} \div P2_{corrected}$

2) Engine Temperatures

The non-dimensional group is $T \div T2$, where T2 is the engine face total temperature;

$$(T \div T2)_{test} = (T \div T2)_{corrected}$$

$$\Rightarrow T_{corrected} = T_{test} \bullet T2_{corrected} \div T2_{test}$$

$$= T_{test} \div (T2_{test} \div T2_{corrected})$$

$$= T_{test} \div \Theta$$

where Θ conventionally represents $T2_{test} \div T2_{corrected}$

3) Net Thrust

The semi-dimensional group is $FN \div Pamb$, where Pamb is the local ambient static pressure;

$$(FN \div Pamb)_{test} = (FN \div Pamb)_{corrected}$$

$$\Rightarrow FN_{corrected} = FN_{test} \bullet Pamb_{corrected} \div Pamb_{test}$$

$$= FN_{test} \div (Pamb_{test} \div Pamb_{corrected})$$

$$= FN_{test} \div \delta_{amb}$$

where δ_{amb} represents $Pamb_{test} \div Pamb_{corrected}$

4) Fuel Flow

The semi-dimensional group is $WFE \div (P2\sqrt{T2})$;

$$(WFE \div (P2\sqrt{T2}))_{test} = (WFE \div (P2\sqrt{T2}))_{corrected}$$

$$\Rightarrow WFE_{corrected} = WFE_{test} \bullet \frac{(P2\sqrt{T2})_{corrected}}{(P2\sqrt{T2})_{test}}$$

$$= WFE_{test} \div (\delta \bullet \sqrt{\Theta})$$

5) Shaft Speeds

The semi-dimensional group is $N \div \sqrt{T2}$;

$$(N \div \sqrt{T2})_{test} = (N \div \sqrt{T2})_{corrected}$$

$$\Rightarrow N_{corrected} = N_{test} \bullet \sqrt{T2}_{corrected} \div \sqrt{T2}_{test}$$

$$= N_{test} \div (\sqrt{T2}_{test} \div \sqrt{T2}_{corrected})$$

$$= N_{test} \div \sqrt{\Theta}$$

6) Airflow

The semi-dimensional group is $W\sqrt{T2} \div P2$;

$$(W\sqrt{T2} \div P2)_{test} = (W\sqrt{T2} \div P2)_{corrected}$$

$$\Rightarrow W_{corrected} = W_{test} \bullet \frac{(\sqrt{T2} \div P2)_{test}}{(\sqrt{T2} \div P2)_{corrected}}$$

$$= W_{test} \bullet \sqrt{\Theta} \div \delta$$

However, the above groups are not in fact constant as flight conditions vary, so for accurate performance analysis it is necessary to take this into account. The two principal departures from non- or semi-dimensionality are changes in specific heat (which depend on the levels of temperature in the engine, which themselves depend on T2), and Reynold's Number effects on the components (which depend on P2 and, to a smaller degree, T2).

Variations of P2 from nominal ISA conditions are rarely more than 1% on the sea level beds, but variations of T2 are much larger. Accounting of the departures from non-dimensionality due to T2 variations is done by modifying the power that Θ is raised to in the above expressions; hence their name 'theta exponents'. Typical theta exponents are shown in Table 7.

Parameter	Ideal Exponent	Real Exponent
Temperatures	1.0	0.98 to 1.03
Pressures	0.0	0.0 to 0.05
Fuel Flow	0.5	0.65 to 0.75
Speeds	0.5	0.49 to 0.5
Airflow	0.5	0.48 to 0.52

Table 7: Typical theta exponents

The exponents are derived by running a performance synthesis program over a range of inlet temperatures at several flight conditions and power settings, and observing how the various parameters change. The large change from ideal to actual exponent in the case of fuel flow comes from the fact that the temperature rise charts (which give fuel/air ratio) are derived using variable specific heats for air.

Other corrections are also applied, such as:

1) corrections from the actual test intake to a standard flight or ideal (100% recovery) intake;

2) corrections from the humidity of the test flight condition to zero humidity, taking account of the different gas properties of dry and humid air;

3) corrections for the effects of condensation of atmospheric water vapour in the intake, together with subsequent re-evaporation of the water in the engine;

4) corrections for the effects of test installation features, such as instrumentation losses and intake boundary layer blockage (which affects fan performance);

5) corrections to the fuel flow for differences between the test fuel calorific value and the calorific value of standard fuel.

With the exception of condensation corrections (which are still the subject of intense research because the physics of condensation and super-saturation in aero-engines are so complex) and calorific value corrections (which are done by factoring fuel flow by the ratio (test fuel calorific value + 100)÷(standard fuel calorific value + 100); the 100 is an empirical factor to convert calorific value to enthalpy at a typical combustion temperature), all the above correction factors can be derived using performance synthesis programs, run with and without the effect to be corrected out to derive semi-empirical factors. Another method of correcting out these various effects is to derive, from the test measurements, a model of the actual engine, and then run the model at the standard conditions; this is discussed in detail later.

Sometimes, all the measured data is corrected first, before the core flow calculations and derivation of unmeasured parameters takes place. This approach has now fallen out of favour because the shifts of component working points that can be introduced in the correction process at high non-dimensional power settings can introduce inconsistencies between the 'corrected' analysis done by the performance analyst and the 'raw' analysis done by component specialists on engine data.

A15 Calculation of Component Performance

Having calculated flow, pressure and temperature at every station in the engine, calculation of component performance parameters such as efficiencies and working points is very simple:

1) Compressor pressure ratio = $P_{out} \div P_{in}$

   Compressor non-dimensional speed = $N \div \sqrt{T_{in}}$

   Compressor non-dimensional flow = $(W\sqrt{T} \div P)_{in}$

   Compressor efficiency = $$\frac{(P_{out} \div P_{in})^{((\gamma-1)\div\gamma)}-1}{(T_{out} \div T_{in})-1}$$

2) Turbine non-dimensional power = $C_p \bullet (T_{in} - T_{out}) \div T_{in}$

   Turbine non-dimensional speed = $N \div \sqrt{T_{in}}$

   Turbine non-dimensional flow = $(W\sqrt{T} \div P)_{in}$

   Turbine efficiency = $$\frac{1-(T_{out} \div T_{in})}{1-(P_{out} \div P_{in})^{((\gamma-1)\div\gamma)}}$$

3) Nozzle discharge coefficient =

$$\frac{\text{Effective area from } (W\sqrt{T} \div P)_{in} \text{ and Q from } P_{in} \div \text{Pamb}}{\text{Geometric Area}}$$

   Nozzle velocity coefficient =

$$\frac{\text{Actual Thrust}}{\text{Ideal Thrust from } (FG \div W\sqrt{T}) \text{ (from } P_{in} \div \text{Pamb)}, W_{in}, T_{in}}$$

4) Duct pressure loss = $(P_{in} - P_{out}) \div P_{in}$, if P_{in}, P_{out} measured

   etc

Other engine parameters, such as SFC (=WFE÷FN) and thermal and propulsive efficiencies, can also be calculated.

A16 Measurement Error

Errors in the measurements made on an engine can have a major effect on the analysis, and the performance analyst should always be aware of the possibility of their occurrence.

Measurement error is defined as a difference between the observed reading of a parameter and its 'true' value, defined either as the value that a standards authority such as the National Physical Laboratory would record or, more practically, as a datum standard that is representative of the quantity being measured, eg from 'rig standard' instrumentation. It has two components:

1) A random component (known as (non-)repeatability, random error or precision error) caused by numerous uncontrolled small effects which cause disagreements between repeated measurements of the same quantity;

2) A fixed component (known as bias, systematic error or constant error) which is caused by changes in the measurement equipment relative to the standard; these changes remain fixed, however often the measurement is repeated. Examples are:

   - Bent/broken/blocked sensor heads;

   - Incorrect calibration of transducers;

   - Defects such as leaks in pressure measurement tubes, incorrect measurement of cold junction temperature, or leaks in fuel lines.

Repeatability errors can be minimised by averaging many samples of the measurement in question, since the repeatability of an average is better than the repeatability of an individual reading. They can also be 'smoothed out' by curve-fitting parameters of interest against appropriate power-level parameters (eg SFC can be plotted against FN, compressor efficiency can be plotted against either FN or compressor inlet $W\sqrt{T}\div P$), and then interpolating values from the curve-fit. Bias errors are much more difficult to deal with, since they can only be detected analytically, either by comparing redundant parameters and cross-plotting by the performance analyst or by sophisticated tools such as the Kalman Filter.

Measurement errors show up in a variety of ways:

1) If a parameter is measured a number of times at a particular station (such as by individually-read Pitot tappings or by different types of instruments that should have a fixed relationship to each other), then individual readings can be compared both with their neighbours (on a 'profile plot') and with the average.

This process is particularly good for detecting problems such as pressure line leaks (where the suspect reading reads either cell pressure, under-cowl pressure or ambient pressure if the leak is large, or drifts further away from the 'normal' profile as engine power is increased if the leak is small) and short-circuit or open-circuit thermocouples;

2) Plotting one parameter against another is also a good way of looking for measurement inconsistency, both to check the resulting relationship with other test data (if available) or pre-test predictions and to check if the resulting relationship is 'smooth'. It should be noted that any shift seen in a relationship could be caused by:

   - an error in either the Y parameter or the X parameter; plotting both against a third parameter can sometimes resolve which one is erroneous;

   - genuine shifts in component performance; these usually show up by changing several relationships simultaneously.

3) Calculation of 'impossible' component performance (such as efficiencies greater than 100%, negative pressure losses, compressor working lines above surge or below choke, physically unreachable compressor flows at a non-dimensional speed or nozzle coefficients very far away from unity) is a clear indication that one or more measurements are erroneous;

4) 'Reciprocal' changes in component efficiencies, where one component seems too 'good' while another (on the same shaft, say, or immediately upstream/downstream) seems too 'bad', can be used as indications of potential errors.

It should be noted that the presence of 'reciprocal' changes or shifts in relationships do not 'prove' the existence of measurement errors, only indicate that they might be present. A common fallacy is to assume that measurement errors can be found by looking at the effects of component performance changes on such overall parameters as SFC and TET; however, such 'accounting checks', if done properly by including all component performance parameters (ie nozzle performance as well as component efficiencies), merely show that 'goodness' in some components caused by measurement error is exactly cancelled out by 'badness' in others, leaving the overall parameters unchanged. A high HP Compressor exit temperature (T3), for instance, will reduce calculated HP Compressor efficiency, but increase HP Turbine efficiency and excess cooling bleed; these changes will exactly cancel out, to leave SFC (=WFE÷FN) unchanged (which is reasonable, since WFE and FN measurements are unaffected

by any errors in T3). By a similar argument, all the calculated shifts in component efficiencies, nozzle performance, etc will 'explain' all the shifts in parameter relationships such as SFC vs FN, TET vs TGT (Turbine Gas Temperature), compressor working lines, etc; 'goodness' cancels out 'badness' to leave relationships (that are themselves unaffected by errors) unchanged. The performance analyst needs to use skill and judgement to assess whether the analysis is 'credible', based in large measure on other information such as expected component efficiencies and nozzle performance parameters and a knowledge of potential hardware problems and how these can affect the engine's aero-thermodynamic behaviour.

A17 Iterative Analysis

So far, the discussion of analysis methods has concentrated on the calculation of unmeasured parameters and component performance parameters directly from measurements. While this 'traditional' method generally works well (and, indeed, may form part of a contract between the engine manufacturer and the customer and/or certifying authority that lays down agreed calculations for proving engine acceptability), there are a number of problems that have led to the development of a technique called Iterative Analysis that uses pre-test models of the engine being analysed as the starting point for the analysis process. These problems include:

1) potential inconsistencies between the analysis and synthesis processes as engine modelling becomes more sophisticated;

2) the inability of the 'traditional' analysis to proceed if significant measurements (such as those needed to calculate core flow) are missing;

3) large departures from non-dimensionality when the engine is tested at conditions far removed from standard, making the correction processes described incorrect;

4) the reliance on the skill of the performance analyst to detect and remove measurement errors from the analysis; this can be extremely time-consuming and frustrating if several errors are present.

Note that this newer method will be different to the 'contract thermodynamics' referred to earlier; it supplements, but does not usually replace, calculations agreed with the customer or done for historical consistency.

To understand Iterative Analysis, it is instructive to compare analysis and synthesis programs:

1) An analysis program calculates, from measurements taken at a defined power level and set of flight conditions (engine inlet total pressure and temperature, as well as nozzle exhaust static pressure) the air mass flow, total pressure and total temperature at each station in the engine, as well as fuel flow, thrust and shaft speeds. Some of these parameters will be measured directly; others will be calculated using the laws of conservation of mass and energy, or derived by making assumptions about pressure losses, etc. Knowing these parameters, the individual component performance parameters (eg efficiency, non-dimensional flow and speed, pressure ratio) can be calculated;

2) A synthesis program works in the opposite direction: using predictions of component performance, it calculates, by iteration, a series of working points on these characteristics that satisfy the laws of conservation of mass and energy, at a defined power level and set of flight conditions. In doing so, it derives the air mass flow, total pressure and total temperature at each station in the engine, as well as fuel flow, thrust and shaft speeds.

It follows that, if the component performance assumptions made in a synthesis are modified so that, when a synthesis is run at the test power level and flight conditions, the measurements taken on that test are reproduced, then an analysis will have been done, since, at the end of this process, all the parameters mentioned above will have been calculated. The process is iterative, hence Iterative Analysis.

Note that one measurement, such as fuel flow, is needed to define the power level of the engine, and other measurements are needed to define the flight conditions. Any extra measurements that are taken are reproduced by varying as many component performance assumptions as there are extra measurements.

The following examples illustrate the above statements. If the only measurement taken on an engine (in addition to those necessary to determine the flight conditions) is fuel flow, then the best estimate of the performance of that engine is obtained by running a synthesis model of that engine at the measured fuel flow and flight conditions. If fuel flow and HP Compressor delivery pressure (P3) are measured, then the HP Compressor efficiency (say) will have to be varied so that the measured pressure is reproduced when the above synthesis is run at the measured fuel flow. If fuel flow, HP Compressor delivery total pressure and HP Compressor delivery total temperature (T3) are measured, then both the HP Compressor and HP Turbine efficiencies (say) will have to be varied in order to reproduce the measurements.

Note that it is an assumption, based on all the available information, that the HP components are the ones to be changed. It may, in fact, have been other components that have changed, but it is impossible to say categorically what has changed given the information available. The choice of which component assumptions to vary is a best guess; as more measurements are taken, so more component performance assumptions can be varied, and a more complete picture of the actual component performance built up.

Having converted the analysis process from one of direct calculation to one of varying component performance assumptions within a synthesis model, it can be seen that this method of analysis is merely an extension of the calculations done in a synthesis. This brings with it a number of advantages:

1) The thermodynamic assumptions and data (including such items as parasitic losses, etc) are identical for both synthesis and analysis;

2) The analysis is able to proceed if measurements are missing, by using component performance assumptions that would be used in a synthesis;

3) The changes made to the component performance assumptions in order to reproduce the measurements are known. This means that:

   - The analysis automatically 'accounts'; the analysed component performance changes will, by definition, account for the observed measurement values.

   - The changes made to the component performance assumptions can be fed back into a synthesis to easily produce a synthesis model of the engine being tested, for running at other flight conditions.

   - As an extension of the above, the necessity to produce correction factors to correct the measurements to standard day conditions is eliminated. The analysis can be done at actual conditions (inlet total pressure and temperature, intake configuration, humidity, ram ratio, etc); the resulting component performance changes can be fixed, then the program can be run again, this time as a synthesis at corrected conditions, to derive what the measurements would have been had the engine been run at standard day conditions, with standard intake configuration, etc.

   - Reciprocal changes, eg a positive delta on HP Compressor efficiency coupled with a negative delta on HP Turbine efficiency, are much easier to spot, and can be used to diagnose measurement errors.

As stated previously, each measurement input to an Iterative Analysis program over and above a measurement used to define the power level of the engine requires the definition of a component performance parameter (eg compressor efficiency) that can be changed in order to reproduce that measurement. Consideration of the functions of the components (eg compressors produce pressure ratio, so outlet pressure is associated with efficiency: turbines produce work to drive compressors, so compressor outlet temperature is associated with turbine efficiency: ducts produce pressure loss, so that outlet pressure is associated with duct loss: nozzles produce thrust and determine airflow, so engine gross thrust and total inlet airflow are associated with nozzle thrust and discharge coefficients) determine which component performance parameter changes are best associated with each measurement. The relationships between measurement and component performance parameters need not be unique, but may depend on the presence or absence of other measurements; the choice is purely one of engineering judgement.

APPENDIX B: CALCULATION OF OBSERVABILITY EIGENVALUES AND EIGENVECTORS

1) Let the matrix (dimensions (m•n)) being analysed be denoted by $\underline{C}$. Since the angles between the equations denoted by $\underline{C}$ depend on ratios of elements by row, we first have to normalise $\underline{C}$ by row to produce a new matrix $\underline{D}$ with rows which are of unit length. This matrix $\underline{D}$ can be written as:

$$\underline{D} = \begin{pmatrix} \underline{d}_1 \\ \underline{d}_2 \\ \cdot \\ \cdot \\ \underline{d}_m \end{pmatrix}$$

where $\underline{d}_1$, $\underline{d}_2$, ... are row vectors of unit length. We are looking for a column vector $\underline{u}$, itself also of unit length, which is as closely orthogonal as possible to $\underline{d}_1$, $\underline{d}_2$, ..., ie:

$$L = (\underline{d}_1 \bullet \underline{u})^2 + (\underline{d}_2 \bullet \underline{u})^2 + ...$$

is a minimum.

2) This can be written as:

$$L = \underline{u}^T \bullet (\underline{d}_1^T \bullet \underline{d}_1 + \underline{d}_2^T \bullet \underline{d}_2 + ...) \bullet \underline{u}$$

$$= \underline{u}^T \bullet \underline{D}^T \bullet \underline{D} \bullet \underline{u}$$

3) The objective is to minimise L, subject to the constraint:

$$\underline{u}^T \bullet \underline{u} = 1$$

which arises because all vectors have unit length. The function to be minimised then becomes:

$$L = \underline{u}^T \bullet \underline{D}^T \bullet \underline{D} \bullet \underline{u} + \lambda \bullet (\underline{u}^T \bullet \underline{u} - 1)$$

where λ is a scalar.

4) $$\frac{\delta L}{\delta \underline{u}} = \frac{\delta}{\delta \underline{u}} (\underline{u}^T \bullet \underline{D}^T \bullet \underline{D} \bullet \underline{u} + \lambda \bullet (\underline{u}^T \bullet \underline{u} - 1)) = 0$$

$$2 \bullet \underline{D}^T \bullet \underline{D} \bullet \underline{u} - 2 \bullet \lambda \bullet \underline{I} \bullet \underline{u} = 0$$

$$(\underline{D}^T \bullet \underline{D} - \lambda \bullet \underline{I}) \bullet \underline{u} = 0$$

This has a non-trivial solution only if the determinant of

$$(\underline{D}^T \bullet \underline{D} - \lambda \bullet \underline{I}) = 0.$$

5) The equation $\det[(\underline{D}^T \bullet \underline{D} - \lambda \bullet \underline{I})] = 0$ is the characteristic equation for $\underline{D}^T \bullet \underline{D}$: values of λ that satisfy it are called Eigenvalues, each of which has a corresponding Eigenvector $\underline{u}$, which satisfies the equation:

$$\underline{D}^T \bullet \underline{D} \bullet \underline{u} = \lambda \bullet \underline{u}$$

The smallest Eigenvalue corresponds to the most orthogonal Eigenvector, which points in the direction of weakest observability.

6) It should be noted that there are as many Eigenvalues and Eigenvectors as there are dimensions of $\underline{D}^T \bullet \underline{D}$, which has dimensions $(n \bullet n)$; therefore the total number of Eigenvalues and Eigenvectors is equal to the total number of component changes and sensor biasses in $\underline{C}$. It should also be noted that, since $\underline{D}^T \bullet \underline{D}$ is symmetric, the Eigenvalues and Eigenvectors are real, and the Eigenvectors are orthogonal.

APPENDIX C: CALCULATION OF SENSOR NON-REPEATABILITY STANDARD DEVIATIONS

The calculations in this Appendix make use of the following statistical result:

$$\text{Standard deviation of average} = \frac{\text{Standard deviation of individual reading}}{\sqrt{(\text{Number of readings in average})}}$$

It should also be noted that the non-repeatability values are quoted maxima: for the purposes of this work, they have been interpreted as representing ±3 standard deviations (within which, according to Normal Distribution tables, just over 99.7% of readings would lie).

1) EPR standard deviation

3 standard deviations of single EPR reading = 0.262%
Number of readings per data scan = 8

Therefore EPR standard deviation = 0.262 ÷ (3 • √8)
= 0.031%

2) Inlet Total Pressure (P2) standard deviation

3 standard deviations of single P2 reading = 0.272%
Number of readings per data scan = 8

Therefore P2 standard deviation = 0.272 ÷ (3 • √8)
= 0.032%

3) Inlet Total Temperature (T2) standard deviation:

3 standard deviations of single T2 reading = 0.087%
Number of readings per data scan = 2

Therefore T2 standard deviation = 0.087 ÷ (3 • √2)
= 0.021%

4) Fuel Flow (WFE) standard deviation

3 standard deviations of single WFE reading = 0.3%
Number of readings per data scan = 1

Therefore WFE standard deviation = 0.3 ÷ 3
= 0.1%

5) HPC Entry Total Pressure (P26) standard deviation

3 standard deviations of single P26 reading = 0.262%
Number of readings per data scan = 5

Therefore P26 standard deviation = 0.262 ÷ (3 • √5)
= 0.039%

6) HPC Entry Total Temperature (T26) standard deviation

3 standard deviations of single T26 reading = 0.15%
Number of readings per data scan = 6

Therefore T26 standard deviation = 0.15 ÷ (3 • √6)
= 0.02%

7) HPC Exit Total Pressure (P3) standard deviation

3 standard deviations of single P3 reading = 0.306%
Number of readings per data scan = 1

Therefore P3 standard deviation = 0.306 ÷ 3
= 0.102%

8) HPC Exit Total Temperature (T3) standard deviation

3 standard deviations of single T3 reading = 0.252%
Number of readings per data scan = 1

Therefore T3 standard deviation = 0.252 ÷ 3
= 0.084%

9) LPT Exit Total Temperature (T49) standard deviation

3 standard deviations of single T49 reading = 0.062%
Number of readings per data scan = 6

Therefore T49 standard deviation = 0.062 ÷ (3 • √6)
= 0.008%

10) Fan Tip Exit Total Pressure (P13) standard deviation

3 standard deviations of single P13 reading = 0.279%
Number of readings per data scan = 8

Therefore P13 standard deviation = 0.279 ÷ (3 • √8)
= 0.033%

11) LP Speed (XNL) standard deviation

3 standard deviations of single XNL reading = 0.022%
Number of readings per data scan = 1

Therefore XNL standard deviation = 0.022 ÷ 3
= 0.007%

12) HP Speed (XNH) standard deviation

3 standard deviations of single XNH reading = 0.022%
Number of readings per data scan = 1

Therefore XNH standard deviation = 0.022 ÷ 3
= 0.007%

13) Net Thrust (FN) standard deviation

3 standard deviations of single FN reading = 0.442%
Number of readings per data scan = 1

Therefore FN standard deviation = 0.442 ÷ 3
= 0.147%

14) Total Inlet Airflow (W1A) standard deviation

Airmeter Total Pressure standard deviation = 0.0032%
Airmeter Static Pressure standard deviation = 0.0063%
Airmeter Total Temperature standard dev'n = 0.021%

+1% Airmeter Total Pressure => +1.0% W√T÷AP
+1% Airmeter Static Pressure => -1.5% W√T÷AP

W1A = (W√T÷AP) • Airmeter Area • Airmeter Total Pressure ÷ √(Airmeter Total Temperature)

Therefore, by considering the effects of the above non-repeatabilities on each of the terms in the above equation, then taking the root-sum-square, the W1A standard deviation becomes:

$$\sqrt{(2\bullet(1\bullet0.0032)^2 + (1.5\bullet0.0063)^2 + (0.5\bullet0.021)^2)}$$
= 0.015%